GEOCHEMISTRY OF STREAMS, SOILS, AND PERMAFROST AND THE GEOCHEMICAL EFFECTS OF CLIMATE CHANGE IN A CONTINUOUS PERMAFROST REGION, ARCTIC ALASKA, USA

by

Kate A. Keller

A dissertation submitted in partial fulfillment
of the requirements for the degree of
Doctor of Philosophy
(Geology)
in The University of Michigan
2006

Doctoral Committee:

Professor Joel D. Blum, Co-chair
Professor George W. Kling II, Co-chair
Professor Stephen E. Kesler
Professor Donald R. Zak
Assistant Professor Ingrid L. Hendy

ACKNOWLEDGEMENTS

I extend my gratitude to Dr. Joel Blum for his support during the course of my doctoral research; without his intellectual and practical support this research would not have been possible. I also thank Dr. George Kling and Dr. Donald Zak, whose interesting ideas and enthusiasm for science helped increase the breadth of my research and the depth of my permafrost sampling trenches. Comments, criticism, and insight from committee members Dr. Stephen Kesler and Dr. Ingrid Hendy also substantially improved the quality of this dissertation.

I would also like to acknowledge my family who supported and inspired me during this research: Dr. Steven Keller, and Susan, Noah, John, and Reno Keller. Many colleagues and friends at University of Michigan and other institutions also provided advice, assistance, and analytical expertise critical to this project, so I would like to thank Dr. Chris Smith, Amanda Ash Dasch, Abir Biswas, Carmen Nezat, Kelsey Johnson, Martin Reich, Dr. Kristi Judd, Heather Adams, Amanda Field, Brendan O'Donnell, Dr. Brian Kennedy, Dr. Tom Douglas, Dr. Andrea Klaue, Dr. Jamie Gleason, and Marcus Johnson.

TABLE OF CONTENTS

LIST OF TABLES

LIST OF FIGURES

LIST OF APPENDICES

ABSTRACT

GEOCHEMISTRY OF STREAMS, SOILS, AND PERMAFROST AND THE GEOCHEMICAL EFFECTS OF CLIMATE CHANGE IN A CONTINUOUS PERMAFROST REGION, ARCTIC ALASKA, USA

Climate warming can impact arctic ecosystems by altering watershed geochemistry through permafrost degradation and increased mineral weathering. This dissertation evaluated the importance of these changes in arctic Alaska by examining permafrost and soil geochemistry, mineral weathering, and changes in stream geochemistry.

Elemental and $^{87}Sr/^{86}Sr$ geochemistry of streams and soils, permafrost, and soil parent materials from glacial deposit surfaces of varying ages were evaluated. Carbonate content increases with soil depth across all surfaces, and exchangeable P, K, and Ca concentrations are significantly ($p<0.05$) greater in permafrost than in active-layer mineral soil. These results suggest that increasing thaw depth will increase carbonate alkalinity, Ca, K, and P supply to soils and streams across the region. Elemental depletion factors for a subset of these soils forming a chronosequence indicate that carbonate weathering is the dominant weathering process, and long-term weathering rates are 0.5-11 meq m^{-2} yr^{-1}.

Based on increasing Ca/Na and Ca/Ba and decreasing $^{87}Sr/^{86}Sr$ with depth in soils and permafrost, elemental ratios and $^{87}Sr/^{86}Sr$ in an arctic stream were used as tracers of the maximum depth of soil water flow and therefore changes in integrated thaw depth across the watershed. From 1994 to 2004, mean $^{87}Sr/^{86}Sr$ values in low-discharge late summer stream water decreased from 0.7122 to 0.7119 (R^2=0.62, p=0.012), and Ca/Na and Ca/Ba showed significant increasing trends that were consistent with increasing depth of soil water flowpaths. These trends provide new evidence for increasing thaw depth, despite the lack of measured increases using traditional thaw probe techniques.

The effects of an in-stream thermokarst feature on stream chemistry were also investigated. Solute concentrations, alkalinity, and conductivity were elevated downstream from the thermokarst. Estimates suggest geochemical changes may be detectable downstream in rivers up to 100 times the size of the original affected stream. These data further support the use of stream geochemistry as an indicator of spatially heterogeneous permafrost degradation.

This research suggests that permafrost degradation on the Alaskan North Slope is exposing previously frozen carbonate minerals to weathering, thereby influencing stream geochemistry. These geochemical changes are an important consideration when examining the overall impact of climate change on arctic ecosystems.

CHAPTER 1

INTRODUCTION: CHANGING CLIMATE AND WATERSHED GEOCHEMISTRY IN THE ARCTIC

Introduction

Climate change in permafrost regions. Climate models predict that global climate change will have an amplified effect in the arctic relative to temperate and tropical regions (Walsh and Crane, 1992; Fyfe et al., 1999; Shindell et al., 1999) and recent studies support this hypothesis (Majorowicz and Skinner, 2001; Moritz et al., 2002; Majorowicz et al., 2004). In arctic Alaska, temperature records show a mean annual increase of 2.4°C from 1974 to 2003 (Alaska Climate Research Center, 2003). The impacts of warming climate in the Arctic include effects on biodiversity (Ruess et al., 1999), plant growth (Arft et al., 1999), and carbon storage in tundra soils (Waelbroek et al., 1997). The research presented here indicates that climate change will also affect soil and stream geochemistry, due to thawing of permafrost.

Permafrost underlies 20% of the Earth's surface, including most arctic soils (Easterbrook, 1999). Evidence suggests that warming climate is increasing the thickness of the active (seasonally thawed) layer and degrading permafrost in

the Arctic. Although models suggest current (Chen et al., 2003) and future increases in active layer thickness (Stendel and Christensen, 2002), there have been limited direct measurements of such changes. These measurements include thaw depth increases at a few sites (Brown et al., 2000; Pavlov and Moskalenko, 2002) and observations of accelerated degradation of ground ice on the Arctic Coastal Plain from 1945-2001 (Shur et al., 2003; Jorgenson et al., 2006). Increasing permafrost borehole temperatures (Osterkamp, 2005) show no increases in active layer thickness but do indicate degradation of permafrost.

Thawing of permafrost increases the total amount of mineral soil that is exposed to cation exchange and weathering. Exposure of minerals that were previously inhibited from weathering is an effect of climate change specific to permafrost regions, and may cause changes in chemical weathering and watershed geochemistry not seen in temperate or tropical regions. In order to understand the potential effects of climate change, it is necessary to characterize arctic stream, soil, and permafrost geochemistry, and mineral weathering rates, to establish baselines against which future changes can be measured.

Overview of chapters

In order to predict how climate change may impact watershed geochemistry in the Arctic, this dissertation aims to evaluate the geochemistry of the permafrost, the relationship between mineral weathering and stream and soil geochemistry in permafrost regions, and changes in stream geochemistry that are already occurring as a result of permafrost degradation. Many geochemical

and geologic methods were employed in these investigations, including thin section mineral identification, various laboratory leach and digestion procedures, major and trace element analyses, radiogenic isotope analyses, and mixing and weathering calculations. This array of approaches has resulted in a comprehensive set of geochemical data for soils and streams extending north from the Toolik Lake area on the Alaskan North Slope. This data set provides the basis for discussion of some of the ecological and geochemical implications of increasing thaw depth, and also introduces a new and sensitive hydrogeochemical method for evaluating changes in thaw depth that may be applicable in many permafrost regions.

Chapter 2 presents and discusses stream, soil, and permafrost geochemical data for several geomorphic surfaces in the Alaskan arctic; this chapter is in press as a paper, co-authored with Joel Blum and George Kling, in *Arctic, Antarctic, and Alpine Research* (Keller et al., 2006a). Chapter 3 uses data presented in chapter 2 to estimate long-term chemical weathering rates for four of the surfaces that form a glacial chronosequence on the Alaskan North Slope.

Chapters 4 and 5 both examine the effects of permafrost degradation on stream geochemistry, but from different perspectives. Chapter 4 takes advantage of our knowledge of permafrost geochemistry to predict and detect trends in stream geochemistry that indicate incremental permafrost degradation, and introduces a geochemical-tracer method of monitoring integrated thaw depth across a watershed. This chapter is in review at the journal *Geology* (Keller et al., 2006b). Chapter 5 examines the effects of larger-scale permafrost

degradation, as typified by thermokarst formation, on the chemistry of a small stream and estimates how these effects might resonate through larger arctic watersheds.

References Cited

Alaska Climate Research Center, 2003: Temperature Change in Alaska 1974-2003, http://climate.gi.alaska.edu/ClimTrends/Change/7403Change.html.

Arft, A. M., Walker, M. D., Gurevitch, J., Alatalo, J. M., Bret-Harte, M. S., Dale, M., Diemer, M., Gugerli, F., Henry, G. H. R., Jones, M. H., Hollister, R. D., Jonsdottir, I. S., Laine, K., Levesque, E., Marion, G. M., Molau, U., Molgaard, P., Nordenhall, U., Raszhivin, V., Robinson, C. H., Starr, G., Stenstrom, A., Stenstrom, M., Totland, O., Turner, P. L., Walker, L. J., Webber, P. J., Welker, J. M., and Wookey, P. A., 1999: Responses of tundra plants to experimental warming: Meta-analysis of the international tundra experiment. *Ecological Monographs,* 69: 491-511.

Brown, J. G., Kling, G. W., Hinkel, K. M., Hinzman, L. D., Nelson, F. E., Romanovsky, V., and Shiklomanov, N. I., 2000: Arctic Alaska and Seward Peninsula, in Brown, J. G., Hinkel K. M., and Nelson F. E. (eds.): The circumpolar active layer monitoring (CALM) program: Research designs and initial results. *Polar Geography,* 24: 165-258.

Chen, W., Zhang, Y., Cihlar, J., Smith, S., and Riseborough, D., 2003: Changes in soil temperature and active layer thickness during the twentieth century in a region in western Canada. *Journal of Geophysical Research-Atmospheres,* 108: Art. No. 4696.

Easterbrook, D. J., 1999: *Surface processes and landforms*. second edition ed. New Jersey: Prentice Hall, 546 pp.

Fyfe, J. C., Boer, G. J., and Flato, G. M., 1999: The Arctic and Antarctic Oscillations and their projected changes under global warming. *Geophysical Research Letters,* 26: 1601-1604.

Jorgenson, M. T., Shur, Y. L., and Pullman, E. R., 2006: Abrupt increase in permafrost degradation in Arctic Alaska. *Geophysical Research Letters,* 33: Art. No. L02503, doi: 02510.01029.02005GL024960, 022006.

Keller, K., Blum, J. D., and Kling, G. W., 2006a: Geochemistry of soils and streams on surfaces of varying ages in arctic Alaska. *Arctic, Antarctic, and Alpine Research,* in press.

Keller, K., Blum, J. D., and Kling, G. W., 2006b: Stream geochemistry as an indicator of increasing thaw depth in an arctic watershed. *Geology,* In review.

Majorowicz, J. A. and Skinner, W. R., 2001: Reconstruction of the surface warming history of western interior Canada from borehole temperature profiles and other climate information. *Climate Research,* 16: 157-167.

Majorowicz, J. A., Skinner, W. R., and Safanda, J., 2004: Large ground warming in the Canadian Arctic inferred from inversions of temperature logs. *Earth and Planetary Science Letters,* 221: 15-25.

Moritz, R. E., Bitz, C. M., and Steig, E. J., 2002: Dynamics of recent climate change in the Arctic. *Science,* 297: 1497-1502.

Osterkamp, T. E., 2005: The recent warming of permafrost in Alaska. *Global and Planetary Change,* 49: 187-202.

Pavlov, A. V. and Moskalenko, N. G., 2002: The thermal regime of soils in the north of Western Siberia. *Permafrost and Periglacial Processes,* 13: 43-51.

Ruess, L., Michelsen, A., Schmidt, I. K., and Jonasson, S., 1999: Simulated climate change affecting microorganisms, nematode density, and biodiversity in subarctic soils. *Plant and Soil,* 212: 63-73.

Shindell, D. T., Miller, R. L., Schmidt, G. A., and Pandolfo, L., 1999: Simulation of recent northern winter climate trends by greenhouse-gas forcing. *Nature,* 399: 452-455.

Shur, Y., Jorgenson, M. T., and Pullman, E. R., 2003: Widespread degradation of ice wedges on the Arctic Coastal Plain in northern Alaska in response to the recent warmer climate. *Eos Trans. AGU,* 84: Fall Meet. Suppl., Abstract C11A-05.

Stendel, M. and Christensen, J. H., 2002: Impact of global warming on permafrost conditions in a coupled GCM. *Geophysical Research Letters,* 29: Art. No. 1632.

Waelbroek, C., Monfray, P., Oechel, W. C., Hastings, S., and Vourlitis, G., 1997: The impact of permafrost thawing on the carbon dynamics of tundra. *Geophysical Research Letters,* 24: 229-232.

Walsh, J. E. and Crane, R. G., 1992: A comparison of GCM simulations of arctic climate. *Geophysical Research Letters,* 19: 29-32.

CHAPTER 2

GEOCHEMISTRY OF SOILS AND STREAMS ON SURFACES OF VARYING AGES IN ARCTIC ALASKA

Abstract

Climate warming may bring about geochemical changes in arctic regions as a result of increasing thaw depth. In order to better understand current watershed geochemistry and mineral weathering and provide a basis for predicting the geochemical effects of active-layer thickness increase, we examined elemental chemistry and $^{87}Sr/^{86}Sr$ of streams and sequential and total digests of soils, permafrost, and soil parent materials from seven glacial deposit surfaces of varying geomorphic ages in arctic Alaska in the vicinity of the Philip Smith Mountains quadrangle (69°N, 150°W). We found overall significantly ($p<0.05$) greater exchangeable K concentrations, exchangeable and acid digestible P and Ca concentrations, acid digestible and total Ca/Na and Ca/Sr, and lower acid digestible $^{87}Sr/^{86}Sr$ in permafrost than in active-layer mineral soil. Of the surfaces with similar parent material, stream and soil data suggest that weathering has progressively depleted calcium carbonate in the active layer with increasing surface age. Our results suggest that increasing thaw depth will lead

to increasing carbonate and Ca supply to soils and streams, as well as spatially variable increases in P and K supply. Geochemical differences between active-layer soil and permafrost suggest the possibility of using stream geochemistry to detect changes in active-layer thickness in watersheds.

Introduction

Chemical weathering of minerals is an integral part of soil formation and is ecologically important as a source of nutrients such as phosphorus, potassium, and calcium (Schlesinger, 1997); silicate weathering is geologically important as a sink for atmospheric carbon in the long term carbon cycle (Walker et al., 1981). It is important to understand mineral weathering and related soil and stream geochemistry in arctic regions because global climate change may cause changes in both the nature and extent of mineral weathering in these regions. Continuous permafrost in arctic regions restricts mineral weathering to the active (seasonally thawed) layer, and warming climate is likely to cause increased active-layer thickness (Anisimov et al., 1997). Increased active-layer thickness will allow minerals previously contained in permafrost to weather, thereby increasing the total mineral surface area that is exposed to weathering. Additionally, permafrost in some areas may contain very soluble minerals that largely have been removed by weathering in overlying thawed soils. Thawing and weathering of these minerals could cause potentially important changes in stream and soil geochemistry for years to come; the nature of these changes will depend on the spatial and temporal progression of permafrost degradation.

Much progress has been made towards understanding soil chemistry and mineral weathering on the North Slope of Alaska. Soils on the North Slope were classified and physically described in early work by Tedrow et al. (1958) and in more recent studies by Ping (1998) and Munroe and Bockheim (2001). In an investigation of the soil chemistry differences between non-acidic and acidic tundra, Bockheim et al. (1998) analyzed soil exchangeable chemistry and other soil characteristics across the Kuparuk River Basin of the North Slope, an area that overlaps the study area of this paper and includes loess, till, and colluvium deposits of different ages. Their study found a relationship between non-acidic tundra soils and greater amounts of exchangeable base cations. Munroe and Bockheim (2001) found that among the four most recently deglaciated surfaces in this region, soil profile concentrations of weathering products (clay and silt) increased significantly with age, suggesting that even in areas where cryoturbation is common, surface age is a factor in mineral weathering and soil development.

Although cycling of biogeochemically important elements such as carbon and nitrogen in soils and catchments of the Alaskan Arctic has been the subject of many studies (e.g. Giblin et al., 1991; Nadelhoffer et al., 1991; Hobbie et al., 2002; Judd and Kling, 2002), the geochemistry of other elements including macro- and micronutrients released by mineral weathering is less well known. Stutter and Billet (2003) described the stream and soil chemistry of a Swedish arctic region more recently glaciated than the study area of this paper, but with similar sedimentary bedrock (including sandstone and limestone units), and

found the system to be dominated by carbonate dissolution. Kling et al. (1992) investigated the chemistry of lakes and rivers over a wide region of the Alaskan North Slope and interpreted the water chemistry in the region of this study to also be dominated by the products of carbonate dissolution and related to surface age.

Both terrestrial (Shaver and Chapin, 1995) and aquatic (Hobbie et al., 1999) ecosystems in this region are nutrient limited, either by P alone or by N and P. Therefore, enhanced release of mineral nutrients via weathering of newly thawed minerals may have an important ecological impact. Hobbie et al. (1999) measured a twofold increase in P concentrations in a stream passing through glacial deposits disturbed by construction and predicted that weathering of thawed permafrost minerals may increase aquatic P availability, causing bottom-up trophic effects.

Objective. Because of the potential for a unique, permafrost-related geochemical response of arctic systems to climate change, it is important to understand the current mineral weathering processes and geochemical characteristics of these systems. The objective of this study was to describe the elemental chemistry of soils and streams in the central Alaskan North Slope, examine mineral weathering as a function of surface age, and address the geochemical implications of thaw depth increases brought about by climate change. To accomplish these goals, we analyzed stream water and several chemical fractions of soil and bedrock, and used elemental and Sr isotope ratios to identify the mineral sources of weathering products. These results will serve to

further our understanding of weathering in arctic regions, as well as provide baseline information for predicting how warming climate may influence the biogeochemistry of ecosystems.

Study Area

Field research was conducted on the eastern North Slope of arctic Alaska near the foothills of the Brooks Range (Figure 2-1), primarily in the Philip Smith Mountains quadrangle (69°N, 150°W). The entire region is underlain by continuous permafrost (Brown and Krieg, 1983). For the years 1990-2000, the mean active-layer thickness at three sites within the study area (Happy Valley, Imnavait Creek, and Toolik Lake) ranged from 33-60 cm (Brown et al., 2002); the maximum thaw depth we observed during field work was 80 cm. Mean annual air temperatures on this part of the North Slope range from –5.9°C in the Brooks Range to –12.8°C at Prudhoe Bay (Haugen, 1982). The dominant vegetation types include tussock tundra, wet sedge tundra, and riparian willow communities (Giblin et al., 1991). The landscape descends from the steep, rocky foothills of the Brooks Range to gently rolling tundra with poorly developed drainage and many kettle and thermokarst lakes.

North of the foothills, the landscape is developed on till and outwash formed during several glaciations of varying ages, during which glaciers moved northward from the Brooks Range (Hamilton, 1978; Brown and Krieg, 1983; Hamilton, 2003). The oldest and most northerly recognizable glacial deposits resulted from the Gunsight Mountain (GM) glaciation, which is inferred to have

occurred in the late Tertiary based on the similarity of erosional features to Pliocene deposits south of the Brooks Range (Hamilton, 1994). The second oldest glacial deposits resulted from the Anaktuvuk River (AR) glaciation, which is assigned an early Pleistocene age by paleomagnetic analysis of overlying sediments (Hamilton, 1986) and correlations with other Alaskan glacial sequences (Hamilton, 1994). The next two younger glaciations are each broken up into separate units consisting of advances and readvances separated by interglacial periods. The Sagavanirktok River glaciation is dated broadly to the middle Pleistocene (780,000-125,000 years B. P.; Hamilton, 2003) based on paleomagnetic data and correlation to glaciations elsewhere in Alaska (Hamilton 1994), and is separated into two units: Sagavanirktok River 1 (Sag1) and 2 (Sag2). At least five separate phases of the Itkillik glaciation have been identified (Hamilton, 2003), but for the purpose of simplification in this paper we use the three main phases initially described by Hamilton and Porter (1975) and used by Hamilton (1986): Itkillik I (It1), Itkillik II (It2) and the latest Itkillik II re-advance (It3). It1 deposits are beyond the range of radiocarbon dating (>40 ka) but have an inferred age between 50-120 ka; radiocarbon dating suggests ages between approximately 11.5-24 ka for It2 deposits and 11.4 ka-12.8 for It3 deposits (Hamilton, 1986; 2003). These surfaces have loess cover ranging from greater than 15 meters on the oldest surfaces, through thin but still continuous cover on intermediate-aged surfaces, to loess-free moraine crests on the youngest surfaces (Hamilton, 1994; 2003).

The bedrock formations in the Brooks Range foothills, from which the glacial till is derived, consist primarily of conglomerates, sandstones, and limestones, with some shale and phyllite (Menzie et al., 1985; Mull and Adams, 1985). Based on the gentle topography of the youngest (It3) moraines, Hamilton (2003) inferred that they contain abundant fine sediments derived from large nearby lake beds and therefore may be compositionally different than other glacial deposits.

The soils developed on these deglaciated surfaces are classified broadly as Gelisols, and more specifically as Turbels and Orthels, depending on the amount of apparent cryoturbation (Munroe and Bockheim, 2001). In most areas, the mineral soil is overlain by a thick (ten or more centimeters) organic horizon. The soils are characterized by medium texture, poor drainage, and cryogenic features such as warped horizons and ice lenses (Ping et al., 1998).

Methods

Water sampling and analysis. We sampled small first- or second-order streams in watersheds entirely contained within each of the seven glacial surfaces of different ages in the study area, and within each of the major bedrock types in the foothills north of the Brooks Range (Figure 1); we also sampled the major rivers (up to fourth order) in the study area. Precipitation samples were collected in acid-washed polyethylene containers. All water samples were filtered through 0.45 μm polypropylene filters into acid-washed polyethylene

bottles in the field, acidified with ultra-pure hydrochloric acid, and refrigerated at <10°C until analysis.

All water samples were analyzed using a Perkin Elmer Optima 3300 DV Inductively Coupled Plasma Optical Emission Spectrometer (ICP-OES) using five- to eight-point calibration curves for element concentrations (including Ba, Ca, Fe, K, Mg, Na, S, Si, and Sr). Two High-Purity® standards (Trace Metals in Drinking Water and River Sediment-B) and one in-house standard were used for quality control. These standards were analyzed to within ±10% of the known values for Fe and Sr; ±17% for S, and ±5% for all other elements.

Soil sampling and analysis. During late July and August of 2002 and 2003, two to four soil sampling pits on each glacial deposit surface were excavated (Figure 2-1), with the exception of the GM surface, on which a single large trench was excavated and sampled on opposite sides. Sites were randomly selected on flat (slope <2°) moraine crests or shoulders. Vegetation at the pit sites indicated that all of the sites except one were located on moist acidic tundra; one of the lt2 pit sites was located on non-acidic tundra. Each pit was excavated through active-layer soil and at least several cm into frozen ground. Soil profiles and visible horizons were measured and described, and homogenized samples were taken from each visible horizon. We took samples from 3-6 horizons per pit, usually consisting of layers designated "O" (peat), "A" (an oxidized layer with live roots), "B1" (the upper section of a thick gleyed layer), "B2" (the lower section of the same layer; this division was meant to split the thick "B" horizon approximately in half in order to look for differences with depth), "P1"

(the first few cm of thickly laminated frozen soil, which may infrequently be part of the active layer), and "P2" (deeper, thinly laminated sediment in permafrost). Several soil profiles contained evidence of cryoturbation such as irregular horizon boundaries or buried peat inclusions. A deeper (~3m) permafrost sample (labeled Sag1-DP on Figure 2-1 and in tables) was obtained from the Sag1 surface from the site of a thermokarst tundra collapse within a few days of that event.

Soil samples were dried at 35°C and mineral soils were sieved to separate the <2mm size fraction, which was used for further analyses. We consider the >2mm fraction to contribute a negligible amount to overall mineral weathering of the soil due to its low ratio of surface area to volume; the >2mm fraction appeared to consist mostly of chert pebbles and quartzite cobbles and was on average less than 35% by mass of each sample. Percent organic matter was determined for samples from one representative pit on several surfaces by loss on ignition (LOI) via combustion at 450°C for 24 hours, following the method of Heiri et al (2001).

Following the methods of Blum et al. (2002), 0.5 g soil samples were leached and digested sequentially with 5mL of each of the following ultra-pure solutions: (1) 1M NH_4Cl (pH=7) at room temperature for 20 hours to obtain the exchangeable fraction; (2) 1M HNO_3 at room temperature for 20 hours to dissolve easily soluble minerals (which in these soils are mostly carbonates but include minor amounts of phosphate and some sulfides) and to leach remaining labile elements bound to organics; and (3) concentrated HNO_3 at 150°C for 3 hours to partially digest less soluble but still potentially weatherable minerals

such as biotite, plagioclase, potassium feldspar, sulfides, and some oxides and clays. For convenience, we will refer to the solutions obtained via the second and third steps in the sequential digest procedure as the "cold acid digestible" and "hot acid digestible" fractions respectively. While we aim to estimate "easily weatherable" and "less weatherable" fractions of the soil with these sequential digests, these digests are operationally defined and thus do not represent clearly defined reservoirs within the soil. Furthermore, while elemental P and S (possibly occurring as PO_4^{3-} and SO_4^{2-}) released by NH_4Cl are not necessarily "exchangeable," they represent the most labile fraction of those elements, and for convenience they are referred to as part of the exchangeable fraction.

To obtain a total digest of mineral soil samples, about 0.1 g of each sample was fused with 1 g of technical grade $LiBO_2$ in a graphite crucible at 1100°C, then dissolved in approximately 60 mL of trace metal grade 5% HNO_3 and filtered through 25µm pore size cellulose fiber paper. Two procedural blanks ($LiBO_2$ with no sample added) and two USGS Geochemical Reference Standards were also digested.

The soil leachate and digest solutions were analyzed for elemental concentrations by ICP-OES using six- to nine-point calibration curves. Quality control standards included High-Purity® ICP-Stock Solution for Si and CRM Soil Solution A and Trace Metals in Drinking Water for other elements. For the sequential digest solutions, these standards were analyzed within ±7% for Ba, Ca, Fe, K, Na, and Sr; ±12% for Si, and ±14% for P and S in the same concentration ranges as the samples. For the total digests, these standards plus

an in-house standard were analyzed to within ±7% for Ba, P, and Si; and ±12% for Ca, Fe, K, Na, S, Sr in the same concentration ranges as the samples.

Bedrock sampling and analysis. Samples of each major rock unit on the eastern North Slope (Philip Smith Quadrangle) were collected during the summer of 2002. Where possible bedrock samples were collected from outcrops in the same watersheds in which streams were sampled.

Polished thin sections were made of each rock sample and mineral constituents were identified visually using a petrographic microscope or by an energy dispersive spectrometer (EDS) on a Hitachi S3200N scanning electron microscope (SEM). Subsamples of each rock sample were pulverized in a tungsten carbide ring mill and then subjected to the same sequential leach and digest procedure described above. After the hot acid digest, the remaining sample was digested with a mixture of concentrated ultra-pure HF, HNO_3, and HCl until all sample was in solution. The leachate and digest solution was analyzed by ICP-OES as described above.

Sr isotopic analyses. Sr was separated from selected water samples and soil and rock leachate and digest solutions by eluting a subsample through Eichrom Sr-Spec resin in a quartz cation exchange column. Fifty to 100 ng of Sr along with 1 ng of H_3PO_4 were then loaded onto a tungsten filament with Ta_2O_5 powder matrix. $^{87}Sr/^{86}Sr$ was determined by multiple-collector thermal ionization mass spectrometry (TIMS) on a Finnigan MAT 262. To correct for instrumental mass bias, $^{86}Sr/^{88}Sr$ was normalized to 0.1194. Between 50-200 replicate $^{87}Sr/^{86}Sr$ ratios were measured for each sample. Internal precision ($\pm 2\sigma$)

calculated from these replicates was generally less than ±0.000030; exceptions are noted in tables and graphs. The Sr standard NBS-987 was analyzed after every 12 samples with a mean value of 0.710231±0.000016 (2σ) during the period of sample analyses.

Results

Bedrock composition and geochemistry. Based on the location and extent of rock unit outcrops in the eastern Brooks Range foothills and on cobbles found in soil pits by us and by Hamilton (2003), we identified six units (as mapped by Mull and Adams (1985)) likely to comprise the bulk of the glacial till in the study area: the Devonian Beaucoup phyllite (Dbs), the Devonian Ear Peak sandstone member of the Kanayut conglomerate and sandstone (Dke), the Permian-Mississippian Lisburne limestone (PMl), the Permian Echooka shale (Pe), the Cretaceous Fortress Mountain conglomerate and sandstone (Kf), and the Cretaceous Nanushuk sandstone (Kn). Because the Kn crops out north of the Sagavanirktok River glacial deposits, it is likely included only in the older and more northerly Gunsight and Anaktuvuk glacial deposits.

Visual and SEM thin section analyses suggest that all three sandstones (Dke, Kf, Kn) are composed primarily of quartz and chert and contain minor amounts of biotite/vermiculite, muscovite, and oxide and sulfide minerals; the Kf and Kn also contain minor plagioclase and glauconite. The limestone unit (PMl) appeared chert-rich and argillaceous, which is consistent with the description of this unit by Moore et al. (1994).

The composition of sequential and bulk digests of these six units is reported in Table 2-1. As expected, the limestone had the lowest $^{87}Sr/^{86}Sr$ values and highest Ca/Sr of the six units; the phyllite (Dbs) and the Devonian sandstone (Dke) had the highest exchangeable and cold acid digestible fraction $^{87}Sr/^{86}Sr$ values. The elemental ratios Ca/Na and Ca/Sr are often used as indicators of calcium carbonate contribution because calcium carbonate has high Ca but low Na and Sr concentrations, whereas the reverse is true for many common silicate minerals. Strontium isotope ratios can be used similarly because most carbonates have low $^{87}Sr/^{86}Sr$ while many silicate minerals have higher $^{87}Sr/^{86}Sr$ values (e. g. Palmer and Edmond, 1992). Because the carbonate and silicate rocks in this area follow these general patterns, we use the elemental concentration ratios Ca/Na and Ca/Sr and the isotope ratio $^{87}Sr/^{86}Sr$ as indicators of the calcium carbonate contribution to soil fractions and stream water solutes.

Soil geochemistry. Geochemical characteristics of the soil exchangeable fraction, cold acid digestible fraction, hot acid digestible fraction and total soil digests are reported in Tables 2-2 through 2-5. The lt2 surface has the highest exchangeable Ca concentrations, Ca/Na, and Ca/Sr (Table 2-2). In the mineral soil of most profiles, there is a trend of increasing Ca concentrations and Ca/Sr and decreasing $^{87}Sr/^{86}Sr$ with depth (Table 2-2). Statistical tests (ANOVA or Welch ANOVA where the variances are unequal) were performed on concentration data for select elements that were log-transformed to induce normal distribution. Although data sets for individual surfaces are not large enough to test reliably, statistical analyses of data from all surfaces combined

show some significant ($p<0.05$) differences between permafrost and active-layer mineral soil chemistry: exchangeable fraction Ca, K, and P concentrations are significantly greater in the permafrost (all "P" horizons) than in active-layer mineral soil (all "A" and "B" horizons). Despite these overall statistically significant differences, the magnitudes of within-surface differences between permafrost and active-layer mineral soil exchangeable fraction elemental concentrations vary substantially among surfaces (Table 2-2).

The cold acid digestible fractions of the It2, AR, and GM soil profiles have greater Ca concentrations and Ca/Sr and lower $^{87}Sr/^{86}Sr$ than those of the other surfaces (Table 2-3). The cold acid digestible fraction of the mineral soil shows a general pattern across all surfaces of increasing Ca concentrations and Ca/Sr and decreasing $^{87}Sr/^{86}Sr$ with depth, and on some surfaces P concentrations also increase with depth. Both Ca and P cold acid digestible fraction concentrations are significantly ($p\leq0.05$) greater in the permafrost than in the active-layer mineral soil when data from all surfaces are analyzed, and the differences in cold acid digestible fraction K concentrations are nearly significant ($p=0.06$). These differences between active-layer mineral soil and permafrost vary by surface: all surfaces have higher permafrost concentrations of Ca; all surfaces except the GM and It2 have higher permafrost concentrations of K; and cold acid digestible fraction P concentrations are higher in the permafrost on four of the surfaces.

The hot acid digestible fractions of mineral soil horizons on all surfaces contain some Ca, but have lower Ca/Sr and higher $^{87}Sr/^{86}Sr$ than either the exchangeable or cold acid digestible fractions (Table 2-4). This suggests that the

majority of carbonate was dissolved before this step in the sequential digest procedure and that the Ca in this fraction is largely the result of silicate mineral dissolution.

The total digests of the mineral soil (Table 2-5) show that Ca generally increases with depth on each surface. The lt2, AR, and GM surfaces have the highest Ca concentrations. On average, SiO_2 comprises approximately 80% of the total mineral soil mass. For a few samples, elemental concentrations from the acid digests sum to slightly more than the total digest concentration. These values are within analytical errors propagated through the sum in all except for the Ca values for the Sag1 deep permafrost sample. This discrepancy is likely the result of sample heterogeneity.

Stream geochemistry. In streams on glacial deposit surfaces, dissolved Ca concentrations ranged from 12 µmol/L on the Sag1 surface to 594 µmol/L on the lt2 surface. Streams draining only limestone bedrock had Ca concentrations up to 1606 µmol/L (Table 2-6). Dissolved P concentrations were generally less than 1 µmol/L, but several streams on the lt2 surface had concentrations greater than 10 µmol/L. Dissolved Si concentrations were less than 1µmol/L in two streams that were lake outlets, but other Si concentrations ranged from 10-87 µmol/L. $^{87}Sr/^{86}Sr$ ranged from 0.71023-0.71881 in streams draining glacial deposit surfaces and from 0.70847-0.71989 in streams draining bedrock surfaces.

Discussion

Analysis of soil parent material variability. Before we can evaluate whether geochemical patterns are dependent on varying degrees of weathering on geomorphic surfaces of different ages, we must ascertain the compositional variability of the glacial till soil parent among the surfaces. Figure 2-2 shows a comparison of the $^{87}Sr/^{86}Sr$ of the hot acid digestible fractions of the soil profiles on each surface. Because easily weathered material has already been removed from this fraction by previous steps in the sequential digest procedure, we make the assumption that the chemistry of this fraction reflects minerals that would only be affected by intense weathering, making them unlikely to have been significantly affected yet by weathering in this arctic region. Therefore, the $^{87}Sr/^{86}Sr$ and elemental ratios of this fraction should be very similar for soils with similar parent material, regardless of their age. We used $^{87}Sr/^{86}Sr$ rather than elemental ratios as an indicator of differences in parent material because different parent materials of the same type (e. g. different sandstone units) may have very similar elemental ratios due to similar mineralogical compositions, but because of their unique protoliths, they are more likely to have detectable differences in $^{87}Sr/^{86}Sr$. We examined the $^{87}Sr/^{86}Sr$ of the hot acid digestible fraction with respect to depth, to account for any minor effects of weathering or addition of new material (e.g. eolian loess) to the soil profile.

Overall the composition of the parent material has low variability but showed some grouping among the different surfaces. The GM and AR profiles have significantly lower mean $^{87}Sr/^{86}Sr$ than the other surfaces (Figure 2-2;

$p<0.05$). This suggests that the AR and GM soils are derived from different parent material than the other surfaces. Differences in parent material may be explained by the incorporation of various rock units in different proportions based on different surface expressions of these units at the time of the glacial advances. Additionally, rock units (the Kn and three minor units not analyzed here) that outcrop north of the Sag1 surface may have been incorporated into the GM and AR parent till. It is also possible that long-term eolian loess deposition has contributed to these differences in soil composition. The $^{87}Sr/^{86}Sr$ of the hot acid digestible fraction of the It1, It2, It 3, Sag1, and Sag2 soil profiles is similar, suggesting that these surfaces have similar parent material, although the $^{87}Sr/^{86}Sr$ of the upper part of the It3 profile is slightly higher than that of the other surfaces. This is consistent with the suggestion by Hamilton (2003) that the It3 surface was derived from slightly different parent material than the It1 and It2 surfaces, based on surficial geomorphology. For the purposes of further analyses with respect to surface age, we will consider only the It1, It2, Sag1, and Sag2 to be derived from similar parent material.

Besides these overall differences among the profiles from each surface, each individual profile shows a pattern of increasing hot acid digestible fraction $^{87}Sr/^{86}Sr$ with increasing depth within the active layer (down to approximately 50 cm; Figure 2-2). The most likely explanation for this is eolian deposition of a weathering-resistant mineral, with lower $^{87}Sr/^{86}Sr$ than the soil parent material, which is mixed down through the active layer by cryoturbation or water movement. Such dust could be derived from the Dke sandstone or resistant

minerals in the PMI (Table 2-1), or from sediments outside the study region. This dust may also have a carbonate component that contributes to the exchangeable and cold acid digestible fractions. However, the effects of this input as shown by increasing $^{87}Sr/^{86}Sr$ with depth seem to be of similar magnitude in the hot acid digestible fraction, so we can assume that age comparisons between these surfaces based on the other fractions are not substantially affected. An alternate explanation for the pattern of increasing $^{87}Sr/^{86}Sr$ with depth in the active layer could be removal by weathering of a resistant mineral with relatively high $^{87}Sr/^{86}Sr$ (such as biotite) in the upper part of the active layer, but this seems unlikely due to the low weathering intensity of this environment as evidenced by the relatively slow carbonate weathering described in the next section.

Carbonate weathering and its relationship to surface age. Calcite depletion via weathering in the active layer is indicated on every surface, by decreasing $^{87}Sr/^{86}Sr$ and increasing Ca/Na and Ca/Sr with depth (Figure 2-3), and by greater Ca concentrations in permafrost than in active layer mineral soil as described in the results section. These geochemical trends suggest increasing carbonate mineral concentration in the soil with depth, as frequency of thaw and hence weathering intensity decreases. These results may explain the findings of Everett et al. (1989), who monitored the seasonal geochemistry of the Imnavait stream on the Sag1 surface and found that streamwater Ca concentrations were greatest in the late summer, corresponding to deep seasonal thaw.

When considering only the surfaces with similar parent material (It1, It2, Sag1 and Sag2), some patterns related to surface age become apparent. The

mean $^{87}Sr/^{86}Sr$ values of the active-layer cold acid digestible fraction are lowest on the youngest surface (It2) and highest on the oldest (Sag1), with overlapping values for the two other surfaces (Figure 2-3c). The decrease in mean cold acid digestible fraction $^{87}Sr/^{86}Sr$ between the permafrost and the "A" horizon is least on the youngest surface. The youngest surface also has the highest exchangeable, acid digestible, and total Ca concentrations and Ca/Sr (Tables 2, 3, and 5). These data suggest that weathering has progressively depleted the calcite in the active layer over time on these surfaces. Furthermore, mean cold acid digestible fraction $^{87}Sr/^{86}Sr$ values for shallow permafrost ("P" samples from within soil pits, excluding the Sag1 deep permafrost sample) increase with surface age among the four surfaces derived from similar parent material (Figure 2-3c, Table 2-3). This trend suggests that the currently frozen soil has been episodically thawed during past intervals of warmer climate and has undergone some weathering or was mixed with weathered material via cryoturbation during these intervals.

Both stream and soil geochemistry suggest that differences in carbonate weathering drive not only depth-related geochemical differences within individual soil profiles, but also age-related differences in whole watershed geochemistry. Simple chemical mixing lines drawn between end-members formed by the cold acid digestible fractions of the PMI limestone (high Ca/Sr, low $^{87}Sr/^{86}Sr$), Dke sandstone (low Ca/Sr, high $^{87}Sr/^{86}Sr$), and Kf sandstone (low Ca/Sr, low $^{87}Sr/^{86}Sr$) represent the expected composition of waters containing easily weathered solutes derived from these units based on varying proportional contributions from

each unit by mass (Figure 2-4). These mixing lines define a range containing 7 out of 15 streams draining watersheds developed on different glacial till surfaces. Streams draining PMl-based watersheds have a lower mean Ca/Sr and very slightly higher mean $^{87}Sr/^{86}Sr$ than the cold acid digestible fraction of PMl samples (Figure 2-4, hatched line end-members). This may be explained by a greater influence of precipitation on these watersheds, or a fraction of the PMl which is more soluble under natural conditions and differs chemically from the fraction digestible with stronger acid in the laboratory, or both. The slightly higher Ca/Sr and $^{87}Sr/^{86}Sr$ of streams draining Dke sandstone and undifferentiated Kanayut conglomerate (MDk) bedrock may be explained by contributions from other members of the MDk, as well as the slightly higher $^{87}Sr/^{86}Sr$ of the exchangeable fraction of the Dke.

Simple chemical mixing lines drawn between the mean Ca/Sr and $^{87}Sr/^{86}Sr$ of precipitation samples, streams draining PMl limestone bedrock, and streams draining Dke/MDk bedrock (Figure 2-4, hatched lines) represent the expected composition of waters containing solutes derived from a combination of inputs based on the solutes measured in unit-specific streams and precipitation. All but one of the 15 glacial till surface streams sampled are contained within these mixing lines (Figure 2-4). The reasons that these end-members predict water composition more accurately than the range defined by the cold acid digestible fraction of rock units are likely that (1) the effects of precipitation and other members of the MDk are incorporated and (2) they are based on

weathering in natural settings, rather than on an operationally defined laboratory cold acid digest.

Within the ranges defined by both sets of mixing lines, most streams on younger (It3, It2, and It1) surfaces have $^{87}Sr/^{86}Sr$ ratios similar to those of streams draining limestone bedrock and the cold acid digestible fraction of limestone, but lake outlet streams on the It2 surface have higher $^{87}Sr/^{86}Sr$. The Ca/Sr ratios of these streams vary widely, perhaps reflecting varying effects of precipitation in different watersheds or at the different times when the streams were sampled. The effects of precipitation on the $^{87}Sr/^{86}Sr$ of these streams would be nearly undetectable because the difference between the $^{87}Sr/^{86}Sr$ of precipitation and streams draining PMI watersheds is less than 0.0002. Streams on older (Sag2 and Sag1) surfaces have Ca/Sr and $^{87}Sr/^{86}Sr$ ratios similar to those of streams draining Dke/MDk bedrock and the cold acid digestible fraction of Dke sandstone, suggesting much less carbonate influence on these surfaces than on younger surfaces. Streams on very old (AR and GM) surfaces have Ca/Sr and $^{87}Sr/^{86}Sr$ which fall very close to the Kf-PMI mixing line, suggesting that the weathering products dissolved in these streams are primarily derived from these two end-members, or perhaps an end-member with similar chemistry such as the Kn (Table 2-1). The chemistry of the GM and AR streams suggests little input of the Dke/Mdk end-member, consistent with the differences in parent material between these and younger surfaces discussed above.

The effects of weathering on shallow mineral soils of different ages was examined by plotting cold acid digestible Ca/Sr vs. $^{87}Sr/^{86}Sr$ for soil "A" horizon

samples from all glacial deposit surfaces along with the mixing lines from the cold acid digestible fraction rock unit end-members described above (Figure 2-5). Ca/Sr and $^{87}Sr/^{86}Sr$ for the GM, AR, and It2 surfaces fall outside and below the range defined by the mixing lines, suggesting that their chemistry has been influenced by input from precipitation, or low-$^{87}Sr/^{86}Sr$ loess deposition, or both. Data from the It3, It1, and Sag2 surfaces overlap, consistent with the overlapping $^{87}Sr/^{86}Sr$ values for It1 and Sag2 soils in Figure 2-3, but despite the clear differences in the stream water Ca/Sr vs. $^{87}Sr/^{86}Sr$ for these surfaces (Figure 2-4). This may be because, as discussed above, the cold acid digestible fraction represents an estimate of potentially "easily weatherable" minerals, but does not necessarily reflect what is actually being weathered. Therefore the It3, It1, and Sag2 surfaces could have similar reservoirs of "easily weatherable" minerals as estimated by the digest, yet release into streams very different weathering products that represent the most soluble part of the "easily weatherable" fraction. Cryoturbation may also play a role in keeping the cold acid digestible fraction similar in soils close in age (like the It1 and Sag2) via the upwards mixing of less-weathered minerals from deeper, less frequently thawed layers.

Despite the overlapping values of data from the It3, It1, and Sag2 surfaces, samples from the youngest (It2) of the four surfaces with similar parent material generally have the highest Ca/Sr and lowest $^{87}Sr/^{86}Sr$, while samples from the oldest (Sag1) of these four surfaces have the lowest Ca/Sr and highest $^{87}Sr/^{86}Sr$, plotting near the Dke digest end-member. These data suggest that carbonate weathering causes detectable geochemical differences to develop in

the cold acid digestible fraction of shallow mineral soil over hundreds of thousands of years. Additional research will be necessary to explore the relationship between the timescale at which the effects of weathering are apparent and the rate of cryoturbation.

These results show that carbonate content decreases in soils and carbonate weathering products decrease in streams with increasing surface age, but the carbonate weathering regime is still generally dominant even on older surfaces. This interpretation is consistent with previous studies of aquatic and soil chemistry in this region (Kling et al., 1992) and similar arctic regions (Stutter and Billet, 2003). The decrease in carbonate weathering over time (driven by a depletion of carbonate minerals via weathering) that we interpret from these data is similar to changes that take place in a much shorter time (thousands rather than hundreds of thousands of years) in tropical and temperate climates (e.g. Lichter, 1998). Despite the extended timeframe, this change in the carbonate content of soils with time supports the suggestion of Munroe and Bockheim (2001) that the traditional soil chronosequence model relating age to soil properties is applicable even in cryoturbated soils.

Silicate weathering. The presence of dissolved Si in low but detectable levels in streams on almost every geomorphic surface in our study area suggests that some silicate weathering is occurring; the range of dissolved streamwater Si concentrations in this study is similar to those reported for streams in similar arctic and subarctic systems with sedimentary or mixed bedrock influences (Huh et al., 1998; Millot et al., 2003; Stutter and Billet, 2003; Humborg et al., 2004).

The inference that silicate minerals are weathering is consistent with the observed lower concentrations of K in the cold acid digestible fraction of active-layer mineral soil compared to permafrost on six out of the seven surfaces examined in this study. At least some of this K is likely derived from the most soluble silicate minerals contained in parent material sandstones, which have between 2-10 times the amount of cold acid digestible fraction K than the limestone unit (Table 2-1).

Nutrient release via mineral weathering. The ecological influence of weathering in this region is reflected in the exchangeable fraction of soils. Exchangeable $^{87}Sr/^{86}Sr$ and cold acid digestible fraction $^{87}Sr/^{86}Sr$ for each soil horizon are well correlated (R^2=0.74) across all surfaces in this study. This suggests that locally-derived mineral weathering products are the primary source of exchangeable Sr, and therefore probably also the source of ecologically important elements like Ca, P, and K, to the watersheds on these surfaces.

We did not perform soil extractions specifically designed to determine the reservoirs of P in these soils. However, the ratio of Ca to P in the cold acid digestible fraction of active-layer mineral soil samples on all surfaces is consistently greater than or equal to 1.67 (Figure 2-6), which is the Ca/P of apatite ($Ca_5(PO_4)_3(F,Cl,OH)$), the major P-bearing mineral in rocks. Ca/P is lowest and nearest to 1.67 in Sag1 soils, which have the least carbonate content as determined by Ca/Sr and $^{87}Sr/^{86}Sr$. Only 3 out of 52 active-layer mineral soil samples with measurable cold acid digestible fraction P have a Ca/P ratio less than 1.67 (lower by at most only 26%), suggesting that apatite is the primary

source of P in this fraction. High Fe concentrations in the hot acid digestible fraction suggest the possibility that some of the P in this fraction is bound to Fe hydroxide species. However, P and Fe concentrations in this fraction are poorly correlated, so it is likely that P in this fraction is bound in other (e.g. organic) forms as well.

Geochemical implications of increasing thaw depth. Our results suggest several possible geochemical consequences of increased active-layer thickness brought about by warming climate. The most conspicuous is increasing carbonate and Ca supply to soil and stream water with increasing active-layer thickness. This change would be ubiquitous across the study area, as all profiles exhibit geochemical indicators of increasing calcite content with depth, and analysis of data from all surfaces shows that cold acid digestible fraction Ca concentrations are significantly higher in the permafrost than in the active layer. The increased carbonate in soils brought about by calcite dissolution may lead to increased pH of acidic tundra, and potentially related changes in vegetation (Bockheim et al., 1998), but these changes would happen concurrently with and could be mitigated by changes in organic matter decomposition and organic acid production that may accompany warmer conditions and deeper thaw.

In addition to increasing carbonate dissolution and general base cation release, our measurements suggest that increased active-layer thickness may increase mineral weathering release of two nutrients, P and K. On all surfaces there were significantly greater concentrations of exchangeable K in the

permafrost than in the active-layer mineral soil. Both exchangeable and cold acid digestible fraction P concentrations were significantly greater in the permafrost than in the active-layer mineral soil overall. The mean increase in P between these layers was 28% for the exchangeable fraction and 61% for the cold acid digestible fraction. The deep permafrost sample from the Sag1 surface was enriched in cold acid digestible fraction P compared to active-layer soil (including "O" horizons) or shallow permafrost on any surface. Despite these mean differences in K and P between permafrost and active-layer mineral soil, the surface-specific differences between active-layer mineral soil and permafrost concentrations of these elements are variable. For example, the It2 surface has active-layer mineral soil concentrations of cold acid digestible fraction P that are actually higher than shallow permafrost concentrations, whereas the It3 and Sag1 surfaces have shallow permafrost concentrations of cold acid digestible fraction P that are more than double the concentrations found in active-layer mineral soil.

These data support the predictions of Hobbie et al. (1999) that thawing of permafrost could increase P availability to ecosystems, and provide more information regarding possible mechanisms of P release. Because the permafrost contains small but significantly greater concentrations of exchangeable P than the active layer, increases in available P may occur concurrently with permafrost thawing. Subsequent to initial thaw depth increases, a larger increase in newly available P may occur gradually as previously frozen minerals weather. Based on the differences in exchangeable and cold acid

digestible P concentration profiles between surfaces, it is reasonable to expect that different geographic areas or watersheds may undergo different degrees of increased P availability. Some areas, such as those with already high cold acid digestible fraction P in the active layer (It2 and AR) or those where past weathering of currently frozen soil has depleted P in the first few centimeters of permafrost (Sag2), may change little in P availability until large increases (tens of centimeters) in thaw depth occur. Thaw-depth driven increases in K availability are also likely to be spatially variable, based on differences in the exchangeable and cold acid digestible fraction K depth profiles among surfaces.

Sulfur concentrations in soil show no statistically significant increase from the active-layer mineral soil to the permafrost across all surfaces for any fraction, but several individual surfaces have higher S concentrations in the permafrost than in the active-layer mineral soil in the exchangeable (It3, It2, GM), cold acid digestible (It3, It1), or hot acid digestible (It3, It2, It1) fractions (Tables 2, 3, and 4). The Sag1 deep permafrost sample has exchangeable and cold acid digestible fraction S concentrations 100% and 25% greater, respectively, than any active-layer sample from any surface, including O horizon samples. Our analyses do not distinguish whether the S in these soils is inorganically or organically bound, but both forms are likely because the soils are organic rich and the sandstone units of the parent material contain accessory sulfide minerals. Sulfur may be an important control on Hg methylation via sulfate-reducing bacteria (Compeau and Bartha, 1985; Gilmour et al., 1992); methylation of Hg in high arctic wetlands is an important step in Hg bioaccumulation in arctic

food chains, although soils there appear to have low levels of sulfate-reducing bacteria (Loseto et al., 2004). Further study of the forms and concentrations of S in the permafrost may shed light on how increased thaw depth will influence SO_4 concentrations in arctic surface waters, potentially affecting Hg methylation pathways.

Use of stream geochemistry as a monitor of thaw depth. The geochemical profiles of soils on the central North Slope described in this study may provide a useful tool for qualitatively detecting watershed-scale changes in thaw depth. We hypothesize that in watersheds which have sufficient changes in soil geochemistry with depth, such as the $^{87}Sr/^{86}Sr$ or Ca/Sr trends described in this study (Figure 2-3), stream geochemistry may reflect increases in thaw depth. Specifically, we predict that as thaw depth increases in this study area, more carbonate weathering products will be dissolved in late summer streamwater, and will be detectable as increases in streamwater elemental ratios such as Ca/Sr and decreases in streamwater $^{87}Sr/^{86}Sr$ over periods of many years. On some surfaces with very pronounced geochemical differences between active-layer mineral soil and permafrost, such as the It1 surface, regular analysis of stream geochemistry may signal watershed-scale permafrost degradation before it is detectable by traditional physical (e.g., steel probe) methods of measuring thaw depth. Even in permafrost regions with non-carbonate-dominated soil parent material, less intensely weathered soil at depth may provide a geochemical signature as soils thaw more deeply.

Conclusion

Analysis of stream and soil geochemistry on arctic Alaskan glacial till deposits of varying ages indicates that carbonate weathering is the major controlling factor of geochemical trends related to soil depth and surface age. Carbonate minerals have been depleted by weathering in the active layer on every geomorphic surface, and on the four surfaces with similar parent material, stream and soil geochemistry suggest progressive carbonate depletion with time over hundreds of thousands of years. Dissolved Si concentrations in streams are similar to those in other arctic watersheds, suggesting that silicate weathering is also occurring on these surfaces, but at a much slower rate than carbonate weathering.

Compared to active-layer mineral soils, permafrost has overall greater exchangeable K concentrations, exchangeable and acid digestible P and Ca concentrations, and carbonate content. Some glacial deposit surfaces also have higher S concentrations in permafrost than in active-layer soils. The magnitude of the geochemical differences between permafrost and active-layer soils varies among different surfaces. The results of this study suggest that increasing thaw depth brought about by climate change will lead to overall (albeit spatially variable) increases in carbonate, Ca, P, K, and S supply to soils and streams. This increase may occur concurrently with increased maximum thaw as the exchangeable fraction becomes available, and then progressively as soluble minerals begin to weather. The nature of these geochemical changes will depend on the rate of thaw; changes are likely to be gradual overall but could be

locally abrupt in areas of rapid thermokarst formation. Based on geochemical differences between active-layer soil and permafrost, stream geochemistry may be a useful qualitative monitor of watershed-scale changes in thaw depth.

Acknowledgements

At the time this dissertation is submitted, this chapter was in press as a paper of the same title in *Arctic, Antarctic, and Alpine Research*, with Joel D. Blum and George W. Kling as co-authors; they contributed much to the writing and editing of this chapter. We thank D. Zak, H. Adams, and K. Judd for help in the field. Funds for field research were provided by grants from the Geological Society of America and the University of Michigan Geological Sciences and Ecology and Evolutionary Biology departments. Research was also supported by NSF DEB-0423385, DEB 97-26837, ATM-0439620, and ARC-0435893. We appreciate thoughtful reviews by Michael Gooseff, Suzanne Anderson, and two anonymous reviewers.

Table 2-1: Chemistry of local rock units likely incorporated into glacial till deposits.

Fm. name	rock type	fraction	Ba µmol/g	Ca µmol/g	Fe µmol/g	K µmol/g	Mg µmol/g	Na µmol/g	P µmol/g	S µmol/g	Si µmol/g	Sr µmol/g	Ca/Na (molar)	Ca/Sr (molar)	$^{87}Sr/^{86}Sr$
Dbs	phyllite/slate	exch.	0.051	25.3	1.22	6.92	13.6	2.64	<0.09	1.77	0.83	0.110	9.6	230	0.727052
Dke	ss/cong.	exch.	0.031	2.94	0.63	9.68	4.12	1.59	<0.09	0.15	0.30	0.020	1.8	147	0.723253
PMI	limestone	exch.	0.009	132	0.28	1.19	2.63	0.40	0.23	<0.08	0.36	0.092	326	1430	0.708986
Pe	shale	exch.	1.35	30.9	1.28	12.7	10.9	0.53	<0.09	0.42	4.79	0.097	58.7	319	0.715667
Kf	sandstone	exch.	2.57	11.9	0.14	20.4	19.4	4.50	<0.09	0.40	0.64	0.052	2.6	227	0.717860
Kn	sandstone	exch.	0.277	35.1	0.47	6.46	12.3	4.35	<0.09	4.13	<0.06	0.066	8.1	533	0.713092
Dbs	phyllite/slate	cold dig.	0.016	660	348	4.17	314	0.62	20.4	54.6	60.4	0.831	1060	793	0.725383
Dke	ss/cong.	cold dig.	0.085	12.3	67.5	6.12	6.73	0.47	2.88	<0.08	39.2	0.029	26.3	425	0.719324
PMI	limestone	cold dig.	0.044	5970	1.02	1.01	35.9	0.09	17.1	<0.08	6.66	1.69	64000	3530	0.708058
Pe	shale	cold dig.	2.97	55.4	80.6	8.29	71.3	<0.073	2.01	1.74	44.6	0.103	>758	540	0.714122
Kf	sandstone	cold dig.	2.49	45.7	141	12.5	97.5	3.12	21.2	2.71	97.3	0.096	14.7	477	0.712404
Kn	sandstone	cold dig.	0.415	85.1	127	2.69	62.4	<0.073	15.8	23.7	84.5	0.122	>1160	695	0.713419
Dbs	phyllite/slate	hot dig.	<0.001	15.1	518	13.2	252	<0.073	<0.09	19.2	350	0.060	>207	251	0.731134
Dke	ss/cong.	hot dig.	<0.001	<0.04	229	20.1	8.04	<0.073	2.30	0.15	150	0.060	-	<0.59	0.723511
PMI	limestone	hot dig.	0.019	534	2.38	1.19	2.17	<0.073	1.37	0.18	14.0	0.099	>7310	5380	0.713099
Pe	shale	hot dig.	0.097	<0.04	365	51.5	196	<0.073	<0.09	1.29	184	0.022	-	<1.60	0.753962
Kf	sandstone	hot dig.	1.52	<0.04	189	57.1	127	11.1	3.73	2.50	281	0.031	<0.003	<1.11	0.735151
Kn	sandstone	hot dig.	0.610	5.67	334	41.9	210	1.27	0.37	6.44	495	0.057	4.5	100	0.727727
Dbs	phyllite/slate	res. dig.	2.66	<0.04	91.3	452	1.32	290	0.28	1.48	1090	0.263	>0.0001	<0.13	0.740233
Dke	ss/cong.	res. dig.	<0.001	<0.04	109	27.8	6.26	<0.073	0.95	<0.08	1560	0.208	-	<0.17	0.714283
PMI	limestone	res. dig.	0.035	1.23	0.17	0.50	<0.0001	<0.073	<0.09	0.47	547	0.007	>16.4	168	0.708846
Pe	shale	res. dig.	1.22	<0.04	259	583	41.2	91.3	0.22	1.25	780	0.412	<0.0003	<0.085	0.741406
Kf	sandstone	res. dig.	2.30	<0.04	26.9	50.7	29.2	95.1	0.29	1.82	939	0.162	<0.0004	<0.22	0.715210
Kn	sandstone	res. dig.	4.31	5.83	91.9	319	44.2	273	1.65	1.00	926	0.638	0.02	9.1	0.723082

PMI elemental data and cold digestible $^{87}Sr/^{86}Sr$ represent a mean of data from 5 samples of the PMI from different locations and members; other PMI $^{87}Sr/^{86}Sr$ data and data for all other units are from one representative sample. Errors for elemental data and $^{87}Sr/^{86}Sr$ reported in text. Exch.=exchangeable fraction; cold dig.=cold acid digestible fraction; hot dig.=hot acid digestible fraction; res. dig.=residual (HF) digest fraction.

Table 2-2: Mean exchangeable soil fraction (per gram dry soil)

surface	horizon	depth cm	Ba µmol/g	Ca µmol/g	Fe µmol/g	K µmol/g	Na µmol/g	P µmol/g	S µmol/g	Si µmol/g	Sr µmol/g	Ca/Na (molar)	Ca/Sr (molar)	$^{87}Sr/^{86}Sr$**
It3	O	0-7	0.163	92.0	3.31	7.12	0.22	0.58	0.91	2.49	0.087	420	1062	0.713660
(n=4)	A	7-19	0.296	7.29	0.80	1.42	0.10	0.02	0.07	1.05	0.011	70.4	687	0.720245*
	B1	19-39	0.374	6.55	0.98	1.49	0.12	0.03	0.14	0.60	0.011	55.8	577	0.720483
	B2	39-60	0.518	7.27	0.87	2.61	0.11	0.02	0.19	0.41	0.013	63.6	543	0.719548
	P	62-71	0.779	13.1	3.64	4.62	0.16	0.10	0.47	1.87	0.027	84.1	490	0.716431
It2	O	0-16	0.448	174	1.63	1.12	0.34	0.43	2.88	0.80	0.109	509	1596	0.709544
(n=3)	A	18-29	0.700	52.7	2.31	0.81	0.11	0.12	0.11	1.75	0.041	489	1282	0.710457
	B1	29-46	0.753	57.9	1.99	1.65	0.15	0.08	0.48	1.92	0.040	395	1450	0.709485
	B2	46-62	0.428	83.3	3.95	2.14	0.20	0.15	2.82	3.05	0.060	425	1397	0.709496*
	P	66-73	0.302	88.5	1.85	2.47	0.55	0.10	4.74	1.12	0.071	162	1244	0.709585
It1	O***	0-7	0.384	20.5	2.69	7.10	0.20	0.18	1.41	0.44	0.033	105	627	0.721412*
(n=3)	A	8-23	0.296	4.71	1.03	0.64	0.06	0.02	0.12	0.31	0.007	78.1	657	0.718664
	B1	23-40	0.373	5.48	0.60	0.69	0.06	0.04	0.11	0.22	0.009	93.2	642	0.718510*
	B2	35-49	0.552	6.80	1.50	0.75	0.10	0.05	0.07	0.82	0.010	65.5	701	0.717530
	P1	49-60	0.501	7.38	2.98	0.96	0.10	0.07	0.10	1.60	0.009	75.5	797	0.715944
	P2	62-69	0.489	34.7	0.42	1.76	0.10	0.04	0.14	0.28	0.037	359	951	0.711278
Sag2	O	0-8	0.242	32.0	2.72	6.55	0.34	0.68	1.49	0.91	0.048	93.7	670	0.716872
(n=3)	A	8-25	0.409	4.77	0.58	0.85	0.10	0.05	0.15	0.35	0.009	47.9	541	0.720050
	B1	25-42	0.861	14.2	1.93	1.43	0.23	0.06	0.09	1.52	0.023	61.8	612	0.720851*
	B2	38-55	0.365	3.05	1.52	0.66	0.15	0.04	0.11	1.33	0.006	19.9	504	0.717221
	P1	55-69	0.495	5.39	0.95	1.24	0.15	0.02	0.08	0.49	0.011	35.2	486	0.715970
	P2	71-75	0.861	21.5	1.41	2.43	0.20	0.06	0.14	0.78	0.030	105	709	0.716069*
Sag1	O	0-13	0.543	30.6	3.13	3.56	0.29	0.21	1.18	0.65	0.044	106	696	0.717314
(n=2)	A	13-22	0.611	12.3	1.76	1.22	0.14	0.08	0.34	1.20	0.018	88.0	668	0.717041
	B1	22-40	0.580	5.89	0.45	0.82	0.15	0.04	0.10	0.37	0.009	39.0	635	0.719167
	B2	35-50	0.727	7.17	0.85	1.29	0.16	0.03	0.15	0.54	0.011	44.3	630	0.717241*
	P	50-58	0.680	7.24	2.85	1.62	0.17	0.07	0.20	1.84	0.011	41.5	656	0.716745*
Sag1-DP	P (deep)	200-300	0.340	79.4	0.74	1.74	<0.04	0.10	5.88	1.85	0.102	<1980	780	0.713109
AR	O	0-11	0.116	68.6	0.78	4.56	0.26	0.87	1.20	0.48	0.070	269	980	0.708721
(n=3)	A	11-27	0.458	67.1	3.29	1.34	0.21	0.19	0.35	2.10	0.076	322	880	0.708773
	B1	27-50	0.549	73.7	1.38	1.38	0.23	0.09	0.06	1.94	0.080	318	925	0.708416
	B2	45-75	0.616	78.2	1.89	1.50	0.21	0.12	0. 0	1.61	0.084	367	931	0.708313*
	P1	70-80	0.691	75.7	1.29	1.56	0.27	0.07	0.08	0.87	0.075	282	1010	0.708253
	P2	85-93	0.688	68.6	4.42	1.55	0.19	0.15	0.01	2.76	0.073	356	942	0.708296
GM	Oe	0-13	0.185	38.5	1.87	5.93	0.31	0.73	0.86	0.77	0.053	125	731	0.710621*
(n=2)	B1	13-35	0.755	28.5	1.95	1.10	0.39	0.02	0.24	0.61	0.042	73.1	673	0.711741*
	B2	38-44	0.828	39.0	5.19	1.17	0.42	0.08	0.20	3.16	0.057	92.2	690	0.710258
	IIOa	44-55	0.431	105	3.16	1.04	0.26	0.23	1.21	0.76	0.112	405	937	0.710080
	P1	50-54	0.327	82.8	3.23	1.11	0.19	0.23	0.88	2.17	0.099	425	833	0.709814*
	IIB	57-90	0.278	150	2.28	1.93	0.36	0.16	0.74	1.64	0.145	421	1040	0.709412
	P2	100-110	0.289	85.0	0.59	1.90	0.73	0.05	1.61	0.59	0.155	116	548	0.710615

Errors for elemental data and $^{87}Sr/^{86}Sr$ as reported in text, except: *error (2σ) greater than 0.000030 but less than 0.000075. ** n=1 for all $^{87}Sr/^{86}Sr$ data. ***n=2 for It1 O horizon.

Table 2-3: Mean cold acid digestible soil fraction (per gram dry soil)

surface	horizon	depth cm	Ba µmol/g	Ca µmol/g	Fe µmol/g	K µmol/g	Na µmol/g	P µmol/g	S µmol/g	Si µmol/g	Sr µmol/g	Ca/Na (molar)	Ca/Sr (molar)	$^{87}Sr/^{86}Sr$**
It3	O	0-7	0.682	183	57.3	3.97	0.45	5.12	0.58	29.4	0.144	405	1270	0.713346
(n=4)	A	7-19	0.123	7.77	147	1.41	0.29	2.06	0.68	42.1	0.011	26.7	681	0.713351
	B1	19-39	0.191	8.54	173	1.46	0.28	1.82	0.58	44.7	0.013	30.6	660	0.714043
	B2	39-60	0.189	8.76	157	1.80	0.28	3.05	0.75	44.7	0.013	31.4	672	0.713707
	P	62-71	0.399	12.6	285	2.46	0.44	8.31	1.25	51.7	0.014	28.9	875	0.713848
It2	O	0-16	2.17	360	53.8	1.01	0.56	4.70	5.90	11.9	0.218	646	1650	0.710522
(n=3)	A	18-29	1.09	60.7	119	1.35	0.39	11.3	2.47	59.8	0.070	156	864	0.710246
	B1	29-46	1.34	62.4	122	1.79	0.46	11.2	4.05	68.8	0.072	136	869	0.709875
	B2	46-62	2.17	122	117	1.99	0.41	12.2	7.12	72.2	0.118	297	1040	0.709850
	P	66-73	2.39	257	125	1.97	0.42	9.76	4.01	66.9	0.195	610	1320	0.709610
It1	O*	0-7	0.350	10.4	68.1	3.64	0.18	3.73	1.19	18.8	0.017	59.3	627	0.720647
(n=3)	A	8-23	0.152	6.03	125	0.95	0.10	2.04	0.34	28.5	0.009	62.5	702	0.713331
	B1	23-40	0.180	8.67	121	1.04	0.10	3.23	0.39	32.1	0.012	88.3	729	0.712963
	B2	35-49	0.186	7.23	124	1.14	0.13	3.10	0.19	39.2	0.011	57.6	658	0.712858
	P1	49-60	0.136	6.28	95.7	1.11	0.13	2.41	0.31	31.9	0.009	47.8	685	0.712326
	P2	62-69	0.423	79.8	125	1.40	0.09	5.60	0.64	42.2	0.052	929	1540	0.710896
Sag2	O	0-8	0.537	28.1	52.1	2.91	0.44	5.93	1.33	13.2	0.039	64.6	714	0.715214
(n=3)	A	8-25	0.182	6.84	92.0	1.01	0.13	2.36	0.33	31.1	0.009	50.9	758	0.712909
	B1	25-42	0.414	7.99	138	1.52	0.14	2.71	0.86	45.1	0.011	57.5	703	0.713031
	B2	38-55	0.079	4.04	60.5	0.94	0.18	3.05	0.15	26.9	0.006	22.3	672	0.712395
	P1	55-69	0.128	5.99	65.4	1.25	0.18	2.44	0.38	28.1	0.009	33.1	655	0.712871
	P2	71-75	0.493	12.2	95.4	1.57	0.11	2.18	0.70	37.0	0.015	114	807	0.712010
Sag1	O	0-13	0.677	22.6	85.8	3.28	0.40	3.03	1.56	23.2	0.030	57.1	749	0.715044
(n=2)	A	13-22	0.272	4.0	133	1.29	0.23	1.54	0.66	34.4	0.006	17.0	669	0.713519
	B1	22-40	0.147	2.65	104	1.26	0.26	1.36	0.28	35.9	0.004	10.1	649	0.713252
	B2	35-50	0.186	3.29	115	1.34	0.27	1.84	0.34	39.1	0.005	12.0	602	0.713607
	P	50-58	0.235	6.16	166	1.53	0.31	4.38	0.45	41.4	0.008	20.0	738	0.713144
Sag1-DP	P (deep)	200-300	1.75	244	236	1.46	18.8	21.5	9.08	169	0.279	13.0	874	0.711083
AR	O	0-11	0.391	166	37.1	4.89	0.40	6.33	1.82	16.3	0.154	418	1080	0.708762
(n=3)	A	11-27	0.727	82.7	171	1.97	0.73	19.7	1.66	65.2	0.164	113	503	0.709060
	B1	27-50	0.726	183	137	2.37	0.63	20.3	0.90	85.9	0.213	288	857	0.708580
	B2	45-75	0.446	280	70.8	2.16	0.49	13.2	0.01	66.4	0.250	573	1120	0.708235
	P1	70-80	0.777	423	142	2.59	0.80	20.8	0.12	92.8	0.353	530	1200	0.708352
	P2	85-93	0.740	320	94.2	2.45	0.58	19.0	0.01	84.3	0.309	549	1040	0.708425
GM	Oe	0-13	0.394	54.8	29.4	6.32	0.34	5.52	1.21	7.06	0.075	160	729	0.710627
(n=2)	B1	13-35	0.310	14.1	162	3.18	1.21	4.66	3.19	62.6	0.029	11.6	490	0.711870
	B2	38-44	0.467	18.3	286	1.86	0.39	3.20	1.72	57.0	0.034	47.3	538	0.711035
	IIOa	44-55	1.10	186	241	3.73	1.24	7.52	5.48	44.0	0.219	150	849	0.710836
	P1	50-54	0.811	101	131	1.96	0.34	6.93	2.43	36.7	0.132	295	762	0.709522
	IIB	57-90	1.05	342	139	4.22	1.34	9.92	3.85	64.0	0.313	255	1090	0.709681
	P2	100-110	1.07	1220	177	3.21	1.37	13.9	2.55	72.4	0.850	891	1440	0.709076

Errors for elemental data and $^{87}Sr/^{86}Sr$ as reported in text; maximum error (2σ) for any $^{87}Sr/^{86}Sr$ value used in calculating means is 0.000068. *For $^{87}Sr/^{86}Sr$: n=3 for It3, n=1 for AR and GM; for other surfaces, n is as reported.

Table 2-4: Mean hot acid digestible soil fraction (per gram dry soil).

surface	horizon	depth cm	Ba μmol/g	Ca μmol/g	Fe μmol/g	K μmol/g	Na μmol/g	P μmol/g	S μmol/g	Si μmol/g	Sr μmol/g	Ca/Na (molar)	Ca/Sr (molar)	$^{87}Sr/^{86}Sr$***
It3	O	0-7	0.309	51.2	196	5.42	16.7	13.0	26.2	10.5	0.045	3.07	1150	0.714412
(n=4)	A	7-19	0.125	2.44	359	8.40	12.9	5.56	3.09	49.3	0.015	0.19	168	0.731134
	B1	19-39	0.145	2.37	409	10.1	13.0	6.74	3.77	44.2	0.014	0.18	173	0.732188
	B2	39-60	0.183	2.17	441	14.3	12.9	8.67	5.75	68.2	0.019	0.17	113	0.733771*
	P	62-71	0.253	4.38	263	9.05	17.0	7.22	10.6	4.12	0.010	0.26	436	0.730624
It2	O	0-16	0.949	87.9	95.1	.78	16.7	15.4	101	9.41	0.056	5.27	1570	0.709652*
(n=3)	A	18-29	0.284	3.91	298	5.22	11.5	6.81	13.6	87.8	0.009	0.34	429	0.720106
	B1	29-46	0.342	4.10	342	7.61	11.5	4.55	14.6	102	0.012	0.36	340	0.720671*
	B2	46-62	0.353	7.20	341	10.5	11.2	7.20	24.5	47.9	0.015	0.64	485	0.725481
	P	66-73	0.324	13.2	395	4.94	8.34	8.20	27.1	50.9	0.019	1.58	710	0.715267
It1	O****	0-7	0.296	6.06	317	9.33	17.2	23.2	25.9	15.4	0.012	0.35	526	0.724344
(n=3)	A	8-23	0.107	1.76	330	5.85	12.1	5.35	2.54	60.4	0.008	0.15	231	0.727602*
	B1	23-40	0.103	1.69	285	6.82	12.5	4.53	2.45	81.9	0.009	0.14	191	0.730939
	B2	35-49	0.191	2.46	399	7.38	18.4	8.26	2.41	3.19	0.010	0.13	254	0.731677
	P1	49-60	0.192	2.70	394	8.64	17.9	7.61	1.98	4.57	0.010	0.15	275	0.732349
	P2	62-69	0.160	2.77	411	15.0	12.0	6.70	8.16	114	0.017	0.23	163	0.733956
Sag2	O	0-8	0.238	11.8	156	5.12	17.5	17.5	23.9	8.03	0.016	0.67	752	0.720922*
(n=3)	A	8-25	0.126	2.14	283	5.86	12.0	5.98	3.10	45.3	0.007	0.18	295	0.722058
	B1	25-42	0.231	2.38	343	9.99	11.9	7.13	6.14	54.2	0.012	0.20	190	0.722017
	B2	38-55	0.187	3.45	216	4.52	18.3	2.95	1.38	4.15	0.009	0.19	394	0.723151
	P1	55-69	0.191	3.08	386	4.25	17.5	7.44	3.01	4.87	0.007	0.18	465	0.721817*
	P2	71-75	0.209	2.10	386	8.62	12.0	5.38	5.55	67.8	0.010	0.17	206	0.723476
Sag1	O	0-13	0.363	7.92	176	8.86	17.1	21.5	27.5	2.43	0.019	0.46	409	0.722149**
(n=2)	A	13-22	0.307	4.20	459	10.1	18.2	12.1	6.59	4.87	0.018	0.23	227	0.723068
	B1	22-40	0.247	4.30	364	7.33	17.8	7.31	1.91	4.88	0.016	0.24	274	0.722645**
	B2	35-50	0.248	3.88	371	7.76	18.4	7.16	1.56	0.94	0.016	0.21	250	0.723827
	P	50-58	0.274	5.15	302	7.92	16.6	5.88	2.30	5.19	0.014	0.31	369	0.725281
Sag1-DP	P (deep)	200-300	0.257	12.7	435	9.86	18.1	4.10	6.02	3.51	0.041	0.70	309	0.726095
AR	O	0-11	0.348	70.0	136	4.30	16.0	20.9	58.4	19.8	0.069	4.36	1020	0.708900*
(n=3)	A	11-27	0.394	14.4	385	3.26	8.52	19.7	20.4	9.08	0.036	1.68	397	0.713011**
	B1	27-50	0.450	14.7	535	7.76	17.6	11.3	8.80	5.44	0.027	0.84	538	0.711376
	B2	45-75	0.359	18.9	502	6.69	16.6	9.57	3.99	2.67	0.027	1.14	708	0.713535
	P1	70-80	0.402	20.1	508	8.50	17.8	8.94	4.06	3.25	0.028	1.13	723	0.711658
	P2	85-93	0.386	9.08	491	7.97	17.2	9.73	4.64	1.91	0.022	0.53	407	0.716740*
GM	Oe	0-13	0.457	48.1	68.9	5.85	15.9	21.7	38.7	16.2	0.062	3.02	781	0.712801**
(n=2)	B1	13-35	0.297	5.67	234	6.72	17.5	7.95	9.44	5.31	0.019	0.32	300	0.713987*
	B2	38-44	0.360	5.84	460	8.00	17.1	9.02	8.52	5.91	0.021	0.34	283	0.714585*
	IIOa	44-55	0.438	60.6	204	4.96	16.4	15.9	48.5	16.1	0.066	3.68	919	0.713590*
	P1	50-54	0.428	25.2	189	8.38	17.7	11.5	36.1	19.2	0.042	1.43	604	0.713149*
	IIB	57-90	0.463	58.4	209	14.4	18.1	8.30	46.1	12.6	0.066	3.22	890	0.712507**
	P2	100-110	0.340	31.7	211	14.0	18.8	5.23	23.2	4.57	0.046	1.69	684	0.714035**

Errors for elemental data and $^{87}Sr/^{86}Sr$ as reported in text, except: *error (2σ) greater than 0.000030 but less than 0.000075 **error (2σ) greater than 0.000075 but less than 0.000211. ***n=1 for all $^{87}Sr/^{86}Sr$ data. ****n=2 for It1 O horizon.

Table 2-5: Total soil digest chemistry (per gram dry soil)

surface	horizon	depth	Ba	Ca	Fe	K	Na	P	Si	Sr	Ca/Na	Ca/Sr	fraction	LOI
		cm	μmol/g	μmol/g	μmol/g	μmol/g	μmol/g	μmol/g	μmol/g	μmol/g	(molar)	(molar)	< 2mm	%
lt3	O	0-7	-	-	-	-	-	-	-	-	-	-	-	-
(n=4)	A	7-19	3.01	20.5	547	282	128	12.73	13600	0.583	0.017	35.2	76%	5%
	B1	19-39	3.50	19.9	685	325	129	14.68	14100	0.624	0.018	31.9	76%	7%
	B2	39-60	3.51	19.7	644	327	122	16.77	12800	0.585	0.019	33.7	80%	8%
	P	62-71	4.66	35.1	730	383	128	23.84	13200	0.643	0.023	54.6	63%	-
lt2	O	0-16	-	-	-	-	-	-	-	-	-	-	-	-
(n=3)	A	18-29	4.77	124	504	213	151	22.23	13900	0.577	0.023	214	65%	12%
	B1	29-46	5.32	113	565	271	155	19.90	14000	0.591	0.023	192	52%	20%
	B2	46-62	5.73	202	606	265	141	23.04	12400	0.626	0.024	323	59%	8%
	P	66-73	6.67	330	831	335	168	27.77	11800	0.759	0.021	434	82%	7%
lt1	O*	0-7	-	-	-	-	-	-	-	-	-	-	-	-
(n=3)	A	8-23	2.65	18.2	541	251	148	12.80	15300	0.508	0.019	35.8	49%	5%
	B1	23-40	2.85	18.7	484	262	118	15.31	15400	0.526	0.019	35.5	57%	8%
	B2	35-49	3.30	20.4	638	286	108	17.46	15100	0.562	0.020	36.3	54%	-
	P1	49-60	3.24	19.9	586	304	112	15.13	17200	0.555	0.020	35.9	53%	-
	P2	62-69	3.45	108	653	305	117	16.98	15100	0.635	0.020	170	71%	10%
Sag2	O	0-8	-	-	-	-	-	-	-	-	-	-	-	-
(n=3)	A	8-25	2.66	19.4	466	197	101	14.25	15600	0.466	0.021	41.6	66%	7%
	B1	25-42	4.37	30.1	705	315	124	20.55	13500	0.517	0.024	58.3	79%	23%
	B2	38-55	2.61	23.8	343	195	115	8.60	16100	0.505	0.019	47.1	69%	-
	P1	55-69	2.55	22.5	514	179	93.5	14.53	15200	0.454	0.021	49.4	61%	-
	P2	71-75	3.82	37.5	743	265	112	17.95	13400	0.432	0.026	86.8	77%	22%
Sag1	O	0-13	-	-	-	-	-	-	-	-	-	-	-	-
(n=2)	A	13-22	3.67	29.3	565	236	137	17.1	14000	0.560	0.023	52.3	69%	15%
	B1	22-40	3.55	26.6	519	229	157	12.36	14000	0.548	0.023	48.5	65%	7%
	B2	35-50	4.08	26.8	586	264	167	13.29	14400	0.576	0.024	46.5	58%	-
	P	50-58	3.77	25.9	525	243	140	13.79	14200	0.570	0.024	45.4	61%	7%
Sag1-DP	P (deep)	200-300	7.13	255	896	675	153	29.46	13400	1.14	0.019	224	88%	-
AR	O	0-11	-	-	-	-	-	-	-	-	-	-	-	-
(n=3)	A	11-27	4.13	138	581	200	181	30.1	11900	0.589	0.021	234	46%	-
	B1	27-50	5.34	270	631	267	239	31.6	13500	0.797	0.019	339	40%	-
	B2	45-75	4.58	428	529	255	199	26.89	11900	0.858	0.017	498	30%	-
	P1	70-80	5.45	483	593	268	235	32.41	13000	0.915	0.020	528	41%	-
	P2	85-93	5.25	612	596	277	227	48.97	13700	1.27	0.019	480	37%	-
GM	Oe	0-13	-	-	-	-	-	-	-	-	-	-	-	-
(n=2)	B1	13-35	4.47	67.6	475	259	222	20.99	13200	0.685	0.023	98.7	47%	-
	B2	38-44	4.37	75.7	845	209	183	20.33	12600	0.682	0.024	111	76%	-
	IIOa	44-55	3.16	289	379	128	95.5	28.8	5860	0.614	0.032	471	69%	-
	P1	50-54	3.65	219	336	164	126	24.9	8240	0.659	0.028	333	57%	-
	IIB	57-90	4.60	593	396	249	203	25.30	10600	0.982	0.020	604	79%	-
	P2	100-110	4.82	1320	452	283	208	27.27	11400	1.63	0.011	814	57%	-

Errors for elemental data as reported in text.

Table 2-6: Water chemistry for streams on different glacial deposit and bedrock surfaces.

Surface	stream name	date sampled	Ba µmol/L	Ca µmol/L	Fe µmol/L	K µmol/L	Mg µmol/L	Na µmol/L	S µmol/L	Si µmol/L	Sr µmol/L	Ca/Na (molar)	Ca/Sr (molar)	$^{87}Sr/^{86}Sr$
It3	1) It 3 stream	7/29/02	0.08	551.3	3.88	2.3	104.9	36	20.8	67.6	0.740	15	745	0.710391*
	2) Island Lake outlet	8/2/02	0.13	522.0	<0.08	10.3	183.5	77	20.7	85.9	0.736	6.8	709	0.710234
It2 (outwash)	3) I minus outlet	6/27/02	0.10	219.6	1.03	8.3	61.5	16	20.8	78.2	0.760	14	289	0.713132
	4) I minus inlet	6/27/02	0.07	136.3	2.26	4.8	37.9	13	20.8	78.8	0.766	11	178	0.712971
	5) TW stream (lower)	7/21/02	0.10	269.2	0.96	1.0	57.6	7	20.8	77.9	0.761	40	354	0.713314
	6) Milky Way (upper)	8/10/02	0.12	255.4	1.56	2.3	62.7	27	18.4	40.3	0.205	9.4	1244	0.712085*
It2 (till)	7) N1 inlet	7/11/02	0.09	543.5	0.64	1.2	117.5	13	20.8	80.3	0.752	42	722	0.710600*
	8) I1 outlet	8/7/02	0.03	123.1	1.34	6.4	36.5	14	8.1	0.9	0.102	8.8	1204	0.715188**
	9) I4 outlet	8/7/02	0.05	104.9	2.65	5.0	34.7	13	8.5	<0.4	0.096	7.8	1093	0.715593
	10) I2 outlet	8/7/02	0.07	129.7	4.61	6.7	50.5	14	6.8	10.4	0.131	9.4	988	0.716473*
It1	11) I6 HW inlet	8/8/02	0.08	594.3	9.20	1.0	97.9	20	6.4	34.6	0.404	30	1471	0.711281
	12) I8 Headwater	6/26/02	0.06	168.1	2.32	2.8	52.7	13	20.8	78.8	0.764	13	220	0.713464*
	13) It 1 stream	7/15/02	0.25	440.6	<0.08	2.5	73.4	19	20.8	76.2	0.746	23	590	0.710995
Sag2	14) E5 inlet S	7/30/02	0.07	44.2	6.37	0.7	20.2	11	3.1	37.2	0.046	4.0	958	0.716328
	15) E5 inlet W	8/13/02	0.09	19.7	2.02	0.3	12.2	13	8.5	43.6	0.025	1.6	796	0.718806
Sag1	16) Imnavait (weir)	8/1/02	0.08	28.1	13.55	0.6	14.2	4	1.2	20.2	0.036	7	777	0.716905
	17) Toolik R. trib.	8/16/02	0.06	11.7	8.36	0.5	10.9	4	2.6	29.0	0.018	3	654	0.717341
AR	18) Anaktuvuk stream	8/15/03	0.08	78.2	4.55	0.6	18.3	12	2.3	47.1	0.079	6.7	990	0.712417
GM	19) Gunsight stream	8/16/03	0.07	165.8	5.62	<0.3	44.2	9	3.5	58.7	0.148	20	1120	0.711356
multiple surfaces	20) Kuparuk R.	8/7/02	0.28	199.1	0.37	6.6	71.2	78	20.8	65.3	0.745	2.6	267	0.707878**
	21) Sagavanirktok R.	7/31/02	0.22	924.3	<0.08	8.9	282.5	80	20.7	76.8	0.635	12	1456	0.710453
carbonate bedrock	22) Atigun R. trib.	7/29/02	0.26	1559.1	<0.08	13.3	287.4	97	20.6	80.2	0.678	16	2301	0.710550*
	23) Kayak Creek	8/7/02	0.13	1605.7	<0.08	7.5	166.3	20	20.8	80.9	0.569	79	2821	0.708469
	24) Aufeis stream	7/31/02	0.35	1226.5	<0.08	5.4	272.0	21	20.8	71.0	0.707	58	1736	0.708802
mixed bedrock	25) Trevor Creek	8/7/02	0.30	706.7	<0.08	10.5	264.2	94	20.7	83.6	0.704	7.5	1003	0.714855*
	26) Atigun R.	7/29/02	0.18	691.1	<0.08	12.2	324.6	122	20.7	80.8	0.697	5.67	991	0.714458
	27) Bad Idea stream	8/18/03	0.18	866.5	<0.08	14.8	167.5	169	397.0	34.7	1.495	5.14	580	0.711382
	28) Holden Creek	8/18/03	0.09	569.4	0.14	8.6	102.4	88	122.5	21.2	1.212	6.4	470	0.709772
	29) Roche Moutonee Cr.	8/18/03	0.12	372.6	0.16	9.9	110.1	56	83.0	24.0	0.465	6.7	802	0.713843
silicate bedrock	30) Atigun R. headwater	8/7/02	0.07	570.4	<0.08	12.2	395.8	271	20.7	77.5	0.686	2.11	832	0.719655*
	31) Underwillow stream	8/18/03	0.27	254.5	0.30	22.7	194.9	296	318.6	31.6	0.502	.86	507	0.719893
precipi-tation	field station precip. 1	8/5/02	<0.01	102.2	<0.08	83.5	4.4	218	20.8	92.3	0.770	0.47	133	0.709485**
	field station precip. 2	8/6/02	0.03	84.9	<0.08	19.0	2.1	57	20.8	92.0	0.772	1.5	110	0.708781*

Errors for elemental data and $^{87}Sr/^{86}Sr$ as reported in text, except: *error (2σ) greater than 0.000030 but less than 0.000051 **error (2σ) greater than 0.000051 but less than 0.000165.

Figure 2-1. Map of study area with locations of soil (triangle) and stream (square) sampling sites. Glacial deposit and bedrock boundaries after Hamilton (1978; 2003), Mull and Adams (1985) and Brown and Krieg (1983).

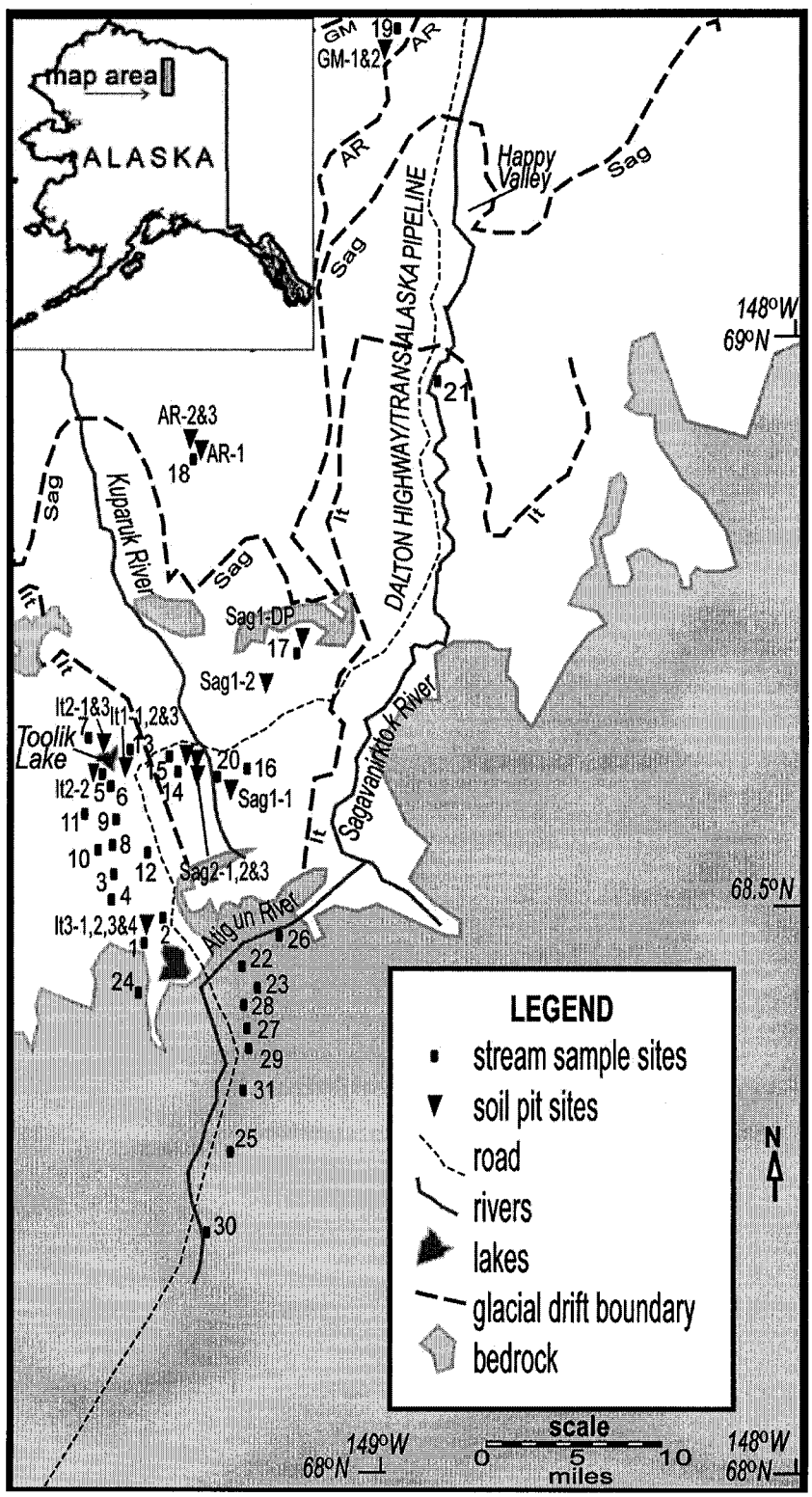

Figure 2-2. Hot acid digestible fraction $^{87}Sr/^{86}Sr$ of soil horizon samples vs. mean horizon depth. $^{87}Sr/^{86}Sr$ analytical errors are reported in table 2-4.

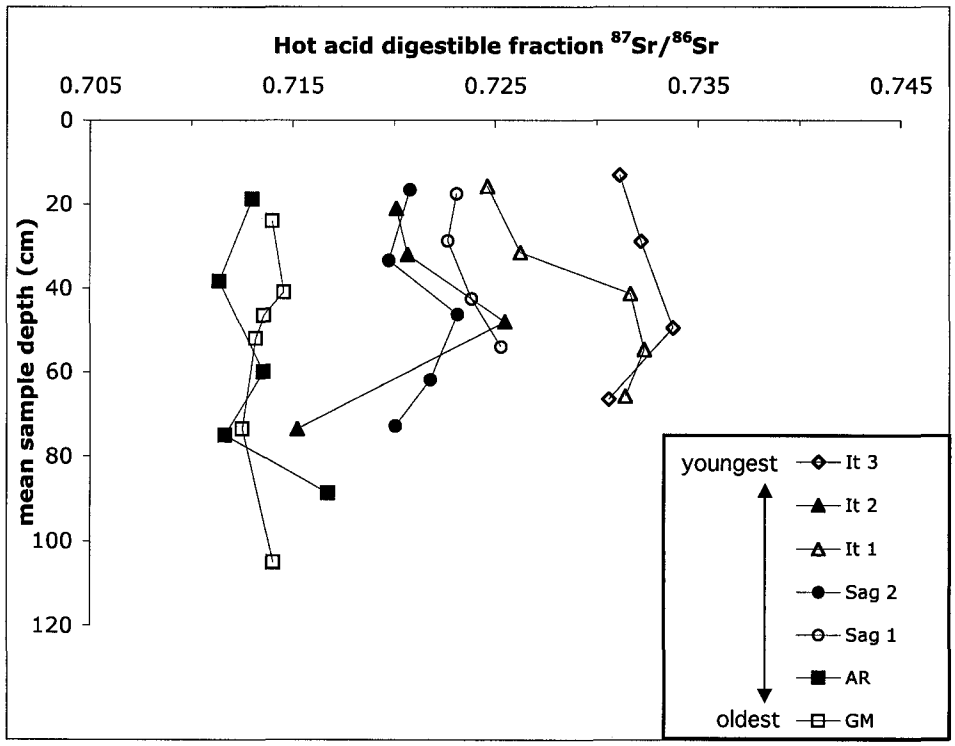

Figure 2-3. Cold acid digestible Ca/Na, Ca/Sr, and $^{87}Sr/^{86}Sr$ of soil horizon samples vs. mean sample depth. Elemental ratios are molar. Analytical errors are reported in the text.

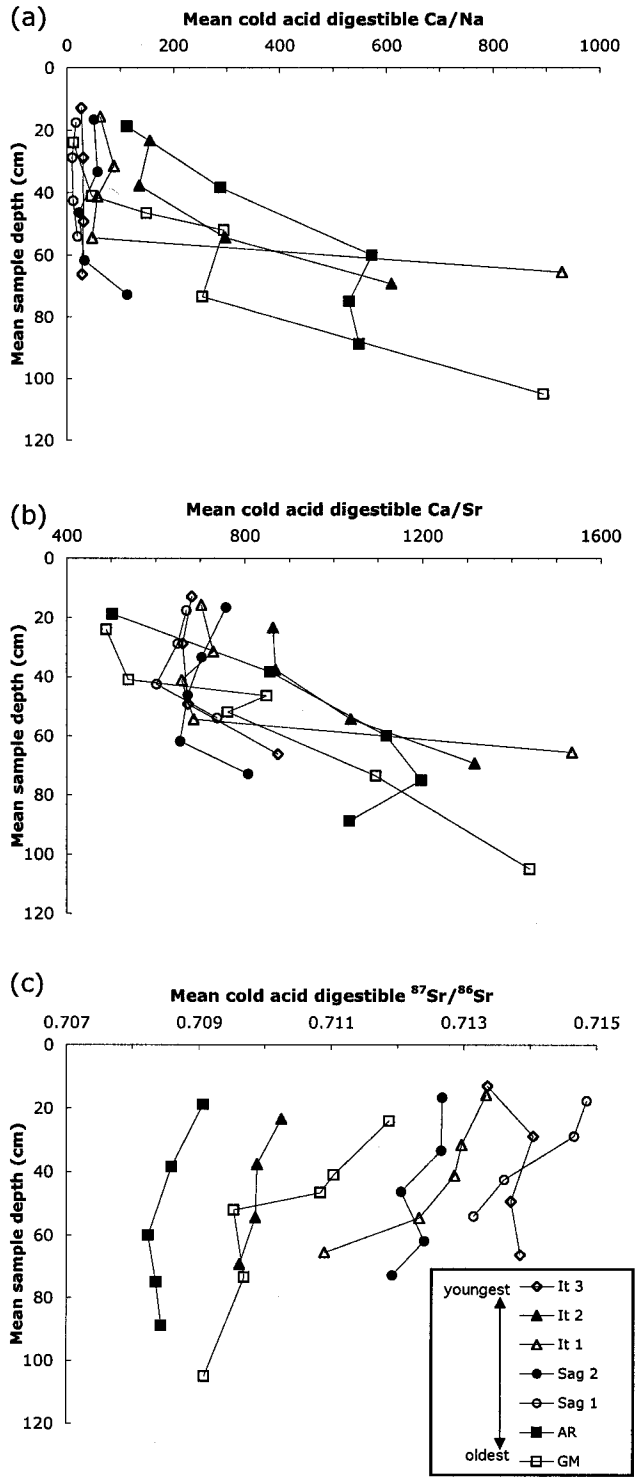

Figure 2-4. $^{87}Sr/^{86}Sr$ vs. Ca/Sr of stream water samples from glacial deposit surfaces. Dashed lines connecting the cold acid digestible fraction values of PMl, Dke, and Kf rock units (see table 2-3) represent simple chemical mixing lines for these end-members. Hatched lines connecting the mean values for precipitation and streams draining PMl and Dke/MDk units represent simple chemical mixing lines for these end-members. Ca/Sr is a molar ratio. Error bars represent propagated Ca/Sr analytical errors; $^{87}Sr/^{86}Sr$ errors are smaller than the symbol size and are reported in Table 2-6.

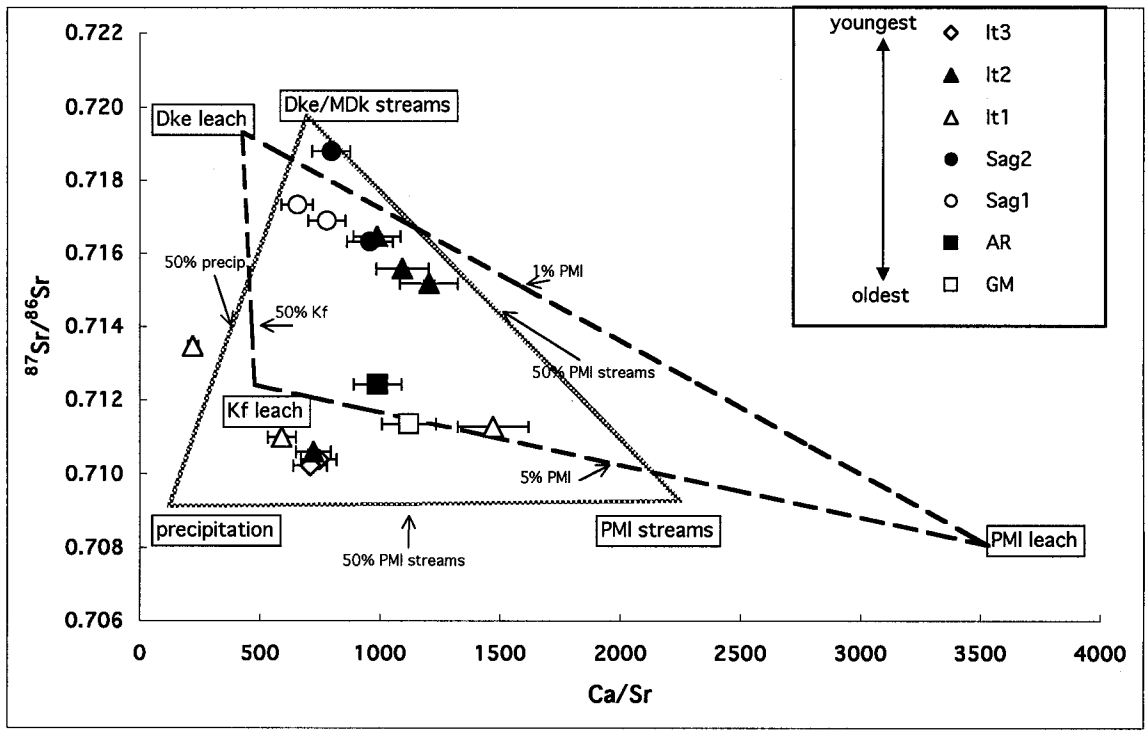

Figure 2-5. Cold acid digestible fraction $^{87}Sr/^{86}Sr$ vs. Ca/Sr of soil "A" horizon samples from glacial deposit surfaces. Dashed lines connecting the cold acid digestible fraction values of PMI, Dke, and Kf rock units (see table 2-3) represent simple chemical mixing lines for these end-members, as in Figure 4. Ca/Sr is a molar ratio. Error bars represent propagated Ca/Sr analytical errors; $^{87}Sr/^{86}Sr$ errors are smaller than the symbol size and are reported in Table 2-3.

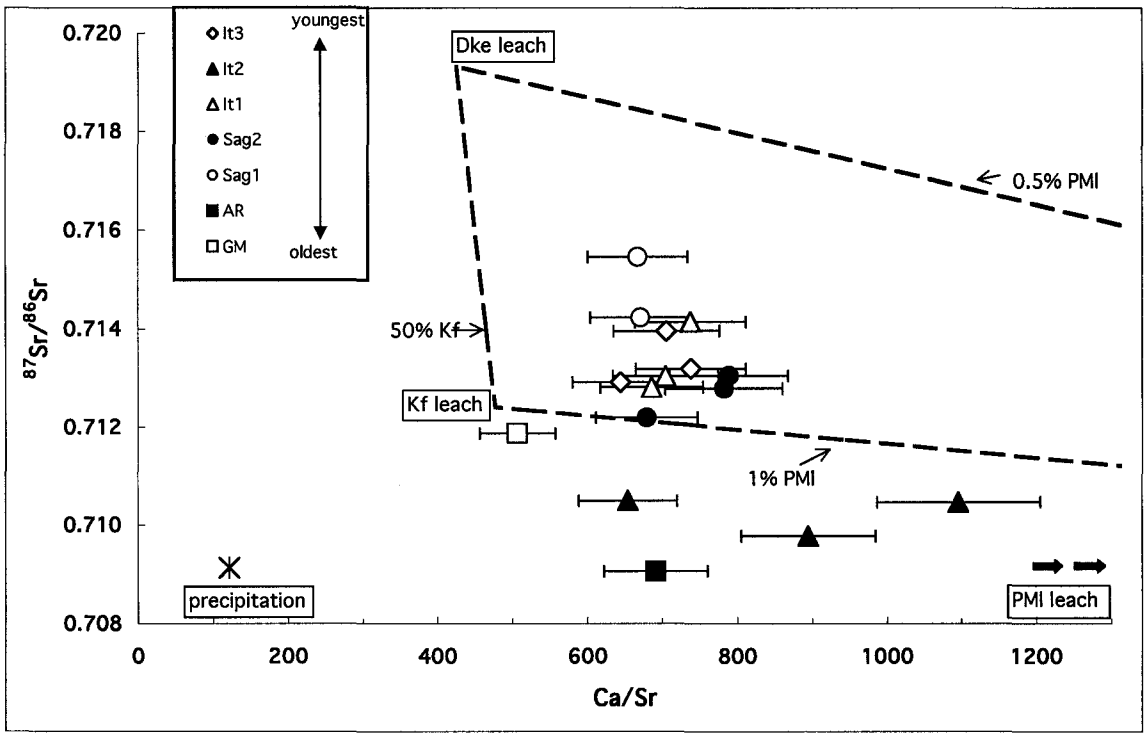

Figure 2-6. Cold acid digestible fraction Ca (µmol/g) vs. cold acid digestible fraction P (µmol/g) in active-layer mineral soil samples from different glacial surfaces. The dashed line represents the Ca/P of apatite (1.67). Analytical errors are reported in the text.

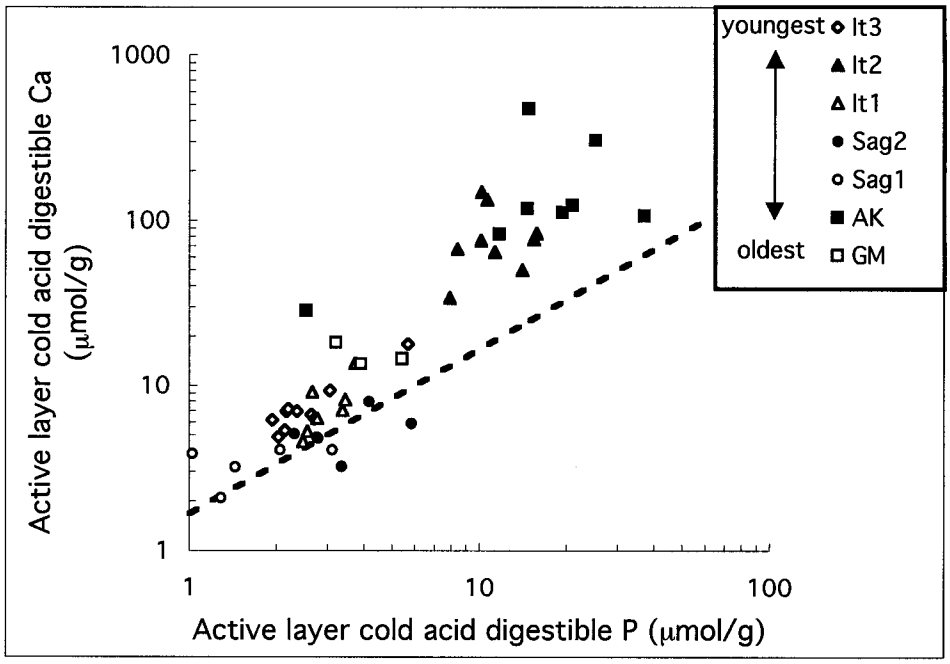

References Cited

Anisimov, O. A., Shiklomanov, N. I., and Nelson, F. E., 1997: Global warming and active-layer thickness: results from transient general circulation models. *Global and Planetary Change,* 15: 61-77.

Blum, J. D., Klaue, A., Nezat, C. A., Driscoll, C. T., Johnson, C. E., Siccama, T. G., Eagar, C., Fahey, T. J., and Likens, G. E., 2002: Mycorrhizal weathering of apatite as an important calcium source in base-poor forest ecosystems. *Nature,* 417: 729-731.

Bockheim, J. G., Walker, D. A., Everett, L. R., Nelson, F. E., and Shiklomanov, N. I., 1998: Soils and cryoturbation in moist nonacidic and acidic tundra in the Kuparuk River Basin, Arctic Alaska, U. S. A. *Arctic and Alpine Research,* 30: 166-174.

Brown, J. and Krieg, R. A., 1983: *Guidebook to permafrost and related features along the Elliot and Dalton Highways, Fox to Prudhoe Bay, Alaska.* University of Alaska-Fairbanks, University of Alaska-Fairbanks.

Brown, J. G., Kling, G. W., Hinkel, K. M., Hinzman, L. D., Nelson, F. E., Romanovsky, V., and Shiklomanov, N. I., 2002: Arctic Alaska and Seward Peninsula, in Brown, J. G., Hinkel K. M., and Nelson F. E. (eds.): The circumpolar active layer monitoring (CALM) program: Research designs and initial results. *Polar Geography,* 24: 165-258.

Compeau, G. C. and Bartha, R., 1985: Sulfate-reducing bacteria: Principal methylators of mercury in anoxic estuarine sediment. *Applied Environmental Microbiology,* 50: 498-502.

Everett, K. R., Marion, G. M., and Kane, D. L., 1989: Seasonal geochemistry of an arctic tundra drainage-basin. *Holarctic Ecology,* 12: 279-289.

Giblin, A. E., Nadelhoffer, K. J., Shaver, G. R., Laundre, J. A., and McKerrow, A. J., 1991: Biogeochemical diversity along a riverside toposequence in arctic Alaska. *Ecological Monographs,* 61: 415-436.

Gilmour, C. C., Henry, E. A., and Mitchell, R., 1992: Sulfate stimulation of mercury methylation in fresh-water sediments. *Environmental Science & Technology,* 26: 2281-2287.

Hamilton, T. D. and Porter, S. C., 1975: Itkillik glaciation in the Brooks Range, northern Alaska. *Quaternary Research,* 5: 471-497.

Hamilton, T. D., 1978: Surficial geologic map of the Philip Smith Mountains Quadrangle, Alaska, MF-879. Reston, VA: Department of the Interior, United States Geological Survey.

Hamilton, T. D., 1986: Late Cenozoic glaciation of the Central Brooks Range. *In* Hamilton, T. D., Reed, K. M., and Thorson, R. M. (eds.), *Glaciation in Alaska: the geologic record.* Anchorage, AK: Alaska Geological Society, 265.

Hamilton, T. D., 1994: Late Cenozoic glaciation of Alaska. *In* Plafker, G. (ed.), *The geology of Alaska*. Boulder, CO: Geological Society of America, 1055.

Hamilton, T. D., 2003: *Glacial geology of Toolik Lake and the Upper Kuparuk River region*. Fairbanks, Alaska: Alaska Geobotany Center, Institute of Arctic Biology, University of Alaska Fairbanks, 24 pp.

Haugen, R. K., 1982: Climate of remote areas in north-central Alaska, 1975-1979 summary, *U. S. Army Cold Regions Research and Engineering Laboratory Report*, 110.

Heiri, O., Lotter, A. F., and Lemcke, G., 2001: Loss on ignition as a method for estimating organic and carbonate content in sediments: reproducibility and comparability of results. *Journal of Paleolimnology,* 25: 101-110.

Hobbie, J. E., Peterson, B. J., Bettez, N., Deegan, L., O'Brien, W. J., Kling, G. W., Kipphut, G. W., Bowden, W. B., and Hershey, A. E., 1999: Impact of global change on the biogeochemistry and ecology of an Arctic freshwater system. *Polar Research,* 18: 207-214.

Hobbie, S. E., Miley, T. A., and Weiss, M. S., 2002: Carbon and nitrogen cycling in soils from acidic and nonacidic tundra with different glacial histories in Northern Alaska. *Ecosystems,* 5: 761-774.

Huh, Y., Tsoi, M.-Y., Zaitsev, A., and Edmond, J. M., 1998: The fluvial geochemistry of the rivers of Eastern Siberia: I. Tributaries of the Lena River draining the sedimentary platform of the Siberian Craton. *Geochimica et Cosmochimica Acta,* 62: 1657-1676.

Humborg, C., Smedberg, E., Blomqvist, S., Morth, C.-M., Brink, J., Rahm, L., Danielsson, A., and Sahlberg, J., 2004: Nutrient variations in boreal and subarctic Swedish rivers: Landscape control of land-sea fluxes. *Limnology and Oceanography,* 49: 1871-1883.

Judd, K. E. and Kling, G. W., 2002: Production and export of dissolved C in arctic tundra mesocosms: the roles of vegetation and water flow. *Biogeochemistry,* 60: 213-234.

Kling, G. W., O'Brien, J., Miller, M. C., and Hershey, A. E., 1992: The biogeochemistry and zoogeography of lakes and rivers in arctic Alaska. *Hydrobiologia,* 240: 1-14.

Lichter, J., 1998: Rates of weathering and chemical depletion in soils across a chronosequence of Lake Michigan sand dunes. *Geoderma,* 85: 255-282.

Loseto, L. L., Siciliano, S. D., and Lean, D. R. S., 2004: Methylmercury production in High Arctic wetlands. *Environmental Toxicology and Chemistry,* 23: 17-23.

Menzie, W. D., Reiser, H. N., Brosge, W. P., and Detterman, R. L., 1985: Map showing distribution of mineral resources (excepting oil and gas) in the Philip Smith Mountains quadrangle, Alaska (Map MF-879-C). Reston: United States Geological Survey.

Millot, R., Gaillardet, J., Dupre, B., and Allegre, C. J., 2003: Northern latitude chemical weathering rates: Clues from the Mackenzie River Basin, Canada. *Geochimica et Cosmochimica Acta,* 67: 1305-1329.

Moore, T. E., Wallace, W. K., Bird, K. J., Karl, S. M., Mull, C. G., and Dillon, J. T., 1994: Geology of northern Alaska. *In* Plafker, G. and Berg, H. C. (eds.), *The Geology of Alaska*. Boulder, Colorado: Geological Society of America.

Mull, C. G. and Adams, K. E., 1985: *Bedrock Geology of the eastern Koyukuk Basin, central Brooks Range, and east central Arctic Slope along the Dalton Highway, Yukon River to Prudhoe Bay*. Anchorage: Alaska Department of Natural Resources, Division of Geological and Geophysical Surveys, 309 pp.

Munroe, J. S. and Bockheim, J. G., 2001: Soil development in low-arctic tundra of the northern Brooks Range, Alaska, USA. *Arctic and Alpine Research,* 33: 78-87.

Nadelhoffer, K. J., Giblin, A. E., Shaver, G. R., and Laundre, J. A., 1991: Effects of temperature and substrate quality on element mineralization in six arctic soils. *Ecology,* 72: 242-253.

Palmer, M. R. and Edmond, J. M., 1992: Controls over the strontium isotope composition of river water. *Geochimica et Cosmochimica Acta,* 56: 2099-2111.

Ping, C. L., Bockheim, J. G., Kimble, J. M., Michaelson, G. J., and Walker, D. A., 1998: Characteristics of cryogenic soils along a latitudinal transect in Arctic Alaska. *Journal of Geophysical Research-Atmospheres,* 103: 28917-28928.

Schlesinger, W. H., 1997: *Biogeochemistry: an analysis of global change*. second edition ed. San Diego: Academic Press.

Shaver, G. R. and Chapin, F. S., 1995: Long-term responses to factorial NPK fertilizer treatment by Alaskan wet and moist tundra sedge species. *Ecography,* 18: 259-275.

Stutter, M. I. and Billet, M. F., 2003: Biogeochemical controls on streamwater and soil solution chemistry in a High Arctic environment. *Geoderma,* 113: 127-146.

Tedrow, J. C. F., Drew, J. V., Hill, D. E., and Douglas, L. A., 1958: Major genetic soils of the arctic slope of Alaska. *Journal of Soil Science,* 9: 33-45.

Walker, J. C. G., Hays, P. B., and Kasting, J. F., 1981: A negative feedback mechanism for the long-term stabilization of Earth's surface temperature. *Journal of Geophysical Research,* 86: 9776-9782.

CHAPTER 3

ESTIMATES OF WEATHERING RATES IN ARCTIC SOILS DEVELOPED ON A GLACIAL CHRONOSEQUENCE

Abstract

In order to understand the relationship between climate and chemical weathering, it is important to quantify chemical weathering rates in arctic regions. I calculated elemental depletion factors and estimated long-term weathering rates for four glacial surfaces in arctic Alaska ranging in age from 11 to 780 ka. The soils on these surfaces were developed on carbonate-rich glacial deposits. Ca, Mg, and K depletion decreased with depth on the two younger surfaces. There were no consistent trends with depth on the older surfaces, but Ca was depleted compared to the parent material and to other elements on all surfaces, suggesting that carbonate weathering is the dominant weathering process in this region. There were no consistent trends in depletion with surface age, probably as a result of cryoturbation in the soil profiles. Interpretation of depletion profiles was confounded by the effects of cryoturbation and difficulty in identifying unweathered parent material. Long-term weathering rate estimates for these arctic soils on carbonate-rich parent material ranged from 0.5 to 11 meq m^{-2} yr^{-1}. These rates have a power-law relationship with age similar to that calculated for soils developed on silicate parent material in temperate regions.

Introduction

Because weathering of silicate minerals acts as a negative feedback regulating global climate in the long-term carbon cycle (Walker et al., 1981; Berner et al., 1983), much research has been conducted on chemical weathering rates in tropical and temperate ecosystems, where weathering rates are relatively high (e.g. White and Blum, 1995; Dahlgren et al., 1997; Louvat and Allegre, 1997; Wood et al., 1997; White et al., 1998). Less attention has been focused on weathering in cold regions, where chemical weathering rates are usually lower. However, understanding both silicate and carbonate weathering rates in these regions of climatic extremes is important in order to further develop a knowledge of the relationship between mineral weathering and climate.

Climate is one of the most important controls on chemical weathering, and influences other controls such as biotic and mechanical processes. Climate can have such an important influence on weathering processes and soil development that in some instances it can outweigh differences in soil parent material (Easterbrook, 1999). One reason climate is a dominant control is that it determines the availability of water, a necessary component of chemical weathering reactions, at the Earth's surface. The mean annual precipitation is generally the most important control on the amount of water available to participate in weathering reactions, but temperature also plays a role. In many areas, freezing temperatures prevent the interaction of liquid water with mineral surfaces seasonally, or in permafrost regions, year-round. In addition to

influencing water availability, warmer temperatures accelerate the weathering rates of many minerals by increasing mineral solubility (with a few important exceptions, most notably calcite) (White et al., 1999). Overall, climates that are both warm and wet produce the highest weathering rates (White and Blum, 1995).

Permafrost regions are usually considered to be areas of low weathering rates because by definition, permafrost prevents the chemical interaction of water with mineral weathering surfaces by freezing the system (Easterbrook, 1999). In fact, past reports have suggested that arctic soils show little or no chemical alteration and that soil development is dominated by mechanical processes (e.g.Reiger, 1974). However, recent research has demonstrated the significance of chemical weathering to ecosystem processes and soil formation even in permafrost regions. For example, podzolization of soils occurs in some areas of Antarctica (Beyer et al., 2000), chemical weathering leads to acidic soil conditions in the Swedish Arctic (Darmody et al., 2000), and chemical denudation rates were shown to exceed mechanical denudation rates in arctic Greenland (Hasholt and Hagedorn, 2000).

Even though climate suppresses weathering rates in cold climates, arctic permafrost regions may be the most susceptible to climate-driven increases in chemical weathering for two reasons. First, climate models predict that global climate change will have an amplified effect in the Arctic relative to temperate and tropical regions (Walsh and Crane, 1992; Fyfe et al., 1999; Shindell et al., 1999). Second, most arctic soils are underlain by permafrost (Easterbrook,

1999) and a warming climate may increase active layer thickness in these areas, increasing the total mineral volume that is exposed to weathering. Exposure of minerals that were previously inhibited from weathering is an effect of climate change specific to permafrost regions, and may cause dramatic increases in chemical weathering not seen in temperate or tropical regions. It is important to document current and long-term chemical weathering rates and patterns in arctic regions, in order to further develop the relationship between climate and weathering rates, to understand the contribution of weathering in permafrost regions to global geochemical cycles, and to provide a baseline for any climate-related changes that may occur.

Objective. Previous studies have used elemental depletion factors to calculate long-term weathering rates for soils developed on single glacial deposits (April et al., 1986; Kirkwood and Nesbitt, 1991) or glacial deposit chronosequences (Taylor and Blum, 1995) in temperate regions. The objective of this study is to estimate long-term chemical weathering rates by using elemental depletion factors from soils developed on four mixed-sedimentary glacial deposit surfaces of different ages on the eastern North Slope of Alaska. We aim to characterize carbonate vs. silicate mineral weathering in soils with mixed parent material and delineate a relationship between weathering rate and soil age in arctic regions.

Study area

This study was conducted on the arctic Alaskan North Slope in the vicinity of Toolik Lake and the Dalton Highway crossing of the Kuparuk River (roughly 68.5°N, 149.3°W). North of the Brooks Range, the landscape of the Alaskan tundra is underlain by continuous permafrost. The soils developed on these surfaces are Gelisols, classified specifically as Turbels and Orthels, depending on the amount of apparent cryoturbation (Munroe and Bockheim, 2001). In most areas, the mineral soil is overlain by a thick (ten or more centimeters) organic horizon. The soils are characterized by medium texture, poor drainage, and cryogenic features such as warped horizons and ice lenses (Ping et al., 1998).

The soils are developed on till and outwash from four major glaciations of varying ages (Hamilton, 1978, 2003). During these glaciations, alpine glaciers advanced northward out of the Brooks Range (Hamilton, 2003). Because this paper uses geochemical methods to assess weathering rates, I focus on the two main glacial deposits found by Keller et al. (2006) to have similar till geochemistry: the Sagavanirktok River glacial deposits and the Itkillik glacial deposits. Though the parent glacial till was deposited on these surfaces at different times, it originated from the same Brooks Range bedrock, and is compositionally similar. Evidence of this similarity was found by Keller et al. (2006): digests of only the weathering-resistant mineral fraction of these soils had only slightly different $^{87}Sr/^{86}Sr$, suggesting that the original parent material was

compositionally similar, and the overall geochemical differences in the soils are due to weathering over time.

These glaciations are each sub-divided into separate units consisting of advances and readvances separated by interglacial periods. The older of the two, the Sagavanirktok River glaciation, is dated broadly to the middle Pleistocene, or 780,000-125,000 years B. P. (Hamilton, 2003) based on paleomagnetic data and correlation to glaciations elsewhere in Alaska (Hamilton 1994). The Sagavanirktok River glaciation is separated into two units: Sagavanirktok River 1 (Sag1) and Sagavanirktok River 2 (Sag2). There are at least three Itkillik glaciation surfaces; in this study we only discuss data from the Itkillik I (It1) and Itkillik II (It2) surfaces. It1 deposits are older than the range of radiocarbon dating (>40 ka) but have an inferred age between 120 ka-50 ka. Radiocarbon dating yields ages between approximately 24 and 11.5 ka for It2 deposits (Hamilton, 1986, 2003). The Sagavanirktok River glacial deposit surfaces have thin but continuous eolian loess cover; the Itkillik glacial deposit surfaces have some loess cover but can have loess-free moraine crests (Hamilton, 1994, 2003).

The bedrock formations in the Brooks Range foothills, from which most glacial till is likely derived, consist primarily of conglomerates, sandstones, and limestones, with some shale and phyllite (Menzie et al., 1985; Mull and Adams, 1985). The limestone unit (Lisburne limestone) is chert-rich and argillaceous (Moore et al., 1994). The composition of the sandstone units (Kanayut conglomerate-sandstone and Fortress Mountain conglomerate-sandstone) likely

included in the till of the surfaces in this study is predominantly quartz and chert, with minor biotite-vermiculite, muscovite, oxides (including rutile and iron oxides), and sulfides in some samples. The Fortress Mountain sandstone also includes minor plagioclase and glauconite (Keller et al., 2006). Based on the mineral composition of the parent material, the major weathering processes in these soils are likely to be carbonate dissolution, releasing Ca and Mg, followed by biotite weathering to form vermiculite and releasing K.

Methods

Field methods. During July and August of 2002 and 2003 (during the time of maximum thaw), I excavated two to four soil sampling pits on each Itkillik and Sagavanirktok River glacial deposit surface. Sites were randomly selected on flat (slope <2°) moraine crests or shoulders. The vegetation that was present indicated that all of the pit sites except one were located on moist acidic tundra; one of the It2 pit sites was located on non-acidic tundra (Hobbie et al., 2002). Each pit was excavated through the active layer soil and several cm into the frozen ground. The soil profile and visible horizons were then measured and described, and homogenized samples were taken from each visible horizon. I took 3-6 mineral soil horizon samples per pit, usually consisting of horizons labeled "A" (an oxidized layer with live roots), "B1" (roughly the upper half of a thick gleyed layer), "B2" (the lower part of the same layer), "P1" (the first few cm of thickly laminated frozen soil, which may infrequently be part of the active layer), and "P2" (deeper, thinly laminated and solidly frozen permafrost

sediment). I also obtained a deeper (~3m) permafrost sample from the Sag1 surface from the site of a thermokarst tundra collapse within a few days of that event.

Laboratory methods. Samples were dried at 35°C and sieved to separate the <2mm size fraction, which was used for further analyses. The >2mm fraction is considered to contribute a negligible amount to overall mineral weathering of the soil due to its low ratio of surface area to volume; the >2mm fraction appeared to consist mostly of chert pebbles and quartzite cobbles and was on average less than 35% by mass of each sample.

To obtain a total digest of mineral soil samples, about 0.1 g of each sample was fused with 1 g of technical grade $LiBO_2$ in a graphite crucible at 1100°C, then dissolved in approximately 60 mL of trace metal grade 5% HNO_3 and filtered through 25µm pore size cellulose fiber paper. For quality assurance, two procedural blanks ($LiBO_2$ with no sample added) and two USGS Geochemical Reference Standards were also digested.

The $LiBO_2$ digest solutions were analyzed for elemental concentrations (including Ca, K, Mg, Na, P, Ti, and Zr) by ICP-OES using six- to nine-point calibration curves. Quality control standards included High-Purity® ICP-Stock Solution for Si and CRM Soil Solution A and Trace Metals in Drinking Water for other elements. These standards plus an in-house standard were analyzed to within ±7% for P, Ti, and Zr; ±12% for Ca, K, Na; and ±13% for Mg in the same concentration ranges as the samples.

Soil depletion profile calculation. Depletion factors show the proportion of an element lost from a soil horizon via weathering of soil minerals (or gained via eolian deposition) compared to the concentration of that element relative to an immobile element like titanium (Ti) or zirconium (Zr) in the parent material. Based on total digest data for the <2mm fraction, depletion factors ($d_{X,h}$) were calculated for each major cation (X) in the <2mm fraction of each mineral soil horizon (h) on the It2, It1, Sag2, and Sag1 surfaces using the equation: $d_{X,h}=(X_h/Zr_h)/(X_p/Zr_p)$, where the subscript p represents concentrations in the parent material and the units are mmol/g.

We used Zr rather than Ti for the calculations. Variability throughout the profiles was similar for the two elements: the mean X_h/X_p ± the standard deviation for all horizons on all surfaces is 0.7±0.08 for Ti and 0.9±0.1 for Zr (see Zr_h/Zr_p profile in Figure 3-1). However, ANOVAs performed on the Ti_h/Ti_p values of all horizons by surface indicate that the Sag1 and It1 surfaces have significantly different values (p=0.002) than the Sag2 and It2 surfaces. This creates a clustered effect among surfaces of alternating ages that is unlikely to be based on real differences in overall parent material composition and that may cause artifacts in the depletion factors and weathering calculations. An ANOVA performed on the Zr_h/Zr_p values across profiles indicates only the It2 surface has significantly different values than the other three; this may be based on actual slight differences in the parent material of this surface (Keller et al., 2006). Finally, the Zr_h/Zr_p values were closer to 1 on all surfaces than the Ti_h/Ti_p values, which is more consistent with the assumption that this element is immobile and

that there has been no dilation of the soil. Keller et al. (2006; Chapter 2) reported oxide minerals in SEM analyses of the sandstones from which the parent till was derived; in some samples of the extensive Mississippian-Devonian Kanayut conglomerate/sandstone these oxides included rutile (TiO_2). It is possible that the sample chosen to represent parent material and some surfaces were enriched in rutile-bearing sandstone, leading to the Ti_h/Ti_p ratios less than 1 across all surfaces and the clustering effect among surfaces. For these reasons, Zr was the better choice of the two commonly used immobile elements for this study.

I made four assumptions common to other studies in calculating long-term weathering rates. The first, as discussed above, is that Zr is immobile throughout the profile (Kirkwood and Nesbitt, 1991; Bain et al., 1993). Second, I assumed that there has been little mechanical erosion of soil; we minimized this possibility by sampling on relatively flat moraine crests as suggested by Taylor and Blum (1995). The third assumption (Taylor and Blum, 1995) is that there has been no significant eolian loess addition. This risk was also minimized by sampling on moraine crests, where the younger surfaces have been described as loess-free but the older surfaces may have some thin loess cover (Hamilton, 1994, 2003). Finally, I assumed the >2mm fraction does not weather appreciably (Nezat et al., 2004).

The depletion factor calculations also depend largely on what sample or samples are assumed to represent parent material, which is not as straightforward in this region as it is in some others because of the variable till

composition and the type of bedrock from which the till is derived. The glacial till in the study area is derived substantially from carbonates and shales, which can be mechanically ground into silt- and clay-sized particles during glacial transport. Therefore it was difficult to distinguish between (frozen) unweathered parent material and the (frozen) lowermost weathered mineral soil horizons in the field based on visual or textural characteristics (as it is for soils developed on crystalline bedrock, which often have "C" horizons containing recognizable fragments of bedrock). Furthermore, permafrost samples from individual pits proved unsuitable representations of parent material as they were not deep enough to have been excluded from weathering or cryoturbation during warmer periods, as will be discussed later. Therefore, for parent material values, a deep permafrost sample from 200-300 cm below the tundra was used; this sample was collected from a thermokarst collapse on the Sag1 surface (Chapters 2 and 4). Despite the slight compositional differences that might exist in the original till among the four different surfaces, this deep and solidly frozen sample was the closest available representation of original, unweathered parent material for all surfaces.

Long-term chemical weathering rate calculation. We used the depletion factors calculated above to estimate long-term chemical weathering rates for each surface following the method of Taylor and Blum (1995). We first calculated the total amount of each element that would have been in a 1 m^2 section of the unweathered parent material on any surface using the equation $U_{X,h}=(X_p)(\rho)(F_h)(T_h)$. In this equation X_p is the concentration of element X in the

parent material, ρ is the density of the parent material (we used the average density of 34 soil and permafrost samples from all four surfaces, 1.17 g/cm^3), F_h is the mean mass fraction of material <2mm in grain size, and T_h is the mean thickness of each horizon. The values of $U_{X,h}$ were then summed for each surface for a total initial amount of each element for that surface prior to weathering, I_X.

Next, the current amount of each element in a 1m^2 section on each surface was calculated using the depletion factors, with the equation $L_{X,h}= (d_{X,h})(U_{X,h})$. This equation does not take into account specific density of each horizon and therefore assumes equal density with the parent material, which for this area is a reasonable assumption; from our limited number of density samples there was no consistent trend of dilation or compaction within or between surfaces, or between active-layer soils and permafrost. We then summed $L_{X,h}$ over each surface profile to obtain a total amount of element X currently present in that profile, P_X. The total amount of each element weathered in a 1m^2 section of each surface was calculated by subtracting the current amount of each element present from the initial amount of that element present in the parent: $W_X=I_X-P_X$. W_X was then divided by Hamilton's (1986; 2003) ranges of inferred and radiocarbon ages for each surface to estimate a range of weathering rates for each element on each surface. A range of total weathering rates of major cations (Ca+K+Mg+Na) for each surface, R_{LT} in meq m^{-2} yr^{-1}, can then be calculated.

Results and Discussion

Depletion factors. Depletion factors and Zr concentration ratios calculated for the mean soil profile geochemical data are plotted in Figure 3-1. Zr increases or stays relatively consistent in concentration towards the top of three of the profiles, except for a slight decrease (from 1.1 to 0.9) towards the top of the oldest (Sag1) profile. The overall consistent or increasing concentrations suggest that Zr is in fact immobile; the decrease at the top of the oldest (Sag1) soil profile is most likely a result of loess input to this surface or parent heterogeneity. This slight decrease is noted as a caveat for further weathering calculations based on the assumption of Zr immobility, but it should not affect them substantially.

The depletion profiles in Figure 3-1 show that Ca, Mg, and K are generally depleted in the active layer relative to the permafrost on the two younger surfaces (It1 and 2). The older surfaces (Sag1 and 2) show less consistent within-profile trends; the exception is a slightly decreasing trend for Ca toward the surface of the Sag2 profile. Ca, a proxy for calcite weathering in these soils, is extremely depleted compared to the parent material on the three older surfaces and is depleted in the active layer compared to the permafrost in the three younger soil profiles. This suggests that carbonate weathering is the dominant weathering process in this area, which was predicted based on the prevalence of carbonates in the parent material. Silicate weathering intensity (as represented here by the K depletion factor, as a proxy for the biotite found in the parent material) appears to decrease with depth on the It2 and It1 surfaces, but

the other surfaces do not show a clear trend. Depletion factors indicate that K, like Ca, is depleted in the active layer compared to the permafrost in the three younger soil profiles.

Trends with geomorphic surface age in both Ca and K depletion factors are unclear; depletion of these elements appears to increase with age among the Sag1, It1, and It2 surfaces, but the values are too variable within the Sag2 profile to evaluate whether this surface falls in line with this trend. The youngest (It2) surface shows the least amount of depletion for all elements in all horizons except for K in the top horizon (and in fact this surface sometimes has a depletion factor greater than 1, probably indicating a discrepancy between the actual parent material for this surface and the sample assumed to represent parent material). However, the three older surfaces do not show a consistent pattern with age.

This lack of both age-related trends and within-profile trends on the older surfaces, along with our observations of cryoturbation features during sampling, suggests that cryoturbation may have mixed the soil on these surfaces to the extent that weathering patterns with depth and age are not detectable, with the exception of some trends associated with carbonate weathering. The fact that most of the observable trends on the older surfaces (Ca on It1 and Sag2, Mg on It1) relate to calcite weathering could suggest that calcite weathers in frequently thawed soil faster than cryoturbation can replenish it with unweathered minerals from less-frequently thawed layers.

The lack of significant trends in depletion factors contrasts with the more consistent changes in concentrations of carbonate weathering products and geochemical indicators of the carbonate content in streams and soils which correlate with both geomorphic surface age and horizon depth presented by Keller et al. (2006; Chapter 2). Ca depletion factors do not decrease consistently with depth throughout the active layer on all surfaces, as would be predicted based on the trends in carbonate weathering intensity interpreted from $^{87}Sr/^{86}Sr$ trends with depth (Keller et al., 2006).

There are several potential reasons for the lack of a clear trend in soil depletion factors with surface age. First, there are weaknesses with the assumption that sediments now frozen in permafrost on the Sag1 surface constitute representative parent material from all surfaces. The lower horizons on the It2 surface have Ca depletion factors greater than 1, as well as absolute Ca concentrations slightly greater than those of the Sag1 material used as a parent material proxy (0.33 vs. 0.26 mmol/g), indicating that at least the It2 surface had parent material which started with higher Ca concentrations (probably due to a higher proportion of carbonates in the till) compared to the Sag1 material. Furthermore, though these sediments are currently buried fairly deeply and frozen, they may have been subjected to weathering during periods of warmer climate or diluted by weathered sediments via cryoturbation since the onset of soil development hundreds of thousands of years ago.

Another possible reason that the depletion factors do not show expected patterns is the effect of cryoturbation throughout the soil profiles. Numerous

studies have suggested the importance of cryoturbation in soil profiles in this area (e.g. Ping et al., 1998; Swanson et al., 1999; Munroe and Bockheim, 2001). It is possible that even in soil profiles where no cryoturbation features are currently visible, some cryoturbation has occurred in the past, and the visible evidence (e.g. warped horizon boundaries) has been erased by soil processes (e.g. discoloration by redox reactions) but the soil minerals remain physically relocated. Bockheim et al. (1998) found that cryoturbation contributes to maintaining non-acidic tundra, which has high levels of exchangeable Ca and other base cations. The data presented here suggest that even in moist acidic tundra with lower levels of cryoturbation, the effects of cryoturbation mix soil minerals throughout the profile enough to confound detection of a relationship between weathering intensity and depth (e.g. the Sag2, and Sag1 profiles in figure 3-1). Therefore, on surfaces of all geomorphic ages and acidity conditions, cryoturbation may play an important role in the release of mineral nutrients to the ecosystem via the upward mixing of less-weathered minerals.

Long-term chemical weathering rates. Long-term chemical weathering rates calculated using the depletion factors are presented in Table 3-1. Because only one of the glacial deposit surfaces is radiocarbon dated within a narrow age range and the others have broad inferred age ranges (Hamilton, 1986, 2003), we estimated ranges of long-term weathering rates for each of the It2 and It1 surfaces, and one range for the entire Sag2-Sag1 glaciation using the ages bracketing that period. Despite the difficulties in interpreting depletion factors discussed above, the accuracy of this calculation should be less affected by the

mixing effects of cryoturbation. If only active-layer soils are analyzed, long-term weathering rate calculations could be affected by cryoturbation, which, by physically replenishing unweathered material, can lead to soils appearing less chemically weathered and to the calculation of an artificially low long-term weathering rate. To avoid this, we included the upper permafrost, below which cryoturbation is unlikely to occur, in our analyses. However, as discussed above, it is impossible to know the extent of soil mixing during earlier periods of warmer climate, so it is possible that some of the estimated rates are too low because of past cryoturbation. The previously discussed concerns regarding the identification of unweathered parent material also affect the R_{LT} calculation, and because the parent material sample used does not appear to be a suitable proxy for It2 parent material, the R_{LT} estimate for that surface is likely somewhat low.

Our calculated estimates for total R_{LT} as well as long-term weathering rates of Ca and Mg for the two younger surfaces are roughly 10-20 times lower than rates calculated by Lichter (1998) for soils developed on 4000 year old temperate sand dunes that also included carbonate minerals. These lower rates are congruent with the older age and colder climate of our study area. For both our study area and the soils in Lichter's (1998) study, the dominant weathering process is carbonate dissolution which is not decreased by lower temperature. Still, because of the very short duration of soil thaw, the colder climate of our study area would still be expected to lead to lower carbonate (and therefore overall) weathering rates.

Some silicate weathering rates and weathering rates of accessory minerals, however, were unexpectedly high when compared to the temperate sand dune study. The estimated weathering rates for K on the It1 and It2 surfaces were tens of times higher than those in the sand dune study, and the weathering rate of P on the It1 surface was roughly double that of the sand dune study, despite the age and climate differences. These differences might be attributable to differences in parent material mineralogy. The K in this study is derived from biotite, whereas the K in the sand dune study was derived from potassium feldspar (Lichter, 1998), which is slightly more resistant to weathering (Easterbrook, 1999). In the arctic study area, chemistry of the rock units suggests the P is associated with sandstones, shales, and carbonates, and soil chemistry Ca:P ratios suggest that the mineral form of the P is apatite (Keller et al., 2006). In the sand dune study, the source of P is also hypothesized to be apatite, although chemical data suggest it is primarily biogenic apatite (i.e. shell fragments), which may affect how it is weathered; it may also become immobilized in the soil after weathering (Lichter, 1998).

There is some difficulty in comparing long-term weathering rates calculated from soil profiles and present-day weathering rates calculated from watershed cation fluxes, because watershed flux calculations integrate over a large spatial area but only a short time (the duration of the study), while soil calculations usually average a few points on a surface but integrate over a very long time. Therefore, calculations of present-day rates may be influenced by short term variability in the weathering rate, whereas calculations of long-term rates

(especially single-soil-profile studies) are more likely influenced by spatial variability. Despite these general difficulties with comparison, Taylor and Blum (1995) derived an equation suggesting that present-day weathering rates should be approximately one-third the value of long-term weathering rates at any point in time for a particular soil. Although present-day estimates are not available for this study area due to lack of atmospheric deposition data, we can compare the long-term weathering rates calculated in this study to the present-day rates calculated for the mixed carbonate and silicate sedimentary Mackenzie River basin in a thorough study by Millot et al. (2003). Rivers in the Mackenzie River drainage area have carbonate denudation rates between 2 and 58 tons/(km^2*yr) and total denudation rates between roughly 3 and 59 tons/(km^2*yr) (Millot et al., 2003); these rates are approximately 1/3 to 1/7 the long-term rates calculated for this study of Alaskan soils (13-410 tons/(km^2*yr) total). This relationship is similar to the 1/3 ratio between long-term and present day weathering rates predicted by Taylor and Blum (1995), although our long-term rates are slightly higher than expected. The slightly higher values for our estimates likely reflect differences in parent material between the North Slope and the Mackenzie River basin, which includes some metamorphic units and is primarily bedrock rather than glacial till.

Taylor and Blum (1995) demonstrated a power-law relationship between soil age and weathering rate for soils developed on silicate parent material (Figure 3-2): $R_{LT}=215t^{(-0.71)}$, with R_{LT} in meq m^{-2} yr^{-1} and t in thousands of years. This equation was based on soils developed in temperate climates on granitic parent material, but the rates calculated in this study (Table 3-1) suggest that a power-

law relationship between long-term weathering rate and age exists in the arctic on carbonate-rich parent material as well. When all the age-range data for all the surfaces is included, the equation that best defines this relationship is $R_{LT}=74.9t^{(-0.66)}$, which has an R^2 of 0.74 with the data points from the study. If the data from the It2 surface is excluded on the basis that the depletion factors greater than 1 for Ca, Mg, Na, and P may indicate a slightly different parent material and therefore an inaccurate calculation of R_{LT}, the equation for the best-fit line becomes $R_{LT}=1089t^{(-1.14)}$, which has an R^2 of 0.98 (Figure 3-2). This line has a steeper slope than that based on granitic parent material, which might be expected given the faster initial weathering rates of carbonate parent material. The steepness of the line may also be affected if older surfaces have artificially low estimates of R_{LT} due to cryoturbation, but it is difficult to determine whether this is a factor without another carbonate system for comparison.

Conclusion

I calculated elemental depletion factors and long-term weathering rates for four 11-780 ka carbonate-rich glacial deposit surfaces using Zr as the immobile element, and using a deep permafrost sample from the oldest surface as a proxy for parent material. The results showed a correlation between Ca, Mg, and K depletion factors with depth on the younger surfaces, but there were no consistent trends on the older surfaces, for other elements, or for surface age, probably as a result of cryoturbation in the soil profiles. Ca is generally depleted compared to the parent material on all surfaces, suggesting that carbonate

weathering is the dominant weathering process in this region as predicted. Calculating depletion factors in this permafrost region presented unique problems related to cryoturbation and assumptions regarding parent material. Long-term weathering rate estimates suggest that the carbonate-dominated rates in this area have a power-law relationship with age similar to, but steeper than, that of silicate rates in temperate regions.

Table 3-1: Long-term weathering rates and related values estimated for soils on each glacial surface. The R_{LT} estimated for the Sag2 surface uses the lower end of the inferred age range for the entire Sag glaciation, the Sag1 estimate uses the upper end.

Glacial surface	surface age range (ka)*	total amount weathered (W_X, in mol/m^2) Ca	K	Mg	Na	total R_{LT} (meq/(m^2*yr))
It 2	11.5-24	6.0	121.7	3.3	-16.4	5.2-10.8
It 1	50-120	96.2	174.8	75.4	15.5	4.5-10.7
Sag 2	125-780	131.0	248.5	85.6	22.0	5.6
Sag 1		77.4	145.1	56.7	-0.8	0.5

Figure 3-1: Depletion factors for five elements, and Zr concentration ratios plotted vs. depth in each profile on the four glacial surfaces.

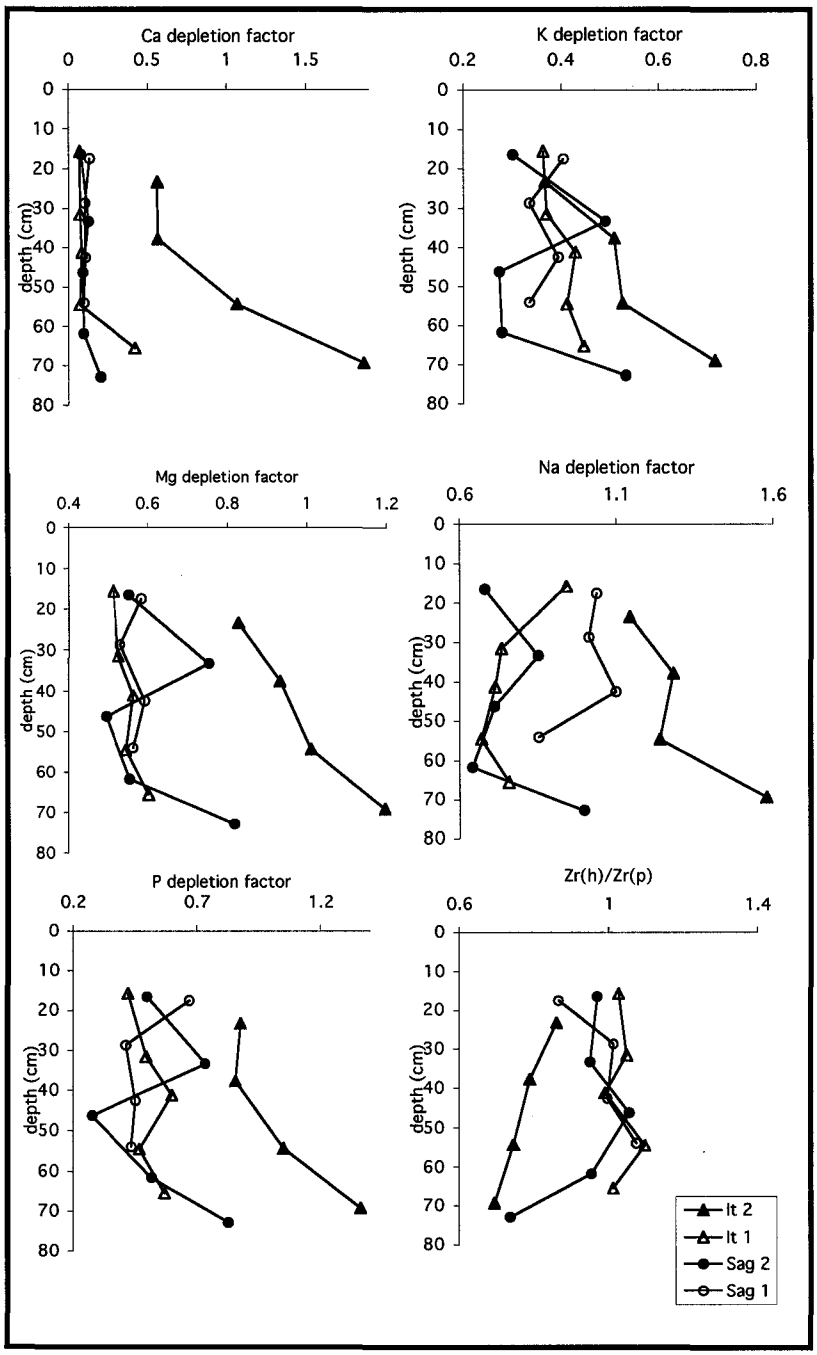

Figure 3-2: Log-log plot of long-term weathering rates vs. soil age for a temperate granitic chronosequence (open circles) calculated by Taylor and Blum (1995) and for the mixed sedimentary chronosequence in this study (closed squares). Dashed line is the best-fit curve to the granitic chronosequence; solid line shows the best-fit curve for the data from this study.

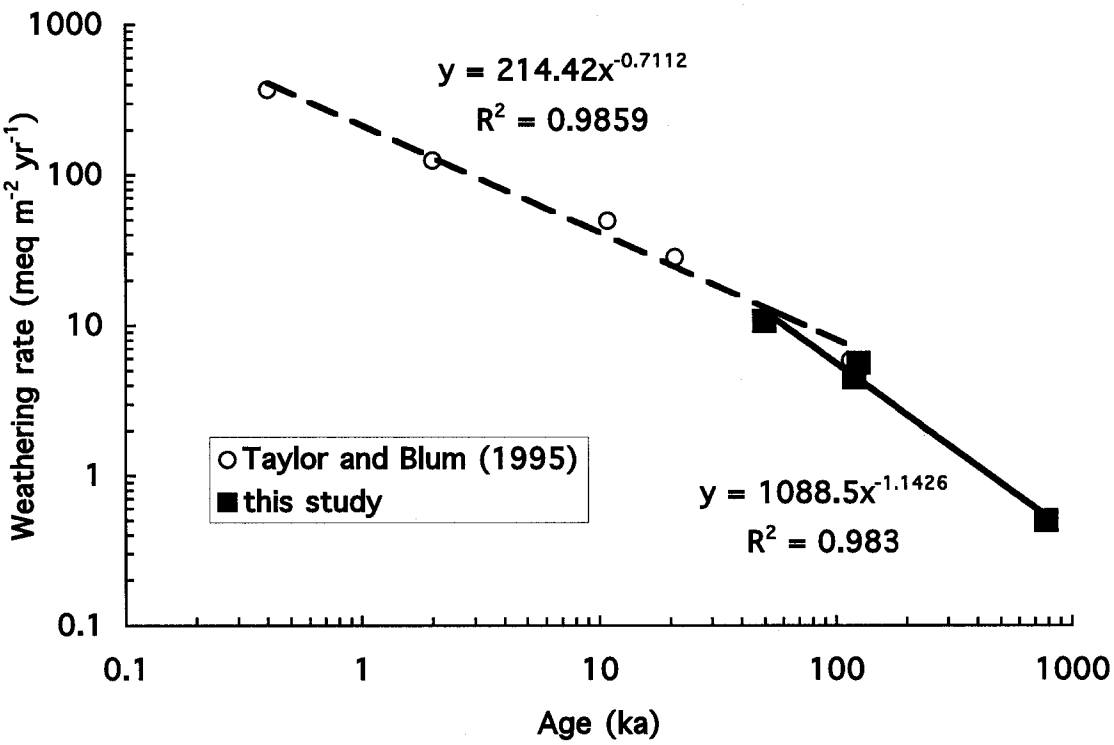

References Cited

April, R. H., Newton, R. M., and Coles, L. T., 1986: Chemical weathering in two Adirondack watersheds: past and present-day rates. *Geological Society of America Bulletin,* 97: 1232-1238.

Bain, D. C., Mellor, A., Robertsonrintoul, M. S. E., and Buckland, S. T., 1993: Variations in Weathering Processes and Rates with Time in a Chronosequence of Soils from Glen-Feshie, Scotland. *Geoderma,* 57: 275-293.

Berner, R. A., Lasaga, A. C., and Garrels, R. M., 1983: The carbonate-silicate geochemical cycle and its effect on atmospheric carbon dioxide over the past 100 million years. *American Journal of Science,* 283: 641-683.

Beyer, L., Pingpank, K., Wriedt, G., and Bolter, M., 2000: Soil formation in coastal continental Antarctica (Wilkes Land). *Geoderma,* 95: 283-304.

Dahlgren, R. A., Boettinger, J. L., Huntington, G. L., and Amundson, R. G., 1997: Soil development along an elevational transect in the western Sierra Nevada, California. *Geoderma,* 78: 207-236.

Darmody, R. G., Thorn, C. E., Dixon, J. C., and Schlyter, P., 2000: Soils and landscapes of Karkevagge, Swedish Lapland. *Soil Science Society of America journal,* 64: 1455-1466.

Easterbrook, D. J., 1999: *Surface processes and landforms*. second edition ed. New Jersey: Prentice Hall, 546 pp.

Fyfe, J. C., Boer, G. J., and Flato, G. M., 1999: The Arctic and Antarctic Oscillations and their projected changes under global warming. *Geophysical Research Letters,* 26: 1601-1604.

Hamilton, T. D., 1978: Surficial geologic map of the Philip Smith Mountains Quadrangle, Alaska, MF-879. Reston, VA: Department of the Interior, United States Geological Survey.

Hamilton, T. D., 1986: Late Cenozoic glaciation of the Central Brooks Range. *In* Hamilton, T. D., Reed, K. M., and Thorson, R. M. (eds.), *Glaciation in Alaska: the geologic record.* Anchorage, AK: Alaska Geological Society, 265.

Hamilton, T. D., 1994: Late Cenozoic glaciation of Alaska. *In* Plafker, G. (ed.), *The geology of Alaska.* Boulder, CO: Geological Society of America, 1055.

Hamilton, T. D., 2003: *Glacial geology of Toolik Lake and the Upper Kuparuk River region*. Fairbanks, Alaska: Alaska Geobotany Center, Institute of Arctic Biology, University of Alaska Fairbanks, 24 pp.

Hasholt, B. and Hagedorn, B., 2000: Hydrology and geochemistry of river-borne material in a high arctic drainage system, Zackenburg, Northeast Greenland. *Arctic, Antarctic and Alpine research,* 32: 84-94.

Hobbie, S. E., Miley, T. A., and Weiss, M. S., 2002: Carbon and nitrogen cycling in soils from acidic and nonacidic tundra with different glacial histories in Northern Alaska. *Ecosystems,* 5: 761-774.

Keller, K., Blum, J. D., and Kling, G. W., 2006: Geochemistry of soils and streams on surfaces of varying ages in arctic Alaska. *Arctic, Antarctic, and Alpine Research,* in press.

Kirkwood, D. E. and Nesbitt, H. W., 1991: Formation and Evolution of Soils from an Acidified Watershed - Plastic Lake, Ontario, Canada. *Geochimica et Cosmochimica Acta,* 55: 1295-1308.

Lichter, J., 1998: Rates of weathering and chemical depletion in soils across a chronosequence of Lake Michigan sand dunes. *Geoderma,* 85: 255-282.

Louvat, P. and Allegre, C. J., 1997: Present denudation rates on the island of Reunion determined by river geochemistry: Basalt weathering and mass budget between chemical and mechanical erosions. *Geochimica et Cosmochimica Acta,* 61: 3645-3669.

Menzie, W. D., Reiser, H. N., Brosge, W. P., and Detterman, R. L., 1985: Map showing distribution of mineral resources (excepting oil and gas) in the Philip Smith Mountains quadrangle, Alaska (Map MF-879-C). Reston: United States Geological Survey.

Millot, R., Gaillardet, J., Dupre, B., and Allegre, C. J., 2003: Northern latitude chemical weathering rates: Clues from the Mackenzie River Basin, Canada. *Geochimica et Cosmochimica Acta,* 67: 1305-1329.

Moore, T. E., Wallace, W. K., Bird, K. J., Karl, S. M., Mull, C. G., and Dillon, J. T., 1994: Geology of northern Alaska. *In* Plafker, G. and Berg, H. C. (eds.), *The Geology of Alaska*. Boulder, Colorado: Geological Society of America.

Mull, C. G. and Adams, K. E., 1985: *Bedrock Geology of the eastern Koyukuk Basin, central Brooks Range, and east central Arctic Slope along the Dalton Highway, Yukon River to Prudhoe Bay*. Anchorage: Alaska Department of Natural Resources, Division of Geological and Geophysical Surveys, 309 pp.

Munroe, J. S. and Bockheim, J. G., 2001: Soil development in low-arctic tundra of the northern Brooks Range, Alaska, USA. *Arctic and Alpine Research,* 33: 78-87.

Nezat, C. A., Blum, J. D., Klaue, A., Johnson, C. E., and Siccama, T. G., 2004: Influence of landscape position and vegetation on long-term weathering rates at the Hubbard Brook Experimental Forest, New Hampshire, USA. *Geochimica et Cosmochimica Acta,* 68: 3065-3078.

Ping, C. L., Bockheim, J. G., Kimble, J. M., Michaelson, G. J., and Walker, D. A., 1998: Characteristics of cryogenic soils along a latitudinal transect in Arctic Alaska. *Journal of Geophysical Research-Atmospheres,* 103: 28917-28928.

Reiger, S., 1974: Arctic soils. *In* Ives, J. D. and Bary, R. G. (eds.), *Arctic and Alpine Environments*. London: Methuen, 749-769.

Shindell, D. T., Miller, R. L., Schmidt, G. A., and Pandolfo, L., 1999: Simulation of recent northern winter climate trends by greenhouse-gas forcing. *Nature,* 399: 452-455.

Swanson, D. K., Ping, C. L., and Michaelson, G. J., 1999: Diapirism in soils due to thaw of ice-rich material near the permafrost table. *Permafrost and Periglacial Processes,* 10: 349-367.

Taylor, A. and Blum, J. D., 1995: Relation between soil age and silicate weathering rates determined from the chemical evolution of a glacial chronosequence. *Geology,* 25: 382-383.

Walker, J. C. G., Hays, P. B., and Kasting, J. F., 1981: A negative feedback mechanism for the long-term stabilization of Earth's surface temperature. *Journal of Geophysical Research,* 86: 9776-9782.

Walsh, J. E. and Crane, R. G., 1992: A comparison of GCM simulations of arctic climate. *Geophysical Research Letters,* 19: 29-32.

White, A. F. and Blum, A. E., 1995: Effects of climate on chemical weathering in watersheds. *Geochimica et Cosmochimica Acta,* 59: 1729-1747.

White, A. F., Blum, A. E., Schulz, M. S., Vivit, D. V., Stonestrom, D. A., Larsen, M., Murphy, S. F., and Eberl, D., 1998: Chemical weathering in a tropical watershed, Luquillo mountains, Puerto Rico: I. Long-term versus short-term weathering fluxes. *Geochimica et Cosmochimica Acta,* 62: 209-226.

White, A. F., Blum, A. E., Bullen, T. D., Vivit, D. V., Schulz, M., and Fitzpatrick, J., 1999: The effect of temperature on experimental and natural chemical weathering rates of granitoid rocks. *Geochimica et Cosmochimica Acta,* 63: 3277-3291.

Wood, A. K. H., Ahmad, Z., Shazili, N. A. M., Yaakob, R., and Carpenter, R., 1997: Geochemistry of sediments in Johor Strait between Malaysia and Singapore. *Continental Shelf Research,* 17: 1207-1228.

CHAPTER 4

STREAM GEOCHEMISTRY AS AN INDICATOR OF THAW DEPTH IN AN ARCTIC WATERSHED

Abstract

Permafrost influences arctic hydrology, ecology, and society; understanding the response of permafrost to recent warming is critical to predicting the regional effects of global climate change. Recent research suggests that thaw depth may be increasing in response to warming, but physical thaw depth surveys in the Alaskan arctic are not sensitive enough to detect incremental increases and cannot measure increases in the thaw bulbs beneath lakes and streams. Here we demonstrate the use of geochemical tracers in stream water to assess changes in thaw depth in an arctic watershed. Based on marked differences in geochemistry with depth in soils and permafrost on the Alaskan North Slope, we used $^{87}Sr/^{86}Sr$ and elemental ratios in an arctic stream as tracers of the maximum depth of soil water flow and therefore integrated thaw depth in the watershed. From 1994 to 2004, mean low-discharge late summer stream $^{87}Sr/^{86}Sr$ decreased from 0.7122 to 0.7119 (R^2=0.62, p=0.012), and Ca/Na and Ca/Ba showed significant increasing trends that were consistent with increasing depth of soil water flowpaths, providing new evidence for increasing

thaw depth. Stream geochemistry may be useful as a qualitative indicator of changes in thaw depth in other areas where permafrost and active-layer soil geochemistry differs.

Introduction

Arctic Alaskan temperature records show a mean annual increase of 2.4°C from 1974 to 2003 (Alaska Climate Research Center, 2003). An important consequence of warming climate in these regions is increasing summer thaw depth (active layer thickness), which impacts hydrology (Michel and Vaneverdingen, 1994; Rouse et al., 1997), mineral weathering and nutrient supply (Keller et al., 2006), vegetation growth (Lloyd et al., 2003), organic carbon storage and decomposition (Waelbroek et al., 1997; Turestsky et al., 2002), and engineered structures (Nelson et al., 2001). There is considerable direct, physical evidence for increasing thaw depth and permafrost degradation in discontinuous permafrost zones (Jorgenson et al., 2001; Payette et al., 2004; Camill, 2005). In addition, models suggest that active layer thickness in some continuous permafrost zones has already increased up to 21% over the 20th century (Chen et al., 2003), and predict further increases of up to 40% by the end of the 21st century (Stendel and Christensen, 2002).

However, direct measurement of increases in active layer thickness in continuous permafrost regions has been less conclusive. Temperature increases of 2-4°C have been observed since 1977 at still-frozen depths in the continuous permafrost of arctic Alaska (Osterkamp, 2005), and a single-station

measurement in Siberia showed increases in active layer thickness (Pavlov and Moskalenko, 2002). Yet out of 12 thaw depth surveys from the continuous permafrost zone of arctic Alaska, only two surveys (near Barrow) showed a weak trend of increasing active layer thickness (Brown et al., 2000; Hinkel and Nelson, 2003). These large-scale thaw depth surveys are complicated by spatial heterogeneity in active layer thickness caused by variability in soil moisture content, small-scale topography, and larger landscape features (Hinkel and Nelson, 2003).

Because of this spatial variability in active layer thickness, traditional thaw depth surveys, which make many physical measurements over a large area using graduated steel probes, are not sensitive enough to detect small changes in active layer thickness. For example, over a 1 km^2 watershed near Toolik Lake in arctic Alaska, mean August thaw depth from 1990-2005 was 39.0 cm and the mean standard deviation of these yearly measurements was 8.8 cm or about 23% of the mean (n=3551 total measurements; 170-288 measurements per year) (Arctic Long Term Ecological Research Site, 2005a). More importantly, increases in active layer thickness may be concentrated in areas where thaw depth is difficult to measure. For example, thaw bulbs beneath lakes and streams are likely locations for active layer thickness increases because hyporheic waters have been shown to be important conduits of heat transfer in permafrost zones (Conovitz et al., 2006). Here, as an alternative to traditional physical measurements of thaw depth, we use geochemical tracers in stream water that spatially integrate over the watershed, avoiding difficulties caused by small-scale

spatial variation and physical barriers, and allowing detection of an increase in thaw depth.

Strontium isotope and elemental ratios have been used extensively to trace water sources and hydrologic flowpaths and are often more sensitive to subtle changes in flowpaths than elemental concentrations (Blum and Erel, 2004). For instance, Hogan and Blum (2003) used $^{87}Sr/^{86}Sr$, Ca/Sr, and Ba/Sr in a granitic watershed to distinguish groundwater, shallow subsurface flow, and throughfall contributions to a stream during rain events. Land et al. (2000) used these same geochemical tracers in a subarctic granitic watershed to separate contributions to a stream from three subsurface flowpaths based on the geochemical profile created by decreasing weathering intensity with depth. Bullen and Kendall (1998) used $^{87}Sr/^{86}Sr$ and other tracers in a Vermont watershed to discriminate between carbonate-free flowpaths and flowpaths influenced by carbonate weathering.

Arctic Alaskan permafrost and infrequently thawed soils developed on several expansive glacial till surfaces of different ages have substantially higher concentrations of carbonate minerals than the more weathered soils in the active layer above them (Keller et al., 2006). Specifically, in the "easily weatherable," mostly carbonate fraction of the mineral soil (as estimated by a 1M HNO_3 soil digest), Ca/Na and Ca/Ba generally increase with depth and reach their maxima in the permafrost, whereas $^{87}Sr/^{86}Sr$ decreases with depth (Figure 4-1). Because carbonate content increases with depth in the soil and permafrost profile, in the case of increasing active layer thickness, water traveling along the deepest

possible soil flowpath will incorporate increasing amounts of carbonate weathering products. Therefore, any increase in active layer thickness should result in increasing Ca/Na and Ca/Ba and decreasing $^{87}Sr/^{86}Sr$ in late summer deep soil flowpath contributions to stream water. In order to best detect these deep soil flowpath contributions in stream water chemistry and minimize the variations caused by dilution of deep flowpath geochemical signals by overland or shallow flow during or after precipitation events, measurements can be restricted to low-discharge conditions. This allows the use of $^{87}Sr/^{86}Sr$, Ca/Na, and Ca/Ba as qualitative indicators of increases in the maximum depth of soil water flow and integrated thaw depth across the watershed.

The objective of this study was to detect increases in thaw depth indicated by changes over time in the $^{87}Sr/^{86}Sr$, Ca/Na, and Ca/Ba values of late summer, low-discharge samples of an arctic stream. We predicted that $^{87}Sr/^{86}Sr$ would decrease while Ca/Na and Ca/Ba would increase as a result of increasing spatially integrated soil water flowpaths. To accomplish this objective, we measured the elemental concentrations and $^{87}Sr/^{86}Sr$ of samples taken during 1994-2004 from Toolik Inlet stream in arctic Alaska.

Study area

Toolik Inlet stream was sampled near where it enters Toolik Lake (68°38'N, 149°36'W, Figure 4-2) in the foothills of the North Slope of the Brooks Range, Alaska, USA. The Toolik Inlet stream watershed is underlain by soils and continuous permafrost with the average geochemical profiles shown in Figure 4-

1. The soils are developed on two relatively young (roughly 100-50 ka and 25-10 ka) glacial till and outwash deposits comprised primarily of sedimentary rocks, including carbonates (Mull and Adams, 1985; Hamilton, 2003). The soils are gelisols (Munroe and Bockheim, 2001) and consist of a thick organic layer, which is the primary soil water flowpath, overlying mineral soil with lower hydrologic conductivity (Hinzman et al., 1991). The watershed is dominated by upland tussock tundra vegetation, and includes riparian birch-willow and wet sedge vegetation. Toolik Inlet stream is a third-order tundra stream; it drains a 46.6 km^2 watershed that includes several lakes. Summer thaw lasts from late May through September; during this time active layer thickness reaches 0.3-1.0 m (Kling et al., 2000). This watershed is transected by a two-lane gravel road (the Dalton Highway) and an elevated section of the Trans-Alaska Pipeline, which were completed in 1977 and have been relatively unchanged since then; thus, we believe they have no influence on the time-dependent trends of interest in this study.

Methods and Data analysis

Toolik Inlet stream stage height and flow measurements were recorded every thirty seconds on a datalogger and averaged hourly to calculate discharge (Arctic Long Term Ecological Research Site, 2005b). Stream water samples were collected weekly during the late summers (July 1-August 21) of 1994-2004, excluding 1995 when no sample collection occurred at this site. Stream water samples were filtered through either borosilicate glass fiber filters (1994-2001) or

0.45 micron polypropylene filters (2002-2004). They were acidified with tracemetal grade (1994-2001, 2004) or ultrapure HCl (2002-2003) immediately after collection and refrigerated at 10°C until analysis. Four replicate stream samples were taken in 2002 to test for differences in results between samples collected using borosilicate glass filters and trace-metal grade acid versus those collected using polypropylene filters and ultrapure acid. No significant differences in $^{87}Sr/^{86}Sr$ between the paired samples were found in a paired t-test ($p=0.8$); only one of the four sample pairs had $^{87}Sr/^{86}Sr$ values that differed by more than the 2σ analytical error, and they differed by less than 0.008%.

Samples were analyzed for elemental concentrations by inductively coupled plasma optical emission spectrometry. One in-house standard and two NIST traceable commercial standards were used for quality control; these standards were analyzed to within ±7% of the known value for Ba, ±6% for Ca, and ±8% for Na. Sr was separated by elution through Sr-specific resin (Eichrom) in quartz cation exchange columns and approximately 75 ng of Sr was loaded onto a tungsten filament with Ta_2O_5 powder. The Sr isotopic ratio was determined by thermal ionization mass spectrometry using a Finnigan MAT 262. Internal precision ($\pm 2\sigma$) of 100-200 ratios for each sample was less than ±0.000035, and replicate analyses of NBS987 yielded $^{87}Sr/^{86}Sr$ of 0.710233 ±0.000004 (2σ, n=112).

To better isolate the deep soil flowpath geochemical signal, we restricted the data set to samples taken during "low-discharge" conditions. This is necessary because precipitation events can cause saturation of the organic mat

and shallow soils, which have high acid digestible $^{87}Sr/^{86}Sr$ values (up to 0.72065 for organic mat (Keller et al., 2006); soil values shown in Figure 4-1). As a result, the high $^{87}Sr/^{86}Sr$ signal of water from these shallow and overland flowpaths overwhelms the geochemical signal of deep flowpaths that may indicate changes in active layer thickness. The evidence for this process is a positive correlation between Toolik Inlet stream water $^{87}Sr/^{86}Sr$ values and the natural log of stream discharge (R^2=0.41, p<0.0001, n=87). When the data set is restricted to "low discharge" samples taken when discharge was less than the 1994-2004 summer (June 1-August 21) mean discharge of 1.1 m^3/s, $^{87}Sr/^{86}Sr$ is less strongly correlated to discharge (R^2=0.24, p<0.0001, n=58); suggesting that variations in $^{87}Sr/^{86}Sr$ in this sample set are less influenced by varying shallow flowpath contributions. In subsequent analyses, we consider time trends for only low-discharge (<1.1 m^3/s) conditions; as a result of this restriction, all 2003 samples are eliminated due to high discharge on each sampling date.

Results and Discussion

Between 1994 and 2004, late summer Toolik Inlet stream water $^{87}Sr/^{86}Sr$ decreases significantly and is correlated with year (Figure 4-3A). Over the same time period, there are significant increases in both late summer Ca/Ba (Figure 4-3B) and Ca/Na (Figure 4-3C). When considering all three trends, the best-fit lines were simple linear regressions, as shown in Figure 4-3. The elemental ratios (Ca/Ba and Ca/Na) also showed significant trends with time even when the data were not restricted to low-discharge samples (p<0.0001, n=88 for both). It

is unlikely that the observed geochemical trends with time could be related to changing patterns of discharge because there is no correlation between year and discharge when samples were taken, either for the low-discharge sample set (R^2=0.008, p=0.51) or for the entire July-August 21 sample set (R^2=0.02, p=0.19). Therefore, these results are consistent with a greater influence of carbonate dissolution on stream geochemistry as a result of increasing depth of deep flowpaths, indicating increased thaw depth between 1994 and 2004.

The trends in stream geochemistry suggest that seasonally and spatially integrated thaw depth has increased in the Toolik Inlet stream watershed from 1994 to 2004, but do not indicate where in the watershed or to what extent. Furthermore, the mode of thaw depth increase or permafrost degradation is unknown. Thaw depth increases could be relatively uniform across the watershed or spatially patchy, occurring predominantly under surface waters or other places where the insulating soil organic mat is thin. It is possible that the trends are due to occasional melting of small areas of permafrost (e.g. small thermokarst slumps) rather than progressive thaw with time. It is also possible that some of the observed geochemical trend is due to an earlier and longer seasonal thaw of deep active layer soils, although this scenario would also likely result in an increase in thaw depth due to heat transfer through these soils into the upper permafrost.

The geochemical changes we observe in stream water indicate that thaw depth has increased over an 11-year observation period. In the two extreme cases there could be either a thin layer of material that is reacting extensively

with soil solution, or a thick layer that is reacting incompletely. We constrained the minimum thickness of active layer increase needed to cause the observed stream water $^{87}Sr/^{86}Sr$ changes with a simple mass balance calculation based on the extreme assumption that all newly thawed soil carbonate completely reacted with soil water each season. We estimated the July and August flux of Sr from Toolik Inlet stream (for July-August mean Q=1.2 m^3/s, [Sr]=0.23 μmol/L). We then calculated the amount of Sr with the $^{87}Sr/^{86}Sr$ of the upper permafrost necessary to produce the observed trend, assuming that the younger surface covers 34% of the watershed, and the remainder is covered by the older surface (Hamilton, 2003). A 3x deionized water (pH=5.5) batch leach of permafrost samples at 20°C for 72 hours yielded Sr concentrations and isotope ratios (older surface: 0.005 umol/L, 0.711711; younger surface: 0.009 umol/L, 0.710103) that were used to estimate the maximum effect of soil thawing on stream chemistry. Averaging over the entire watershed (46.6 km^2) we find that only 1.3 cm of permafrost would have to thaw between 1994 and 2004 and react with soil water to produce the observed effect on stream water. Because natural waters likely react less completely with soil and permafrost than in our laboratory batch leach, this is a low estimate of the newly thawed layer thickness. In addition, thaw is likely to be spatially heterogeneous and perhaps concentrated beneath lakes and streams or in other areas with reduced organic mat thickness. Despite the simplified nature of this calculation, it illustrates that a small amount of permafrost thaw could produce changes in stream geochemistry, yet be too small or physically inaccessible to detect by traditional measurements of thaw depth.

Implications and Conclusions

The geochemical method we used here to detect a change in thaw depth across the Toolik Inlet stream watershed may be applicable to many different permafrost areas where streams are (or were) sampled regularly. Soil geochemical profiles of other landscape surfaces on the North Slope have increasing carbonate content with depth (Keller et al., 2006), and in the Canadian Arctic on a different type of parent material, soils also have a depth-dependent geochemical profile (Kokelj et al., 2002). Less-intensely weathered soil at depth may provide geochemical gradients in many permafrost regions sufficient to cause changes in stream geochemistry as a result of changes in active layer thickness. Based on the results of this study, we propose that that (1) thaw depth has increased in this part of the Arctic and has influenced surface water chemistry, and (2) stream geochemistry provides a sensitive, albeit qualitative, indicator of thaw depth that may be useful in many areas as a compliment or an alternative to physical thaw depth surveys.

Acknowledgements

A slightly shortened version of this paper is currently in review in *Geology* under the same title as the Chapter in this dissertation, with Joel Blum and George Kling as co-authors. This study was supported by National Science Foundation grants DEB-0423385, DEB 97-26837, ATM-0439620, and ARC-

0435893. Field work was supported by a student grant from the Geological Society of America to Keller. We thank B. Kennedy for thoughtful comments.

Figure 4-1: Mean 1M HNO_3 cold acid digestible A) $^{87}Sr/^{86}Sr$, B) Ca/Ba, and C) Ca/Na of each mineral soil horizon vs. mean horizon depth for the older and younger geomorphic surfaces developed on glacial till underlying the Toolik Inlet stream watershed. The lowermost points on each surface represent permafrost. Elemental ratios are calculated from measurements made in mol/g with an analytical error of <±7%; $^{87}Sr/^{86}Sr$ analytical error (2σ) is <±0.000040. Error bars represent standard error (n=3). Detailed data and methods reported in Keller et al. (Keller et al., 2006).

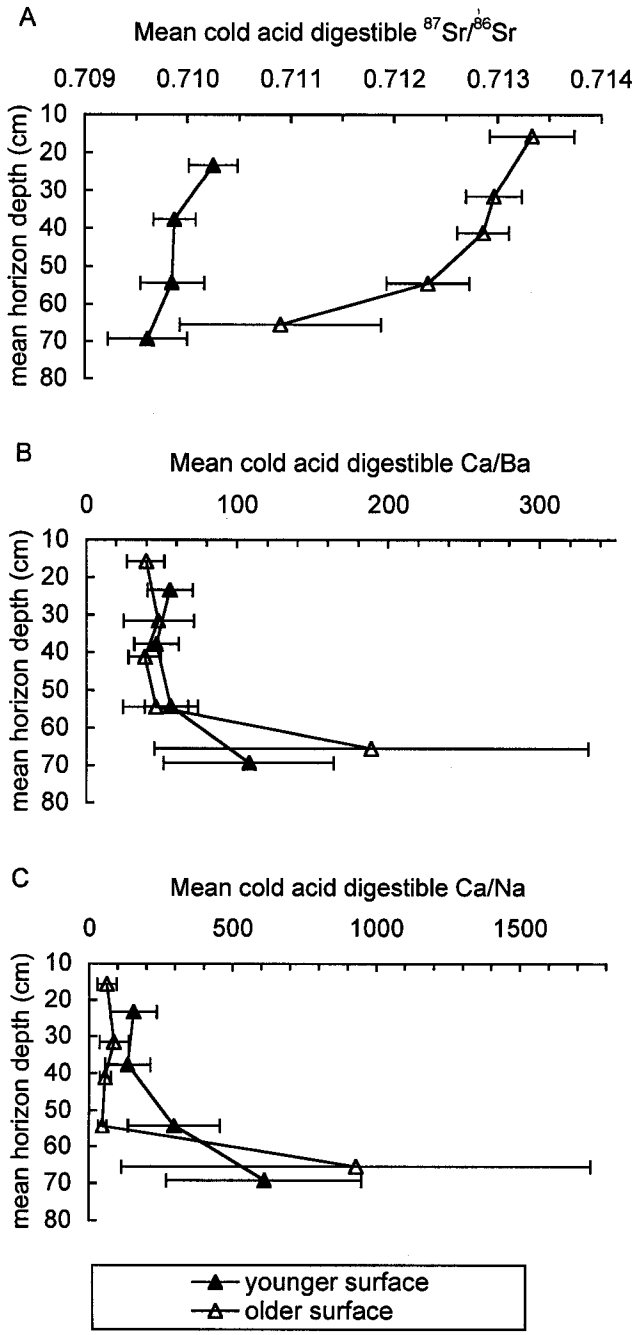

Figure 4-2: Map of Toolik Inlet stream watershed and sampling site. Shaded regions show area covered by Itkillik 1 (older) and Itkillik 2 (younger) glacial till and outwash surfaces referred to in Figure 4-1.

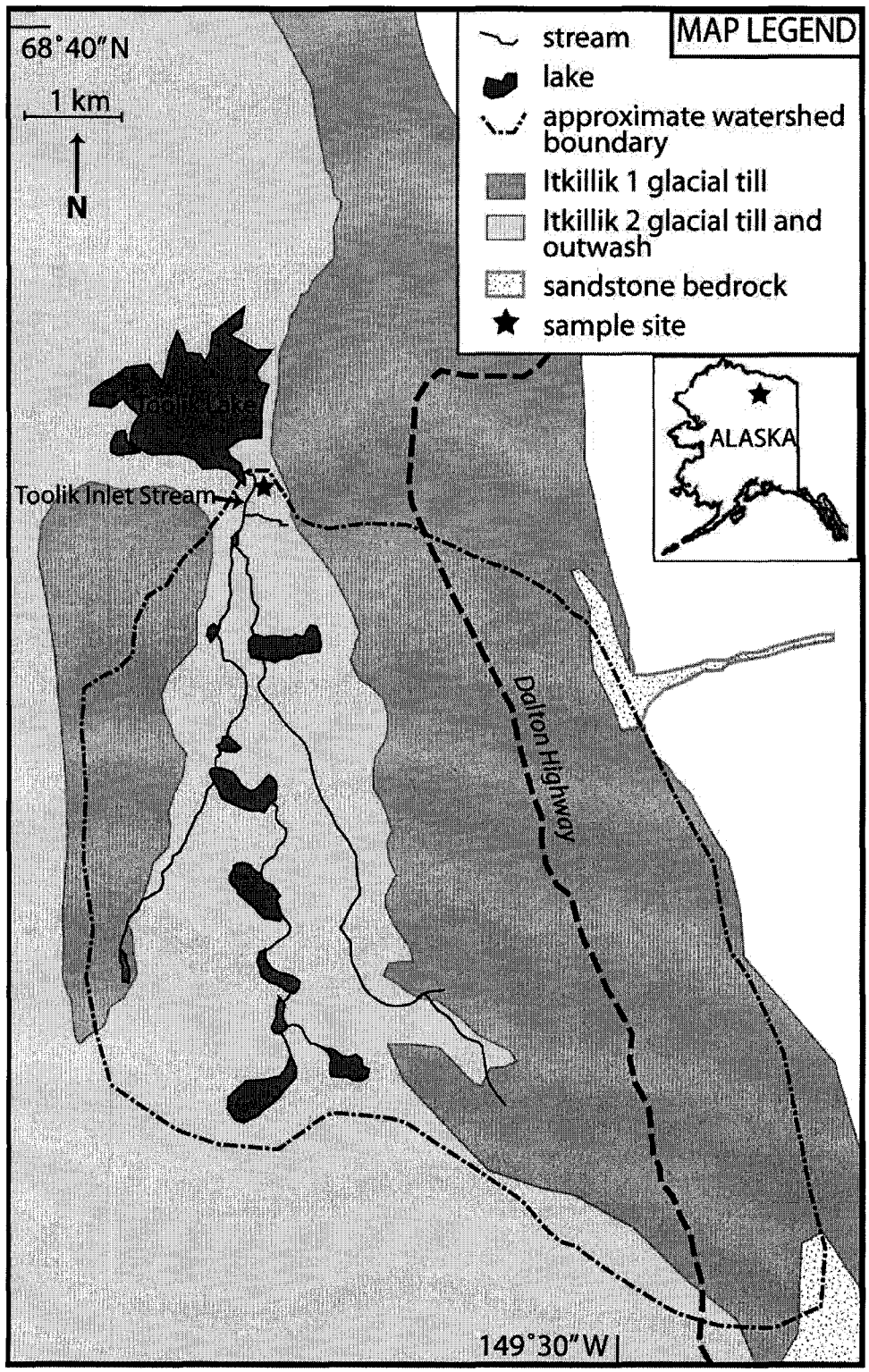

Figure 4-3. Toolik Inlet stream July-August 21 low discharge (<1.1m3/s) stream water geochemistry vs. year. A) $^{87}Sr/^{86}Sr$: R^2=0.36, p<0.0001, n=58 total samples; R^2=0.62, p=0.012, n=9 yearly means; B) Ca/Ba: R^2=0.38, p<0.0001, n=58 total samples; R^2=0.65, p=0.009, n=9 yearly means; and C) Ca/Na: R^2=0.22, p<0.0022, n=58 total samples; R^2=0.44, p=0.052, n=9 yearly means. Closed symbols represent individual data points; open symbols represent the yearly mean. $^{87}Sr/^{86}Sr$ error (2s) is <±0.000035. Propagated analytical error for elemental ratios is <±10%.

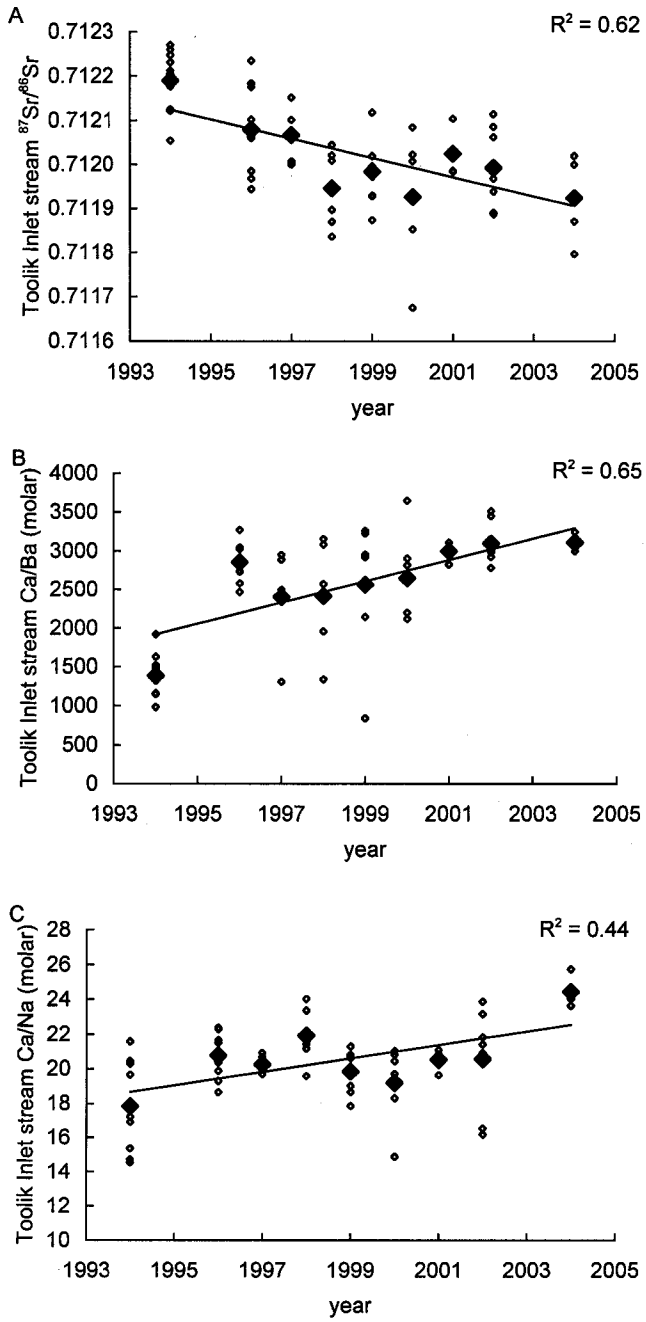

References Cited

Alaska Climate Research Center, 2003: Temperature Change in Alaska 1974-2003, http://climate.gi.alaska.edu/ClimTrends/Change/7403Change.html.

Arctic Long Term Ecological Research Site, 2005a: Biannual thaw depth survey data, http://ecosystems.mbl.edu/ARC/.

Arctic Long Term Ecological Research Site, 2005b: Toolik Lake inlet stream discharge measurements, http://ecosystems.mbl.edu/ARC/.

Blum, J. D. and Erel, Y., 2004: Radiogenic isotopes in weathering and hydrology. *In* Drever, J. I. (ed.), *Surface and Ground water, Weathering, and Soils.* Oxford: Elsevier-Pergamon, 365-392.

Brown, J. G., Kling, G. W., Hinkel, K. M., Hinzman, L. D., Nelson, F. E., Romanovsky, V., and Shiklomanov, N. I., 2000: Arctic Alaska and Seward Peninsula, in Brown, J. G., Hinkel K. M., and Nelson F. E. (eds.): The circumpolar active layer monitoring (CALM) program: Research designs and initial results. *Polar Geography,* 24: 165-258.

Bullen, T. D. and Kendall, C., 1998: Tracing of weathering reactions and water flowpaths: a multi-isotope approach. *In* Kendall, C. and McDonnell, J. J. (eds.), *Isotope tracers in catchment hydrology.* Amsterdam, The Netherlands: Elsevier Science, 611-646.

Camill, P., 2005: Permafrost thaw accelerates in boreal peatlands during late-20th century climate warming. *Climatic Change,* 68: 135-152.

Chen, W., Zhang, Y., Cihlar, J., Smith, S., and Riseborough, D., 2003: Changes in soil temperature and active layer thickness during the twentieth century in a region in western Canada. *Journal of Geophysical Research-Atmospheres,* 108: Art. No. 4696.

Conovitz, P. A., MacDonald, L. H., and McKnight, D. M., 2006: Spatial and temporal active layer dynamics along three glacial meltwater streams in the McMurdo Dry Valleys, Antarctica. *Arctic Antarctic and Alpine Research,* 38: 42-53.

Hamilton, T. D., 2003: *Glacial geology of Toolik Lake and the Upper Kuparuk River region.* Fairbanks, Alaska: Alaska Geobotany Center, Institute of Arctic Biology, University of Alaska Fairbanks, 24 pp.

Hinkel, K. M. and Nelson, F. E., 2003: Spatial and temporal patterns of active layer thickness at Circumpolar Active Layer Monitoring (CALM) sites in northern Alaska, 1995-2000. *Journal of Geophysical Research-Atmospheres,* 108: Art. No. 8168.

Hinzman, L. D., Kane, D. L., Gieck, R. E., and Everett, K. R., 1991: Hydrologic and thermal-properties of the active layer in the Alaskan Arctic. *Cold Regions Science and Technology,* 19: 95-110.

Hogan, J. F. and Blum, J. D., 2003: Tracing hydrologic flow paths in a small forested watershed using variations in 87Sr/86Sr, [Ca]/[Sr], [Ba]/[Sr] and delta-18O. *Water Resources Research,* 39.

Jorgenson, M. T., Racine, C. H., Walters, J. C., and Osterkamp, T. E., 2001: Permafrost degradation and ecological changes associated with a warming climate in central Alaska. *Climatic Change,* 48: 551-579.

Keller, K., Blum, J. D., and Kling, G. W., 2006: Geochemistry of soils and streams on surfaces of varying ages in arctic Alaska. *Arctic, Antarctic, and Alpine Research,* in press.

Kling, G. W., Kipphut, G. W., Miller, M. M., and O'Brien, W. J., 2000: Integration of lakes and streams in a landscape perspective: the importance of material processing on spatial patterns and temporal coherence. *Freshwater Biology,* 43: 477-497.

Kokelj, S. V., Smith, C. A. S., and Burn, C. R., 2002: Physical and chemical characteristics of the active layer and permafrost, Herschel Island, western Arctic Coast, Canada. *Permafrost and Periglacial Processes,* 13: 171-185.

Land, M. and Ohlander, B., 2000: Chemical weathering rates, erosion rates and mobility of major and trace elements in a boreal granitic till. *Aquatic Geochemistry,* 6: 435-460.

Lloyd, A. H., Yoshikawa, K., Fastie, C. L., Hinzman, L. D., and Fraver, M., 2003: Effects of permafrost degradation on woody vegetation at arctic treeline on the Seward Peninsula, Alaska. *Permafrost and Periglacial Processes,* 14: 93-101.

Michel, F. A. and Vaneverdingen, R. O., 1994: Changes in hydrogeologic regimes in permafrost regions due to cimatic-change. *Permafrost and Periglacial Processes,* 5: 191-195.

Mull, C. G. and Adams, K. E., 1985: *Bedrock Geology of the eastern Koyukuk Basin, central Brooks Range, and east central Arctic Slope along the Dalton Highway, Yukon River to Prudhoe Bay.* Anchorage: Alaska Department of Natural Resources, Division of Geological and Geophysical Surveys, 309 pp.

Munroe, J. S. and Bockheim, J. G., 2001: Soil development in low-arctic tundra of the northern Brooks Range, Alaska, USA. *Arctic and Alpine Research,* 33: 78-87.

Nelson, F. E., Anisimov, O. A., and Shiklomanov, N. I., 2001: Subsidence risk from thawing permafrost. *Nature,* 410: 889-890.

Osterkamp, T. E., 2005: The recent warming of permafrost in Alaska. *Global and Planetary Change,* 49: 187-202.

Pavlov, A. V. and Moskalenko, N. G., 2002: The thermal regime of soils in the north of Western Siberia. *Permafrost and Periglacial Processes,* 13: 43-51.

Payette, S., Delwaide, A., Caccianiga, M., and Beauchemin, M., 2004: Accelerated thawing of subarctic peatland permafrost over the last 50 years. *Geophysical Research Letters,* 31: Art.No. L18208.

Rouse, W. R., Douglas, M. S. V., Hecky, R. E., Hershey, A. E., Kling, G. W., Lesack, L., Marsh, P., McDonald, M., Nicholson, B. J., Roulet, N. T., and Smol, J. P., 1997: Effects of climate change on the freshwaters of arctic and subarctic North America. *Hydrological Processes,* 11: 873-902.

Stendel, M. and Christensen, J. H., 2002: Impact of global warming on permafrost conditions in a coupled GCM. *Geophysical Research Letters,* 29: Art. No. 1632.

Turestsky, M. R., Wieder, R. K., and Vitt, D. H., 2002: Boreal peatland C fluxes under varying permafrost regimes. *Soil Biology and Biochemistry,* 34: 907-912.

Waelbroek, C., Monfray, P., Oechel, W. C., Hastings, S., and Vourlitis, G., 1997: The impact of permafrost thawing on the carbon dynamics of tundra. *Geophysical Research Letters,* 24: 229-232.

CHAPTER 5

EFFECTS OF THERMOKARST FORMATION ON THE GEOCHEMISTRY OF A TUNDRA STREAM IN ARCTIC ALASKA, USA

Abstract

One likely effect of climate warming in permafrost regions is increased occurrence of thermokarst, which has the potential to substantially impact watershed geochemistry. Here I investigate the effects on stream chemistry of an in-stream thermokarst caused by the melting of a hyporheic ice wedge in a small watershed in arctic Alaska, sampled within a few days of its collapse in 2003 and again in 2005. At both sampling times, conductivity was more than doubled and solute concentrations and alkalinity were substantially higher in the streamwater downstream from the thermokarst compared to upstream. The upstream-versus-downstream differences in alkalinity, conductivity, and most dissolved elements were slightly smaller in 2005 compared to 2003. Ca was the dominant cation in the exchangeable fraction of permafrost and in the ice wedge exposed by the thermokarst. Carbonate dissolution is indicated as a major factor in the observed changes in stream chemistry. Analysis of Ca/Sr vs. $^{87}Sr/^{86}Sr$ ratios in 2003 and 2005 stream samples suggest that melting ice may have had an initial influence on stream chemistry, but by 2005 the dominant influence was ion exchange and dissolution of exposed sediments. Estimates suggest

geochemical changes may be detectable downstream in rivers up to 100 times the size of the original affected stream.

Introduction

Permafrost underlies 25% of the northern hemisphere (Brown et al., 1997), and has important effects on ecology, hydrology, and engineering in cold regions (Michel and Vaneverdingen, 1994; Nelson et al., 2001; Turestsky et al., 2002; Lloyd et al., 2003). Climate change is already causing permafrost degradation in regions with discontinuous permafrost (Osterkamp and Romanovsky, 1999; Osterkamp et al., 2000; Jorgenson et al., 2001; Payette et al., 2004), and models predict substantial increases in active layer thickness in continuous permafrost zones in the next century (Stendel and Christensen, 2002). Permafrost degradation can affect ecosystems and the landscape in many ways (Jorgenson and Osterkamp, 2005); the increased occurrence of thermokarst is one important effect.

Thermokarst involves the settling or collapse of the ground surface due to thawing of ground ice or degradation of ice-rich permafrost. Often, these collapsed features are then filled with water (Jorgenson and Osterkamp, 2005). Therefore, thermokarst plays an important role in arctic and subarctic hydrology. Thermokarst is involved in the formation of thaw lakes and beaded streams, both of which are common features of hydrologic systems developed in permafrost regions. Many observations support the thermokarst origin of thaw lakes (Jorgenson and Osterkamp, 2005); less is known about the formation of beaded

streams, but evidence suggests the pools that form the "beads" are products of thermal erosion of the intersections of interconnecting ice wedges which outline high-center ice-wedge polygons (Hopkins et al., 1955; Oswood et al., 1989).

Observations suggest that thermokarst can be triggered by surface disturbances to the insulating vegetation, including fire (Mackay, 1970; Lewkowicz and Harris, 2005) construction (Tucker et al., 2004), vehicle traffic (Slaughter et al., 1990), trampling (Mackay, 1970), or by overall environmental changes in hydrology and climate (White et al., 1969; Jorgenson and Osterkamp, 2005). Because thermokarst formation is often dependent on localized disturbances which form positive feedbacks, an isolated occurrence is a poor indicator of climate change (Harris, 2002). However, climate change is likely to cause increased incidence of thermokarst via permafrost degradation and associated hydrological changes; increases in thermokarst formation have already been reported in many areas.

Increases in thermokarst as a mode of permafrost degradation in response to recent periods of warm climate are most noticeable in discontinuous permafrost zones such as Alaskan boreal forests (Osterkamp and Romanovsky, 1999; Osterkamp et al., 2000; Jorgenson et al., 2001) and palsa bogs in Canada (Laberge and Payette, 1995; Beilman, 2001) and Scandinavia (Luoto and Seppala, 2003; Payette et al., 2004). However, increased thermokarst formation has been documented even in continuous permafrost in the Alaskan Arctic: field studies and analysis of aerial photography indicates that there has been widespread and accelerated degradation of the ice wedges on the Arctic Coastal

Plain west of the Colville Delta from 1945-2001 (Shur et al., 2003; Jorgenson et al., 2006).

Because of the likelihood of increased occurrences of thermokarst with continuing climate change, it is important to understand the potential impacts of thermokarst on ecosystems. Aside from the hydrological impact of increased numbers of thaw pools and lakes, increased thermokarst may also affect other ecosystem functions. Thermokarst features have been shown to create soil drainage conditions that facilitate establishment of shrub and tree species (Lloyd et al., 2003) and decrease plant community diversity (Truett and Kertell, 1992).

Thermokarst also has the potential to substantially affect streamwater chemistry. Whether it occurs in a palsa bog, as a tundra thaw lake or slump, or as part of a beaded stream, thermokarst formation nearly always involves the relatively sudden interaction of previously frozen mineral sediments with varying amounts of water, leading to cation exchange and weathering reactions that can have significant impacts on the watershed despite the relative rarity of the event. A recent study comparing the chemistry of small delta thaw lakes in arctic watersheds with and without thermokarst slumping showed that major cation (Ca, Mg, Na, K) concentrations, SO_4, pH, and conductivity were significantly higher, while DOC was significantly lower, in lakes affected by thermokarst (Kokelj et al., 2005). The effects on lake water chemistry were detectable even when thermokarst covered only a small percentage of the watershed area, and the elevated ionic concentrations lasted for several decades after the slumps occurred.

The effects of thermokarst on streams and river systems are less well studied than the effects on lakes. In addition, because the occurrence of thermokarsts is not often observed, the immediate effects of thermokarsts on surface water chemistry are not documented. I investigated the effects of a within-stream thermokarst formation on the geochemistry of a first-order arctic tundra stream within days of its formation. Preliminary studies of this stream showed elevated NH_4, PO_4, and total suspended sediment downstream of the thermokarst in the month after thermokarst formation (Bowden et al., 2004). Here I examine stream geochemistry approximately four days after and two years after thermokarst occurrence, as well as the geochemistry of the associated sediments and ice wedge, in order to evaluate both the geochemical effects of thermokarst over time and the mechanisms responsible for these effects.

Study Area

The thermokarst site is on the central North Slope of Alaska at 68.692°N, 149.203°W. The surrounding vegetation is tussock tundra. This site is underlain by glacial till from the older of two advances of the Sagavanirktok River glaciation, which has been roughly dated to the middle Pleistocene (Hamilton, 2003). Till is derived from local sedimentary and metasedimentary rock units including carbonates (Mull and Adams, 1985) and is covered with a thin but continuous layer of loess (Hamilton, 2003). Previous work has shown that while most of the carbonate has weathered out of the active (seasonally thawed) layer

on this surface, carbonate minerals are still abundant in the permafrost (Keller et al., 2006).

The thermokarst occurred in a first-order, peat-bottomed tundra stream in the Toolik River and Kuparuk River watersheds, roughly 500 m south of the junction of this stream with the East Fork of the Toolik River (Figure 5-1A). The thermokarst is believed to have been initiated when an ice wedge in the hyporheic zone melted rapidly. This caused sediments in the streambed to erode and form a roughly 50-100 m long tunnel, leading to the collapse of the overlying tundra (Figure 5-1B) on approximately 12 August, 2003 (as reported by a local helicopter pilot). The collapse occurred after several rainy days. This thermokarst created a >7m high waterfall in the stream (Figure 5-1C), displaced the stream course several tens of meters (Figure 5-2), and exposed large banks of peat, active layer mineral soils, permafrost sediments, and ice on either side of the stream for approximately 200 m downstream of the waterfall.

Several ice features were visible in the banks in the days after the thermokarst occurred; the largest appeared to be a remnant of the partially melted ice wedge complex. The shape of the thermokarst indicated that the axis of the primary melted ice wedge was likely parallel to the current stream course; however, the remaining ice wedge was approximately perpendicular to the bank and ~8 m high (Figure 5-1D). This suggests that the melting may have started at the junction of two wedges, as is hypothesized for the cause of pools in beaded streams (Hopkins et al., 1955; Oswood et al., 1989).

Two distinct layers in the permafrost were observed at the thermokarst feature: one shallower (1-2m below the tundra surface) sandy layer, and one deeper (2-3 m) with less sand and more visible clay and silt. Both permafrost layers had several small (3-20 cm thick) interbedded ice lenses. The permafrost sediments and ice features exposed by the thermokarst at this site, and the stream above and below the collapsed area, were sampled on 16 August, 2003, and the stream was sampled again on 9 July, 2005.

Methods

Homogenized samples of permafrost sediments from the two layers, labeled Permafrost 1 (shallower sample) and Permafrost 2 (deeper sample) were collected with a sharp stainless steel trowel from the exposed banks. The samples were allowed to thaw at about 2°C, then dried at 35°C. The dried samples were sieved to separate the <2 mm fraction, which was used for further analyses; the >2 mm fraction is usually considered to contribute a negligible amount to geochemical reactions due to its low surface area to volume ratio. Following the methods of Blum et al. (2002) and as described in Keller et al. (2006), 0.5 g of each sediment sample was leached and digested sequentially with 1M NH_4Cl at room temperature for 20 hours, 1M HNO_3 at room temperature for 20 hours, and concentrated HNO_3 at 150°C for 3 hours. These leachates were used to estimate the major and trace element concentration of the exchangeable fraction, easily weatherable minerals, and minerals more resistant to weathering, respectively. Subsamples of the sediments were also completely

digested for chemical analysis via the $LiBO_2$ fusion method described in Keller et al. (2006).

Samples of the large ice wedge and a smaller ice lens associated with the Permafrost 2 sample were also collected from the banks of the thermokarst structure. Samples of ice were scraped into clean polyethylene bags using a stainless steel knife, and allowed to thaw at about 2°C. Small amounts of sediment contained in each ice sample settled during thawing and the liquid was then poured into a separate bottle. The thawed ice samples were subsequently treated in the same way as the stream water samples described below.

Stream water was collected approximately 25 m upstream of the waterfall caused by the thermokarst formation, and approximately 200 m downstream of the waterfall, just beyond the collapsed area on both sampling dates. In 2005, additional samples were collected approximately 1 m and 100 m downstream of the waterfall within the collapse area. Conductivity was measured in the field. All water samples were filtered through 0.45-micron disposable polypropylene filters into acid-washed polyethylene bottles, and then samples for elemental analysis were acidified with ultra-pure hydrochloric acid to prevent precipitation of dissolved ions. The water was refrigerated in the dark until analysis.

The stream water, the three types of soil leachate and the $LiBO_2$ digest solutions were analyzed for elemental concentrations (including Al, Ba, Ca, Fe, K, Li, Mg, Mn, Na, Ni, P, Rb, S, Si, Sr, Ti, V, Zn, and Zr) by ICP-OES using five- to nine-point calibration curves. Quality control standards included High-Purity ICP-Stock Solution CRM Soil Solution A, CRM River Sediment B, and Trace

Metals in Drinking Water. For the water samples, these standards were analyzed to within ±10% of the known values for Al, Fe, and Sr; ±17% for P and S, and ±5% for all other elements. For the leachates, standards were analyzed to within ±12% for Al, Mg, Mn, and Si, ±14% for P and S, and ±7% for other elements in the same concentration ranges as the samples. For the total digests, the commercial standards plus an in-house standard were analyzed to within ±7% for Ba, Mn, P, Si, Ti, V, Zn, and Zr; ±12% for Al, Ca, Fe, K, Na, Ni, S, Sr; and ±13% for Mg in the same concentration ranges as the samples. Alkalinity was determined on unacidified stream water samples by titration on a Radiometer autotitrator followed by Gran analysis of the titration curves.

A pure 50-100 ng Sr fraction was separated from selected water and sediment leachate samples by eluting a subsample through Eichrom Sr-Spec resin in a quartz cation exchange column. The Sr samples along with 1 ng H_3PO_4 were then transferred onto tungsten filaments with Ta_2O_5 powder. Sr isotope ratios ($^{87}Sr/^{86}Sr$) were determined by thermal ionization mass spectrometry (TIMS) on a Finnigan MAT 262. To correct for machine mass bias, $^{86}Sr/^{88}Sr$ was normalized to 0.1194. Between 50 and 200 replicate $^{87}Sr/^{86}Sr$ measurements were made for each sample. Machine error ($\pm 2\sigma$) calculated from these replicates was generally less than ±0.000030. The Sr standard NBS-987 was analyzed after every 12 samples with a mean value of 0.710233±0.000016 ($\pm 2\sigma$, n=112) during sample analyses.

Results and Discussion

The results of the sequential leach and digest and the total digest of the permafrost sediments are shown in Table 5-1. The deeper permafrost sample has higher concentrations of most measured exchangeable and acid digestible elements than the shallower sample. The shallower sample has a higher total concentration of Si and a lower total concentration of Al than the deeper sample. These elemental data, along with the visibly sandy texture of the shallow sample, suggests the shallower sample may have a higher percentage of quartz while the deeper sample may contain more clay and non-quartz minerals such as calcite and biotite. The dominant cation in the exchangeable and cold acid digestible fractions for both samples is Ca, and the $^{87}Sr/^{86}Sr$ of these fractions is lower than active-layer soils on this surface, nearer the 1M HNO_3-digestible value of local limestone units of 0.708058 (Keller et al., 2006). This supports a previous study indicating the presence of carbonate in these permafrost sediments (Keller et al., 2006).

Table 5-1 also shows the concentrations of solutes in the ice wedge and an ice lens included in the deeper permafrost sediments. Ca and Mg were the dominant cations in both ice features, suggesting the influence of carbonate from the sediments in this area on both samples. While the ice wedge and the smaller lens had similar concentrations of Ca and Sr, the ice wedge had lower concentrations of the other measured elements. These results are consistent with analyses of ground ice from the Canadian Arctic coast by Kokelj et al. (2002) that found generally lower solutes in ice-wedge ice than in tabular ice. The

relatively low solute levels in ice-wedge ice are also congruent with the hypothesis that ice wedges form by snow melting into thermal contraction cracks in the tundra (Pewe, 1966), allowing the snowmelt to avoid much interaction with sediment and remain relatively dilute except for the most easily soluble ions.

Solute concentrations in both ground ice features were greater than or similar to solute concentrations for most elements in the undisturbed stream sample; for Ca they were approximately 100 times greater in the ice features (Table 5-1). The finding that ground ice solute concentrations are generally greater than or equal to surface water concentrations is also consistent with similar measurements by Kokelj et al. (2002). This difference would be expected because water in small tundra streams is for the most part isolated from mineral sediments by the peat layer on the stream bed, while ground ice water interacts with mineral sediments to some extent before freezing.

The effects of the thermokarst on dissolved major and minor elements, conductivity, and alkalinity of the stream in 2003 and 2005 are shown in Figure 5-3. At both sampling times, concentrations of all elements, conductivity, and alkalinity were greater in the stream sample taken 200 m downstream of the thermokarst than in the sample upstream of the thermokarst, indicating that the thermokarst affected stream chemistry both immediately and throughout the subsequent thawed seasons for two years. The mechanisms responsible could be melting of ice-bound solutes, cation exchange, mineral weathering, or varying combinations of these at different times. The element with the greatest absolute difference in upstream-downstream concentration both years was Ca, which

along with the changes in alkalinity suggests that carbonate dissolution was a large factor in the observed chemical changes. A simple carbonate-saturation calculation for a stream at these conditions (roughly 10°C and pH=6.5 as measured in 2005) based on equations and equilibrium constants given in Drever (1997) shows that the stream water was not carbonate saturated at either sampling time; in 2003, it had about one-third the alkalinity of the carbonate-saturated level.

After Ca, the elements with the largest absolute upstream-downstream concentration differences were Si in 2003 and Fe in 2005. Due to seasonal changes in solute concentrations in the upstream reach of the stream, it is difficult to compare percentage change between years, however, K had the largest percentage increase (>2000%) from upstream to downstream concentrations in both years. Phosphorus (P) was also measured but not included in the graph; the only stream sample with dissolved P levels above the ICP-OES analytical limit of detection of 0.02 mg/L was the 2003 downstream sample, which had 0.09 mg/L.

The upstream-downstream differences in alkalinity, conductivity, and most dissolved elements decrease slightly in 2005 compared to 2003. While the change in conductivity downstream of the thermokarst only decreases by 9% in 2005 compared to 2003, the change in alkalinity decreases by 60% and the upstream-downstream difference in some dissolved elements drops even more (74% for Al, 64% for Si). This may suggest that there was a limited supply of these elements readily soluble (e.g. frozen in ice) or exchangeable, which is

becoming exhausted. The exceptions to this trend are dissolved Fe, Mn, Na, Ni, S, and Zn. The upstream-downstream differences for these elements are larger in 2005 than in 2003, perhaps indicating that these elements are contained in slightly more resistant minerals (such as sulfides, which are a part of the parent till (Keller et al., 2006) for Fe, Zn, and S) or bound to organic compounds which become progressively easier to break down after increased exposure and mechanical stress or oxidation.

There is also a marked increase in the upstream concentration of Fe, and small increases in Mn, Ni, S, and Zn, in 2005 compared to 2003. This may be due simply to natural variability of flowpaths or ecological processes in the watershed. In a similar small stream (Imnavait Creek) near this study area, Fe and Mn concentrations varied by a factor of four, and Zn concentrations varied by a factor of ten, throughout the course of one summer (Arctic LTER, unpublished data). However, it is also possible that the increases in these elements in this study could indicate the oxidation of sediments and the release of redox-sensitive elements in the upstream reach of the stream. One explanation for this is the exposure of previously buried peat, which could be the first step in another thermokarst event.

The elevation in conductivity, alkalinity, and Ca, Mg, Na, K, and S concentrations in natural water affected by thermokarst in this study is consistent with the results of Kokelj et al. (2005), who found similar results in their study of thermokarst-affected lakes in the Mackenzie Delta, Canada, which are also in carbonate-rich glacial deposits. The Mackenzie Delta environment and

thermokarst differed from that of this study in several ways: both pristine and thermokarst-affected Mackenzie Delta lakes had generally higher solute concentrations than the stream in this study, the thermokarst occurred in the form of retrogressive lakeshore slumps rather than melting of hyporheic ice-wedges (i.e. horizontally adjacent to the aquatic feature rather than under it), many of the thermokarst slumps observed were inactive, and the ages of the inactive thermokarst slumps affecting the lakes were only roughly known. The magnitude of the increases of some cation concentrations between pristine and thermokarst-affected waters in both studies, however, is comparable: for example, the mean Ca concentration in the thermokarst-affected Mackenzie Delta lakes increased approximately 650% over the pristine lakes, and in the stream in this study in 2005 the increase was approximately 500%. Despite the different environmental factors between the two studies, this comparison suggests that when soluble minerals like calcium carbonate are present, even different forms of thermokarst in different hydrologic features may have some similar effects on water chemistry.

In 2005, in addition to the 25 m upstream and 200 m downstream samples, intermediate stream samples were obtained in the collapsed area to examine the geochemical gradient along this stream reach. Major element chemistry and $^{87}Sr/^{86}Sr$ for these samples is shown in Figure 5-4. Ca, K, and Mg concentrations all increase at the start of the thermokarst feature compared to upstream concentrations and continue to increase in stream water as the stream passes through the collapsed area. Fe decreases slightly at the start of the

thermokarst feature compared to its upstream concentration, but then increases similar to Ca. This initial decrease in dissolved Fe might be explained by adsorption of dissolved Fe onto suspended clay particles released by the thermokarst. Dissolved Si increases through the collapse, but starts to decrease after the end of the collapsed area, at the 200 m sample. This decrease may be caused by dilution by runoff with lower Si levels. The $^{87}Sr/^{86}Sr$ ratio decreases in both the 1 m and 100 m downstream samples as it is influenced by carbonate-rich sediments, but like dissolved Si, this value also shows signs of beginning a return to "normal" stream values at the 200 m sample, which is higher than the samples taken within the collapsed area. The soil organic horizon in this area has a relatively high exchangeable $^{87}Sr/^{86}Sr$ of 0.717314 (Keller et al., 2006), therefore, depending on precipitation conditions, it may be possible for overland flow to influence this value even at this short distance from the thermokarst.

These results indicate that the effects of thermokarst on stream chemistry changed slightly over two years. Examination of isotopic and elemental ratios may help clarify the reasons for the changes. Figure 5-5 shows the streamwater $^{87}Sr/^{86}Sr$ vs Ca/Sr ratios upstream and downstream from the thermokarst in 2003 and 2005 along with the ratios of the exchangeable and cold acid digestible fractions of the shallow and deep permafrost samples and the ice wedge. Both water samples taken downstream of the thermokarst have reduced $^{87}Sr/^{86}Sr$ and elevated Ca/Sr compared to the upstream samples, suggesting that permafrost sediments and ice exposed by the thermokarst influenced stream chemistry. But while the 2003 downstream water sample plots between the sediment values and

the ice wedge value, the 2005 downstream water sample has a Ca/Sr value more similar to the sediment exchangeable and digestable fraction values. Comparing Ca/Na values (not shown) of these samples yields a somewhat similar pattern, with the 2003 downstream sample closer than the 2005 sample to the ice wedge value. This could indicate that the ice wedge or other ice features were still melting early after the initial thermokarst event and influencing stream chemistry, but by July of 2005 the ice had stopped melting or had melted away, so elemental stream chemistry was primarily influenced by ion exchange and dissolution of exposed sediments.

Some simple calculations indicate the plausibility of the hypothesis that melting ice wedges can strongly influence stream chemistry. A mixing equation between 2003 upstream values and ice wedge values (Figure 5-5, dashed line) suggests that, because ice wedge solute concentrations are higher than stream solute concentrations, only a small amount of ice wedge water is needed to have a substantial impact on stream chemistry. I also estimated the amount of water from the melting ice wedge and other ground ice as approximately 875 cubic meters in the first four days (based on the estimate of 50 by 5 by 5 m for the volume of the initial void left by the thermokarst and assuming 50% of that was filled by ice, based on our observations of the remaining ice wedge and our analysis of the frozen sediment as up to 25% water) and compared that to the amount of water flowing through the stream in that time period based on an estimate of 0.01 m^3/s for average non-storm-event discharge from published data for a slightly larger arctic stream (Oswood et al., 1989). Using these numbers, in

the first four days, melting ice would have accounted for 20% of the total downstream discharge. If 75% of the ice melted during the first day of the thermokarst, it would have accounted for 50% of the discharge on that day, and if only 5% was melting by the fourth day it still would have been 5% of the discharge. According to the mixing line calculation in Figure 5-5, even at the lower estimates, the melting ground ice would have an impact on stream chemistry for these first few days. It is unlikely that the influence of melting ground ice could have lasted much longer than a few days, since by the time the site was sampled much of the massive ground ice was gone and the Ca/Sr value of the stream was already well off the calculated ice-stream mixing line; however, because multiple samples were not taken in 2003, it is difficult to estimate how quickly the stream chemistry values were changing during this time.

Implications

The results of this study demonstrate that an in-stream thermokarst can substantially impact the chemistry of the stream in which it occurs, in addition to the obvious local changes in topography and hydrology caused by thermokarst. This small stream, however, is not isolated but part of a larger watershed, so these effects have the potential to impact downstream ecosystems as well. In order to determine how far downstream the chemical impact of the thermokarst would be detectable, I did a simple calculation to estimate the thermokarst effect on stream chemistry at four points draining successively larger areas: the confluence of the thermokarst-affected stream with the East Fork of the Toolik;

the East Fork of the Toolik over 7 km downstream, just before its confluence with the main Toolik River; the Toolik River approximately 120 km N of the thermokarst; and the mouth of the Kuparuk River (which drains the Toolik watershed), approximately 200 km N of the thermokarst at the Arctic Ocean. I used published estimates of watershed areas (McNamara et al., 1998; Best et al., 2005) for the large watersheds and estimated the two smallest watershed areas and the thermokarst-affected stream watershed area (~2 km^2) from topographic maps; for the purposes of this calculation I assumed discharge to be proportional to watershed area. Ion concentration and alkalinity measurements from summer 1988 for the Kuparuk River (Kling et al., 1992) were used in the calculation. For other river chemistry estimates, no direct measurements of the rivers in question were available so I used analogous streams, which are similar in size and flow over similar landscape surfaces to the streams in question: July 1990 measurements from an upstream point on the Kuparuk (Kling et al., 1992) were used for the Toolik River, August 2002 measurements of Imnavait Creek (Keller et al., 2006) were used for the East Fork of the Toolik River near the confluence, and the August 2002 measurements of the upstream portion of the thermokarst-affected stream were used the confluence of the East Fork Toolik-thermokarst stream confluence. With these watershed area and total river chemistry estimates, assuming discharge is proportional to watershed area, and knowing the portion of the river chemistry contributed by the thermokarst-affected stream before the thermokarst (the upstream measurements), I calculated an

estimate of the ion concentration of the portion of total river chemistry contributed by the remainder of each watershed, based on the equation:

$$K_{tsu}*A_{ts}+K_{rw}*(1-A_{ts})=K_{total}$$

where K_{tsu} is the ion concentration in the thermokarst-affected stream (before the thermokarst, as estimated by the upstream measurement), A_{ts} is the area of the thermokarst-affected watershed as a proportion of the total watershed area, K_{rw} is the ion concentration contribution from the rest of the watershed, and K_{total} is the total ion concentration in river water. Assuming the contribution from the "rest of the watershed" remains the same, I then calculate how the total river chemistry would change based solely on the changes in the thermokarst-affected stream in 2002, by replacing K_{tsu} with K_{tsd} (the ion concentration in the thermokarst affected stream, downstream of the thermokarst) in the equation. Similar calculations were made to estimate changes in $^{87}Sr/^{86}Sr$ which included a factor to normalize to published Sr concentrations for the streams in a mixing equation similar to those presented in Faure (1986). The results for each watershed are displayed in Table 5-2.

The estimates reported in Table 5-2 highlight that while a thermokarst in a first-order tundra watershed is unlikely to cause detectable ion chemistry changes in a major river like the Kuparuk, it certainly will influence the next stream it joins. It also, has the potential to cause detectable changes in watersheds 20 times the size in which it occurred, depending on the baseline solute load of the streams. While estimates of potential changes in $^{87}Sr/^{86}Sr$ for the larger watersheds were not possible due to lack of published data, the

significant changes (compared to analytical sensitivity) in this value in the smaller watersheds suggest that thermokarst-induced changes in this ratio may be detectable even in larger watersheds. Furthermore, while one isolated thermokarst may not substantially influence the overall ion concentrations, alkalinity, or even $^{87}Sr/^{86}Sr$ of a large river system, warming-induced increases in thermokarst activity may eventually lead to detectable changes in river chemistry even on larger scales.

Conclusions

I sampled in-stream thermokarst on the Alaskan North Slope approximately four days after it occurred in summer 2003 and again in summer 2005. At both sampling times, all dissolved element concentrations, alkalinity, and conductivity were higher in the sample downstream from the thermokarst than in the upstream sample. Dissolved Ca showed the greatest absolute difference in upstream vs. downstream concentrations in both years, which along with the changes in alkalinity suggests carbonate dissolution as a major factor in the observed chemical changes. The upstream-downstream differences in alkalinity, conductivity, and most dissolved elements were slightly smaller in 2005 compared to 2003. Of two observable permafrost layers revealed by the thermokarst, the deeper (2-3 m), clay-rich layer had higher concentrations of exchangeable and cold 1M acid digestible elements than the shallower (1-2 m), sandier layer; in both layers, Ca was the dominant cation in the exchangeable and cold 1M acid digestible fractions. Ca and Mg were also the dominant cations

measured in an ice wedge and an ice lens exposed by the thermokarst. Analysis of Ca/Sr vs. $^{87}Sr/^{86}Sr$ ratios in 2003 and 2005 stream samples suggest that melting ice had a strong initial influence on stream chemistry, but by 2005 stream chemistry was primarily influenced by ion exchange and dissolution of exposed sediments. Calculated estimates of the potential effect of this thermokarst on larger watersheds indicate that small thermokarsts may have detectable effects on stream chemistry in watersheds tens of times the size in which they occur.

Table 5-1: Elemental concentrations of ice features and sequential and total digests of permafrost samples from thermokarst. Errors for elemental measurements as reported in text. NA=sample not analyzed for element or isotopic ratio due to methodological or processing constraints.

Sample	Al	Ba	Ca	Fe	K	Mg	Mn	Na	Ni	P	S	Si	Sr	Zn	$^{87}Sr/^{86}Sr$	error(2σ)
	dissolved solids mg/L															
Ice wedge	0.004	0.22	50.8	0.004	2.46	6.43	<0.001	1.38	NA	0.0286	NA	0.86	0.175	NA	0.713126	0.000017
Ice lens in Permafrost 2	0.393	0.09	53.5	0.191	6.34	11.37	0.003	25.11	NA	0.0448	NA	1.57	0.183	NA	0.713940	0.000026
	NH_4Cl exchangeable fraction mg/g															
Permafrost 1 (1.5-2m)	0.114	0.04	0.8	0.38	0.002	0.07	0.05	<0.001	<0.001	0.009	0.018	0.01	0.002	0.0010	0.712331	0.000018
Permafrost 2 (2-3m)	0.032	0.05	3.2	0.04	0.068	0.16	0.01	<0.001	<0.001	0.003	0.188	0.05	0.009	0.0005	0.713109	0.000012
	cold 1M HNO_3 digestible fraction mg/g															
Permafrost 1 (1.5-2m)	1.80	0.07	1.2	6.6	<0.002	0.23	0.11	0.42	0.012	0.38	0.037	1.30	0.004	0.019	0.711629	0.000011
Permafrost 2 (2-3m)	4.32	0.24	9.8	13.2	0.057	1.77	0.86	0.43	0.047	0.67	0.29	4.73	0.024	0.070	0.711083	0.000010
	hot concentrated HNO_3 digestible fraction mg/g															
Permafrost 1 (1.5-2m)	4.48	0.02	0.2	12.6	0.081	1.50	0.08	0.41	<0.003	0.1067	0.148	0.03	0.001	0.025	0.724539	0.000019
Permafrost 2 (2-3m)	9.108	0.04	0.5	24.3	0.386	3.41	0.21	0.42	<0.003	0.1271	0.193	0.10	0.004	0.052	0.726095	0.000013
	total $LiBO_2$ digest mg/g															
Permafrost 1 (1.5-2m)	30.25	0.31	2.0	18.8	6.237	2.75	0.19	1.91	NA	0.7429	NA	458	0.038	0.041	NA	NA
Permafrost 2 (2-3m)	101.4	0.98	10.2	50.0	26.4	9.37	0.89	3.52	NA	0.9123	NA	377	0.100	0.134	NA	NA

Table 5-2: Percent difference between measured or analog stream ion concentrations, alkalinity, and $^{87}Sr/^{86}Sr$ and the calculated post-thermokarst estimates for these values as described in the text. Where alkalinity or $^{87}Sr/^{86}Sr$ data were not published for the streams or analogous streams, no calculated differences are reported as indicated by (--). (Note that these are not predictions of actual changes in river chemistry caused by the 2002 thermokarst.)

Stream	baseline ion values used	watershed area (km^2)	Ca	K	Mg	Mn	Na	S	alk	$^{87}Sr/^{86}Sr$
Kuparuk total	**Kuparuk total (Kling et al, 1992)**	8140	0.01%	0.03%	0.01%	0.18%	0.00%	0.01%	0.00%	(--)
Toolik River	**Kuparuk upstream (Kling et al, 1992)**	233	1.01%	1.50%	0.46%	12.3%	0.21%	0.05%	0.63%	(--)
East Fork before Toolik confluence	**Imnavait Creek (Keller et al, 2006)**	54	14.8%	90.1%	4.92%	8.33%	7.49%	6.64%	(--)	-0.086%
East Fork Toolik at thermokarst stream conf.	**Upstream from thermokarst, this study**	12	160%	457%	29.1%	35.8%	32.3%	14.0%	13.3%	-0.395%

Figure 5-1: Map and photos (from August 2003) of thermokarst site. A: Map showing location of thermokarst site. B: Aerial view of tundra collapse caused by thermokarst; collapsed area is about 50 m long. C: Waterfall caused by thermokarst viewed from within collapsed area. Tundra vegetation and sediment slumping is visible on either side. D: Remnant ice wedge exposed by thermokarst in collapsed area.

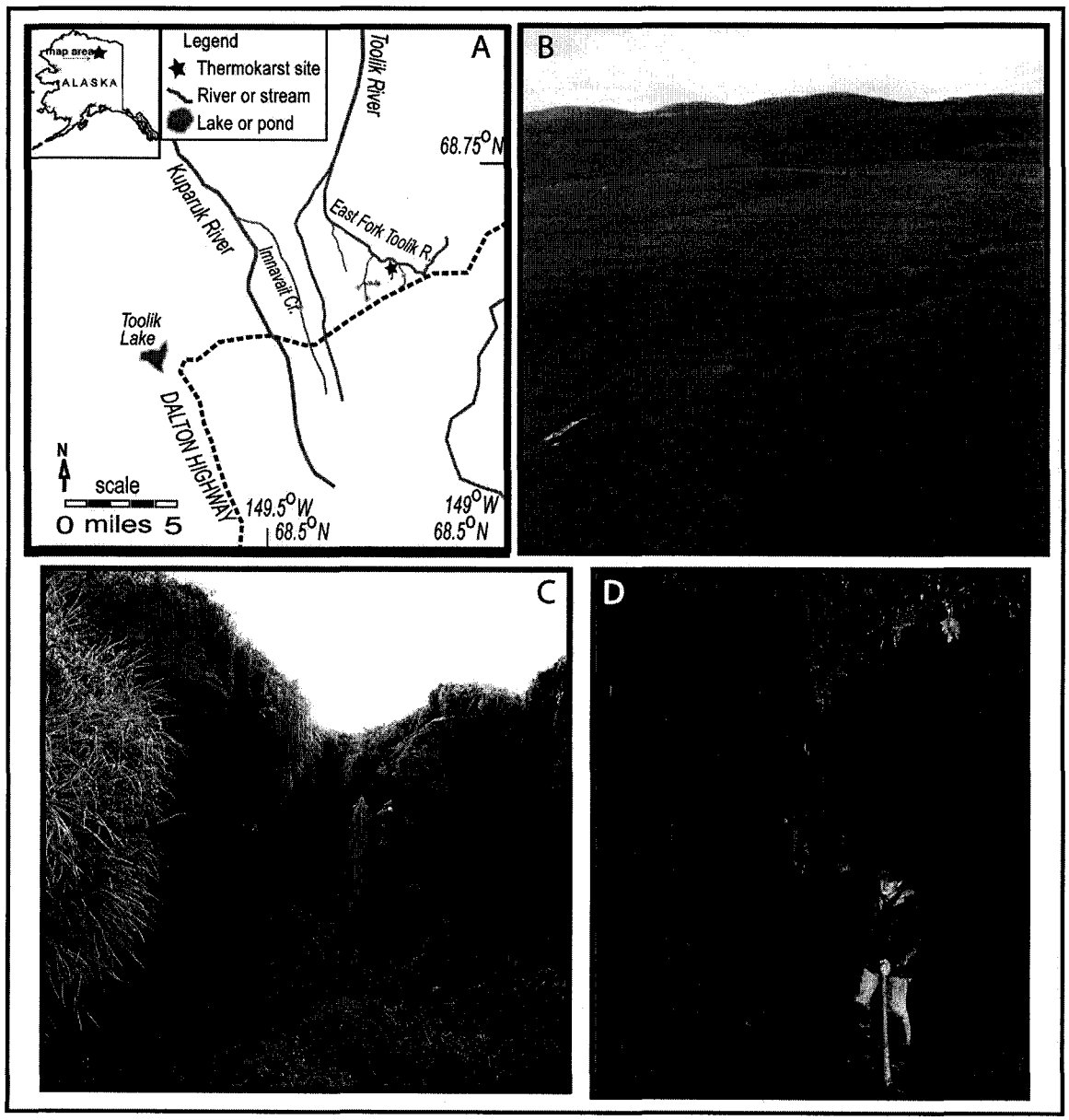

Figure 5-2: Map outline of thermokarst collapse area. Dark solid line shows the direction of the diverted stream course and outlines the collapse extent as of July 2005. Dot symbols indicate sampling or GPS data collection points.

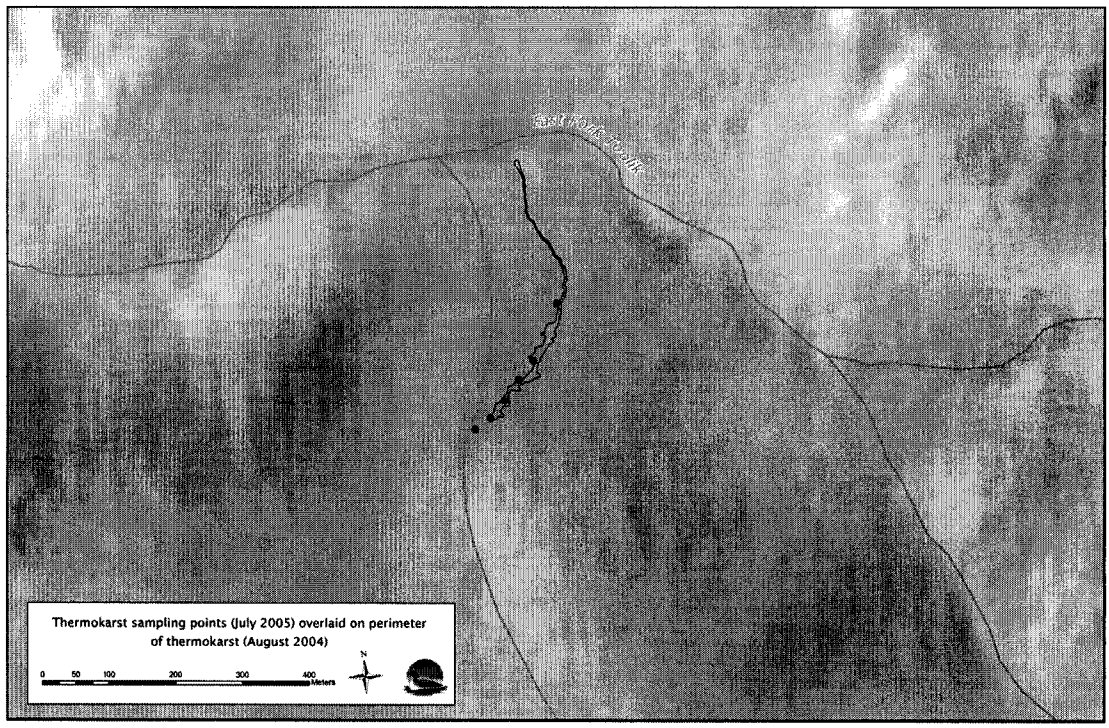

Figure 5-3: 2003 and 2005 stream water elemental concentrations, conductivity, and alkalinity.

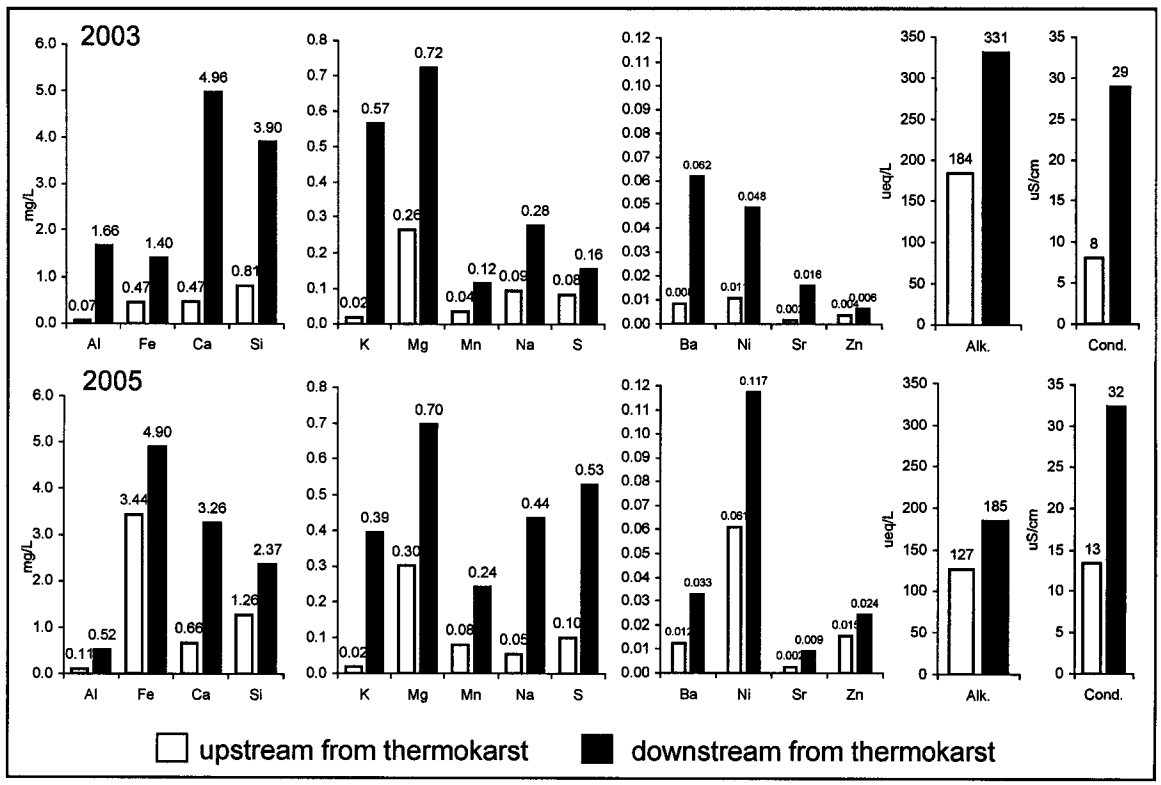

Figure 5-4: 2005 stream chemistry (solute concentrations in mg/L) vs. distance downstream from thermokarst. Negative distance (first points) are upstream from thermokarst.

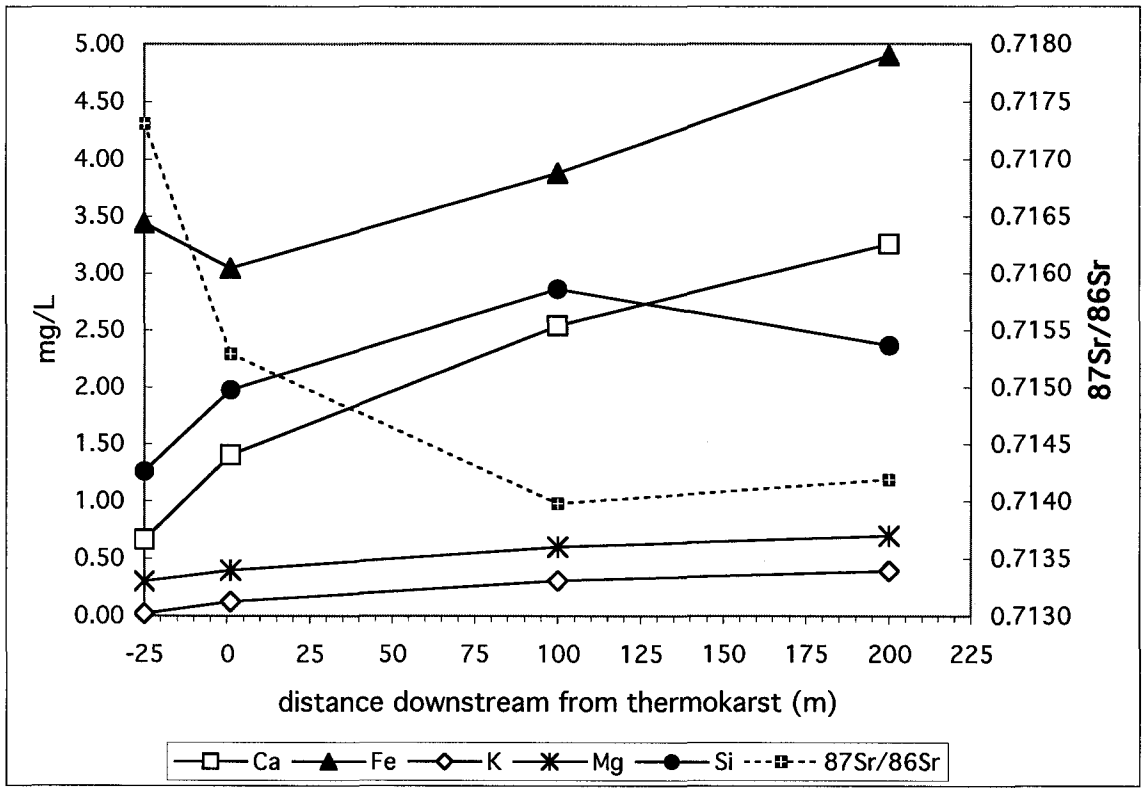

Figure 5-5: $^{87}Sr/^{86}Sr$ vs Ca/Sr (molar ratio) for stream water, ice, and sediment exchangeable and acid digestible fraction samples from the thermokarst feature. Propagated Ca/Sr error is 7%; error for $^{87}Sr/^{86}Sr$ ratios is less than 0.000040. Arrows link upstream water samples to their downstream counterparts from the same date. The dashed line shows a mixing calculation between the ice wedge and the upstream 2003 sample, with the 5% and 1% ice wedge fractions indicated.

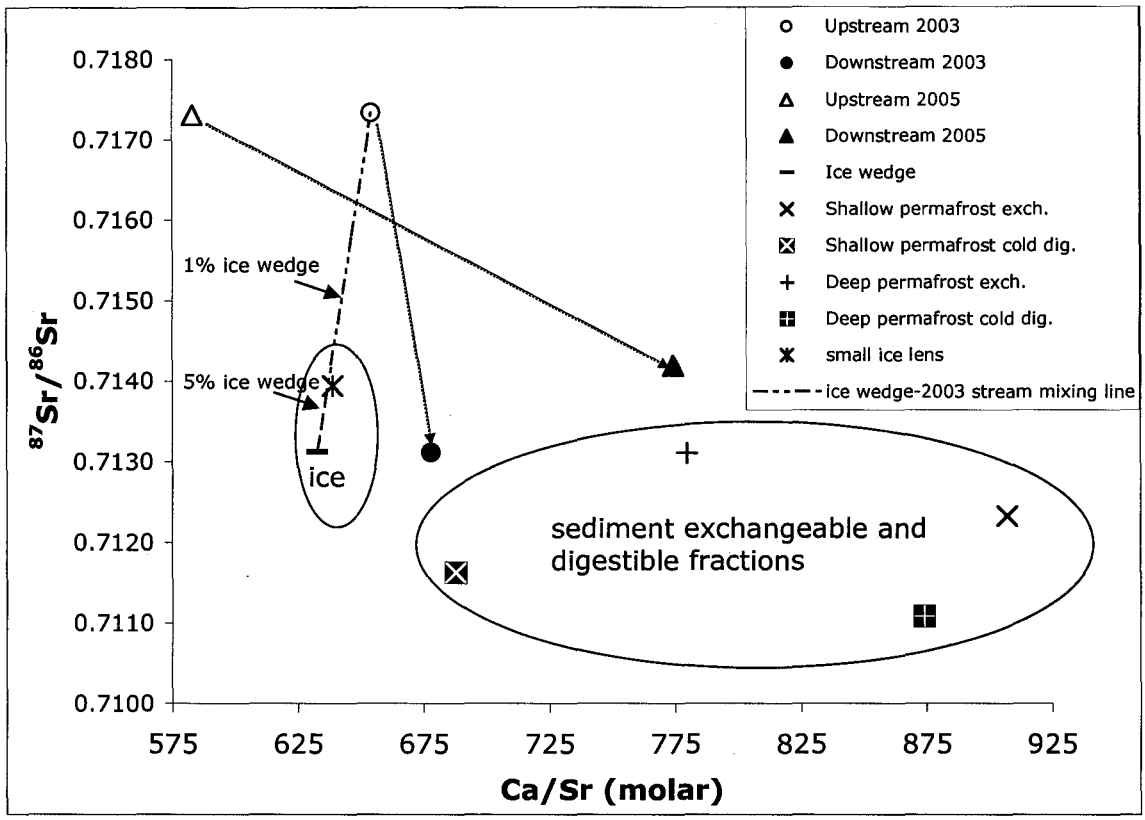

References Cited

Beilman, D. W., 2001: Plant community and diversity change due to localized permafrost dynamics in bogs of western Canada. *Canadian Journal of Botany-Revue Canadienne de Botanique,* 79: 983-993.

Best, H., McNamara, J. P., and Liberty, L., 2005: Association of ice and river channel morphology determined using ground-penetrating radar in the Kuparuk River, Alaska. *Arctic Antarctic and Alpine Research,* 37: 157-162.

Blum, J. D., Klaue, A., Nezat, C. A., Driscoll, C. T., Johnson, C. E., Siccama, T. G., Eagar, C., Fahey, T. J., and Likens, G. E., 2002: Mycorrhizal weathering of apatite as an important calcium source in base-poor forest ecosystems. *Nature,* 417: 729-731.

Bowden, W. B., Gooseff, M. N., Bradford, J. H., and McNamara, J. P., 2004: Potential impacts of increased thermokarst activity on aquatic ecosystems in arctic landscapes. *Eos Trans. AGU,* 85: Abstract 83725-81535.

Brown, J., Ferrians, O. J. J., Heginbottom, J. A., and Melnikov, E. S., 1997: CP-45: Circum-Arctic map of permafrost and ground-ice conditions. Reston, VA: U. S. Geological Survey.

Drever, J. I., 1997: *The Geochemistry of Natural Waters.* 3rd edition ed. Upper Saddle River, New Jersey: Prentice-Hall, Inc.

Faure, G., 1986: *Principles of Isotope Geology.* Second Edition ed. New York, New York: John Wiley and Sons, 589 pp.

Hamilton, T. D., 2003: *Glacial geology of Toolik Lake and the Upper Kuparuk River region.* Fairbanks, Alaska: Alaska Geobotany Center, Institute of Arctic Biology, University of Alaska Fairbanks, 24 pp.

Harris, S. A., 2002: Causes and consequences of rapid thermokarst development in permafrost or glacial terrain. *Permafrost and Periglacial Processes,* 13: 237-242.

Hopkins, D. M., Karlstrom, T. N. V., Black, R. F., Williams, J. R., Pewe, T. L., Fernald, A. T., and Muller, E. H., 1955: Permafrost and ground water in Alaska. *U. S. Geological Survey Professional Paper,* 264-F: 113-146.

Jorgenson, M. T., Racine, C. H., Walters, J. C., and Osterkamp, T. E., 2001: Permafrost degradation and ecological changes associated with a warming climate in central Alaska. *Climatic Change,* 48: 551-579.

Jorgenson, M. T. and Osterkamp, T. E., 2005: Response of boreal ecosystems to varying modes of permafrost degradation. *Canadian Journal of Forest Research,* 35: 2100-2111.

Jorgenson, M. T., Shur, Y. L., and Pullman, E. R., 2006: Abrupt increase in permafrost degradation in Arctic Alaska. *Geophysical Research Letters,* 33: Art. No. L02503, doi: 02510.01029.02005GL024960, 022006.

Keller, K., Blum, J. D., and Kling, G. W., 2006: Geochemistry of soils and streams on surfaces of varying ages in arctic Alaska. *Arctic, Antarctic, and Alpine Research,* in press.

Kling, G. W., O'Brien, J., Miller, M. C., and Hershey, A. E., 1992: The biogeochemistry and zoogeography of lakes and rivers in arctic Alaska. *Hydrobiologia,* 240: 1-14.

Kokelj, S. V., Smith, C. A. S., and Burn, C. R., 2002: Physical and chemical characteristics of the active layer and permafrost, Herschel Island, western Arctic Coast, Canada. *Permafrost and Periglacial Processes,* 13: 171-185.

Kokelj, S. V., Jenkins, R. E., Milburn, D., Burn, C. R., and Snow, N., 2005: The influence of thermokarst disturbance on the water quality of small upland lakes, Mackenzie Delta Region, Northwest Territories, Canada. *Permafrost and Periglacial Processes,* 16: 343-353.

Laberge, M. J. and Payette, S., 1995: Long-term monitoring of permafrost change in a palsa peatland in northern Quebec, Canada:1983-1993. *Arctic and Alpine Research,* 27: 167-171.

Lewkowicz, A. G. and Harris, C., 2005: Morphology and geotechnique of active-layer detachment failures in discontinuous and continuous permafrost, northern Canada. *Geomorphology,* 69: 275-297.

Lloyd, A. H., Yoshikawa, K., Fastie, C. L., Hinzman, L. D., and Fraver, M., 2003: Effects of permafrost degradation on woody vegetation at arctic treeline on the Seward Peninsula, Alaska. *Permafrost and Periglacial Processes,* 14: 93-101.

Luoto, M. and Seppala, M., 2003: Thermokarst ponds as indicators of the former distribution of palsas in Finnish lapland. *Permafrost and Periglacial Processes,* 14: 19-27.

Mackay, J. R., 1970: Disturbances to the tundra and forest tundra environment of the western Arctic. *Canadian Geotechnical Journal,* 7: 420-432.

McNamara, J. P., Kane, D. L., and Hinzman, L. D., 1998: An analysis of streamflow hydrology in the Kuparuk River Basin, Arctic Alaska: a nested watershed approach. *Journal of Hydrology*: 39-57.

Michel, F. A. and Vaneverdingen, R. O., 1994: Changes in hydrogeologic regimes in permafrost regions due to cimatic-change. *Permafrost and Periglacial Processes,* 5: 191-195.

Mull, C. G. and Adams, K. E., 1985: *Bedrock Geology of the eastern Koyukuk Basin, central Brooks Range, and east central Arctic Slope along the Dalton Highway, Yukon River to Prudhoe Bay.* Anchorage: Alaska Department of Natural Resources, Division of Geological and Geophysical Surveys, 309 pp.

Nelson, F. E., Anisimov, O. A., and Shiklomanov, N. I., 2001: Subsidence risk from thawing permafrost. *Nature,* 410: 889-890.

Osterkamp, T. E. and Romanovsky, V. E., 1999: Evidence for warming and thawing of discontinuous permafrost in Alaska. *Permafrost and Periglacial Processes,* 10: 17-37.

Osterkamp, T. E., Viereck, L., Shur, Y., Jorgenson, M. T., Racine, C., Doyle, A., and Boone, R. D., 2000: Observations of thermokarst and its impact on boreal forests in Alaska, USA. *Arctic Antarctic and Alpine Research,* 32: 303-315.

Oswood, M. W., Everett, K. R., and Schell, D. M., 1989: Some physical and chemical characteristics of an arctic beaded stream. *Holarctic Ecology,* 12: 290-295.

Payette, S., Delwaide, A., Caccianiga, M., and Beauchemin, M., 2004: Accelerated thawing of subarctic peatland permafrost over the last 50 years. *Geophysical Research Letters,* 31: Art.No. L18208.

Pewe, T. L., 1966: Ice-wedges in Alaska-- Classification, distribution, and climatic significance. *Permafrost international conference*, 1287: 76-81.

Shur, Y., Jorgenson, M. T., and Pullman, E. R., 2003: Widespread degradation of ice wedges on the Arctic Coastal Plain in northern Alaska in response to the recent warmer climate. *Eos Trans. AGU,* 84: Fall Meet. Suppl., Abstract C11A-05.

Slaughter, C. W., Racine, C. H., Walker, D. A., Johnson, L. A., and Abele, G., 1990: Use of off-road vehicles and mitigation of effects in Alaska permafrost environments: A review. *Environmental Management,* 14: 63-72.

Stendel, M. and Christensen, J. H., 2002: Impact of global warming on permafrost conditions in a coupled GCM. *Geophysical Research Letters,* 29: Art. No. 1632.

Truett, J. C. and Kertell, K., 1992: Tundra disturbance and ecosystem production - implications for impact assessment. *Environmental Management,* 16: 485-494.

Tucker, W., Brigham, L., and Nelson, F., 2004: A new report on permafrost research needs. *Journal of Cold Regions Engineering,* 18: 123-133.

Turestsky, M. R., Wieder, R. K., and Vitt, D. H., 2002: Boreal peatland C fluxes under varying permafrost regimes. *Soil Biology and Biochemistry,* 34: 907-912.

White, S. E., Clark, G. M., and Rapp, A., 1969: Palsa localities in Padjelanta National Park, Swedish Lappland. *Geografiska Annaler Series A-Physical Geography,* 51: 97-103.

CHAPTER 6

CONCLUSION

The Alaskan Arctic has warmed significantly in the last 30 years, and understanding the effects of warming on this region is a first step toward understanding the global sum of the effects of persistent environmental change. The goal of this dissertation was to investigate the geochemistry of the permafrost, the relationship between mineral weathering and stream and soil geochemistry, and changes in stream geochemistry that are already occurring as a result of permafrost degradation in the Alaskan arctic. Overall, the findings presented in the preceding chapters suggest that permafrost degradation and increases in thaw depth are occurring in watersheds on the Alaskan North Slope, and these changes are influencing stream geochemistry.

The comprehensive set of geochemical data for permafrost, soils, and streams in the Toolik Lake area of the Alaskan North Slope indicated that carbonate weathering is the major controlling factor of geochemical trends related to soil depth and surface age. Carbonate minerals have been depleted by weathering in the active layer on every geomorphic surface, and compared to active-layer mineral soils, permafrost has overall greater exchangeable K

concentrations, exchangeable and acid digestible P and Ca concentrations, and carbonate content. These data suggest that increasing thaw depth will lead to spatially variable increases in carbonate and mineral nutrient supply to soils and streams.

Long term weathering rates estimated for a soil chronosequence suggest that weathering rates in these arctic soils developed on carbonate-rich parent material have a power-law relationship with age similar to, but steeper than, that of granitic soils in temperate regions. This relationship between weathering rate and surface age further confirms the importance of mineral weathering to the geochemistry of watersheds in this region.

In an analysis of the effects of sudden permafrost degradation in the form of thermokarst on stream chemistry, dissolved element concentrations, alkalinity, and conductivity were higher in the sample downstream from the thermokarst than in the upstream sample. The results suggest carbonate dissolution as a major factor in the observed chemical changes, and the observed changes decrease slightly over time. Analyses indicate that melting ice had a strong initial influence on stream chemistry, but in two years' time stream chemistry was primarily influenced by ion exchange and dissolution of exposed sediments. Calculations indicate that small thermokarsts may have detectable effects on stream chemistry in watersheds up to tens of times the size in which they occur.

Possibly the most widely applicable and significant part of this dissertation is the demonstration of a new hydrogeochemical method for qualitatively evaluating changes in thaw depth integrated across a watershed, based on

geochemical differences with depth in soils and permafrost in the Alaskan Arctic. Other permafrost soils may also have less-intensely weathered soils at depth that provide geochemical gradients sufficient to cause changes in stream geochemistry as a result of changes in active layer thickness, therefore this method may be applicable in many regions as a compliment or an alternative to less-sensitive physical thaw depth surveys. In this study, this method provided new evidence that previously undetectable thaw depth increases are occurring in this part of the Arctic.

The results presented here supply baseline data for future geochemical comparisons, provide a framework for predicting the types of geochemical changes that might be expected in future warming scenarios, and demonstrate a method for geochemical detection of thaw depth increases in watersheds. This research shows that geochemical effects are an important factor in the overall impact of climate change on arctic ecosystems, and can also serve as an early indicator of climate-induced changes in the cryosphere.

APPENDICES

Appendix A: Rock unit elemental chemistry data.

NH4Cl leach sample number	geo fm	rock type	concentrations mg/g rock Al	Ba	Ca	Fe	K	Li	Mg	Mn	Na	Ni	P	Rb	S	Si	Sr	Ti	V	Zn	Zr	$^{87}Sr/^{86}Sr$	2 sigma
DH-01.05	Hot Springs Pluton	granite	0.01	0.02	0.21	0.01	0.83	0.00	0.15	0.00	0.32	0.00	0.00	0.01	0.00	0.05	0.01	0.00	0.00	0.00	0.00		
DH-02.05	Bonanza Pluton	granite	0.00	0.01	0.16	0.00	0.97	0.00	0.12	0.00	0.21	0.00	0.00	0.00	0.01	0.03	0.01	0.00	0.00	0.00	0.00		
DH-03.06	Ksy	syenite	0.00	0.01	0.27	0.01	1.18	0.00	0.06	0.01	0.32	0.00	0.00	0.00	0.00	0.03	0.02	0.00	0.00	0.00	0.00		
DH-03.07	Kic	cong.	0.13	0.01	1.07	0.25	0.13	0.00	0.10	0.02	0.05	0.00	0.00	0.00	0.00	0.18	0.00	0.00	0.00	0.00	0.00		
DH-03.07B	Kic	skarn cong.	0.00	0.01	0.14	0.02	0.86	0.00	0.16	0.00	0.08	0.00	0.00	0.00	0.21	0.01	0.00	0.00	0.00	0.00	0.00		
DH-C	Dbs	phyllite	0.01	0.01	1.01	0.07	0.27	0.00	0.33	0.04	0.06	0.00	0.00	0.00	0.06	0.02	0.01	0.00	0.00	0.00	0.00	0.727052	0.000017
NS-03.03	Kf	sandstone	0.00	0.35	0.48	0.01	0.80	0.00	0.47	0.00	0.10	0.00	0.00	0.00	0.01	0.02	0.00	0.00	0.00	0.00	0.00	0.717860	0.000019
NS-05.02	Pml	limestone/ chalk	0.00	0.00	2.54	0.00	0.08	0.00	0.10	0.00	0.01	0.00	0.00	0.00	0.00	0.01	0.01	0.00	0.00	0.00	0.00		
NS-05.02b	Pml	limestone/ chalk	0.00	0.00	2.53	0.00	0.01	0.00	0.03	0.00	0.00	0.00	0.00	0.00	0.00	0.00	0.01	0.00	0.00	0.00	0.00		
NS-05.03	Pml	limestone/ chert	0.05	0.00	16.23	0.08	0.10	0.00	0.12	0.00	0.02	0.00	0.03	0.00	0.00	0.03	0.01	0.00	0.00	0.00	0.00	0.708986	0.000026
NS-10.01	MDk	cong.	0.00	0.00	0.06	0.00	0.11	0.00	0.01	0.00	0.01	0.00	0.01	0.00	0.01	0.04	0.00	0.00	0.00	0.00	0.00		
NS-10.01b	MDk	cong.chert clast	0.00	0.05	0.03	0.00	0.07	0.00	0.00	0.00	0.00	0.00	0.00	0.00	0.01	0.05	0.00	0.00	0.00	0.00	0.00		
NS-10.03	MDk	quartzite	0.00	0.01	0.07	0.00	0.03	0.00	0.01	0.00	0.01	0.00	0.00	0.00	0.00	0.09	0.00	0.00	0.00	0.00	0.00		
NS-10.07	MDk	ss w/ slickensides	0.00	0.01	0.12	0.00	0.20	0.00	0.02	0.00	0.01	0.00	0.00	0.00	0.00	0.04	0.00	0.00	0.00	0.00	0.00		
NS-14.04	Pml	chalky limestone	0.00	0.00	2.34	0.00	0.02	0.00	0.04	0.00	0.01	0.00	0.00	0.00	0.00	0.00	0.01	0.00	0.00	0.00	0.00		
NS-14.05	Pe/ TRPss	shale w/ barite nodules	0.05	0.19	1.24	0.07	0.50	0.00	0.26	0.00	0.01	0.00	0.00	0.00	0.01	0.13	0.01	0.00	0.00	0.00	0.00	0.715667	0.000019
NS-14.05b	Pe/ TRPss	barite nodules	0.00	0.03	1.87	0.04	0.37	0.01	0.15	0.00	0.04	0.00	0.26	0.00	0.39	0.02	0.02	0.00	0.00	0.00	0.00		
NS-18.01	Mk	shale	0.11	0.07	2.18	0.23	0.16	0.00	0.08	0.00	0.02	0.00	0.00	0.00	0.00	0.16	0.01	0.00	0.00	0.00	0.00		
NS-20.06	Dke	cong.	0.00	0.00	0.12	0.04	0.38	0.00	0.10	0.04	0.04	0.00	0.00	0.00	0.00	0.01	0.00	0.00	0.00	0.00	0.00	0.723253	0.000027
NS-27.01	MDk	altered cong.	0.00	0.00	2.61	0.06	0.47	0.00	0.65	0.03	0.05	0.00	0.00	0.00	0.01	0.01	0.00	0.00	0.00	0.00	0.00		
NS-27.01b	MDk	altered cong./ vein subsample	0.00	0.00	3.64	0.30	0.11	0.01	0.16	0.14	0.03	0.04	0.01	0.01	0.00	1.06	0.00	0.00	0.00	0.01	0.00		
NS-34.01	Kn	sandstone	0.00	0.04	1.41	0.03	0.25	0.00	0.30	0.00	0.10	0.00	0.00	0.00	0.13	0.00	0.01	0.00	0.00	0.00	0.00	0.713092	0.000019
NS-36.01	PMl	dark limestone	0.00	0.00	2.79	0.00	0.02	0.00	0.03	0.00	0.01	0.00	0.01	0.00	0.00	0.01	0.01	0.00	0.00	0.00	0.00		

cold 1M HNO_3 digest sample number	geo fm	rock type	concentrations mg/g rock Al	Ba	Ca	Fe	K	Li	Mg	Mn	Na	Ni	P	Rb	S	Sl	Sr	Ti	V	Zn	Zr	$^{87}Sr/^{86}Sr$	2 sigma
DH-01.05	Hot Springs Pluton	granite	4.97	0.07	1.77	5.18	1.55	0.02	1.49	0.12	0.56	0.02	0.56	0.01	0.00	1.97	0.01	0.32	0.02	0.02	0.00	0.711032	0.000060
DH-02.05	Bonanza Pluton	granite	5.52	0.07	3.30	4.74	2.36	0.01	1.87	0.14	0.52	0.02	1.32	0.02	0.01	2.06	0.02	0.31	0.02	0.02	0.00	0.710963	0.000011
DH-03.06	Ksy	syenite	3.46	0.03	1.44	0.87	1.35	0.00	0.40	0.06	0.53	0.01	0.49	0.01	0.00	1.17	0.02	0.06	0.01	0.01	0.00	0.709734	0.000018
DH-03.07	Kic	cong.	1.53	0.00	5.98	2.48	0.18	0.00	0.77	0.11	0.07	0.01	0.44	0.00	0.00	1.40	0.02	0.00	0.01	0.02	0.00	0.710071	0.000013
DH-03.07B	Kic	skarn cong.	6.00	0.03	0.41	10.61	0.52	0.01	1.61	0.07	0.05	0.03	0.26	0.00	0.91	3.31	0.01	0.01	0.03	0.03	0.00	0.722249	0.000012
DH-C	Dbs	phyllite	1.96	0.00	26.43	19.42	0.16	0.01	7.64	1.74	0.01	0.02	0.63	0.00	1.75	1.70	0.07	0.00	0.01	0.02	0.00	0.725383	0.000009
NS-03.03	Kf	sandstone	7.13	0.34	1.83	7.87	0.49	0.01	2.37	0.15	0.07	0.03	0.66	0.00	0.09	2.73	0.01	0.01	0.03	0.02	0.00	0.711672	0.000018
NS-05.02	Pml	limestone/ chalk	0.00	0.01	246.36	0.02	0.06	0.00	0.88	0.05	0.00	0.00	0.01	0.00	0.00	0.20	0.13	0.00	0.00	0.01	0.00	0.707928	0.000062
NS-05.02b	Pml	limestone/ chalk	0.00	0.00	252.82	0.03	0.04	0.00	0.87	0.04	0.00	0.00	0.10	0.00	0.00	0.00	0.13	0.00	0.00	0.01	0.00	0.707912	0.000034
NS-05.03	Pml	limestone/ chert	0.22	0.01	67.06	0.20	0.02	0.00	0.24	0.01	0.00	0.01	0.20	0.00	0.00	0.72	0.03	0.00	0.00	0.01	0.00	0.708464	0.000024
NS-10.01	MDk	cong.	0.51	0.00	0.48	1.00	0.08	0.00	0.01	0.01	0.00	0.00	0.26	0.00	0.00	0.44	0.00	0.00	0.00	0.00	0.00	0.715178	0.000036
NS-10.01b	MDk	cong.chert clast	0.08	0.02	0.12	0.49	0.05	0.00	0.00	0.00	0.00	0.00	0.07	0.00	0.00	0.09	0.00	0.00	0.00	0.00	0.00	0.718046	0.000017
NS-10.03	MDk	quartzite ss w/ slickensides	0.16	0.00	0.00	0.14	0.04	0.00	0.00	0.00	0.00	0.00	0.02	0.00	0.01	0.20	0.00	0.00	0.00	0.00	0.00	0.716131	0.000050
NS-10.07	MDk	chalky s	1.17	0.00	0.40	1.25	0.10	0.00	0.02	0.02	0.00	0.01	0.13	0.00	0.17	0.81	0.00	0.00	0.01	0.01	0.00	0.715751	0.000017
NS-14.04	Pml	limestone shale w/ barite	0.00	0.00	340.95	0.01	0.04	0.00	1.30	0.04	0.00	0.00	0.03	0.00	0.00	0.00	0.21	0.00	0.00	0.01	0.00	0.708091	0.000021
NS-14.05	Pe/ TRPss	nodules	1.85	0.41	2.22	4.50	0.32	0.00	1.73	0.14	0.00	0.01	0.06	0.00	0.06	1.25	0.01	0.00	0.01	0.02	0.00	0.713981	0.000016
NS-14.05b	Pe/ TRPss	barite nodules	2.85	0.12	178.31	11.16	0.72	0.03	1.88	0.12	1.48	0.04	94.96	0.00	5.77	4.43	0.50	0.02	0.01	0.20	0.01	0.709960	0.000026
NS-18.01	Mk	shale	4.49	0.04	1.69	7.33	0.12	0.01	1.09	0.09	0.01	0.02	0.10	0.00	0.00	1.82	0.01	0.00	0.02	0.02	0.00	0.709317	0.000071
NS-20.06	Dke	cong.	3.69	0.01	0.49	3.77	0.24	0.00	0.16	0.50	0.01	0.01	0.09	0.00	0.00	1.10	0.00	0.00	0.02	0.00	0.00	0.719324	0.000013
NS-27.01	MDk	altered cong.	6.14	0.03	41.09	64.98	0.26	0.01	8.39	3.16	0.02	0.04	0.19	0.00	0.17	4.61	0.02	0.00	0.03	0.26	0.00	0.715183	0.000090
NS-27.01b	MDk	altered cong./ vein subsample	0.28	0.00	4.88	11.57	0.14	0.01	0.48	0.36	0.00	0.03	0.24	0.01	0.02	0.98	0.00	0.00	0.00	0.04	0.00	0.715464	0.000021
NS-34.01	Kn	sandstone	2.13	0.06	3.41	7.09	0.11	0.01	1.52	0.11	0.00	0.02	0.49	0.00	0.76	2.37	0.01	0.00	0.01	0.04	0.00	0.713419	0.000026
NS-36.01	PMl	dark limestone	0.00	0.00	289.69	0.03	0.03	0.00	1.07	0.03	0.01	0.00	2.31	0.00	0.00	0.01	0.24	0.00	0.00	0.01	0.00	0.707897	0.000016

hot HNO_3 digest sample number	geo fm	rock type	concentrations mg/g rock Al	Ba	Ca	Fe	K	Li	Mg	Mn	Na	Ni	P	Rb	S	Si	Sr	Tl	V	Zn	Zr	$^{87}Sr/^{86}Sr$	2 sigma
DH-01.05	Hot Springs Pluton	granite	12.15	0.15	2.43	14.47	4.65	0.05	4.65	0.28	2.23	0.03	0.00	0.04	0.00	3.36	0.05	1.95	0.05	0.04	0.00		
DH-02.05	Bonanza Pluton	granite	9.52	0.07	2.38	12.34	5.77	0.02	5.94	0.31	1.46	0.02	0.03	0.04	0.01	1.83	0.04	2.24	0.05	0.03	0.00		
DH-03.06	Ksy	syenite	7.00	0.02	1.72	4.33	3.42	0.01	1.66	0.18	1.84	0.02	0.00	0.02	0.00	2.13	0.03	0.89	0.03	0.01	0.00		
DH-03.07	Kic	cong. skarn	6.33	0.00	0.00	13.05	0.41	0.01	4.21	0.25	0.06	0.04	0.00	0.01	0.02	3.90	0.00	0.00	0.03	0.02	0.00		
DH-03.07B	Kic	cong.	11.39	0.02	0.00	20.77	1.47	0.02	3.55	0.10	0.06	0.05	0.08	0.01	0.38	4.93	0.01	0.00	0.05	0.05	0.00		
DH-C	Dbs	phyllite	13.85	0.00	0.61	28.91	0.52	0.03	6.13	0.14	0.00	0.10	0.00	0.01	0.62	9.84	0.01	0.00	0.06	0.09	0.00	0.731134	0.000012
NS-03.03	Kf	sandstone	10.60	0.21	0.00	10.57	2.23	0.01	3.10	0.08	0.26	0.07	0.12	0.01	0.08	7.90	0.00	0.03	0.05	0.02	0.00	0.735151	0.000025
NS-05.02	Pml	limestone/ chalk	0.16	0.00	94.90	0.38	0.05	0.00	0.21	0.02	0.00	0.00	0.18	0.00	0.00	0.50	0.04	0.00	0.00	0.01	0.00		
NS-05.02b	Pml	limestone/ chalk	0.00	0.00	8.60	0.00	0.00	0.00	0.00	0.00	0.00	0.00	0.00	0.01	0.00	0.00	0.00	0.00	0.00	0.00	0.00		
NS-05.03	Pml	limestone/ chert	0.44	0.01	1.07	0.24	0.16	0.00	0.05	0.00	0.00	0.01	0.01	0.00	0.03	1.61	0.00	0.01	0.00	0.00	0.00	0.713099	0.000014
NS-10.01	MDk	cong.	1.17	0.00	0.00	5.74	0.44	0.00	0.04	0.08	0.00	0.02	0.10	0.01	0.00	1.84	0.00	0.00	0.01	0.00	0.00		
NS-10.01b	MDk	cong.chert clast	0.22	0.00	0.00	1.59	0.23	0.00	0.00	0.01	0.00	0.00	0.00	0.01	0.01	0.55	0.00	0.00	0.00	0.00	0.00		
NS-10.03	MDk	quartzite	0.20	0.00	0.00	0.17	0.07	0.00	0.00	0.00	0.00	0.00	0.01	0.01	0.05	0.59	0.00	0.00	0.00	0.00	0.00		
NS-10.07	MDk	ss w/ slickensides	1.62	0.00	0.00	5.95	0.36	0.00	0.02	0.03	0.00	0.02	0.01	0.01	0.05	1.62	0.00	0.00	0.01	0.01	0.00		
NS-14.04	Pml	chalky limestone	0.00	0.00	0.00	0.00	0.00	0.00	0.00	0.00	0.00	0.00	0.00	0.00	0.00	0.00	0.00	0.00	0.00	0.00	0.00		
NS-14.05	Pe/ TRPss	shale w/ barite nodules	10.23	0.01	0.00	20.41	2.01	0.01	4.77	0.07	0.00	0.05	0.00	0.01	0.04	5.18	0.00	0.00	0.05	0.10	0.00	0.753962	0.000022
NS-14.05b	Pe/ TRPss	barite nodules	10.61	0.26	74.81	10.51	3.23	0.14	0.90	0.01	0.30	0.10	32.93	0.01	13.65	9.85	0.00	0.00	0.05	0.18	0.00		
NS-18.01	Mk	shale	11.34	0.00	0.00	31.56	0.77	0.03	3.42	0.56	0.00	0.05	0.04	0.01	0.03	5.39	0.00	0.00	0.05	0.07	0.00		
NS-20.06	Dke	cong.	5.33	0.00	0.00	12.80	0.79	0.00	0.20	0.11	0.00	0.04	0.07	0.01	0.00	4.22	0.01	0.00	0.02	0.01	0.00	0.723511	0.000013
NS-27.01	MDk	altered cong.	5.65	0.00	0.31	27.17	1.02	0.01	0.83	0.29	0.00	0.03	0.15	0.01	0.17	3.44	0.00	0.00	0.03	0.30	0.00		
NS-27.01b	MDk	altered cong./ vein subsample	0.00	0.00	0.00	5.90	0.27	0.02	0.00	0.00	0.00	0.03	0.00	0.03	0.06	3.77	0.00	0.00	0.00	0.04	0.00		
NS-34.01	Kn	sandstone	13.47	0.08	0.23	18.66	1.64	0.03	5.10	0.11	0.03	0.14	0.01	0.01	0.21	13.9	0.00	0.01	0.06	0.07	0.00	0.727727	0.000026
NS-36.01	PMl	dark limestone	0.00	0.00	2.40	0.04	0.03	0.00	0.00	0.00	0.00	0.00	0.02	0.01	0.00	0.02	0.00	0.00	0.00	0.01	0.00		

HF residual digest sample number	geo fm	rock type	concentrations mg/g rock Al	Ba	Ca	Fe	K	Li	Mg	Mn	Na	Ni	P	Rb	S	Si	Sr	Ti	V	Zn	Zr	$^{87}Sr/^{86}Sr$	2 sigma
DH-01.05	Hot Springs Pluton	granite	33.78	0.39	9.37	1.94	14.40	0.01	0.08	0.03	18.63	0.26	0.00	0.06	0.00	25.51	--	0.43	0.16	0.00	0.04		
DH-02.05	Bonanza Pluton	granite	58.50	1.27	15.03	12.88	32.61	0.01	1.44	0.14	21.31	0.10	0.00	0.09	0.00	10.21	--	1.10	0.26	0.01	0.03		
DH-03.06	Ksy	syenite	70.99	0.75	7.69	11.40	54.66	0.01	1.65	0.32	23.06	0.09	0.00	0.18	0.00	8.55	--	0.66	0.31	0.02	0.00		
DH-03.07	Kic	cong.	57.81	0.89	0.39	1.36	37.95	0.01	0.53	0.02	24.98	0.06	0.00	0.11	0.02	5.71	--	0.35	0.26	0.00	0.08		
DH-03.07B	Kic	skarn cong.	10.31	0.09	0.00	2.62	3.96	0.01	0.56	0.01	1.14	0.41	0.00	0.02	0.03	39.21	0.01	1.42	0.05	0.00	0.02		
DH-C	Dbs	phyllite	18.61	0.37	0.00	5.10	17.67	0.02	0.03	0.01	6.67	0.30	0.01	0.05	0.05	30.72	0.02	1.69	0.09	0.01	0.03	0.740233	0.000027
NS-03.03	Kf	sandstone	7.88	0.32	0.00	1.50	1.98	0.01	0.71	0.01	2.19	0.26	0.01	0.01	0.06	26.37	0.01	1.42	0.04	0.00	0.03	0.715210	0.000014
NS-05.02	Pml	limestone/ chalk	0.00	0.00	0.00	0.00	0.00	0.01	0.00	0.00	0.00	0.13	0.00	0.01	0.02	12.84	0.00	0.01	0.00	0.00	0.00		
NS-05.02b	Pml	limestone/ chalk	0.00	0.00	0.00	0.00	0.00	0.01	0.00	0.00	0.00	0.09	0.00	0.01	0.02	8.81	0.00	0.00	0.00	0.00	0.00		
NS-05.03	Pml	limestone/ chert	0.41	0.02	0.25	0.05	0.08	0.00	0.00	0.00	0.00	0.19	0.01	0.00	0.00	18.80	0.00	0.02	0.00	0.00	0.00	0.708846	0.000017
NS-10.01	MDk	cong.	8.43	0.04	0.00	0.95	1.24	0.01	0.16	0.01	0.00	0.32	0.02	0.01	0.02	33.15	0.02	0.51	0.04	0.00	0.01		
NS-10.01b	MDk	cong.chert clast	6.64	0.05	0.00	1.17	2.58	0.01	0.44	0.00	0.00	0.79	0.01	0.02	0.03	76.76	0.02	0.32	0.03	0.00	0.00		
NS-10.03	MDk	quartzite	7.74	0.08	0.00	0.05	0.42	0.01	0.00	0.00	0.00	0.55	0.02	0.01	0.01	57.81	0.02	0.40	0.04	0.00	0.01		
NS-10.07	MDk	ss w/ slickensides	6.89	0.02	0.00	1.30	0.75	0.01	0.07	0.00	0.00	0.41	0.02	0.01	0.02	41.36	0.02	0.38	0.03	0.00	0.00		
NS-14.04	Pml	chalky limestone	0.00	0.00	0.00	0.00	0.00	0.00	0.00	0.00	0.00	0.00	0.00	0.00	0.00	0.00	0.00	0.00	0.00	0.00	0.00		
NS-14.05	Pe/ TRPss	shale w/ barite nodules	23.77	0.17	0.00	14.45	22.80	0.01	1.00	0.02	2.10	0.21	0.01	0.04	0.04	21.92	0.04	2.08	0.11	0.04	0.04	0.741406	0.000016
NS-14.05b	Pe/ TRPss	barite nodules	8.91	0.27	3.49	1.37	2.57	0.10	0.55	0.00	0.34	0.55	1.64	0.01	0.77	53.65	0.03	0.96	0.04	0.01	0.01		
NS-18.01	Mk	shale	18.31	0.34	0.00	20.91	17.44	0.14	0.55	0.26	1.90	0.13	0.13	0.04	0.10	12.97	0.05	2.24	0.09	0.04	0.05		
NS-20.06	Dke	cong.	12.69	0.00	0.00	6.11	1.09	0.01	0.15	0.05	0.00	0.43	0.03	0.01	0.00	43.73	0.02	1.09	0.06	0.00	0.02	0.714283	0.000017
NS-27.01	MDk	altered cong.	5.36	0.00	0.00	3.57	1.58	0.02	0.05	0.02	0.00	0.46	0.02	0.01	0.01	44.96	0.01	1.18	0.03	0.02	0.02		
NS-27.01b	MDk	altered cong./ vein subsample	0.27	0.00	0.00	0.00	0.17	0.04	0.00	0.00	0.00	2.05	0.00	0.03	0.02	209.7	0.00	0.18	0.01	0.00	0.00		
NS-34.01	Kn	sandstone	36.45	0.59	0.23	5.13	12.48	0.02	1.07	0.03	6.28	0.27	0.05	0.04	0.03	26.0	0.06	1.56	0.17	0.01	0.06	0.723082	0.000017
NS-36.01	PMl	dark limestone	0.00	0.00	0.00	0.00	0.02	0.01	0.00	0.00	0.00	0.37	0.00	0.01	0.03	36.37	0.00	0.02	0.00	0.00	0.00		

Appendix B: Soil data for individual sampling pits.

Soil sampling locations and physical data.

sample name	location	glacial surface	latitude (dec. deg. N)	longitude (dec. deg. W.)	min depth cm	max depth cm	mean depth cm	% water	% <2mm	% organic matter det. by LOI	dry density (g/cm^3)
DH-01.07	Hot Springs Pluton	--	66.3417	150.4513	20	25	22.5	43%	76%	14%	
DH-02.07	Bonanza Pluton	--	66.6889	150.6594				14%	73%	4%	
DH-03.09	Jim River Pluton Quarry site	--	66.9910	150.2886	0	10	5	27%	55%	43%	
DH-03.10	Jim River Pluton Quarry site	--	66.9910	150.2886	10	14	12	9%	62%	3%	
DH-03.11	Jim River Pluton Quarry site	--	66.9910	150.2886	14	30	22	7%	64%	3%	
NS-08.07	It 1 pit	It 1	68.6255	149.5774	10	30	20	18%	31%	5%	
NS-08.08	It 1 pit	It 1	68.6255	149.5774	30	50	40	21%	54%	8%	
NS-08.10	It 1 pit	It 1	68.6255	149.5774	65	70	67.5	32%	83%	10%	
NS-13.13	It 2 pit	It 2	68.6412	149.6030	7	17	12				
NS-13.14	It 2 pit	It 2	68.6412	149.6030	17	25	21	24%	71%	12%	
NS-13.15	It 2 pit	It 2	68.6412	149.6030	25	39	32	32%	40%	20%	
NS-13.16	It 2 pit	It 2	68.6412	149.6030	39	57	48	45%	57%	8%	
NS-13.23	It 2 pit	It 2	68.6412	149.6030	72	75	73.5	70%	100%	7%	
NS-22.08	Sag 2 pit	Sag 2	68.6425	149.4591	0	10	5				
NS-22.09	Sag 2 pit	Sag 2	68.6425	149.4591	10	30	20	20%	76%	7%	
NS-22.10	Sag 2 pit	Sag 2	68.6425	149.4591	30	50	40	36%	100%	23%	
NS-22.11	Sag 2 pit	Sag 2	68.6425	149.4591	75	75	75	42%	82%	22%	
NS-22.26	Sag 2 pit- between pit and road- 50 m south of road	Sag 2			0	12	6				
NS-22.27	Sag 2 pit- between pit and road- 50 m south of road	Sag 2			12	20	16	13%	60%	7%	
NS-23A.06	Imnaviat lower slope pit	Sag 1			0	15	7.5				
NS-23A.07	Imnaviat lower slope pit	Sag 1			15	20	17.5	64%	89%	33%	
NS-23A.08	Imnaviat lower slope pit	Sag 1			20	30	25	54%	97%	25%	

sample name	location	glacial surface	latitude (dec. deg. N)	longitude (dec. deg. W.)	min depth cm	max depth cm	mean depth cm	% water	% <2mm	% organic matter det. by LOI	dry density (g/cm^3)
NS-23A.09	Imnaviat lower slope pit	Sag 1			30	50	40	62%	96%	19%	
NS-23B.06	Imnaviat middle slope pit	Sag 1			0	10	5				
NS-23B.07	Imnaviat middle slope pit	Sag 1			10	28	19	43%	98%	16%	
NS-23B.08	Imnaviat middle slope pit	Sag 1			28	50	39	46%	92%	17%	
NS-23C.06	Imnaviat upper slope pit	Sag 1			0	15	7.5				
NS-23C.07	Imnaviat upper slope pit	Sag 1			15	20	17.5	48%	99%	27%	
NS-23C.08	Imnaviat upper slope pit	Sag 1			20	50	35	40%	99%	15%	
NS-23D.07	Imnaviat crest pit	Sag 1	68.6205	149.3080	0	12	6				
NS-23D.08	Imnaviat crest pit	Sag 1	68.6205	149.3080	12	20	16	42%	83%	15%	
NS-23D.09	Imnaviat crest pit	Sag 1	68.6205	149.3080	20	35	27.5	20%	94%	7%	
NS-23D.10	Imnaviat crest pit	Sag 1	68.6205	149.3080	35	60	47.5	22%	87%	7%	
NS-28.07	It 3 pit	It 3	68.4978	149.4833	0	12	6				
NS-28.08	It 3 pit	It 3	68.4978	149.4833	12	20	16	19%	96%	5%	
NS-28.09	It 3 pit	It 3	68.4978	149.4833	20	36	28	24%	98%	7%	
NS-28.10	It 3 pit	It 3	68.4978	149.4833	36	60	48	27%	100%	8%	
NS-29.01	Imnaviat bedrock pit	--			0	10	5	9%	37%	6%	
NS-37.06	Acidic veg pit on It 2 surface	It 2	68.6413	149.6285	0	18	9				
NS-37.07	Acidic veg pit on It 2 surface	It 2	68.6413	149.6285	18	34	26	15%	79%	4%	
NS-37.08	Acidic veg pit on It 2 surface	It 2	68.6413	149.6285	34	50	42	21%	88%	6%	
NS-38.08	Non-acidic veg pit on It 2 surface	It 2	68.6414	149.6279	0	15	7.5				

sample name	location	glacial surface	latitude (dec. deg. N)	longitude (dec. deg. W.)	min depth cm	max depth cm	mean depth cm	% water	% <2mm	% organic matter det. by LOI	dry density (g/cm^3)
NS-38.09	Non-acidic veg pit on lt 2 surface	lt 2	68.6414	149.6279	15	35	25	12%	57%	4%	
NS-38.10	Non-acidic veg pit on lt 2 surface	lt 2	68.6414	149.6279	35	70	52.5	12%	65%	4%	
NS-47.03	Sag 2 E5 10 m from road	Sag 2	68.6425	149.4591	0	10	5				
NS-47.04	Sag 2 E5 10 m from road	Sag 2	68.6425	149.4591	10	30	20	16%	40%	13%	
NS-48.01	middle of Dalton Highway, mile 287	road	68.6425	149.4591			0	4%	35%	2%	
NS-101.01	lt 1 Pit 2	lt 1	68.6251	149.5718	0	6	3	63%			
NS-101.02	lt 1 Pit 2	lt 1	68.6251	149.5718	6	20	13	17%	54%		1.12
NS-101.03	lt 1 Pit 2	lt 1	68.6251	149.5718	20	35	27.5	16%	63%		1.03
NS-101.04	lt 1 Pit 2	lt 1	68.6251	149.5718	35	48	41.5	13%	55%		1.43
NS-101.05	lt 1 Pit 2	lt 1	68.6251	149.5718	48	60	54	18%	42%		
NS-101.06	lt 1 Pit 2	lt 1	68.6251	149.5718	60	68	64	17%	45%		2.20
NS-102.01	lt 1 Pit 3	lt 1	68.6247	149.5708	0	8	4	69%			
NS-102.02	lt 1 Pit 3	lt 1	68.6247	149.5708	8	20	14	21%	62%		1.20
NS-102.03	lt 1 Pit 3	lt 1	68.6247	149.5708	20	34	27	17%	53%		1.39
NS-102.04	lt 1 Pit 3	lt 1	68.6247	149.5708	34	50	42	18%	54%		1.35
NS-102.05	lt 1 Pit 3	lt 1	68.6247	149.5708	50	60	55	23%	65%		
NS-102.06	lt 1 Pit 3	lt 1	68.6247	149.5708	60	70	65	40%	84%		1.22
NS-103.01	Sag 2 Pit 2	Sag 2	68.6451	149.4352	0	9	4.5	82%			
NS-103.02	Sag 2 Pit 2	Sag 2	68.6451	149.4352	9	20	14.5	18%	71%		1.64
NS-103.03	Sag 2 Pit 2	Sag 2	68.6451	149.4352	20	35	27.5	19%	71%		1.74
NS-103.04	Sag 2 Pit 2	Sag 2	68.6451	149.4352	35	50	42.5	17%	71%		1.77
NS-103.05	Sag 2 Pit 2	Sag 2	68.6451	149.4352	50	62	56	13%	66%		1.66
NS-103.06	Sag 2 Pit 2	Sag 2	68.6451	149.4352	62	70	66	19%	78%		
NS-104.01	Sag 2 Pit 3	Sag 2	68.6445	149.4306	0	5	2.5	63%			
NS-104.02	Sag 2 Pit 3	Sag 2	68.6445	149.4306	5	25	15	17%	50%		1.50
NS-104.03	Sag 2 Pit 3	Sag 2	68.6445	149.4306	25	40	32.5	17%	67%		1.72
NS-104.04	Sag 2 Pit 3	Sag 2	68.6445	149.4306	40	60	50	17%	67%		1.58
NS-104.05	Sag 2 Pit 3	Sag 2	68.6445	149.4306	60	75	67.5	17%	56%		1.44

sample name	location	glacial surface	latitude (dec. deg. N)	longitude (dec. deg. W.)	min depth cm	max depth cm	mean depth cm	% water	% <2mm	% organic matter det. by LOI	dry density (g/cm^3)
NS-104.06	Sag 2 Pit 3	Sag 2	68.6445	149.4306	75	80	77.5	21%	70%		
NS-105.01	Sag 1 Pit 2	Sag 1	68.6178	149.3231	0	10	5	71%			0.32
NS-105.02	Sag 1 Pit 2	Sag 1	68.6178	149.3231	10	20	15	27%	78%		
NS-105.03	Sag 1 Pit 2	Sag 1	68.6178	149.3231	20	35	27.5	16%	60%		0.99
NS-105.04	Sag 1 Pit 2	Sag 1	68.6178	149.3231	35	50	42.5	17%	60%		
NS-105.05	Sag 1 Pit 2	Sag 1	68.6178	149.3231	50	55	52.5	19%	59%		
NS-106.01	Sag 1 Pit 3	Sag 1	68.6517	149.3071	0	15	7.5	72%			
NS-106.02	Sag 1 Pit 3	Sag 1	68.6517	149.3071	15	25	20	41%	60%		1.00
NS-106.03	Sag 1 Pit 3	Sag 1	68.6517	149.3071	25	35	30	22%	69%		1.06
NS-106.04	Sag 1 Pit 3	Sag 1	68.6517	149.3071	35	50	42.5	19%	56%		1.00
NS-106.05	Sag 1 Pit 3	Sag 1	68.6517	149.3071	50	61	55.5	32%	64%		0.43
NS-107.01	It 3 Pit 2	It 3	68.5135	149.4667	0	4	2	73%			
NS-107.02	It 3 Pit 2	It 3	68.5135	149.4667	4	15	9.5	26%	56%		
NS-107.03	It 3 Pit 2	It 3	68.5135	149.4667	15	35	25	22%	54%		
NS-107.04	It 3 Pit 2	It 3	68.5135	149.4667	35	60	47.5	23%	71%		
NS-107.05	It 3 Pit 2	It 3	68.5135	149.4667	60	70	65	36%	66%		
NS-108.01	It 3 Pit 3	It 3	68.5117	149.4661	0	8	4	73%			
NS-108.02	It 3 Pit 3	It 3	68.5117	149.4661	8	28	18	25%	63%		1.15
NS-108.03	It 3 Pit 3	It 3	68.5117	149.4661	28	46	37	33%	76%		0.90
NS-108.04	It 3 Pit 3	It 3	68.5117	149.4661	46	60	53	34%	73%		1.20
NS-108.05	It 3 Pit 3	It 3	68.5117	149.4661	60	70	65	68%	73%		0.24
NS-108.06	It 3 Pit 3	It 3	68.5117	149.4661	70	73	71.5	41%	61%		
NS-108.13	It 3 Pit 3	It 3	68.5117	149.4661	60	70	65				
NS-109.01	It 2 Pit 2	It 2	68.6343	149.6415	0	15	7.5	74%			
NS-109.02	It 2 Pit 2	It 2	68.6343	149.6415	15	25	20	66%			
NS-109.03	It 2 Pit 2	It 2	68.6343	149.6415	25	40	32.5	17%	57%		1.52
NS-109.04	It 2 Pit 2	It 2	68.6343	149.6415	40	60	50	18%	62%		1.48
NS-109.05	It 2 Pit 2	It 2	68.6343	149.6415	60	70	65	33%	59%		
NS-110.01	It 2 Pit 3	It 2	68.6414	149.5995	0	11	5.5	70%			
NS-110.02	It 2 Pit 3	It 2	68.6414	149.5995	11	22	16.5	31%	66%		
NS-110.03	It 2 Pit 3	It 2	68.6414	149.5995	22	40	31	19%	55%		
NS-110.04	It 2 Pit 3	It 2	68.6414	149.5995	40	60	50	29%	61%		
NS-110.05	It 2 Pit 3	It 2	68.6414	149.5995	60	70	65	53%	64%		0.55
NS-111.01	It 3 Pit 4	It 3	68.5117	149.4665	0	3	1.5	70%			
NS-111.02	It 3 Pit 4	It 3	68.5117	149.4665	3	13	8	24%	89%		0.95
NS-111.03	It 3 Pit 4	It 3	68.5117	149.4665	13	37	25	28%	75%		0.96
NS-111.04	It 3 Pit 4	It 3	68.5117	149.4665	37	60	48.5	18%	77%		1.11
NS-111.05	It 3 Pit 4	It 3	68.5117	149.4665	60	71	65.5	59%	55%		0.45
NS-112.01	neo 1 pit 1	neo 1			0	4	2	10%	40%		
NS-112.02	neo 1 pit 1	neo 1			4	14	9	7%	33%		

sample name	location	glacial surface	latitude (dec. deg. N)	longitude (dec. deg. W.)	min depth cm	max depth cm	mean depth cm	% water	% <2mm	% organic matter det. by LOI	dry density (g/cm^3)
NS-112.03	neo 1 pit 1	neo 1			0	14	7				
NS-113.01	neo 2 pit 1	neo 2	68.3506	149.5376	0	3	1.5	17%	63%		
NS-113.02	neo 2 pit 1	neo 2	68.3506	149.5376	3	5	4	11%	57%		
NS-113.03	neo 2 pit 1	neo 2	68.3506	149.5376	5	17	11	10%	53%		
NS-113.04	neo 2 pit 1	neo 2	68.3506	149.5376	17	30	23.5	7%	38%		
NS-114.01	neo 3 pit 1	neo 3	68.3776	149.5216	0	1	0.5	73%			
NS-114.02	neo 3 pit 1	neo 3	68.3776	149.5216	1	8	4.5	39%			
NS-114.03	neo 3 pit 1	neo 3	68.3776	149.5216	8	22	15	9%	47%		
NS-114.04	neo 3 pit 1	neo 3	68.3776	149.5216	22	63	42.5	10%	35%		
NS-117.01	Anak Pit 1	Anak	68.9060	149.3842	0	12	6	59%			
NS-117.02	Anak Pit 1	Anak	68.9060	149.3842	12	25	18.5	16%	58%		
NS-117.03	Anak Pit 1	Anak	68.9060	149.3842	25	50	37.5	8%	34%		
NS-117.04	Anak Pit 1	Anak	68.9060	149.3842	50	70	60	8%	25%		
NS-117.05	Anak Pit 1	Anak	68.9060	149.3842	70	80	75	9%	26%		
NS-117.06	Anak Pit 1	Anak	68.9060	149.3842	80	85	82.5	11%	40%		
NS-118.01	Anak Pit 2	Anak	68.9070	149.3842	0	5	2.5	80%			
NS-118.02	Anak Pit 2	Anak	68.9070	149.3842	5	30	17.5	69%			
NS-118.03	Anak Pit 2	Anak	68.9070	149.3842	30	60	45	46%	51%		
NS-118.04	Anak Pit 2	Anak	68.9070	149.3842	60	70	65	68%	53%		0.42
NS-119.01	Anak Pit 3	Anak	68.9070	149.3841	0	15	7.5	81%			
NS-119.02	Anak Pit 3	Anak	68.9070	149.3841	15	25	20	33%	34%		
NS-119.03	Anak Pit 3	Anak	68.9070	149.3841	25	40	32.5	13%	34%		
NS-119.04	Anak Pit 3	Anak	68.9070	149.3841	40	80	60	13%	34%		
NS-119.05	Anak Pit 3	Anak	68.9070	149.3841	80	90	85	19%	43%		
NS-119.06	Anak Pit 3	Anak	68.9070	149.3841	90	100	95	10%	34%		
NS-121.01	Ice Lens Melt-Out	Sag 1	68.6924	149.2033	200	300	250		88%		
NS-121.02	Ice Lens Melt-Out	Sag 1	68.6924	149.2033	150	200	175		37%		

sample name	location	glacial surface	latitude (dec. deg. N)	longitude (dec. deg. W.)	min depth cm	max depth cm	mean depth cm	% water	% <2mm	% organic matter det. by LOI	dry density (g/cm^3)
NS-121.03	Ice Lens Melt-Out	Sag 1	68.6924	149.2033					71%		
NS-122.01	Gunsight Pit 1	Gunsight	69.2663	148.9047	0	16	8	79%			
NS-122.02	Gunsight Pit 1	Gunsight	69.2663	148.9047	16	38	27	23%	37%		
NS-122.03	Gunsight Pit 1	Gunsight	69.2663	148.9047	38	44	41	31%	76%		
NS-122.04	Gunsight Pit 1	Gunsight	69.2663	148.9047	44	50	47	53%	68%		
NS-122.05	Gunsight Pit 1	Gunsight	69.2663	148.9047	50	54	52	64%	57%		
NS-122.06	Gunsight Pit 1	Gunsight	69.2663	148.9047	54	80	67	72%	73%		
NS-122.07	Gunsight Pit 1	Gunsight	69.2663	148.9047	100	110	105	32%	57%		
NS-123.01	Gunsight Pit 2	Gunsight	69.2663	148.9047	0	10	5	81%			
NS-123.02	Gunsight Pit 2	Gunsight	69.2663	148.9047	10	32	21	35%	57%		
NS-123.03	Gunsight Pit 2	Gunsight	69.2663	148.9047	32	60	46	79%	70%		
NS-123.04	Gunsight Pit 2	Gunsight	69.2663	148.9047	60	100	80	74%	85%		
NS-124.01	Gunsight Frost Boil	Gunsight	69.2663	148.9047	0	38	19	21%	44%		
NS-124.02	Gunsight Frost Boil	Gunsight	69.2663	148.9047	38	54	46	22%	51%		
NS-124.03	Gunsight Frost Boil	Gunsight	69.2663	148.9047	54	84	69	25%	39%		

Soil 1M NH_4Cl exchangeable fraction chemistry, mg/g.

sample name	Al	Ba	Ca	Fe	K	Li	Mg	Mn	Na	Ni	P	Rb	S	Si	Sr	Ti	V	Zn	Zr
DH-01.07	0.00	0.06	0.83	0.00	0.06	0.00	0.15	0.01	0.05	0.00	0.00	0.00	0.01	0.01	0.01	0.00	0.00	0.00	0.00
DH-02.07	0.00	0.04	0.05	0.00	0.03	0.00	0.00	0.00	0.00	0.00	0.00	0.00	0.03	0.01	0.00	0.00	0.00	0.00	0.00
DH-03.09	0.06	0.03	0.64	0.02	0.27	0.00	0.12	0.03	0.01	0.00	0.01	0.00	0.03	0.01	0.01	0.00	0.00	0.00	0.00
DH-03.10	0.00	0.00	0.06	0.00	0.04	0.00	0.00	0.00	0.00	0.00	0.00	0.00	0.00	0.00	0.00	0.00	0.00	0.00	0.00
DH-03.11	0.00	0.01	0.26	0.00	0.05	0.00	0.00	0.00	0.01	0.00	0.00	0.00	0.04	0.00	0.00	0.00	0.00	0.00	0.00
NS-08.07	0.00	0.03	0.14	0.01	0.02	0.00	0.02	0.00	0.00	0.00	0.00	0.00	0.00	0.00	0.00	0.00	0.00	0.00	0.00
NS-08.08	0.00	0.06	0.30	0.02	0.03	0.00	0.04	0.00	0.00	0.00	0.00	0.00	0.01	0.00	0.00	0.00	0.00	0.00	0.00
NS-08.10	0.00	0.06	1.41	0.01	0.08	0.00	0.13	0.01	0.00	0.00	0.00	0.00	0.01	0.00	0.01	0.00	0.00	0.00	0.00
NS-13.13	0.01	0.02	4.55	0.04	0.05	0.00	0.26	0.12	0.01		0.01	0.01		0.01	0.01	0.00			
NS-13.14	0.00	0.06	1.70	0.00	0.03	0.00	0.09	0.01	0.00	0.00	0.00	0.00	0.00	0.00	0.00	0.00	0.00	0.00	0.00
NS-13.15	0.00	0.11	2.35	0.02	0.08	0.00	0.22	0.01	0.00	0.00	0.00	0.00	0.01	0.00	0.00	0.00	0.00	0.00	0.00
NS-13.16	0.00	0.03	3.63	0.01	0.11	0.00	0.24	0.03	0.00	0.00	0.00	0.00	0.18	0.00	0.00	0.00	0.00	0.00	0.00
NS-13.23	0.00	0.03	2.74	0.01	0.12	0.00	0.30	0.02	0.02	0.00	0.00	0.00	0.23	0.01	0.00	0.00	0.00	0.00	0.00
NS-22.08	0.02	0.03	1.16	0.06	0.17	0.00	0.25	0.07	0.01		0.03	0.01		0.01	0.00	0.00			
NS-22.09	0.00	0.06	0.34	0.01	0.05	0.00	0.06	0.00	0.00	0.00	0.00	0.00	0.00	0.00	0.00	0.00	0.00	0.00	0.00
NS-22.10	0.02	0.24	1.45	0.04	0.12	0.00	0.21	0.02	0.01	0.00	0.00	0.00	0.00	0.03	0.00	0.00	0.00	0.00	0.00
NS-22.11	0.00	0.25	2.23	0.04	0.20	0.00	0.27	0.02	0.01	0.00	0.00	0.00	0.01	0.01	0.01	0.00	0.00	0.00	0.00
NS-22.26	0.01	0.03	4.85	0.04	0.02	0.00	0.22	0.00	0.01		0.01	0.01		0.00	0.01	0.00			
NS-22.27	0.00	0.03	0.25	0.00	0.03	0.00	0.04	0.00	0.00	0.00	0.00	0.00	0.01	0.00	0.00	0.00	0.00	0.00	0.00
NS-23A.06	0.06	0.12	2.00	0.18	0.28	0.00	0.50	0.44	0.02		0.01	0.01		0.03	0.01	0.00			
NS-23A.07	0.00	0.17	1.28	0.03	0.08	0.00	0.30	0.55	0.00	0.00	0.00	0.00	0.03	0.01	0.01	0.00	0.00	0.00	0.00
NS-23A.08	0.05	0.17	0.96	0.16	0.04	0.00	0.24	0.02	0.00	0.00	0.00	0.00	0.03	0.05	0.00	0.00	0.00	0.00	0.00
NS-23A.09	0.03	0.15	0.72	0.08	0.06	0.00	0.15	0.03	0.00	0.00	0.00	0.00	0.04	0.02	0.00	0.00	0.00	0.00	0.00
NS-23B.06	0.02	0.09	2.15	0.03	0.58	0.00	0.76	0.21	0.02		0.03	0.01		0.05	0.01	0.00			
NS-23B.07	0.03	0.20	1.26	0.09	0.07	0.00	0.41	0.07	0.01	0.00	0.00	0.00	0.01	0.03	0.00	0.00	0.00	0.00	0.00
NS-23B.08	0.06	0.34	1.65	0.18	0.07	0.00	0.44	0.02	0.01	0.00	0.00	0.00	0.02	0.08	0.01	0.00	0.00	0.00	0.00
NS-23C.06	0.01	0.08	2.01	0.01	0.15	0.00	0.47	0.19	0.01		0.00	0.01		0.01	0.01	0.00			
NS-23C.07	0.01	0.13	0.63	0.03	0.09	0.00	0.19	0.09	0.01	0.00	0.00	0.00	0.02	0.02	0.00	0.00	0.00	0.00	0.00
NS-23C.08	0.01	0.11	0.38	0.06	0.09	0.00	0.12	0.04	0.01	0.00	0.00	0.00	0.02	0.00	0.00	0.00	0.00	0.00	0.00
NS-23D.07	0.01	0.05	2.13	0.01	0.21	0.00	0.30	0.26	0.02		0.01	0.01		0.00	0.01	0.00			
NS-23D.08	0.00	0.08	1.19	0.04	0.05	0.00	0.23	0.02	0.01	0.00	0.00	0.00	0.04	0.02	0.00	0.00	0.00	0.00	0.00
NS-23D.09	0.11	0.06	0.69	0.29	0.04	0.00	0.23	0.01	0.01	0.00	0.00	0.00	0.04	0.07	0.00	0.00	0.00	0.00	0.00
NS-23D.10	0.01	0.06	0.60	0.03	0.07	0.00	0.17	0.00	0.01	0.00	0.00	0.00	0.05	0.02	0.00	0.00	0.00	0.00	0.00
NS-28.07	0.03	0.01	2.08	0.13	0.22	0.00	0.39	0.07	0.01		0.01	0.01		0.01	0.01	0.00			
NS-28.08	0.00	0.02	0.14	0.04	0.04	0.00	0.05	0.00	0.00	0.00	0.00	0.00	0.00	0.01	0.00	0.00	0.00	0.00	0.00
NS-28.09	0.00	0.03	0.44	0.03	0.04	0.00	0.13	0.00	0.00	0.00	0.00	0.00	0.00	0.00	0.00	0.00	0.00	0.00	0.00
NS-28.10	0.00	0.03	0.33	0.04	0.06	0.00	0.11	0.00	0.00	0.00	0.00	0.00	0.00	0.00	0.00	0.00	0.00	0.00	0.00
NS-29.01	0.00	0.16	0.98	0.02	0.03	0.00	0.22	0.00	0.00	0.00	0.00	0.00	0.00	0.01	0.01	0.00	0.00	0.00	0.00
NS-37.06	0.05	0.03	2.08	0.13	0.00	0.00	0.21	0.89	0.01		0.01	0.01		0.02	0.01	0.00			
NS-37.07	0.00	0.03	0.37	0.02	0.03	0.00	0.06	0.03	0.00	0.00	0.00	0.00	0.00	0.00	0.00	0.00	0.00	0.00	0.00
NS-37.08	0.00	0.05	0.65	0.02	0.04	0.00	0.10	0.06	0.01	0.00	0.00	0.00	0.01	0.00	0.00	0.00	0.00	0.00	0.00
NS-38.08	0.17	0.06	4.61	0.17	0.00	0.00	0.29	0.00	0.01		0.01	0.01		0.03	0.01	0.00			
NS-38.09	0.00	0.04	1.01	0.02	0.04	0.00	0.07	0.00	0.00	0.00	0.00	0.00	0.00	0.00	0.00	0.00	0.00	0.00	0.00
NS-38.10	0.00	0.06	1.25	0.05	0.05	0.00	0.08	0.00	0.00	0.00	0.00	0.00	0.00	0.01	0.00	0.00	0.00	0.00	0.00
NS-47.03	0.01	0.03	3.63	0.21	0.00	0.00	0.25	0.03	0.01		0.00	0.01		0.01	0.01	0.00			
NS-47.04	0.02	0.08	1.84	0.06	0.04	0.00	0.15	0.00	0.00	0.00	0.00	0.00	0.00	0.02	0.01	0.00	0.00	0.00	0.00
NS-48.01	0.00	0.07	1.62	0.03	0.03	0.00	0.07	0.00	0.02	0.00	0.00	0.00	0.00	0.03	0.00	0.00	0.00	0.00	0.00
NS-101.01	0.10	0.05	0.88	0.13	0.21	0.00	0.15	0.07	0.00	0.00	0.00	0.00	0.04	0.02	0.00	0.00	0.00	0.01	0.00
NS-101.02	0.01	0.05	0.30	0.06	0.03	0.00	0.05	0.04	0.00	0.00	0.00	0.00	0.00	0.01	0.00	0.00	0.00	0.00	0.00
NS-101.03	0.00	0.05	0.24	0.02	0.03	0.00	0.04	0.05	0.00	0.00	0.00	0.00	0.00	0.00	0.00	0.00	0.00	0.00	0.00
NS-101.04	0.02	0.10	0.44	0.10	0.04	0.00	0.07	0.05	0.00	0.00	0.00	0.00	0.00	0.02	0.00	0.00	0.00	0.00	0.00
NS-101.05	0.06	0.10	0.50	0.19	0.04	0.00	0.08	0.04	0.00	0.00	0.00	0.00	0.00	0.06	0.00	0.00	0.00	0.00	0.00
NS-101.06	0.01	0.10	2.68	0.04	0.07	0.00	0.07	0.02	0.00	0.00	0.00	0.00	0.00	0.01	0.00	0.00	0.00	0.00	0.00
NS-102.01	0.10	0.05	0.77	0.17	0.35	0.00	0.18	0.23	0.00	0.00	0.01	0.00	0.05	0.01	0.00	0.00	0.00	0.01	0.00
NS-102.02	0.02	0.04	0.12	0.11	0.03	0.00	0.04	0.09	0.00	0.00	0.00	0.00	0.01	0.01	0.00	0.00	0.00	0.00	0.00
NS-102.03	0.02	0.05	0.11	0.06	0.02	0.00	0.03	0.07	0.00	0.00	0.00	0.00	0.00	0.02	0.00	0.00	0.00	0.00	0.00
NS-102.04	0.02	0.05	0.11	0.07	0.02	0.00	0.03	0.05	0.00	0.00	0.00	0.00	0.00	0.02	0.00	0.00	0.00	0.00	0.00
NS-102.05	0.04	0.04	0.09	0.14	0.03	0.00	0.03	0.08	0.00	0.00	0.00	0.00	0.00	0.03	0.00	0.00	0.00	0.00	0.00

sample name	Al	Ba	Ca	Fe	K	Li	Mg	Mn	Na	Ni	P	Rb	S	Si	Sr	Ti	V	Zn	Zr
NS-102.06	0.01	0.04	0.09	0.02	0.05	0.00	0.02	0.05	0.00	0.00	0.00	0.00	0.00	0.02	0.00	0.00	0.00	0.00	0.00
NS-103.01	0.01	0.03	2.09	0.02	0.38	0.00	0.36	0.28	0.01	0.00	0.02	0.00	0.04	0.02	0.01	0.00	0.00	0.01	0.00
NS-103.02	0.01	0.04	0.14	0.02	0.03	0.00	0.03	0.02	0.00	0.00	0.00	0.00	0.01	0.00	0.00	0.00	0.00	0.00	0.00
NS-103.03	0.10	0.04	0.13	0.26	0.02	0.00	0.05	0.01	0.00	0.00	0.00	0.00	0.01	0.09	0.00	0.00	0.00	0.00	0.00
NS-103.04	0.07	0.03	0.12	0.16	0.02	0.00	0.04	0.01	0.00	0.00	0.00	0.00	0.01	0.07	0.00	0.00	0.00	0.00	0.00
NS-103.05	0.01	0.04	0.12	0.04	0.03	0.00	0.03	0.02	0.00	0.00	0.00	0.00	0.00	0.01	0.00	0.00	0.00	0.00	0.00
NS-103.06	0.01	0.02	0.06	0.02	0.01	0.00	0.01	0.00	0.00	0.00	0.00	0.00	0.00	0.00	0.00	0.00	0.00	0.00	0.00
NS-104.01	0.17	0.04	0.60	0.38	0.22	0.00	0.19	0.05	0.00	0.00	0.01	0.00	0.06	0.05	0.00	0.00	0.00	0.01	0.00
NS-104.02	0.03	0.07	0.09	0.07	0.03	0.00	0.03	0.01	0.00	0.00	0.00	0.00	0.00	0.03	0.00	0.00	0.00	0.00	0.00
NS-104.03	0.02	0.07	0.13	0.02	0.03	0.00	0.04	0.00	0.00	0.00	0.00	0.00	0.00	0.01	0.00	0.00	0.00	0.00	0.00
NS-104.04	0.01	0.07	0.13	0.01	0.03	0.00	0.04	0.00	0.00	0.00	0.00	0.00	0.00	0.01	0.00	0.00	0.00	0.00	0.00
NS-104.05	0.02	0.10	0.31	0.06	0.07	0.00	0.07	0.02	0.01	0.00	0.00	0.00	0.00	0.02	0.00	0.00	0.00	0.00	0.00
NS-104.06	0.05	0.09	0.29	0.18	0.07	0.00	0.06	0.02	0.01	0.00	0.00	0.00	0.00	0.06	0.00	0.00	0.00	0.00	0.00
NS-105.01	0.02	0.07	1.37	0.04	0.15	0.00	0.29	0.09	0.01	0.00	0.01	0.00	0.04	0.01	0.00	0.00	0.00	0.01	0.00
NS-105.02	0.05	0.07	0.39	0.15	0.03	0.00	0.11	0.10	0.00	0.00	0.00	0.00	0.01	0.06	0.00	0.00	0.00	0.00	0.00
NS-105.03	0.01	0.08	0.19	0.01	0.03	0.00	0.05	0.04	0.00	0.00	0.00	0.00	0.00	0.01	0.00	0.00	0.00	0.00	0.00
NS-105.04	0.03	0.09	0.22	0.08	0.03	0.00	0.07	0.05	0.00	0.00	0.00	0.00	0.01	0.02	0.00	0.00	0.00	0.00	0.00
NS-105.05	0.11	0.09	0.24	0.30	0.03	0.00	0.09	0.06	0.00	0.00	0.00	0.00	0.01	0.10	0.00	0.00	0.00	0.00	0.00
NS-106.01	0.18	0.08	1.08	0.31	0.13	0.00	0.20	0.19	0.00	0.00	0.01	0.00	0.04	0.03	0.00	0.00	0.00	0.01	0.00
NS-106.02	0.02	0.09	0.60	0.05	0.06	0.00	0.10	0.19	0.00	0.00	0.00	0.00	0.02	0.01	0.00	0.00	0.00	0.00	0.00
NS-106.03	0.02	0.08	0.28	0.04	0.04	0.00	0.05	0.06	0.00	0.00	0.00	0.00	0.00	0.02	0.00	0.00	0.00	0.00	0.00
NS-106.04	0.01	0.11	0.35	0.02	0.07	0.00	0.06	0.09	0.00	0.00	0.00	0.00	0.00	0.01	0.00	0.00	0.00	0.00	0.00
NS-106.05	0.01	0.10	0.34	0.02	0.10	0.00	0.03	0.21	0.00	0.00	0.00	0.00	0.01	0.01	0.00	0.00	0.00	0.00	0.00
NS-107.01	0.11	0.03	4.35	0.27	0.30	0.00	0.29	0.13	0.00	0.00	0.02	0.00	0.02	0.13	0.01	0.00	0.00	0.00	0.00
NS-107.02	0.01	0.06	0.41	0.02	0.06	0.00	0.09	0.01	0.00	0.00	0.00	0.00	0.01	0.02	0.00	0.00	0.00	0.00	0.00
NS-107.03	0.01	0.06	0.18	0.03	0.04	0.00	0.06	0.04	0.00	0.00	0.00	0.00	0.00	0.01	0.00	0.00	0.00	0.00	0.00
NS-107.04	0.01	0.06	0.17	0.02	0.07	0.00	0.05	0.07	0.00	0.00	0.00	0.00	0.00	0.01	0.00	0.00	0.00	0.00	0.00
NS-107.05	0.01	0.06	0.17	0.03	0.09	0.00	0.05	0.07	0.00	0.00	0.00	0.00	0.01	0.01	0.00	0.00	0.00	0.00	0.00
NS-108.01	0.03	0.02	3.06	0.08	0.29	0.00	0.41	0.10	0.00	0.00	0.01	0.00	0.02	0.03	0.01	0.00	0.00	0.00	0.00
NS-108.02	0.02	0.04	0.34	0.03	0.05	0.00	0.10	0.01	0.00	0.00	0.00	0.00	0.00	0.01	0.00	0.00	0.00	0.00	0.00
NS-108.03	0.02	0.05	0.22	0.05	0.07	0.00	0.07	0.02	0.00	0.00	0.00	0.00	0.00	0.01	0.00	0.00	0.00	0.00	0.00
NS-108.04	0.03	0.11	0.42	0.11	0.14	0.00	0.08	0.10	0.00	0.00	0.00	0.00	0.01	0.03	0.00	0.00	0.00	0.00	0.00
NS-108.05	0.10	0.15	0.96	0.42	0.22	0.00	0.13	0.12	0.00	0.00	0.01	0.00	0.02	0.08	0.00	0.00	0.00	0.00	0.00
NS-108.06	0.07	0.09	0.62	0.22	0.13	0.00	0.10	0.09	0.00	0.00	0.00	0.00	0.01	0.06	0.00	0.00	0.00	0.00	0.00
NS-108.13	--	--	--	--	--	--	--	--	--	--	--	--	--	--	--	--	--	--	--
NS-109.01	0.02	0.05	6.45	0.09	0.06	0.00	0.45	0.04	0.00	0.00	0.01	0.00	0.06	0.01	0.01	0.00	0.00	0.00	0.00
NS-109.02	0.04	0.06	6.22	0.05	0.02	0.00	0.41	0.00	0.00	0.00	0.01	0.00	0.11	0.01	0.01	0.00	0.00	0.00	0.00
NS-109.03	0.11	0.10	1.64	0.29	0.04	0.00	0.15	0.01	0.00	0.00	0.01	0.00	0.00	0.10	0.00	0.00	0.00	0.00	0.00
NS-109.04	0.03	0.08	1.47	0.07	0.07	0.00	0.13	0.00	0.00	0.00	0.00	0.00	0.02	0.04	0.00	0.00	0.00	0.00	0.00
NS-109.05	0.03	0.06	2.09	0.08	0.05	0.00	0.19	0.01	0.00	0.00	0.00	0.00	0.03	0.02	0.00	0.00	0.00	0.00	0.00
NS-110.01	0.12	0.11	9.99	0.17	0.04	0.00	0.53	0.04	0.01	0.00	0.02	0.00	0.10	0.04	0.01	0.00	0.00	0.00	0.00
NS-110.02	0.03	0.13	2.99	0.09	0.03	0.00	0.15	0.01	0.00	0.00	0.00	0.00	0.01	0.04	0.01	0.00	0.00	0.00	0.00
NS-110.03	0.09	0.12	3.15	0.24	0.05	0.00	0.19	0.01	0.01	0.00	0.01	0.00	0.02	0.12	0.00	0.00	0.00	0.00	0.00
NS-110.04	0.18	0.09	4.30	0.57	0.09	0.00	0.25	0.01	0.01	0.00	0.01	0.00	0.06	0.23	0.01	0.00	0.00	0.00	0.00
NS-110.05	0.04	0.06	4.35	0.19	0.08	0.00	0.18	0.00	0.01	0.00	0.01	0.00	0.07	0.05	0.01	0.00	0.00	0.00	0.00
NS-111.01	0.09	0.03	5.27	0.27	0.31	0.00	0.42	0.27	0.00	0.00	0.03	0.00	0.05	0.11	0.01	0.00	0.00	0.00	0.00
NS-111.02	0.05	0.05	0.28	0.08	0.07	0.00	0.11	0.03	0.00	0.00	0.00	0.00	0.00	0.08	0.00	0.00	0.00	0.00	0.00
NS-111.03	0.04	0.06	0.21	0.11	0.09	0.00	0.08	0.03	0.00	0.00	0.00	0.00	0.01	0.04	0.00	0.00	0.00	0.00	0.00
NS-111.04	0.01	0.08	0.26	0.02	0.14	0.00	0.07	0.10	0.00	0.00	0.00	0.00	0.01	0.01	0.00	0.00	0.00	0.00	0.00
NS-111.05	0.08	0.14	0.62	0.26	0.27	0.00	0.11	0.20	0.00	0.00	0.00	0.00	0.02	0.08	0.00	0.00	0.00	0.00	0.00
NS-112.01	0.02	0.07	0.51	0.36	0.07	0.00	0.43	0.01	0.01	0.00	0.01	0.00	0.02	0.03	0.00	0.00	0.00	0.00	0.00
NS-112.02	0.04	0.07	0.48	0.06	0.16	0.00	0.60	0.00	0.01	0.00	0.00	0.00	0.03	0.07	0.01	0.00	0.00	0.00	0.00
NS-112.03	--	--	--	--	--	--	--	--	--	--	--	--	--	--	--	--	--	--	--
NS-113.01	0.01	0.04	0.40	0.04	0.07	0.00	0.42	0.01	0.00	0.00	0.00	0.00	0.01	0.02	0.00	0.00	0.00	0.00	0.00
NS-113.02	0.02	0.04	0.28	0.32	0.05	0.00	0.30	0.01	0.00	0.00	0.00	0.00	0.00	0.04	0.00	0.00	0.00	0.00	0.00
NS-113.03	0.03	0.05	0.33	0.81	0.05	0.00	0.30	0.02	0.00	0.00	0.01	0.00	0.00	0.04	0.00	0.00	0.00	0.00	0.00
NS-113.04	0.05	0.06	0.44	0.09	0.07	0.00	0.43	0.00	0.00	0.00	0.00	0.00	0.01	0.08	0.00	0.00	0.00	0.00	0.00
NS-114.01	0.01	0.00	2.44	0.02	0.17	0.00	0.08	0.01	0.00	0.00	0.07	0.00	0.02	0.00	0.01	0.00	0.00	0.00	0.00
NS-114.02	0.01	0.02	3.74	0.02	0.08	0.00	0.09	0.00	0.00	0.00	0.00	0.00	0.00	0.00	0.01	0.00	0.00	0.00	0.00
NS-114.03	0.07	0.03	1.89	0.25	0.04	0.00	0.06	0.01	0.00	0.00	0.00	0.00	0.00	0.04	0.01	0.00	0.00	0.00	0.00
NS-114.04	0.01	0.03	1.73	0.01	0.03	0.00	0.04	0.00	0.00	0.00	0.00	0.00	0.00	0.00	0.01	0.00	0.00	0.00	0.00
NS-117.01	0.03	0.02	2.64	0.05	0.24	0.00	0.18	0.04	0.00	0.00	0.04	0.00	0.05	0.01	0.01	0.00	0.00	0.01	0.00

sample name	Al	Ba	Ca	Fe	K	Li	Mg	Mn	Na	Ni	P	Rb	S	Si	Sr	Ti	V	Zn	Zr
NS-117.02	0.06	0.07	2.16	0.11	0.04	0.00	0.08	0.01	0.00	0.00	0.00	0.00	0.00	0.07	0.01	0.00	0.00	0.00	0.00
NS-117.03	0.01	0.10	3.21	0.01	0.06	0.00	0.04	0.00	0.01	0.00	0.00	0.00	0.00	0.01	0.01	0.00	0.00	0.00	0.00
NS-117.04	0.07	0.11	3.75	0.18	0.07	0.00	0.07	0.01	0.01	0.00	0.01	0.00	0.00	0.07	0.01	0.00	0.00	0.00	0.00
NS-117.05	0.04	0.11	3.56	0.08	0.07	0.00	0.05	0.00	0.01	0.00	0.00	0.00	0.00	0.04	0.01	0.00	0.00	0.00	0.00
NS-117.06	0.04	0.11	2.89	0.07	0.07	0.00	0.06	0.00	0.00	0.00	0.00	0.00	0.00	0.03	0.01	0.00	0.00	0.00	0.00
NS-118.01	0.03	0.02	1.31	0.04	0.18	0.00	0.09	0.19	0.01	0.00	0.01	0.00	0.02	0.02	0.00	0.00	0.00	0.00	0.00
NS-118.02	0.05	0.07	2.29	0.30	0.08	0.00	0.09	0.18	0.00	0.00	0.01	0.00	0.02	0.02	0.01	0.00	0.00	0.00	0.00
NS-118.03	0.09	0.07	2.72	0.16	0.06	0.00	0.08	0.10	0.01	0.00	0.00	0.00	0.01	0.12	0.01	0.00	0.00	0.00	0.00
NS-118.04	0.05	0.09	2.77	0.11	0.06	0.00	0.06	0.02	0.01	0.00	0.00	0.00	0.01	0.03	0.01	0.00	0.00	0.00	0.00
NS-119.01	0.02	0.01	4.30	0.04	0.12	0.00	0.14	0.05	0.00	0.00	0.04	0.00	0.05	0.01	0.01	0.00	0.00	0.00	0.00
NS-119.02	0.07	0.05	3.61	0.14	0.04	0.00	0.11	0.03	0.01	0.00	0.01	0.00	0.01	0.08	0.01	0.00	0.00	0.00	0.00
NS-119.03	0.04	0.06	2.93	0.06	0.04	0.00	0.03	0.00	0.00	0.00	0.00	0.00	0.00	0.04	0.01	0.00	0.00	0.00	0.00
NS-119.04	0.02	0.06	2.52	0.03	0.05	0.00	0.02	0.00	0.00	0.00	0.00	0.00	0.00	0.02	0.01	0.00	0.00	0.00	0.00
NS-119.05	0.01	0.09	2.77	0.02	0.06	0.00	0.02	0.00	0.00	0.00	0.00	0.00	0.00	0.01	0.01	0.00	0.00	0.00	0.00
NS-119.06	0.16	0.08	2.61	0.42	0.06	0.00	0.08	0.01	0.00	0.00	0.01	0.00	0.00	0.12	0.01	0.00	0.00	0.00	0.00
NS-121.01	0.03	0.05	3.18	0.04	0.07	0.00	0.16	0.01	0.00	0.00	0.00	0.00	0.19	0.05	0.01	0.00	0.00	0.00	0.00
NS-121.02	0.11	0.04	0.76	0.38	0.00	0.00	0.07	0.05	0.00	0.00	0.01	0.00	0.02	0.01	0.00	0.00	0.00	0.00	0.00
NS-121.03	0.03	0.09	3.29	0.04	0.09	0.00	0.13	0.01	0.00	0.00	0.00	0.00	0.07	0.04	0.01	0.00	0.00	0.00	0.00
NS-122.01	0.06	0.02	2.13	0.11	0.23	0.00	0.22	0.04	0.01	0.00	0.03	0.00	0.03	0.04	0.01	0.00	0.00	0.00	0.00
NS-122.02	0.03	0.14	1.41	0.05	0.04	0.00	0.08	0.06	0.01	0.00	0.00	0.00	0.00	0.03	0.00	0.00	0.00	0.00	0.00
NS-122.03	0.08	0.11	1.56	0.29	0.05	0.00	0.11	0.05	0.01	0.00	0.00	0.00	0.01	0.09	0.00	0.00	0.00	0.00	0.00
NS-122.04	0.06	0.09	2.57	0.14	0.04	0.00	0.10	0.08	0.01	0.00	0.00	0.00	0.01	0.02	0.01	0.00	0.00	0.00	0.00
NS-122.05	0.09	0.04	3.32	0.18	0.04	0.00	0.12	0.09	0.00	0.00	0.01	0.00	0.03	0.06	0.01	0.00	0.00	0.00	0.00
NS-122.06	0.08	0.04	5.67	0.18	0.08	0.00	0.23	0.06	0.01	0.00	0.01	0.00	0.04	0.07	0.01	0.00	0.00	0.00	0.00
NS-122.07	0.02	0.04	3.41	0.03	0.07	0.00	0.39	0.01	0.02	0.00	0.00	0.00	0.05	0.02	0.01	0.00	0.00	0.00	0.00
NS-123.01	0.08	0.03	0.96	0.10	0.24	0.00	0.13	0.02	0.01	0.00	0.02	0.00	0.03	0.00	0.00	0.00	0.00	0.01	0.00
NS-123.02	0.14	0.07	0.87	0.17	0.05	0.00	0.08	0.02	0.01	0.00	0.00	0.00	0.01	0.01	0.00	0.00	0.00	0.00	0.00
NS-123.03	0.04	0.03	5.83	0.21	0.04	0.00	0.16	0.11	0.00	0.00	0.01	0.00	0.06	0.03	0.01	0.00	0.00	0.00	0.00
NS-123.04	0.02	0.04	6.38	0.07	0.07	0.00	0.17	0.02	0.01	0.00	0.00	0.00	0.01	0.02	0.01	0.00	0.00	0.00	0.00
NS-124.01	0.02	0.07	3.81	0.02	0.06	0.00	0.05	0.00	0.01	0.00	0.00	0.00	0.00	0.02	0.01	0.00	0.00	0.00	0.00
NS-124.02	0.02	0.05	3.33	0.03	0.06	0.00	0.09	0.04	0.01	0.00	0.00	0.00	0.01	0.01	0.01	0.00	0.00	0.00	0.00
NS-124.03	0.04	0.04	3.77	0.10	0.06	0.00	0.07	0.03	0.00	0.00	0.00	0.00	0.00	0.04	0.01	0.00	0.00	0.00	0.00

Soil cold 1M HNO_3 digestible fraction chemistry, mg/g.

sample name	Al	Ba	Ca	Fe	K	Li	Mg	Mn	Na	Ni	P	Rb	S	Si	Sr	Ti	V	Zn	Zr
DH-01.07	4.14	0.04	0.94	7.77	0.05	0.01	0.70	0.06	0.00	0.01	0.25	0.00	0.02	1.25	0.01	0.11	0.02	0.01	0.00
DH-02.07	11.9	0.04	0.36	5.97	0.06	0.01	1.95	0.09	0.00	0.03	0.05	0.00	0.01	3.32	0.00	0.26	0.05	0.01	0.00
DH-03.09	2.56	0.04	0.49	1.23	0.14	0.00	0.08	0.02	0.00	0.00	0.22	0.00	0.03	0.22	0.01	0.02	0.01	0.01	0.00
DH-03.10	1.32	0.01	0.06	0.58	0.07	0.00	0.03	0.01	0.01	0.00	0.03	0.00	0.01	0.19	0.00	0.01	0.01	0.00	0.00
DH-03.11	13.2	0.01	0.85	3.49	0.06	0.00	0.21	0.05	0.00	0.05	0.52	0.00	0.03	4.89	0.01	0.12	0.06	0.00	0.00
NS-08.07	2.54	0.03	0.37	7.62	0.04	0.00	0.17	0.16	0.00	0.01	0.08	0.00	0.01	0.76	0.00	0.00	0.01	0.01	0.00
NS-08.08	2.97	0.04	0.55	8.20	0.05	0.00	0.18	0.12	0.00	0.01	0.12	0.00	0.02	0.97	0.00	0.00	0.01	0.02	0.00
NS-08.10	1.92	0.07	1.96	9.73	0.05	0.00	0.27	0.29	0.00	0.01	0.18	0.00	0.06	1.04	0.01	0.00	0.01	0.03	0.00
NS-13.13	1.16	0.16	9.72	4.06	0.00	0.00	0.20	2.91	0.02		0.21	0.02		0.17	0.01	0.00			
NS-13.14	3.24	0.15	2.60	9.56	0.04	0.00	0.57	0.92	0.00	0.01	0.35	0.00	0.06	1.47	0.01	0.00	0.01	0.03	0.00
NS-13.15	3.44	0.19	3.05	10.1	0.06	0.00	0.82	0.25	0.00	0.02	0.32	0.00	0.10	1.72	0.01	0.00	0.02	0.04	0.00
NS-13.16	3.46	0.26	5.99	7.92	0.09	0.00	1.22	0.40	0.00	0.02	0.32	0.00	0.12	1.72	0.01	0.00	0.02	0.05	0.00
NS-13.23	3.77	0.36	15.6	9.34	0.09	0.01	2.57	0.72	0.01	0.02	0.40	0.00	0.10	2.40	0.02	0.00	0.02	0.05	0.00
NS-22.08	1.59	0.13	1.51	2.88	0.00	0.00	0.04	0.78	0.02		0.30	0.02		0.28	0.00	0.00			
NS-22.09	3.64	0.05	0.31	5.86	0.04	0.00	0.24	0.18	0.00	0.01	0.00	0.00	0.02	0.97	0.00	0.00	0.02	0.01	0.00
NS-22.10	10.7	0.15	0.52	14.4	0.10	0.00	0.36	0.37	0.00	0.02	0.00	0.00	0.06	2.05	0.00	0.00	0.05	0.02	0.00
NS-22.11	7.03	0.17	0.97	8.87	0.11	0.00	0.24	0.17	0.00	0.02	0.00	0.00	0.04	1.85	0.00	0.00	0.03	0.01	0.00
NS-22.26	2.38	0.13	9.56	3.74	0.00	0.00	0.08	0.04	0.02		0.18	0.02		0.04	0.02	0.00			
NS-22.27	2.14	0.03	0.16	2.66	0.04	0.00	0.15	0.13	0.00	0.00	0.01	0.00	0.01	0.46	0.00	0.00	0.01	0.00	0.00
NS-23A.06	2.00	0.31	2.27	6.42	0.00	0.00	0.31	1.61	0.02		0.18	0.02		0.46	0.01	0.02			
NS-23A.07	4.19	0.23	0.80	31.6	0.04	0.00	0.38	1.19	0.00	0.01	0.00	0.00	0.14	0.93	0.00	0.04	0.02	0.02	0.00
NS-23A.08	4.64	0.23	0.58	17.3	0.05	0.00	0.58	0.10	0.00	0.01	0.00	0.00	0.12	1.23	0.00	0.04	0.02	0.02	0.00
NS-23A.09	3.42	0.18	0.40	6.94	0.04	0.00	0.44	0.03	0.00	0.01	0.04	0.00	0.21	0.96	0.00	0.04	0.02	0.02	0.00
NS-23B.06	0.82	0.23	2.70	1.58	0.00	0.00	0.49	0.37	0.02		0.20	0.02		0.25	0.01	0.00			
NS-23B.07	4.87	0.16	1.07	13.3	0.04	0.01	1.35	0.13	0.00	0.02	0.19	0.00	0.10	1.68	0.00	0.05	0.02	0.03	0.00
NS-23B.08	5.59	0.18	0.93	18.0	0.04	0.01	1.27	0.16	0.00	0.02	0.11	0.00	0.11	1.74	0.00	0.03	0.02	0.03	0.00
NS-23C.06	1.75	0.35	3.17	1.66	0.00	0.00	0.28	0.69	0.02		0.13	0.02		0.15	0.01	0.00			
NS-23C.07	4.90	0.25	0.56	6.10	0.05	0.00	0.57	0.12	0.00	0.01	0.05	0.00	0.13	1.22	0.00	0.06	0.02	0.02	0.00
NS-23C.08	4.03	0.15	0.35	11.2	0.06	0.00	0.58	0.10	0.00	0.01	0.00	0.00	0.09	1.42	0.00	0.07	0.02	0.02	0.00
NS-23D.07	2.14	0.51	4.76	4.61	0.00	0.00	0.46	1.49	0.03		0.18	0.02		0.52	0.02	0.00			
NS-23D.08	7.59	0.55	1.70	18.9	0.05	0.01	2.18	0.15	0.01	0.02	0.22	0.00	0.14	2.56	0.01	0.04	0.03	0.04	0.00
NS-23D.09	4.78	0.35	1.12	12.5	0.04	0.01	1.66	0.06	0.03	0.02	0.25	0.00	0.08	1.94	0.00	0.06	0.02	0.03	0.00
NS-23D.10	4.10	0.38	1.01	9.27	0.05	0.01	1.35	0.04	0.00	0.02	0.33	0.00	0.11	1.72	0.00	0.06	0.02	0.03	0.00
NS-28.07	1.37	0.09	4.53	4.14	0.00	0.00	0.46	1.02	0.02		0.19	0.02		0.56	0.01	0.00			
NS-28.08	1.90	0.02	0.30	5.74	0.04	0.00	0.17	0.23	0.00	0.01	0.03	0.00	0.01	0.70	0.00	0.00	0.01	0.01	0.00
NS-28.09	2.93	0.06	0.60	13.6	0.05	0.00	0.28	0.63	0.00	0.01	0.00	0.00	0.02	1.12	0.00	0.00	0.01	0.02	0.00
NS-28.10	2.56	0.03	0.72	8.33	0.05	0.00	0.23	0.21	0.00	0.01	0.18	0.00	0.02	0.93	0.00	0.00	0.01	0.02	0.00
NS-29.01	3.18	0.19	1.43	3.27	0.04	0.00	1.07	0.28	0.01	0.01	0.31	0.00	0.00	1.10	0.00	0.08	0.01	0.01	0.00
NS-37.06	3.74	0.28	2.42	8.86	0.00	0.00	0.07	8.94	0.02		0.07	0.02		0.66	0.01	0.00			
NS-37.07	1.76	0.03	0.90	5.53	0.04	0.00	0.29	0.24	0.00	0.01	0.32	0.00	0.01	0.91	0.00	0.00	0.01	0.02	0.00
NS-37.08	2.32	0.04	1.15	7.28	0.04	0.00	0.35	0.45	0.00	0.01	0.35	0.00	0.01	1.14	0.00	0.00	0.01	0.02	0.00
NS-38.08	4.49	0.14	6.55	2.64	0.00	0.00	0.29	0.06	0.02		0.02	0.02		0.95	0.01	0.00			
NS-38.09	2.42	0.05	1.87	8.17	0.05	0.00	0.49	0.49	0.00	0.01	0.48	0.00	0.01	1.36	0.01	0.00	0.01	0.03	0.00
NS-38.10	2.48	0.08	1.87	5.35	0.07	0.00	0.51	0.55	0.00	0.02	0.44	0.00	0.01	1.54	0.01	0.00	0.01	0.03	0.00
NS-47.03	1.08	0.13	7.24	18.6	0.00	0.00	0.13	0.81	0.02		0.03	0.02		0.24	0.02	0.01			
NS-47.04	4.12	0.16	1.39	8.47	0.05	0.00	0.26	1.54	0.00	0.01	0.00	0.00	0.03	0.98	0.00	0.01	0.02	0.01	0.00
NS-48.01	1.63	0.13	12.2	3.29	0.05	0.00	1.13	0.25	0.00	0.01	0.44	0.00	0.00	1.30	0.02	0.01	0.01	0.02	0.00
NS-101.01	2.24	0.04	0.38	4.55	0.11	0.00	0.16	0.14	0.00	0.01	0.07	0.00	0.03	0.71	0.00	0.00	0.01	0.01	0.00
NS-101.02	1.95	0.02	0.17	5.70	0.04	0.00	0.18	0.30	0.00	0.01	0.03	0.00	0.01	0.86	0.00	0.00	0.01	0.01	0.00
NS-101.03	1.70	0.02	0.28	5.85	0.04	0.00	0.16	0.27	0.00	0.01	0.10	0.00	0.00	0.85	0.00	0.00	0.01	0.01	0.00
NS-101.04	2.35	0.03	0.33	7.92	0.05	0.00	0.22	0.43	0.00	0.01	0.11	0.00	0.01	1.25	0.00	0.00	0.01	0.02	0.00
NS-101.05	1.97	0.03	0.31	5.73	0.05	0.00	0.16	0.24	0.00	0.01	0.09	0.00	0.01	1.08	0.00	0.00	0.01	0.02	0.00
NS-101.06	2.22	0.09	7.16	8.27	0.06	0.00	0.31	0.79	0.00	0.02	0.14	0.00	0.00	1.60	0.01	0.00	0.01	0.03	0.00
NS-102.01	1.47	0.06	0.46	3.06	0.18	0.00	0.12	0.13	0.00	0.00	0.16	0.00	0.05	0.35	0.00	0.00	0.01	0.01	0.00
NS-102.02	1.69	0.02	0.18	7.62	0.04	0.00	0.13	0.30	0.00	0.01	0.08	0.00	0.01	0.78	0.00	0.00	0.01	0.01	0.00
NS-102.03	1.77	0.01	0.21	6.19	0.04	0.00	0.17	0.27	0.00	0.01	0.08	0.00	0.01	0.88	0.00	0.00	0.01	0.01	0.00
NS-102.04	1.94	0.02	0.25	5.93	0.04	0.00	0.19	0.38	0.00	0.01	0.09	0.00	0.01	0.96	0.00	0.00	0.01	0.01	0.00
NS-102.05	1.40	0.01	0.19	4.97	0.04	0.00	0.11	0.11	0.00	0.01	0.06	0.00	0.01	0.71	0.00	0.00	0.01	0.01	0.00

sample name	Al	Ba	Ca	Fe	K	Li	Mg	Mn	Na	Ni	P	Rb	S	Si	Sr	Ti	V	Zn	Zr
NS-102.06	1.44	0.01	0.48	2.96	0.05	0.00	0.15	0.04	0.00	0.01	0.20	0.00	0.00	0.91	0.00	0.00	0.01	0.01	0.00
NS-103.01	0.95	0.05	1.50	1.86	0.20	0.00	0.23	0.25	0.01	0.00	0.13	0.00	0.03	0.34	0.00	0.00	0.00	0.02	0.00
NS-103.02	1.34	0.01	0.19	5.09	0.04	0.00	0.13	0.06	0.00	0.01	0.09	0.00	0.01	0.68	0.00	0.00	0.01	0.01	0.00
NS-103.03	1.58	0.01	0.20	4.71	0.04	0.00	0.13	0.03	0.00	0.01	0.07	0.00	0.01	0.76	0.00	0.00	0.01	0.01	0.00
NS-103.04	1.37	0.01	0.19	3.97	0.03	0.00	0.12	0.09	0.00	0.01	0.09	0.00	0.00	0.67	0.00	0.00	0.01	0.01	0.00
NS-103.05	1.15	0.01	0.21	2.53	0.04	0.00	0.12	0.03	0.00	0.01	0.06	0.00	0.01	0.73	0.00	0.00	0.01	0.01	0.00
NS-103.06	0.71	0.00	0.21	2.24	0.03	0.00	0.08	0.03	0.00	0.00	0.10	0.00	0.01	0.42	0.00	0.00	0.00	0.00	0.00
NS-104.01	1.54	0.04	0.37	3.99	0.14	0.00	0.13	0.04	0.00	0.00	0.12	0.00	0.05	0.48	0.00	0.01	0.01	0.01	0.00
NS-104.02	1.90	0.01	0.32	4.45	0.04	0.00	0.12	0.01	0.00	0.01	0.13	0.00	0.00	0.97	0.00	0.00	0.01	0.01	0.00
NS-104.03	1.88	0.01	0.24	3.97	0.04	0.00	0.12	0.00	0.01	0.01	0.18	0.00	0.01	0.98	0.00	0.00	0.01	0.01	0.00
NS-104.04	1.64	0.01	0.13	2.79	0.04	0.00	0.10	0.00	0.00	0.01	0.10	0.00	0.01	0.84	0.00	0.00	0.01	0.01	0.00
NS-104.05	1.89	0.02	0.27	4.77	0.05	0.00	0.10	0.01	0.00	0.01	0.10	0.00	0.02	0.84	0.00	0.00	0.01	0.01	0.00
NS-104.06	1.93	0.02	0.28	4.88	0.05	0.00	0.09	0.01	0.00	0.01	0.10	0.00	0.02	0.85	0.00	0.00	0.01	0.01	0.00
NS-105.01	1.91	0.11	1.20	2.70	0.14	0.00	0.23	0.12	0.01	0.00	0.11	0.00	0.05	0.58	0.00	0.01	0.01	0.01	0.00
NS-105.02	2.01	0.03	0.15	6.52	0.05	0.00	0.28	0.40	0.01	0.01	0.03	0.00	0.02	1.00	0.00	0.01	0.01	0.01	0.00
NS-105.03	1.75	0.02	0.13	4.76	0.04	0.00	0.23	0.26	0.01	0.01	0.04	0.00	0.01	0.97	0.00	0.01	0.01	0.01	0.00
NS-105.04	2.00	0.03	0.10	4.81	0.04	0.00	0.27	0.34	0.01	0.01	0.02	0.00	0.01	1.09	0.00	0.01	0.01	0.01	0.00
NS-105.05	1.98	0.03	0.13	9.38	0.05	0.00	0.28	0.57	0.01	0.01	0.08	0.00	0.01	1.24	0.00	0.02	0.01	0.02	0.00
NS-106.01	2.27	0.08	0.61	6.89	0.11	0.00	0.17	0.17	0.01	0.01	0.08	0.00	0.05	0.72	0.00	0.01	0.01	0.01	0.00
NS-106.02	2.60	0.04	0.16	8.28	0.05	0.00	0.18	0.76	0.00	0.01	0.06	0.00	0.03	0.93	0.00	0.01	0.01	0.01	0.00
NS-106.03	2.07	0.02	0.08	6.87	0.05	0.00	0.21	0.23	0.01	0.01	0.04	0.00	0.01	1.04	0.00	0.01	0.01	0.01	0.00
NS-106.04	1.93	0.02	0.16	8.05	0.06	0.00	0.18	0.06	0.01	0.01	0.10	0.00	0.01	1.11	0.00	0.01	0.01	0.01	0.00
NS-106.05	1.75	0.03	0.37	9.17	0.07	0.00	0.13	0.24	0.01	0.01	0.19	0.00	0.01	1.09	0.00	0.01	0.01	0.02	0.00
NS-107.01	1.35	0.10	7.97	2.59	0.18	0.00	0.66	0.99	0.01	0.01	0.18	0.00	0.01	0.93	0.01	0.00	0.01	0.08	0.00
NS-107.02	2.23	0.02	0.37	6.71	0.05	0.00	0.24	0.07	0.01	0.01	0.09	0.00	0.02	1.19	0.00	0.00	0.01	0.01	0.00
NS-107.03	2.09	0.01	0.27	6.52	0.05	0.00	0.26	0.04	0.01	0.01	0.08	0.00	0.00	1.25	0.00	0.00	0.01	0.02	0.00
NS-107.04	1.85	0.01	0.21	5.12	0.06	0.00	0.21	0.06	0.01	0.01	0.07	0.00	0.01	1.11	0.00	0.00	0.01	0.02	0.00
NS-107.05	1.86	0.02	0.38	9.65	0.07	0.00	0.22	0.53	0.01	0.01	0.13	0.00	0.01	1.12	0.00	0.00	0.01	0.02	0.00
NS-108.01	1.93	0.09	9.03	2.75	0.24	0.00	0.85	0.62	0.01	0.01	0.13	0.00	0.02	0.72	0.02	0.00	0.01	0.04	0.00
NS-108.02	2.36	0.01	0.28	6.33	0.06	0.00	0.22	0.06	0.01	0.01	0.07	0.00	0.03	1.13	0.00	0.00	0.01	0.02	0.00
NS-108.03	2.62	0.01	0.25	9.06	0.05	0.00	0.21	0.11	0.01	0.01	0.06	0.00	0.03	1.21	0.00	0.00	0.01	0.02	0.00
NS-108.04	2.93	0.04	0.28	11.8	0.08	0.00	0.20	0.06	0.01	0.01	0.07	0.00	0.03	1.40	0.00	0.00	0.01	0.02	0.00
NS-108.05	2.20	0.05	0.50	13.0	0.08	0.00	0.23	0.34	0.01	0.01	0.18	0.00	0.03	1.03	0.00	0.00	0.01	0.02	0.00
NS-108.06	2.70	0.05	0.57	13.9	0.08	0.00	0.24	0.32	0.01	0.01	0.21	0.00	0.03	1.28	0.00	0.01	0.01	0.02	0.00
NS-108.13	--	--	--	--	--	--	--	--	--	--	--	--	--	--	--	--	--	--	--
NS-109.01	1.43	0.33	15.9	2.48	0.08	0.00	0.54	1.82	0.01	0.00	0.09	0.00	0.12	0.33	0.02	0.00	0.01	0.06	0.00
NS-109.02	2.65	0.22	12.8	1.20	0.05	0.00	0.39	0.02	0.01	0.01	0.13	0.00	0.29	0.54	0.02	0.00	0.01	0.01	0.00
NS-109.03	3.00	0.08	2.01	4.29	0.07	0.01	0.69	0.15	0.01	0.02	0.44	0.00	0.04	2.02	0.01	0.00	0.01	0.02	0.00
NS-109.04	2.60	0.11	1.36	3.72	0.08	0.00	0.49	0.05	0.01	0.02	0.25	0.00	0.09	1.76	0.00	0.00	0.01	0.02	0.00
NS-109.05	3.01	0.18	3.36	6.25	0.06	0.01	0.75	0.15	0.01	0.02	0.49	0.00	0.25	2.15	0.01	0.00	0.01	0.03	0.00
NS-110.01	3.48	0.46	19.2	3.13	0.05	0.00	0.52	1.59	0.01	0.00	0.12	0.00	0.17	0.40	0.03	0.00	0.02	0.01	0.00
NS-110.02	3.33	0.22	2.69	6.07	0.05	0.00	0.58	0.15	0.01	0.02	0.26	0.00	0.14	1.54	0.01	0.00	0.02	0.02	0.00
NS-110.03	3.33	0.25	3.09	6.62	0.07	0.01	1.21	0.45	0.02	0.02	0.48	0.00	0.19	2.32	0.01	0.00	0.02	0.04	0.00
NS-110.04	3.86	0.45	5.37	5.42	0.08	0.01	0.84	0.20	0.02	0.02	0.33	0.00	0.31	2.22	0.01	0.00	0.02	0.02	0.00
NS-110.05	2.22	0.30	5.02	4.65	0.07	0.00	0.49	0.08	0.01	0.01	0.21	0.00	0.16	1.36	0.01	0.00	0.01	0.01	0.00
NS-111.01	1.46	0.09	7.80	3.33	0.19	0.00	0.55	1.40	0.01	0.01	0.14	0.00	0.03	1.09	0.01	0.00	0.01	0.08	0.00
NS-111.02	3.57	0.02	0.29	14.1	0.07	0.00	0.42	0.34	0.01	0.02	0.07	0.00	0.03	1.70	0.00	0.01	0.02	0.02	0.00
NS-111.03	3.06	0.01	0.25	9.47	0.07	0.00	0.31	0.11	0.01	0.01	0.08	0.00	0.03	1.45	0.00	0.00	0.01	0.02	0.00
NS-111.04	2.95	0.03	0.19	9.91	0.09	0.00	0.30	0.04	0.01	0.01	0.06	0.00	0.03	1.58	0.00	0.00	0.01	0.02	0.00
NS-111.05	4.62	0.09	0.60	24.6	0.14	0.00	0.42	0.66	0.01	0.02	0.45	0.00	0.08	2.09	0.00	0.01	0.02	0.04	0.00
NS-112.01	1.12	0.05	2.61	4.05	0.09	0.00	0.51	0.41	0.02	0.01	0.47	0.00	0.00	1.25	0.01	0.00	0.00	0.01	0.00
NS-112.02	0.69	0.04	1.76	12.6	0.12	0.00	2.48	0.33	0.02	0.01	0.18	0.01	0.05	0.68	0.01	0.00	0.00	0.02	0.00
NS-112.03	--	--	--	--	--	--	--	--	--	--	--	--	--	--	--	--	--	--	--
NS-113.01	0.52	0.05	0.94	2.46	0.07	0.00	0.26	0.36	0.01	0.00	0.12	0.00	0.00	0.54	0.00	0.00	0.00	0.01	0.00
NS-113.02	0.50	0.05	1.00	2.06	0.07	0.00	0.23	0.40	0.01	0.01	0.11	0.00	0.00	0.61	0.00	0.00	0.00	0.01	0.00
NS-113.03	0.49	0.05	1.09	1.89	0.07	0.00	0.21	0.34	0.01	0.01	0.12	0.00	0.00	0.61	0.00	0.00	0.00	0.01	0.00
NS-113.04	0.63	0.04	1.37	5.89	0.10	0.00	1.04	0.39	0.01	0.01	0.17	0.00	0.03	0.67	0.00	0.00	0.00	0.01	0.00
NS-114.01	0.33	0.02	10.4	0.40	0.38	0.00	0.24	0.05	0.01	0.00	0.18	0.00	0.02	0.11	0.03	0.00	0.00	0.02	0.00
NS-114.02	1.98	0.04	4.00	2.93	0.06	0.00	0.16	0.11	0.00	0.01	0.06	0.00	0.02	0.85	0.01	0.00	0.01	0.02	0.00
NS-114.03	1.92	0.03	0.94	2.96	0.06	0.00	0.21	0.20	0.00	0.01	0.06	0.00	0.01	1.19	0.00	0.00	0.01	0.01	0.00
NS-114.04	3.10	0.03	1.04	5.85	0.05	0.01	0.49	0.45	0.01	0.02	0.13	0.00	0.00	1.91	0.00	0.00	0.01	0.02	0.00
NS-117.01	1.07	0.04	2.23	2.30	0.16	0.00	0.17	0.09	0.01	0.00	0.15	0.00	0.05	0.44	0.01	0.01	0.00	0.02	0.00

sample name	Al	Ba	Ca	Fe	K	Li	Mg	Mn	Na	Ni	P	Rb	S	Si	Sr	Ti	V	Zn	Zr
NS-117.02	3.07	0.07	1.14	5.01	0.07	0.00	0.44	0.36	0.01	0.02	0.08	0.00	0.01	1.56	0.00	0.00	0.01	0.02	0.00
NS-117.03	3.88	0.09	4.74	4.55	0.10	0.01	1.11	0.31	0.01	0.02	0.45	0.00	0.00	2.13	0.01	0.00	0.02	0.03	0.00
NS-117.04	3.39	0.09	3.34	4.13	0.10	0.01	1.06	0.36	0.01	0.02	0.36	0.01	0.00	1.85	0.01	0.00	0.02	0.02	0.00
NS-117.05	4.79	0.13	5.56	5.59	0.11	0.01	1.12	0.50	0.02	0.02	0.35	0.01	0.00	2.63	0.01	0.00	0.02	0.02	0.00
NS-117.06	4.07	0.14	3.78	5.13	0.11	0.01	1.62	0.73	0.01	0.02	0.53	0.01	0.00	2.29	0.01	0.00	0.02	0.02	0.00
NS-118.01	1.07	0.05	2.25	2.83	0.23	0.00	0.28	0.32	0.01	0.01	0.27	0.00	0.03	0.66	0.01	0.00	0.00	0.02	0.00
NS-118.02	2.95	0.12	4.31	12.7	0.08	0.00	0.36	0.23	0.02	0.01	1.15	0.00	0.07	1.34	0.03	0.01	0.01	0.01	0.00
NS-118.03	3.81	0.14	4.96	12.5	0.09	0.01	0.95	0.82	0.02	0.02	0.65	0.00	0.08	2.45	0.01	0.01	0.02	0.04	0.00
NS-118.04	3.58	0.13	24.3	13.1	0.08	0.01	1.51	1.80	0.02	0.02	0.82	0.00	0.01	2.46	0.04	0.01	0.02	0.05	0.00
NS-119.01	0.69	0.07	15.5	1.08	0.19	0.00	0.33	0.65	0.01	0.00	0.17	0.00	0.09	0.26	0.03	0.00	0.00	0.10	0.00
NS-119.02	4.84	0.12	4.49	11.0	0.08	0.01	1.00	0.90	0.02	0.03	0.60	0.01	0.08	2.60	0.01	0.00	0.02	0.04	0.00
NS-119.03	3.97	0.07	12.3	5.90	0.10	0.01	1.38	0.39	0.02	0.03	0.78	0.00	0.00	2.66	0.03	0.00	0.02	0.03	0.00
NS-119.04	2.69	0.03	19.1	3.78	0.07	0.01	1.62	0.21	0.01	0.02	0.46	0.00	0.00	1.88	0.03	0.00	0.01	0.03	0.00
NS-119.05	3.98	0.07	21.0	5.15	0.10	0.01	1.62	0.38	0.02	0.03	0.77	0.01	0.00	2.73	0.04	0.00	0.02	0.04	0.00
NS-119.06	3.53	0.06	21.9	5.40	0.09	0.01	1.70	0.41	0.02	0.02	0.65	0.01	0.00	2.44	0.04	0.00	0.02	0.04	0.00
NS-121.01	4.32	0.24	9.77	13.2	0.06	0.01	1.77	0.86	0.43	0.05	0.67	0.00	0.29	4.73	0.02	0.00	0.02	0.07	0.00
NS-121.02	1.80	0.07	1.22	6.61	0.00	0.00	0.23	0.11	0.42	0.01	0.38	0.00	0.04	1.30	0.00	0.01	0.01	0.02	0.00
NS-121.03	6.62	0.18	9.90	29.7	0.08	0.01	1.99	1.43	0.44	0.06	0.81	0.00	0.02	6.43	0.02	0.00	0.03	0.13	0.00
NS-122.01	0.87	0.06	3.21	1.57	0.26	0.00	0.28	0.07	0.01	0.00	0.16	0.00	0.03	0.27	0.01	0.00	0.00	0.02	0.00
NS-122.02	3.98	0.04	0.55	10.0	0.06	0.00	0.45	0.25	0.01	0.02	0.12	0.00	0.04	1.79	0.00	0.00	0.02	0.02	0.00
NS-122.03	3.36	0.06	0.73	16.0	0.07	0.00	0.36	0.20	0.01	0.02	0.10	0.00	0.06	1.60	0.00	0.00	0.02	0.02	0.00
NS-122.04	6.13	0.16	2.65	16.8	0.10	0.00	0.35	0.11	0.01	0.02	0.38	0.01	0.14	1.89	0.01	0.02	0.03	0.03	0.00
NS-122.05	2.77	0.11	4.03	7.29	0.08	0.00	0.26	0.11	0.01	0.01	0.21	0.00	0.08	1.03	0.01	0.01	0.01	0.02	0.00
NS-122.06	2.97	0.15	10.3	8.03	0.11	0.00	0.66	0.16	0.01	0.02	0.34	0.01	0.12	1.85	0.02	0.01	0.01	0.04	0.00
NS-122.07	2.61	0.15	49.1	9.90	0.13	0.01	5.91	0.32	0.03	0.02	0.43	0.00	0.08	2.03	0.07	0.01	0.01	0.04	0.00
NS-123.01	1.15	0.05	1.18	1.71	0.24	0.00	0.14	0.02	0.01	0.00	0.18	0.00	0.05	0.13	0.00	0.00	0.00	0.01	0.00
NS-123.02	3.76	0.04	0.58	8.09	0.19	0.00	0.30	0.01	0.04	0.02	0.17	0.04	0.17	1.72	0.00	0.01	0.03	0.03	0.00
NS-123.03	1.37	0.14	12.3	10.1	0.19	0.00	0.27	0.20	0.04	0.01	0.09	0.04	0.21	0.58	0.03	0.01	0.01	0.03	0.00
NS-123.04	2.13	0.14	17.1	7.50	0.22	0.00	2.12	0.23	0.05	0.02	0.27	0.04	0.12	1.74	0.03	0.01	0.02	0.05	0.00
NS-124.01	2.62	0.07	19.4	2.78	0.19	0.01	1.44	0.17	0.04	0.02	0.18	0.04	0.03	1.98	0.02	0.00	0.02	0.03	0.00
NS-124.02	3.24	0.11	4.02	5.77	0.17	0.01	0.93	0.12	0.04	0.02	0.32	0.04	0.10	2.23	0.01	0.01	0.02	0.05	0.00
NS-124.03	2.57	0.10	16.7	9.29	0.18	0.00	1.39	0.41	0.05	0.02	0.33	0.04	0.07	2.01	0.03	0.01	0.02	0.04	0.00

Soil concentrated HNO_3 digestible fraction chemistry, mg/g.

sample name	Al	Ba	Ca	Fe	K	Li	Mg	Mn	Na	Ni	P	Rb	S	Si	Sr	Ti	V	Zn	Zr
DH-01.07	10.0	0.03	0.00	15.1	1.98	0.03	3.34	0.16	0.00	0.07	0.24	0.03	0.25	7.06	0.01	0.58	0.04	0.03	0.00
DH-02.07	13.8	0.02	0.00	23.6	1.73	0.03	5.41	0.23	0.00	0.06	0.14	0.02	0.06	5.62	0.00	0.89	0.06	0.05	0.00
DH-03.09	4.21	0.01	0.23	3.26	0.83	0.00	0.62	0.05	0.28	0.05	0.55	0.01	0.65	4.75	0.01	0.18	0.02	0.01	0.00
DH-03.10	2.51	0.00	0.11	2.21	0.66	0.00	0.44	0.03	0.18	0.03	0.03	0.01	0.03	3.15	0.01	0.30	0.01	0.00	0.00
DH-03.11	3.49	0.00	0.00	5.39	0.31	0.01	1.27	0.10	0.00	0.02	0.15	0.01	0.03	2.18	0.01	0.24	0.02	0.01	0.00
NS-08.07	6.74	0.00	0.00	14.3	0.25	0.01	1.76	0.07	0.00	0.05	0.07	0.01	0.07	4.80	0.00	0.00	0.03	0.04	0.00
NS-08.08	8.62	0.00	0.00	14.5	0.40	0.01	2.00	0.05	0.00	0.07	0.09	0.01	0.14	6.69	0.00	0.00	0.04	0.04	0.00
NS-08.10	11.1	0.01	0.00	23.2	1.03	0.02	2.78	0.12	0.00	0.09	0.14	0.01	0.59	9.26	0.00	0.00	0.05	0.06	0.00
NS-13.13																			
NS-13.14	9.02	0.02	0.00	16.3	0.35	0.02	3.08	0.16	0.00	0.07	0.15	0.01	0.36	7.05	0.00	0.00	0.04	0.05	0.00
NS-13.15	11.8	0.03	0.00	24.2	0.49	0.02	4.27	0.14	0.00	0.08	0.13	0.01	0.41	8.37	0.00	0.00	0.05	0.07	0.00
NS-13.16	9.40	0.04	0.10	14.9	0.79	0.02	3.07	0.11	0.00	0.04	0.11	0.01	0.76	3.82	0.00	0.0	0.04	0.05	0.00
NS-13.23	8.13	0.01	0.39	19.3	0.23	0.02	3.69	0.19	0.00	0.03	0.06	0.01	0.15	2.59	0.00	0.0	0.04	0.05	0.00
NS-22.08																			
NS-22.09	6.81	0.00	0.00	15.6	0.31	0.01	1.27	0.21	0.00	0.04	0.21	0.01	0.16	3.54	0.00	0.00	0.03	0.03	0.00
NS-22.10	18.3	0.04	0.00	29.2	0.77	0.03	1.96	0.31	0.00	0.04	0.39	0.01	0.47	4.39	0.00	0.0	0.08	0.06	0.00
NS-22.11	15.5	0.03	0.00	28.4	0.67	0.02	1.55	0.07	0.00	0.05	0.12	0.01	0.35	5.33	0.00	0.0	0.07	0.04	0.00
NS-22.26																			
NS-22.27	5.15	0.00	0.00	11.2	0.23	0.01	1.02	0.12	0.00	0.03	0.16	0.01	0.15	2.49	0.00	0.00	0.02	0.02	0.00
NS-23A.06																			
NS-23A.07	8.89	0.07	0.08	23.4	0.19	0.02	3.55	0.59	0.00	0.03	0.35	0.01	0.87	3.56	0.00	0.03	0.04	0.04	0.00
NS-23A.08	11.0	0.07	0.27	19.5	0.22	0.02	4.70	0.18	0.00	0.05	0.29	0.01	0.97	5.14	0.00	0.11	0.05	0.05	0.00
NS-23A.09	10.8	0.05	0.54	15.3	0.19	0.02	4.43	0.14	0.00	0.03	0.15	0.01	1.02	2.87	0.00	0.13	0.05	0.05	0.00
NS-23B.06																			
NS-23B.07	13.4	0.04	0.52	23.8	0.18	0.03	7.79	0.26	0.00	0.04	0.18	0.01	0.54	4.25	0.00	0.23	0.06	0.07	0.00
NS-23B.08	15.0	0.05	0.44	27.2	0.20	0.04	7.96	0.30	0.00	0.05	0.19	0.01	0.57	5.64	0.00	0.12	0.07	0.07	0.00
NS-23C.06																			
NS-23C.07	15.5	0.17	0.55	17.1	1.13	0.03	5.63	0.18	0.02	0.09	0.39	0.01	0.90	9.20	0.00	0.47	0.07	0.05	0.00
NS-23C.08	13.5	0.06	0.31	20.3	0.58	0.03	5.63	0.18	0.00	0.06	0.15	0.01	0.49	6.01	0.00	0.34	0.07	0.06	0.00
NS-23D.07																			
NS-23D.08	17.7	0.21	0.92	35.0	0.61	0.04	10.1	0.36	0.00	0.08	0.29	0.01	0.69	8.69	0.00	0.57	0.08	0.08	0.00
NS-23D.09	22.1	0.22	1.53	40.5	0.60	0.05	13.2	0.47	0.03	0.09	0.07	0.01	0.32	9.69	0.00	1.21	0.10	0.10	0.00
NS-23D.10	17.2	0.16	1.29	29.8	0.54	0.04	10.2	0.35	0.00	0.05	0.02	0.01	0.32	5.44	0.00	0.94	0.09	0.09	0.00
NS-28.07																			
NS-28.08	10.1	0.00	0.00	22.4	0.63	0.02	2.87	0.16	0.00	0.05	0.09	0.01	0.07	5.17	0.00	0.00	0.05	0.06	0.00
NS-28.09	9.79	0.00	0.00	28.0	0.69	0.02	2.50	0.22	0.00	0.05	0.18	0.01	0.12	4.69	0.00	0.00	0.05	0.06	0.00
NS-28.10	13.1	0.01	0.00	22.9	1.21	0.02	3.24	0.10	0.00	0.07	0.20	0.01	0.18	7.26	0.00	0.00	0.06	0.07	0.00
NS-29.01	15.4	0.16	2.74	30.8	0.50	0.03	8.92	0.45	0.03	0.04	0.03	0.01	0.13	4.57	0.00	1.58	0.07	0.07	0.00
NS-37.06																			
NS-37.07	7.25	0.00	0.00	13.9	0.49	0.01	2.32	0.08	0.00	0.04	0.07	0.01	0.09	3.87	0.00	0.00	0.03	0.04	0.00
NS-37.08	9.78	0.00	0.00	16.9	0.80	0.02	2.77	0.10	0.00	0.06	0.13	0.01	0.15	6.21	0.00	0.00	0.04	0.05	0.00
NS-38.08																			
NS-38.09	18.6	0.07	0.00	29.8	2.57	0.02	4.10	0.21	0.11	0.12	0.13	0.02	0.16	12.3	0.01	0.02	0.08	0.09	0.00
NS-38.10	12.8	0.05	0.00	24.4	1.82	0.02	2.76	0.32	0.03	0.09	0.13	0.01	0.12	8.74	0.00	0.00	0.06	0.08	0.00
NS-47.03																			
NS-47.04	16.7	0.06	0.00	23.0	1.53	0.02	2.01	1.48	0.03	0.09	0.55	0.02	0.45	9.95	0.00	0.01	0.07	0.05	0.00
NS-48.01	7.90	0.09	1.35	19.3	0.53	0.01	4.33	0.26	0.00	0.05	0.00	0.01	0.27	5.16	0.00	0.95	0.04	0.04	0.00
NS-101.01	6.57	0.04	0.15	26.2	0.44	0.01	1.42	0.17	0.42	0.00	0.68	0.01	0.74	0.70	0.00	0.00	0.02	0.03	0.00
NS-101.02	6.30	0.02	0.10	22.5	0.22	0.01	1.89	0.29	0.42	0.00	0.25	0.01	0.11	0.17	0.00	0.00	0.03	0.04	0.00
NS-101.03	5.74	0.02	0.10	16.3	0.20	0.01	1.83	0.14	0.43	0.00	0.17	0.00	0.05	0.14	0.00	0.00	0.03	0.04	0.00
NS-101.04	7.70	0.03	0.11	25.4	0.39	0.01	2.20	0.28	0.41	0.00	0.32	0.01	0.10	0.12	0.00	0.00	0.04	0.06	0.01
NS-101.05	8.01	0.03	0.10	24.2	0.50	0.01	2.03	0.19	0.44	0.00	0.28	0.01	0.08	0.08	0.00	0.00	0.04	0.05	0.00
NS-101.06	8.38	0.04	0.22	28.7	0.56	0.01	2.32	0.22	0.42	0.00	0.31	0.01	0.17	0.07	0.00	0.00	0.04	0.06	0.01
NS-102.01	3.02	0.05	0.33	9.15	0.29	0.00	0.51	0.10	0.38	0.00	0.75	0.01	0.92	0.17	0.00	0.00	0.01	0.02	0.00
NS-102.02	6.48	0.02	0.11	18.4	0.22	0.01	1.98	0.12	0.42	0.00	0.18	0.01	0.07	0.12	0.00	0.00	0.03	0.04	0.00
NS-102.03	5.70	0.02	0.10	16.9	0.20	0.01	1.80	0.15	0.43	0.00	0.16	0.00	0.05	0.08	0.00	0.00	0.03	0.04	0.00
NS-102.04	5.88	0.02	0.09	19.1	0.19	0.01	1.87	0.35	0.43	0.00	0.19	0.00	0.06	0.06	0.00	0.00	0.03	0.04	0.00
NS-102.05	6.12	0.02	0.11	19.8	0.17	0.01	1.92	0.13	0.39	0.00	0.19	0.01	0.04	0.17	0.00	0.00	0.03	0.04	0.00

sample name	Al	Ba	Ca	Fe	K	Li	Mg	Mn	Na	Ni	P	Rb	S	Si	Sr	Ti	V	Zn	Zr
NS-102.06	5.85	0.02	0.12	17.0	0.16	0.01	1.94	0.11	0.40	0.00	0.17	0.01	0.03	0.28	0.00	0.00	0.02	0.04	0.00
NS-103.01	3.02	0.04	0.76	8.32	0.20	0.00	1.02	0.14	0.39	0.00	0.48	0.00	0.74	0.35	0.00	0.02	0.01	0.02	0.00
NS-103.02	5.75	0.02	0.13	14.0	0.16	0.01	1.88	0.08	0.42	0.00	0.12	0.00	0.07	0.21	0.00	0.00	0.03	0.03	0.00
NS-103.03	7.02	0.03	0.15	16.5	0.21	0.01	2.16	0.09	0.41	0.00	0.14	0.01	0.05	0.09	0.00	0.00	0.03	0.04	0.00
NS-103.04	5.77	0.02	0.15	12.9	0.17	0.01	1.84	0.07	0.41	0.00	0.11	0.00	0.03	0.13	0.00	0.00	0.03	0.03	0.00
NS-103.05	5.86	0.02	0.12	23.4	0.14	0.01	1.80	0.09	0.39	0.00	0.21	0.00	0.04	0.24	0.00	0.00	0.03	0.03	0.00
NS-103.06	3.63	0.01	0.13	10.0	0.06	0.01	1.21	0.05	0.41	0.00	0.08	0.00	0.01	0.31	0.00	0.00	0.02	0.02	0.00
NS-104.01	2.69	0.03	0.19	9.14	0.20	0.00	0.44	0.04	0.41	0.00	0.60	0.01	0.79	0.10	0.00	0.00	0.01	0.01	0.00
NS-104.02	6.90	0.03	0.13	17.8	0.22	0.01	1.71	0.05	0.41	0.00	0.22	0.01	0.07	0.06	0.00	0.00	0.03	0.03	0.00
NS-104.03	6.22	0.03	0.14	11.8	0.19	0.01	1.66	0.05	0.42	0.00	0.12	0.01	0.07	0.09	0.00	0.00	0.03	0.03	0.00
NS-104.04	6.78	0.03	0.13	11.3	0.19	0.01	1.87	0.04	0.43	0.00	0.07	0.01	0.06	0.10	0.00	0.00	0.03	0.03	0.00
NS-104.05	6.43	0.03	0.13	19.7	0.19	0.01	1.58	0.05	0.41	0.00	0.25	0.00	0.15	0.04	0.00	0.00	0.03	0.03	0.00
NS-104.06	7.96	0.04	0.12	26.3	0.28	0.01	1.80	0.08	0.42	0.00	0.30	0.01	0.17	0.07	0.00	0.00	0.03	0.03	0.00
NS-105.01	3.46	0.05	0.34	7.05	0.28	0.00	0.40	0.05	0.40	0.00	0.77	0.01	1.11	0.05	0.00	0.01	0.02	0.02	0.00
NS-105.02	11.1	0.04	0.17	33.4	0.42	0.01	3.36	0.46	0.44	0.00	0.37	0.01	0.15	0.16	0.00	0.01	0.04	0.05	0.01
NS-105.03	8.28	0.04	0.20	21.2	0.32	0.01	2.47	0.15	0.41	0.00	0.23	0.01	0.04	0.02	0.00	0.01	0.04	0.05	0.01
NS-105.04	8.18	0.03	0.15	24.4	0.30	0.01	2.41	0.21	0.43	0.00	0.27	0.00	0.04	0.03	0.00	0.01	0.04	0.05	0.01
NS-105.05	7.77	0.04	0.23	19.2	0.32	0.01	2.41	0.31	0.37	0.00	0.22	0.01	0.06	0.17	0.00	0.01	0.04	0.04	0.00
NS-106.01	5.66	0.05	0.29	12.6	0.41	0.01	0.91	0.08	0.39	0.00	0.56	0.01	0.66	0.09	0.00	0.00	0.03	0.02	0.00
NS-106.02	8.13	0.04	0.17	17.9	0.37	0.01	1.96	0.25	0.40	0.00	0.38	0.01	0.27	0.11	0.00	0.00	0.04	0.04	0.00
NS-106.03	7.91	0.03	0.14	19.5	0.25	0.01	2.32	0.15	0.41	0.00	0.23	0.01	0.08	0.25	0.00	0.01	0.04	0.05	0.01
NS-106.04	7.73	0.03	0.16	17.0	0.31	0.01	2.16	0.08	0.42	0.00	0.17	0.01	0.06	0.03	0.00	0.00	0.04	0.04	0.01
NS-106.05	7.34	0.04	0.18	14.5	0.30	0.01	2.11	0.09	0.40	0.00	0.14	0.01	0.09	0.12	0.00	0.00	0.03	0.04	0.00
NS-107.01	3.63	0.04	1.69	9.84	0.27	0.01	1.24	0.25	0.39	0.00	0.32	0.00	0.58	0.26	0.00	0.00	0.02	0.04	0.00
NS-107.02	7.65	0.02	0.12	18.7	0.27	0.01	2.58	0.09	0.42	0.00	0.18	0.00	0.09	0.17	0.00	0.00	0.04	0.05	0.00
NS-107.03	8.08	0.02	0.12	19.8	0.29	0.01	2.71	0.09	0.42	0.00	0.17	0.00	0.06	0.10	0.00	0.00	0.04	0.05	0.00
NS-107.04	8.46	0.03	0.13	21.6	0.35	0.01	2.84	0.10	0.40	0.00	0.18	0.01	0.07	0.11	0.00	0.00	0.04	0.05	0.00
NS-107.05	6.89	0.03	0.13	14.5	0.32	0.01	2.31	0.11	0.44	0.00	0.12	0.00	0.09	0.11	0.00	0.00	0.03	0.04	0.00
NS-108.01	3.75	0.05	2.91	13.7	0.25	0.01	1.25	0.27	0.38	0.00	0.48	0.00	0.92	0.25	0.01	0.01	0.02	0.04	0.00
NS-108.02	7.26	0.02	0.14	18.5	0.24	0.01	2.30	0.09	0.41	0.00	0.18	0.00	0.12	0.10	0.00	0.00	0.03	0.04	0.00
NS-108.03	8.69	0.03	0.14	25.6	0.38	0.01	2.54	0.12	0.38	0.00	0.27	0.00	0.19	0.13	0.00	0.00	0.04	0.05	0.00
NS-108.04	8.18	0.04	0.09	31.7	0.43	0.01	2.12	0.09	0.42	0.00	0.43	0.01	0.32	0.26	0.00	0.00	0.04	0.05	0.00
NS-108.05	7.13	0.05	0.23	16.2	0.38	0.01	2.12	0.13	0.38	0.00	0.35	0.00	0.61	0.17	0.00	0.00	0.03	0.04	0.00
NS-108.06	5.94	0.03	0.17	15.1	0.28	0.01	1.86	0.08	0.37	0.00	0.25	0.00	0.34	0.13	0.00	0.00	0.03	0.03	0.00
NS-108.13																			
NS-109.01	1.47	0.11	3.10	6.60	0.02	0.00	0.39	0.35	0.38	0.00	0.52	0.00	2.46	0.31	0.00	0.00	0.01	0.02	0.00
NS-109.02	2.08	0.07	1.65	3.92	0.03	0.00	0.43	0.02	0.39	0.00	0.36	0.00	6.01	0.26	0.00	0.00	0.01	0.01	0.00
NS-109.03	5.54	0.03	0.13	18.9	0.22	0.01	1.79	0.09	0.42	0.00	0.23	0.00	0.26	0.15	0.00	0.00	0.03	0.04	0.00
NS-109.04	6.29	0.04	0.20	15.9	0.28	0.01	2.14	0.07	0.41	0.00	0.12	0.00	0.30	0.09	0.00	0.00	0.03	0.04	0.00
NS-109.05	5.04	0.03	0.30	17.3	0.19	0.01	1.79	0.10	0.40	0.00	0.20	0.00	0.60	0.10	0.00	0.00	0.02	0.03	0.00
NS-110.01	1.92	0.17	4.67	5.36	0.03	0.00	0.35	0.37	0.38	0.00	0.51	0.00	2.27	0.24	0.01	0.00	0.01	0.01	0.00
NS-110.02	6.58	0.07	0.34	14.8	0.05	0.01	2.51	0.09	0.38	0.00	0.25	0.00	0.69	0.20	0.00	0.00	0.03	0.03	0.00
NS-110.03	6.13	0.07	0.29	17.1	0.12	0.01	2.71	0.13	0.38	0.00	0.18	0.00	0.69	0.16	0.00	0.00	0.03	0.04	0.00
NS-110.04	7.14	0.08	0.47	24.9	0.26	0.01	2.52	0.12	0.38	0.00	0.36	0.00	1.00	0.11	0.00	0.00	0.03	0.03	0.00
NS-110.05	5.01	0.08	0.67	24.8	0.16	0.01	1.58	0.09	0.38	0.00	0.45	0.00	1.59	0.27	0.00	0.00	0.02	0.02	0.00
NS-111.01	2.84	0.04	1.56	9.20	0.12	0.01	1.02	0.29	0.38	0.00	0.41	0.00	1.02	0.38	0.00	0.01	0.01	0.03	0.00
NS-111.02	6.83	0.02	0.14	20.5	0.17	0.01	2.25	0.16	0.36	0.00	0.23	0.00	0.12	0.10	0.00	0.00	0.03	0.04	0.00
NS-111.03	6.60	0.02	0.12	17.9	0.22	0.01	2.05	0.08	0.39	0.00	0.22	0.00	0.11	0.05	0.00	0.00	0.03	0.04	0.00
NS-111.04	7.06	0.03	0.13	22.4	0.25	0.01	2.11	0.09	0.36	0.00	0.26	0.00	0.16	0.03	0.00	0.00	0.03	0.04	0.00
NS-111.05	6.99	0.04	0.19	13.9	0.41	0.01	1.92	0.10	0.36	0.00	0.26	0.01	0.45	0.08	0.00	0.00	0.03	0.04	0.00
NS-112.01	2.34	0.02	0.06	41.1	0.50	0.00	0.84	0.39	0.42	0.00	0.45	0.01	0.17	0.02	0.00	0.00	0.01	0.08	0.01
NS-112.02	1.90	0.02	0.13	16.8	0.83	0.00	0.52	0.13	0.42	0.00	0.17	0.01	0.29	0.01	0.00	0.00	0.01	0.05	0.00
NS-112.03																			
NS-113.01	1.80	0.02	0.07	41.4	0.26	0.00	0.74	0.43	0.40	0.00	0.34	0.00	0.11	0.02	0.00	0.00	0.01	0.09	0.01
NS-113.02	1.50	0.02	0.05	43.5	0.38	0.00	0.62	0.48	0.40	0.00	0.36	0.00	0.07	0.02	0.00	0.00	0.01	0.09	0.01
NS-113.03	1.51	0.02	0.08	36.7	0.35	0.00	0.55	0.43	0.40	0.00	0.34	0.00	0.08	0.05	0.00	0.00	0.01	0.09	0.01
NS-113.04	1.75	0.02	0.12	20.8	0.62	0.00	0.46	0.18	0.42	0.00	0.20	0.01	0.16	0.02	0.01	0.00	0.01	0.05	0.01
NS-114.01	0.52	0.02	6.62	1.99	0.22	0.00	0.22	0.05	0.37	0.00	0.47	0.00	1.16	0.30	0.02	0.00	0.00	0.01	0.00
NS-114.02	4.03	0.02	0.37	17.0	0.19	0.00	0.48	0.15	0.43	0.00	0.33	0.00	0.71	0.17	0.00	0.00	0.02	0.05	0.00
NS-114.03	4.81	0.02	0.13	23.1	0.17	0.01	1.05	0.31	0.41	0.00	0.19	0.00	0.15	0.17	0.00	0.00	0.02	0.06	0.00
NS-114.04	9.28	0.02	0.13	33.7	0.27	0.01	2.56	0.32	0.41	0.00	0.18	0.01	0.09	0.12	0.00	0.00	0.04	0.09	0.01
NS-117.01	2.69	0.03	0.75	9.76	0.19	0.00	0.58	0.07	0.36	0.00	0.81	0.00	1.93	0.35	0.00	0.01	0.01	0.02	0.00

sample name	Al	Ba	Ca	Fe	K	Li	Mg	Mn	Na	Ni	P	Rb	S	Si	Sr	Ti	V	Zn	Zr
NS-117.02	8.69	0.05	0.25	23.5	0.16	0.02	3.17	0.25	0.39	0.00	0.30	0.00	0.24	0.07	0.00	0.00	0.04	0.05	0.00
NS-117.03	13.5	0.08	0.50	37.7	0.40	0.02	4.77	0.28	0.43	0.00	0.45	0.00	0.16	0.03	0.00	0.00	0.05	0.08	0.01
NS-117.04	9.76	0.06	0.33	28.4	0.24	0.02	3.64	0.28	0.38	0.00	0.37	0.00	0.15	0.06	0.00	0.00	0.04	0.06	0.00
NS-117.05	11.8	0.08	0.45	32.4	0.35	0.02	3.89	0.23	0.42	0.00	0.39	0.00	0.18	0.09	0.00	0.00	0.05	0.07	0.01
NS-117.06	9.07	0.07	0.24	25.8	0.26	0.02	3.35	0.62	0.38	0.00	0.35	0.00	0.13	0.05	0.00	0.00	0.04	0.05	0.00
NS-118.01	4.04	0.06	1.60	9.99	0.25	0.01	1.73	0.26	0.38	0.01	0.49	0.00	0.84	0.94	0.00	0.04	0.02	0.02	0.00
NS-118.02	4.18	0.06	1.05	15.5	0.11	0.01	1.11	0.12	-0.2	0.00	1.11	0.00	1.11	0.41	0.01	0.00	0.02	0.01	0.00
NS-118.03	10.3	0.05	0.45	21.9	0.30	0.02	4.40	0.21	0.39	0.00	0.26	0.00	0.51	0.34	0.00	0.00	0.04	0.05	0.00
NS-118.04	10.6	0.04	0.71	22.1	0.33	0.02	4.68	0.23	0.41	0.00	0.10	0.00	0.12	0.15	0.00	0.00	0.04	0.05	0.00
NS-119.01	1.25	0.05	6.06	3.07	0.06	0.00	0.43	0.24	0.37	0.00	0.64	0.00	2.84	0.38	0.01	0.01	0.01	0.04	0.00
NS-119.02	10.1	0.06	0.42	25.4	0.11	0.02	4.06	0.24	0.39	0.00	0.43	0.00	0.61	0.29	0.00	0.00	0.05	0.05	0.00
NS-119.03	11.2	0.05	0.83	30.0	0.21	0.02	4.61	0.23	0.39	0.00	0.34	0.00	0.17	0.08	0.00	0.00	0.05	0.07	0.00
NS-119.04	10.3	0.04	1.18	27.7	0.29	0.02	4.55	0.22	0.39	0.00	0.23	0.00	0.11	0.09	0.00	0.00	0.04	0.05	0.00
NS-119.05	10.5	0.04	1.26	30.6	0.31	0.02	4.55	0.26	0.39	0.00	0.34	0.00	0.09	0.04	0.00	0.00	0.04	0.06	0.00
NS-119.06	9.44	0.04	0.49	29.0	0.36	0.02	4.06	0.24	0.41	0.00	0.25	0.00	0.16	0.05	0.00	0.01	0.04	0.05	0.00
NS-121.01	9.11	0.04	0.51	24.3	0.39	0.02	3.41	0.21	0.42	0.00	0.13	0.00	0.19	0.10	0.00	0.00	0.04	0.05	0.01
NS-121.02	4.48	0.02	0.17	12.6	0.08	0.01	1.50	0.08	0.41	0.00	0.11	0.00	0.15	0.03	0.00	0.00	0.02	0.03	0.00
NS-121.03	9.99	0.04	0.51	23.1	0.49	0.02	3.66	0.20	0.41	0.00	0.11	0.00	0.14	0.58	0.00	0.00	0.04	0.06	0.01
NS-122.01	2.18	0.07	2.95	4.31	0.29	0.00	0.65	0.07	0.37	0.00	0.58	0.00	1.35	0.70	0.01	0.01	0.01	0.01	0.00
NS-122.02	7.53	0.04	0.22	17.0	0.26	0.01	2.40	0.11	0.40	0.00	0.20	0.00	0.18	0.08	0.00	0.00	0.03	0.04	0.00
NS-122.03	8.32	0.05	0.23	25.7	0.31	0.01	2.60	0.15	0.39	0.00	0.28	0.00	0.27	0.17	0.00	0.00	0.04	0.05	0.00
NS-122.04	4.47	0.04	0.28	8.73	0.20	0.01	1.20	0.04	0.38	0.00	0.52	0.00	0.83	0.41	0.00	0.00	0.02	0.02	0.00
NS-122.05	5.49	0.06	1.01	10.6	0.33	0.01	1.67	0.06	0.41	0.00	0.35	0.00	1.16	0.54	0.00	0.00	0.02	0.03	0.00
NS-122.06	6.71	0.06	1.36	12.0	0.66	0.01	2.45	0.07	0.40	0.00	0.27	0.00	1.55	0.36	0.00	0.01	0.03	0.03	0.00
NS-122.07	6.19	0.05	1.27	11.8	0.55	0.01	2.78	0.09	0.43	0.00	0.16	0.00	0.74	0.13	0.00	0.00	0.03	0.03	0.00
NS-123.01	1.58	0.05	0.91	3.38	0.16	0.00	0.26	0.03	0.36	0.00	0.77	0.00	1.13	0.21	0.00	0.01	0.01	0.01	0.00
NS-123.02	6.35	0.04	0.24	9.13	0.27	0.01	1.83	0.05	0.41	0.00	0.29	0.00	0.42	0.22	0.00	0.00	0.03	0.03	0.00
NS-123.03	3.07	0.08	4.57	14.0	0.19	0.00	0.98	0.10	0.38	0.00	0.46	0.00	2.28	0.50	0.01	0.01	0.01	0.02	0.00
NS-123.04	5.52	0.06	3.31	11.3	0.46	0.01	2.47	0.10	0.43	0.00	0.25	0.00	1.40	0.35	0.01	0.01	0.02	0.03	0.00
NS-124.01	8.38	0.07	1.52	20.0	0.26	0.01	3.13	0.13	0.42	0.00	0.26	0.00	0.22	0.62	0.00	0.00	0.04	0.04	0.00
NS-124.02	8.53	0.06	0.55	17.5	0.33	0.01	3.40	0.12	0.39	0.00	0.19	0.00	0.47	0.30	0.00	0.00	0.03	0.04	0.01
NS-124.03	6.60	0.04	1.07	12.4	0.39	0.01	2.69	0.10	0.43	0.00	0.12	0.00	0.33	0.35	0.00	0.01	0.03	0.03	0.00

Soil residual HF digest chemistry, mg/g, for select samples.

sample name	Al	Ba	Ca	Fe	K	Li	Mg	Mn	Na	Ni	P	Rb	S	Si	Sr	Ti	V	Zn	Zr
DH-02.07	18.2	0.50	8.56	21.5	10.3	0.02	1.45	0.26	12.2	0.10	0.02	0.02	0.01	9.98		2.54	0.09	0.03	0.04
DH-03.10	31.0	0.24	5.03	14.0	26.2	0.01	1.33	0.30	12.4	0.05	0.00	0.08	0.00	5.00		1.34	0.15	0.02	0.01
DH-03.11	11.7	0.13	0.00	6.03	5.50	0.02	0.33	0.02	1.48	0.20	0.08	0.02	0.04	19.2	0.03	2.04	0.06	0.01	0.04
NS-08.07	16.3	0.28	0.00	10.2	11.8	0.03	0.49	0.03	2.88	0.12	0.12	0.04	0.10	12.1	0.05	3.21	0.08	0.02	0.08
NS-08.08	14.9	0.40	0.00	19.3	17.0	0.04	0.52	0.11	3.44	0.07	0.15	0.05	0.21	7.40	0.07	4.58	0.08	0.03	0.12
NS-08.10	7.54	0.19	0.00	5.96	5.75	0.02	0.36	0.03	2.72	0.06	0.07	0.02	0.11	6.12	0.03	1.89	0.04	0.01	0.04
NS-13.14	38.8	0.40	0.08	16.5	12.9	0.03	2.94	0.09	3.24	0.19	0.15	0.05	0.49	20.1	0.05	2.80	0.18	0.04	0.06
NS-13.15	44.6	0.38	0.17	19.8	13.5	0.03	4.05	0.14	3.04	0.14	0.14	0.06	0.18	14.4	0.04	2.72	0.21	0.04	0.05
NS-13.16	16.7	0.13	0.00	9.00	4.97	0.02	0.54	0.05	1.49	0.35	0.17	0.02	0.05	33.8	0.02	1.73	0.08	0.01	0.03
NS-13.23	61.5	0.37	0.0	34.2	15.6	0.05	2.92	0.16	1.52	0.03	0.63	0.08	0.29	3.30	0.04	1.89	0.29	0.05	0.06
NS-22.09	83.4	0.50	0.00	56.0	20.8	0.07	3.89	0.09	2.25	0.11	0.62	0.12	0.35	11.6	0.05	2.64	0.38	0.06	0.07
NS-22.10	15.9	0.12	0.00	11.5	4.37	0.01	0.61	0.10	1.47	0.54	0.20	0.02	0.05	51.6	0.03	1.80	0.08	0.02	0.03
NS-22.11	24.7	0.35	0.39	12.1	7.02	0.02	2.41	0.19	6.31	0.14	0.22	0.02	0.31	13.6	0.03	3.14	0.12	0.02	0.05
NS-22.27	13.7	0.10	0.00	9.89	3.75	0.01	0.52	0.09	1.26	0.46	0.17	0.02	0.05	44.3	0.03	1.54	0.07	0.02	0.03
NS-23A.07	24.9	0.35	0.39	12.1	7.06	0.02	2.42	0.19	6.35	0.14	0.22	0.03	0.31	13.7	0.03	3.16	0.12	0.02	0.05
NS-23A.08	24.3	0.41	0.60	8.9	7.97	0.01	2.19	0.06	9.69	0.03	0.17	0.03	0.28	2.55	0.03	3.40	0.12	0.01	0.05
NS-23A.09	20.0	0.38	0.49	9.18	7.11	0.01	1.81	0.07	9.52	0.06	0.11	0.02	0.40	5.71	0.03	3.34	0.10	0.02	0.05
NS-23B.07	30.0	0.55	0.89	11.0	10.7	0.02	3.11	0.09	11.7	0.04	0.15	0.03	0.18	4.27	0.04	3.69	0.14	0.02	0.06
NS-23B.08	36.0	0.60	0.64	12.5	12.5	0.02	3.95	0.10	9.44	0.03	0.13	0.04	0.20	2.96	0.03	3.99	0.17	0.02	0.07
NS-23C.07	16.5	0.37	0.47	5.04	6.57	0.01	0.76	0.04	10.4	0.07	0.12	0.02	0.12	6.55	0.04	3.35	0.08	0.01	0.05
NS-23C.08	24.7	0.40	0.58	6.1	7.06	0.01	1.56	0.04	10.7	0.03	0.09	0.02	0.10	3.04	0.04	3.32	0.12	0.01	0.05
NS-23D.08	30.7	0.61	0.98	9.7	11.3	0.01	2.41	0.07	11.9	0.06	0.12	0.04	0.14	5.85	0.05	3.72	0.15	0.01	0.06
NS-23D.09	26.7	0.63	1.07	8.0	10.5	0.01	1.65	0.07	14.0	0.10	0.05	0.03	0.08	10.6	0.05	3.27	0.12	0.01	0.05
NS-23D.10	32.9	0.59	1.07	6.78	10.1	0.01	2.38	0.06	13.4	0.21	0.05	0.04	0.09	21.4	0.05	3.33	0.15	0.01	0.06
NS-28.08	16.1	0.17	0.00	4.75	6.92	0.02	0.14	0.02	2.46	0.19	0.07	0.02	0.02	19.1	0.04	2.66	0.08	0.00	0.05
NS-28.09	14.6	0.19	0.00	6.7	8.44	0.02	0.02	0.03	2.33	0.25	0.09	0.03	0.03	24.2	0.03	2.86	0.07	0.01	0.05
NS-28.10	17.9	0.23	0.00	6.25	10.4	0.02	0.10	0.02	2.92	0.16	0.09	0.03	0.05	15.9	0.04	3.05	0.09	0.01	0.07
NS-29.01	19.2	0.67	0.89	9.29	6.25	0.01	0.97	0.08	12.8	0.22	0.10	0.02	0.08	22.6	0.05	3.14	0.10	0.01	0.04
NS-37.07	13.0	0.13	0.00	3.16	5.09	0.01	0.37	0.01	2.55	0.41	0.04	0.02	0.05	41.4	0.03	2.34	0.06	0.00	0.03
NS-37.08	20.1	0.17	0.00	3.63	6.59	0.02	0.76	0.01	2.85	0.26	0.07	0.03	0.06	26.4	0.03	2.70	0.09	0.00	0.04
NS-38.09	14.1	0.15	0.00	4.45	5.86	0.01	0.50	0.03	2.72	0.24	0.05	0.02	0.09	24.7	0.03	2.53	0.07	0.01	0.04
NS-38.10	20.6	0.19	0.00	4.99	7.43	0.01	0.74	0.03	2.68	0.26	0.06	0.03	0.07	27.1	0.03	2.55	0.10	0.01	0.04
NS-47.04	16.0	0.13	0.00	4.10	5.09	0.01	0.33	0.05	1.67	0.11	0.08	0.02	0.04	11.2	0.03	2.22	0.07	0.00	0.04
NS-48.01	17.1	0.31	0.2	4.61	4.82	0.01	0.66	0.05	7.06	0.14	0.03	0.02	0.06	13.9	0.04	1.50	0.08	0.00	0.03

Total soil digest chemistry ($LiBO_2$ fusion method), mg/g.

sample name	Al	Ba	Ca	Fe	K	Mg	Mn	Na	Ni	P	Rb	Si	Sr	Ti	V	Zn	Zr
NS-08.07	46.6	0.39	0.95	30.1	11.2	3.68	0.33	5.60	4.34	0.37	0.05	444	0.04	3.99	0.23	0.06	0.15
NS-08.08	53.6	0.48	1.05	28.3	13.0	4.02	0.20	4.14	3.85	0.66	0.07	410	0.05	3.75	0.25	0.06	0.15
NS-08.10	60.9	0.58	3.98	44.8	15.0	5.19	0.51	3.72	4.32	0.66	0.08	431	0.07	4.57	0.31	0.09	0.17
NS-13.13																	
NS-13.14	47.3	0.63	4.49	28.9	10.1	5.62	0.56	4.77	3.84	0.67	0.04	391	0.05	3.69	0.23	0.08	0.13
NS-13.15	62.5	0.83	4.95	43.6	14.6	7.55	0.45	4.61	3.33	0.70	0.07	346	0.06	4.04	0.30	0.11	0.13
NS-13.16	68.1	0.98	10.2	38.1	16.7	8.65	0.66	4.51	2.83	0.78	0.07	297	0.06	3.99	0.32	0.11	0.11
NS-13.23	81.5	1.14	16.9	52.4	20.0	12.0	1.14	4.91	3.26	0.94	0.10	329	0.09	5.18	0.40	0.12	0.13
NS-22.08																	
NS-22.09	40.9	0.40	0.77	29.9	8.1	2.92	0.46	2.73	4.22	0.51	0.04	436	0.04	2.82	0.19	0.06	0.13
NS-22.10	101	0.99	1.88	72.7	19.5	6.05	0.60	3.12	2.04	1.24	0.12	203	0.05	2.73	0.51	0.12	0.11
NS-22.11	94.3	0.96	2.83	76.6	18.7	5.39	0.31	3.43	2.18	0.90	0.12	218	0.05	2.62	0.47	0.10	0.10
NS-22.26																	
NS-22.27	25.9	0.25	0.60	24.8	5.8	1.87	0.39	2.56	4.31	0.49	0.03	433	0.03	2.05	0.13	0.05	0.09
NS-23A.06																	
NS-23A.07	44.9	1.04	21.6	65.0	8.6	7.63	2.55	7.53	2.06	0.83	0.04	208	0.05	3.44	0.22	0.08	0.08
NS-23A.08	51.5	1.08	3.00	41.3	9.6	8.04	0.34	10.6	2.63	0.61	0.04	268	0.05	4.08	0.25	0.07	0.11
NS-23A.09	52.3	1.08	3.21	29.4	9.4	8.03	0.27	11.4	2.96	0.46	0.04	298	0.05	4.39	0.26	0.07	0.13
NS-23B.06																	
NS-23B.07	58.6	1.08	3.88	40.8	11.9	12.2	0.53	12.4	2.94	0.64	0.04	298	0.05	4.56	0.29	0.09	0.13
NS-23B.08	62.4	1.23	3.46	47.2	13.7	12.6	0.55	10.5	2.81	0.64	0.05	278	0.04	4.81	0.32	0.10	0.13
NS-23C.06																	
NS-23C.07	51.1	1.10	2.72	27.3	9.6	7.84	0.43	12.0	3.00	0.60	0.04	292	0.05	4.39	0.26	0.07	0.12
NS-23C.08	52.0	0.95	2.36	34.3	9.7	8.28	0.37	11.9	3.12	0.42	0.04	313	0.05	4.49	0.26	0.06	0.13
NS-23D.07																	
NS-23D.08	58.5	1.32	4.39	43.6	12.4	12.0	0.46	12.0	2.91	0.72	0.05	287	0.05	4.85	0.30	0.08	0.13
NS-23D.09	56.0	1.20	3.63	39.1	11.2	11.9	0.40	11.9	3.04	0.54	0.05	299	0.05	4.79	0.29	0.08	0.13
NS-23D.10	65.6	1.48	4.28	41.3	13.6	13.9	0.44	13.3	3.41	0.62	0.06	336	0.06	5.43	0.33	0.10	0.14
NS-28.07																	
NS-28.08	43.9	0.33	0.91	27.0	9.2	3.71	0.37	3.15	4.10	0.34	0.05	410	0.05	4.60	0.22	0.05	0.16
NS-28.09	51.9	0.42	0.99	42.3	11.0	4.15	0.81	2.59	3.91	0.45	0.06	388	0.05	4.56	0.26	0.07	0.16
NS-28.10	55.9	0.44	1.23	31.0	12.9	4.47	0.36	2.94	3.78	0.57	0.05	375	0.05	4.73	0.28	0.07	0.18
NS-29.01	50.4	1.35	5.99	37.1	8.1	10.3	1.07	13.6	3.77	0.65	0.03	385	0.06	5.16	0.25	0.07	0.13
NS-37.06																	
NS-37.07	35.9	0.37	1.68	22.6	7.6	3.80	0.40	2.97	4.74	0.61	0.03	479	0.04	3.38	0.18	0.05	0.14
NS-37.08	33.1	0.35	1.58	20.6	7.1	3.32	0.43	2.57	4.61	0.49	0.03	468	0.04	2.92	0.16	0.05	0.11
NS-38.08																	
NS-38.09	37.1	0.42	3.24	31.4	8.1	4.10	0.82	2.54	4.26	0.91	0.04	427	0.04	3.14	0.19	0.07	0.13
NS-38.10	57.0	0.63	4.01	39.9	13.6	5.64	0.50	3.67	4.54	0.82	0.05	536	0.05	3.73	0.25	0.09	0.16
NS-47.03																	
NS-47.04	61.7	0.70	4.25	40.8	10.9	4.19	2.44	2.78	4.61	0.94	0.07	475	0.06	3.92	0.30	0.06	0.19
NS-48.01	30.1	0.73	11.3	23.7	5.7	5.87	0.51	6.48	4.53	0.51	0.02	453	0.06	2.55	0.15	0.05	0.09
NS-101.01																	
NS-101.02	42.8	0.36	0.78	31.5	9.0	3.45	0.55	2.43	4.36	0.42	0.05	431	0.04	4.05	0.22	0.06	0.17
NS-101.03	41.6	0.35	0.72	26.4	8.7	3.38	0.63	2.12	4.60	0.37	0.05	456	0.05	4.23	0.21	0.05	0.18
NS-101.04	56.8	0.54	1.15	41.0	12.7	4.45	0.97	2.90	4.52	0.66	0.07	450	0.05	4.61	0.28	0.08	0.17
NS-101.05	50.6	0.48	1.06	31.5	11.6	3.82	0.51	2.33	4.10	0.53	0.06	405	0.05	3.95	0.25	0.07	0.16
NS-101.06	54.1	0.55	8.38	41.0	12.7	4.32	1.09	2.54	3.92	0.57	0.07	381	0.06	3.84	0.28	0.08	0.15
NS-102.01																	
NS-102.02	41.8	0.34	0.45	29.2	9.2	3.29	0.72	2.17	4.23	0.40	0.04	415	0.04	4.07	0.21	0.05	0.17
NS-102.03	42.7	0.35	0.48	26.4	9.0	3.29	0.46	1.86	4.44	0.39	0.04	435	0.04	4.18	0.21	0.05	0.17
NS-102.04	44.4	0.37	0.49	30.2	9.6	3.61	0.54	2.07	4.02	0.42	0.05	398	0.04	3.93	0.22	0.05	0.14
NS-102.05	51.2	0.41	0.54	34.0	12.2	4.00	0.40	2.83	5.20	0.41	0.05	560	0.05	4.62	0.24	0.06	0.19
NS-102.06	37.4	0.29	0.62	23.7	8.0	3.02	0.21	1.82	4.70	0.35	0.04	461	0.04	4.03	0.19	0.05	0.17
NS-103.01																	
NS-103.02	34.5	0.30	0.84	23.3	7.0	3.07	0.24	2.14	4.68	0.39	0.03	459	0.04	3.61	0.18	0.04	0.18
NS-103.03	38.1	0.34	0.78	22.8	7.7	3.35	0.13	2.57	4.62	0.28	0.03	440	0.04	3.92	0.20	0.05	0.17
NS-103.04	32.5	0.28	0.79	19.6	6.2	2.97	0.18	2.38	4.62	0.27	0.03	435	0.04	3.79	0.17	0.04	0.16
NS-103.05	32.8	0.29	0.60	27.9	6.1	2.82	0.16	1.89	4.83	0.41	0.04	460	0.04	3.33	0.17	0.04	0.17

NS-103.06	23.3	0.21	0.52	15.2	4.7	2.23	0.09	1.62	5.17	0.27	0.02	518	0.03	2.37	0.12	0.03	0.13
NS-104.01																	
NS-104.02	43.8	0.39	0.71	25.0	8.0	3.28	0.09	2.07	4.32	0.42	0.06	417	0.04	3.58	0.22	0.05	0.16
NS-104.03	51.4	0.47	0.97	22.7	9.7	3.89	0.08	2.84	4.52	0.39	0.05	494	0.04	3.88	0.24	0.04	0.18
NS-104.04	46.7	0.44	1.12	18.8	9.1	3.62	0.08	2.91	4.80	0.26	0.06	468	0.05	4.15	0.24	0.05	0.18
NS-104.05	42.3	0.41	1.20	29.5	7.9	3.17	0.10	2.41	4.14	0.49	0.04	396	0.04	3.12	0.22	0.05	0.13
NS-104.06	42.0	0.40	1.16	32.7	7.6	3.04	0.12	2.70	4.01	0.50	0.05	395	0.04	2.78	0.21	0.05	0.12
NS-105.01																	
NS-105.02	39.8	0.45	1.17	33.1	8.0	3.96	1.11	3.61	4.30	0.47	0.04	418	0.05	3.75	0.20	0.07	0.14
NS-105.03	40.5	0.47	1.29	28.0	8.5	3.72	0.43	4.18	4.21	0.40	0.04	395	0.05	4.14	0.22	0.07	0.17
NS-105.04	46.5	0.57	1.24	33.9	9.7	4.26	0.66	4.45	4.29	0.43	0.05	409	0.05	4.24	0.24	0.08	0.18
NS-105.05	40.6	0.50	0.92	28.0	8.4	3.73	0.73	3.69	4.17	0.39	0.05	408	0.05	3.76	0.20	0.06	0.18
NS-106.01																	
NS-106.02	50.6	0.55	1.17	30.0	10.4	3.65	1.44	2.69	3.92	0.59	0.07	370	0.05	4.02	0.27	0.06	0.14
NS-106.03	47.1	0.51	0.84	29.9	9.5	3.75	2.19	3.04	4.07	0.36	0.07	391	0.05	4.27	0.24	0.07	0.15
NS-106.04	52.6	0.55	0.91	31.6	11.0	4.07	0.26	3.25	4.12	0.39	0.07	402	0.05	4.15	0.27	0.07	0.14
NS-106.05	50.8	0.54	1.15	30.6	10.7	3.97	0.62	2.74	4.24	0.46	0.07	387	0.05	4.43	0.28	0.08	0.16
NS-107.01																	
NS-107.02	49.4	0.42	0.78	26.1	10.6	4.21	0.21	2.31	3.69	0.36	0.07	345	0.05	4.29	0.26	0.06	0.13
NS-107.03	58.7	0.49	0.75	31.4	12.6	4.99	0.18	3.15	4.49	0.44	0.07	420	0.06	5.21	0.31	0.07	0.18
NS-107.04	55.8	0.47	0.58	29.8	12.9	4.73	0.26	3.10	3.97	0.38	0.07	378	0.05	4.69	0.29	0.07	0.17
NS-107.05	62.1	0.55	0.91	34.7	14.6	5.14	0.98	3.53	4.56	0.42	0.08	454	0.06	5.00	0.31	0.07	0.19
NS-108.01																	
NS-108.02	53.7	0.42	0.92	31.5	11.8	4.49	0.22	3.12	4.01	0.42	0.06	378	0.05	4.44	0.28	0.06	0.17
NS-108.03	55.5	0.46	0.81	38.9	12.0	4.42	0.28	2.61	3.93	0.45	0.06	371	0.05	4.27	0.29	0.08	0.17
NS-108.04	47.7	0.47	0.75	41.1	10.4	3.60	0.23	1.86	3.70	0.61	0.05	341	0.04	3.26	0.26	0.06	0.11
NS-108.05	57.3	0.67	2.13	46.1	12.7	4.50	0.98	2.15	3.21	0.93	0.06	296	0.05	3.61	0.31	0.06	0.14
NS-108.06	57.5	0.59	1.77	40.3	12.5	4.63	0.65	2.78	3.96	0.78	0.06	393	0.05	3.87	0.29	0.05	0.16
NS-108.13																	
NS-109.01																	
NS-109.02																	
NS-109.03	42.9	0.58	4.33	30.8	8.9	4.50	0.30	2.78	4.58	0.78	0.04	430	0.05	3.75	0.23	0.06	0.15
NS-109.04	45.4	0.62	3.62	25.7	9.4	4.63	0.16	2.99	4.99	0.51	0.06	485	0.05	3.91	0.23	0.05	0.15
NS-109.05	37.0	0.56	6.06	27.1	7.8	3.92	0.27	2.33	4.40	0.62	0.04	432	0.05	3.01	0.19	0.05	0.14
NS-110.01																	
NS-110.02	39.0	0.76	6.04	24.8	6.0	4.75	0.24	2.85	3.90	0.62	0.03	354	0.05	3.26	0.22	0.05	0.13
NS-110.03	37.2	0.74	5.08	25.4	7.8	5.06	0.54	3.08	3.81	0.64	0.04	347	0.05	3.09	0.20	0.08	0.10
NS-110.04	38.1	0.82	8.06	36.3	6.6	4.69	0.29	2.91	3.51	0.74	0.03	315	0.05	3.20	0.21	0.07	0.10
NS-110.05	32.5	0.69	9.51	40.4	6.1	3.30	0.23	2.80	3.42	0.78	0.03	332	0.05	2.48	0.17	0.05	0.09
NS-111.01																	
NS-111.02	57.7	0.48	0.68	37.5	12.6	4.98	0.52	3.19	4.05	0.46	0.06	391	0.06	4.71	0.30	0.08	0.15
NS-111.03	66.8	0.55	0.63	40.5	15.2	5.41	0.31	3.54	4.08	0.48	0.09	402	0.06	4.85	0.34	0.09	0.16
NS-111.04	62.2	0.55	0.61	42.0	15.0	4.94	0.29	3.28	3.59	0.53	0.07	344	0.05	4.39	0.32	0.08	0.15
NS-111.05	70.2	0.74	1.36	44.4	17.8	5.15	0.97	2.81	3.21	0.94	0.09	315	0.06	3.95	0.36	0.09	0.14
NS-112.01	66.3	0.46	1.70	43.2	15.7	3.21	0.70	2.10	3.99	0.70	0.09	370	0.11	5.75	0.35	0.10	0.19
NS-112.02	87.1	0.61	3.89	33.8	26.2	6.98	0.51	1.96	3.69	0.66	0.13	368	0.16	6.09	0.44	0.08	0.19
NS-112.03																	
NS-113.01	63.7	0.41	1.16	39.8	16.4	3.48	0.64	0.60	4.11	0.71	0.08	372	0.12	5.70	0.35	0.10	0.22
NS-113.02	73.3	0.50	1.27	50.8	19.8	3.86	0.86	0.68	4.42	0.82	0.08	460	0.13	6.36	0.36	0.12	0.27
NS-113.03	59.7	0.42	1.12	50.0	15.3	3.11	1.25	0.63	3.99	0.77	0.08	378	0.11	5.54	0.32	0.11	0.22
NS-113.04	80.8	0.52	1.42	29.7	20.4	4.26	0.55	1.16	3.90	0.67	0.10	373	0.15	7.54	0.42	0.06	0.26
NS-114.01																	
NS-114.02	36.4	0.24	4.69	41.6	5.1	1.44	0.94	0.01	3.45	0.46	0.03	317	0.07	3.43	0.20	0.13	0.21
NS-114.03	69.7	0.55	2.60	28.8	10.9	2.90	0.92	0.41	3.89	0.49	0.06	365	0.10	5.89	0.37	0.07	0.19
NS-114.04	92.5	0.65	3.25	47.1	19.3	5.93	0.90	1.30	3.79	0.63	0.12	365	0.10	6.07	0.49	0.11	0.19
NS-117.01																	
NS-117.02	44.0	0.58	4.01	32.4	9.1	5.05	0.65	4.60	4.38	0.56	0.05	422	0.05	3.75	0.23	0.07	0.17
NS-117.03	51.1	0.75	8.30	35.3	10.9	6.35	0.53	4.81	4.18	0.84	0.05	375	0.07	4.20	0.29	0.09	0.17
NS-117.04	36.8	0.55	5.63	25.8	7.6	4.75	0.40	3.50	2.84	0.62	0.04	271	0.05	2.86	0.19	0.06	0.11
NS-117.05	49.5	0.72	7.60	35.2	10.3	5.79	0.58	4.68	4.14	0.87	0.05	369	0.07	4.07	0.28	0.08	0.17
NS-117.06	52.7	0.78	7.07	36.5	11.3	6.65	0.82	5.18	4.38	0.81	0.06	417	0.07	4.05	0.28	0.07	0.17
NS-118.01																	
NS-118.02	32.3	0.50	5.01	29.9	5.9	3.29	0.73	2.92	2.91	1.18	0.03	264	0.04	2.70	0.18	0.04	0.10
NS-118.03	42.4	0.68	6.73	30.8	7.9	5.91	0.88	5.97	3.96	0.94	0.04	395	0.05	3.34	0.22	0.05	0.13
NS-118.04	41.6	0.70	26.2	30.6	8.8	6.24	2.08	5.36	3.94	0.91	0.05	357	0.09	3.45	0.23	0.07	0.14

NS-119.01																	
NS-119.02	44.0	0.61	7.57	34.9	8.4	6.08	1.30	4.97	3.52	1.06	0.05	315	0.06	3.56	0.25	0.09	0.14
NS-119.03	54.3	0.77	17.4	39.7	12.5	7.78	0.76	5.68	3.90	1.15	0.07	364	0.09	3.87	0.29	0.10	0.12
NS-119.04	52.2	0.71	28.7	33.3	12.4	8.13	0.59	5.63	4.07	1.05	0.06	396	0.10	3.79	0.27	0.09	0.15
NS-119.05	55.5	0.82	24.3	33.6	12.3	7.76	0.71	6.14	3.99	1.23	0.07	373	0.08	3.96	0.27	0.10	0.13
NS-119.06	43.6	0.67	42.0	30.0	10.3	6.70	0.60	5.25	3.80	2.22	0.07	353	0.15	3.14	0.22	0.09	0.11
NS-121.01	101	0.98	10.2	50.0	26.4	9.37	0.89	3.52	3.70	0.91	0.13	377	0.10	5.59	0.45	0.13	0.16
NS-121.02	30.3	0.31	2.03	18.8	6.2	2.75	0.19	1.91	4.90	0.74	0.04	458	0.04	2.39	0.14	0.04	0.12
NS-121.03	88.9	0.78	6.24	41.1	22.9	7.69	0.77	2.71	3.60	0.76	0.13	334	0.09	4.78	0.44	0.10	0.13
NS-122.01																	
NS-122.02	51.6	0.67	2.99	31.6	10.3	5.31	0.50	5.15	4.11	0.64	0.08	380	0.06	4.16	0.26	0.06	0.21
NS-122.03	44.1	0.60	3.03	47.2	8.2	4.48	0.48	4.21	3.92	0.63	0.07	354	0.06	3.62	0.22	0.06	0.18
NS-122.04	36.1	0.54	4.87	23.3	7.0	3.15	0.23	3.15	2.66	1.17	0.06	243	0.05	2.81	0.18	0.05	0.13
NS-122.05	32.0	0.50	8.80	18.8	6.4	3.20	0.29	2.90	2.51	0.77	0.05	231	0.06	2.53	0.16	0.04	0.12
NS-122.06	47.5	0.72	21.8	24.7	11.4	5.46	0.39	5.30	3.29	0.83	0.07	350	0.09	3.42	0.21	0.08	0.18
NS-122.07	44.4	0.66	53.1	25.2	11.1	11.0	0.48	4.78	3.20	0.84	0.08	319	0.14	3.40	0.20	0.09	0.18
NS-123.01																	
NS-123.02	46.8	0.56	2.43	21.5	9.9	4.09	0.11	5.05	3.70	0.66	0.07	360	0.06	3.67	0.22	0.06	0.19
NS-123.03	14.2	0.33	18.3	19.0	3.0	1.60	0.38	1.24	0.97	0.62	0.03	86	0.06	1.09	0.07	0.04	0.04
NS-123.04	33.5	0.54	25.8	19.5	8.0	5.51	0.40	4.03	2.58	0.74	0.06	247	0.08	2.72	0.16	0.07	0.15
NS-124.01	34.3	0.47	20.2	18.3	7.0	4.75	0.30	3.78	2.66	0.53	0.05	261	0.05	2.53	0.16	0.06	0.13
NS-124.02	25.8	0.35	4.51	13.6	4.9	3.19	0.18	2.54	2.40	0.48	0.05	215	0.04	2.13	0.13	0.06	0.10
NS-124.03	42.1	0.58	20	24.9	8.6	5.86	0.67	4.92	4.12	0.65	0.07	407	0.08	3.28	0.19	0.10	0.16

$^{87}Sr/^{86}Sr$ of sequential soil leach and digest fractions.

sample name	exch. $^{87}Sr/^{86}Sr$	exch. 2 sigma	cold 1M HNO_3 $^{87}Sr/^{86}Sr$	cold HNO_3 2 sigma	hot HNO_3 $^{87}Sr/^{86}Sr$	hot HNO_3 2 sigma	HF residual $^{87}Sr/^{86}Sr$	HF 2 sigma
DH-01.07			0.707872	0.000014				
DH-02.07			0.709468	0.000013				
DH-03.09			0.709235	0.000010				
DH-03.10			0.708770	0.000035				
DH-03.11			0.708507	0.000011				
NS-08.07			0.712811	0.000018	0.721590	0.000028	0.724546	0.000037
NS-08.08			0.712744	0.000055	0.721545	0.000023	0.725619	0.000027
NS-08.10			0.712404	0.000051	0.728924	0.000009	0.728104	0.000017
NS-13.13	0.712175	0.000019	0.712156	0.000018				
NS-13.14			0.710465	0.000068	0.720106	0.000020	0.723156	0.000044
NS-13.15			0.710055	0.000060	0.720671	0.000032	0.724500	0.000028
NS-13.16			0.709631	0.000043	0.725481	0.000025	0.727459	0.000024
NS-13.23			0.709225	0.000054	0.715267	0.000023	0.728827	0.000019
NS-22.08	0.713771	0.000013	0.713702	0.000027				
NS-22.09	0.713989	0.000031	0.712777	0.000031	0.719524	0.000014	0.722797	0.000027
NS-22.10	0.713286	0.000024	0.713302	0.000023	0.717466	0.000021	0.730348	0.000026
NS-22.11	0.711905	0.000011	0.711978	0.000028	0.716696	0.000020	0.729985	0.000036
NS-22.26	0.709979	0.000023	0.709937	0.000027				
NS-22.27	0.713414	0.000017	0.712500	0.000054	0.725759	0.000285	0.719736	0.000042
NS-23A.06			0.711238	0.000014				
NS-23A.07			0.711095	0.000016				
NS-23A.08			0.710720	0.000023				
NS-23A.09			0.710563	0.000027				
NS-23B.06			0.711286	0.000013				
NS-23B.07			0.710052	0.000018				
NS-23B.08			0.709809	0.000008				
NS-23C.06			0.711428	0.000015				
NS-23C.07			0.710861	0.000017				
NS-23C.08			0.710447	0.000010				
NS-23D.07			0.709935	0.000012				
NS-23D.08			0.709478	0.000010				
NS-23D.09			0.708874	0.000016				
NS-23D.10			0.708737	0.000021				
NS-28.07			0.717712	0.000014				
NS-28.08			0.713960	0.000014				
NS-28.09			0.716672	0.000021				
NS-28.10			0.713674	0.000016				
NS-29.01			0.707821	0.000009				
NS-37.06			0.716050	0.000026				
NS-37.07			0.710876	0.000015				
NS-37.08			0.711492	0.000026				
NS-38.08			0.711661	0.000016				
NS-38.09			0.710095	0.000012				
NS-38.10			0.709931	0.000010				
NS-47.03	0.712250	0.000026	0.712191	0.000017				
NS-47.04	0.712336	0.000019	0.712197	0.000024	0.724495	0.000018	0.723322	0.000184
NS-48.01	0.708697	0.000012	0.708407	0.000026	0.717150	0.000051	0.715325	0.000275
NS-101.01	0.721412	0.000075	0.719918	0.000016	0.724344	0.000021		
NS-101.02	0.718664	0.000017	0.714138	0.000034	0.727602	0.000059		
NS-101.03	0.718510	0.000053	0.712643	0.000046	0.730939	0.000018		
NS-101.04	0.717530	0.000030	0.712608	0.000036	0.731677	0.000018		
NS-101.05	0.715944	0.000026	0.711928	0.000019	0.732349	0.000011		
NS-101.06	0.711278	0.000017	0.709084	0.000011	0.733956	0.000015		
NS-102.01			0.721376	0.000045				
NS-102.02			0.713043	0.000017				
NS-102.03			0.713503	0.000021				
NS-102.04			0.713107	0.000021				
NS-102.05			0.712724	0.000053				

sample name	exch. $^{87}Sr/^{86}Sr$	exch. 2 sigma	cold 1M HNO_3 $^{87}Sr/^{86}Sr$	cold HNO_3 2 sigma	hot HNO_3 $^{87}Sr/^{86}Sr$	hot HNO_3 2 sigma	HF residual $^{87}Sr/^{86}Sr$	HF 2 sigma
NS-102.06			0.711201	0.000016				
NS-103.01			0.714775	0.000019				
NS-103.02			0.712194	0.000020				
NS-103.03			0.711913	0.000009				
NS-103.04			0.711713	0.000014				
NS-103.05			0.711934	0.000014				
NS-103.06			0.711735	0.000011				
NS-104.01	0.716872	0.000018	0.716725	0.000016	0.720922	0.000031		
NS-104.02	0.720050	0.000022	0.713041	0.000019	0.722058	0.000024		
NS-104.03	0.720851	0.000061	0.712759	0.000042	0.722017	0.000017		
NS-104.04	0.717221	0.000019	0.712395	0.000027	0.723151	0.000022		
NS-104.05	0.715970	0.000026	0.712871	0.000035	0.721817	0.000071		
NS-104.06	0.716069	0.000042	0.712042	0.000021	0.723476	0.000020		
NS-105.01			0.716527	0.000019				
NS-105.02			0.714233	0.000047				
NS-105.03			0.714439	0.000044				
NS-105.04			0.713450	0.000024				
NS-105.05			0.713205	0.000038				
NS-106.01	0.717314	0.000027	0.717177	0.000024	0.722149	0.000211		
NS-106.02	0.717041	0.000030	0.715464	0.000021	0.723068	0.000035		
NS-106.03	0.719167	0.000026	0.714871	0.000041	0.722645	0.000124		
NS-106.04	0.717241	0.000044	0.713764	0.000038	0.723827	0.000023		
NS-106.05	0.716745	0.000037	0.713083	0.000027	0.725281	0.000013		
NS-107.01			0.710658	0.000013				
NS-107.02			0.713181	0.000021				
NS-107.03			0.712895	0.000014				
NS-107.04			0.712948	0.000017				
NS-107.05			0.713676	0.000097				
NS-108.01	0.713660	0.000019	0.711668	0.000027	0.714412	0.000017		
NS-108.02	0.720245	0.000044	0.712911	0.000060	0.731134	0.000015		
NS-108.03	0.720483	0.000025	0.712561	0.000033	0.732188	0.000015		
NS-108.04	0.719548	0.000020	0.714498	0.000027	0.733771	0.000041		
NS-108.05	0.716431	0.000020	0.714446	0.000020	0.728717	0.000027		
NS-108.06	0.716577	0.000024	0.713592	0.000019	0.732531	0.000011		
NS-108.13								
NS-109.01			0.709777	0.000014				
NS-109.02			0.709902	0.000018				
NS-109.03			0.710496	0.000017				
NS-109.04			0.710104	0.000020				
NS-109.05			0.710460	0.000018				
NS-110.01	0.709544	0.000022	0.709569	0.000021	0.709652	0.000048		
NS-110.02	0.710457	0.000017	0.709777	0.000016	0.714322	0.000029		
NS-110.03	0.709485	0.000022	0.709465	0.000013	0.718904	0.000012		
NS-110.04	0.709496	0.000042	0.709459	0.000014	0.716494	0.000083		
NS-110.05	0.709585	0.000019	0.709995	0.000016	0.713268	0.000024		
NS-112.01			0.711660	0.000013				
NS-112.02			0.712769	0.000016				
NS-112.03								
NS-113.01			0.711735	0.000014				
NS-113.02			0.709851	0.000016				
NS-113.03			0.710660	0.000018				
NS-113.04			0.711563	0.000021				
NS-114.01			0.708409	0.000015				
NS-114.02			0.708445	0.000021				
NS-114.03			0.709356	0.000015				
NS-114.04			0.709386	0.000013				
NS-119.01	0.708721	0.000023	0.708762	0.000013	0.708900	0.000041		
NS-119.02	0.708773	0.000017	0.709060	0.000015	0.713011	0.000081		
NS-119.03	0.708416	0.000018	0.708580	0.000011	0.711376	0.000015		
NS-119.04	0.708313	0.000033	0.708235	0.000021	0.713535	0.000019		
NS-119.05	0.708253	0.000015	0.708352	0.000017	0.711658	0.000016		
NS-119.06	0.708296	0.000016	0.708425	0.000012	0.716740	0.000035		

sample name	exch. $^{87}Sr/^{86}Sr$	exch. 2 sigma	cold 1M HNO_3 $^{87}Sr/^{86}Sr$	cold HNO_3 2 sigma	hot HNO_3 $^{87}Sr/^{86}Sr$	hot HNO_3 2 sigma	HF residual $^{87}Sr/^{86}Sr$	HF 2 sigma
NS-121.02	0.712331	0.000018	0.711629	0.000011	0.724539	0.000019		
NS-121.03	0.713058	0.000012	0.711070	0.000008	0.727403	0.000036		
NS-122.01	0.710621	0.000044	0.710627	0.000014	0.712801	0.000183		
NS-122.02	0.711741	0.000071	0.711870	0.000022	0.713987	0.000041		
NS-122.03	0.710258	0.000023	0.711035	0.000023	0.714585	0.000031		
NS-122.04	0.710080	0.000023	0.710836	0.000028	0.713590	0.000064		
NS-122.05	0.709814	0.000037	0.709522	0.000023	0.713149	0.000051		
NS-122.06	0.709412	0.000028	0.709681	0.000019	0.712507	0.000076		
NS-122.07	0.710615	0.000028	0.709076	0.000018	0.714035	0.000158		

Appendix C: Stream location and chemistry data.

Location, physical data, and $^{87}Sr/^{86}Sr$.

sample number	LTER ID	Date	location name	surface	latitude (dec. deg. N)	longitude (dec. deg. W.)	temp. (deg. C)	pH	$^{87}Sr/^{86}Sr$	2 sigma
2005-tk1	2005-1002	7/9/05	Toolik River Ice Lens Melt-Out Upstream	Sag 1	68.6924	149.2033			0.717309	0.000017
2005-tk2	2005-1003	7/9/05	Toolik River Ice Lens Melt-Out Downstream	Sag 1	68.6924	149.2033			0.715290	0.000016
2005-tk3	2005-1004	7/9/05	Toolik River Ice Lens Melt-Out Downstream	Sag 1	68.6924	149.2033			0.713982	0.000014
2005-tk4	2005-1005	7/9/05	Toolik River Ice Lens Melt-Out Downstream	Sag 1	68.6924	149.2033			0.714190	0.000037
DH-01.01	2002-1134	6/13/02	Hot Springs Pluton	silicate bedrock	66.3806	150.5062	15			
DH-02.01	2002-1135	6/13/02	Bonanza Pluton	silicate bedrock	66.6985	150.6630	12			
DH-03.01	2002-1136	7/21/02	Jim River Pluton Quarry site	silicate bedrock	66.9934	150.2951	12			
DH-04.01	2002-1137	7/21/02	Jim River Pluton Kmz stream	silicate bedrock	66.9824	150.3215				
DH-05.01	2002-1138	7/21/02	Jim River Pluton boggy stream	silicate bedrock	66.9636	150.3693				
DH-06.01	2002-1139	7/21/02	Jim River	silicate bedrock	66.8843	150.5250				
DH-101.01		8/16/03	Bonanza Creek	silicate bedrock					0.713436	0.000021
DH-130.01		8/18/03	Yukon River	mixed bedrock					0.713228	0.000021
KP-02.01		8/16/03	Kanuti Stream	Kanuti pl.	66.4748	150.6651			0.709260	0.000017
NS-00.00	2002-1140	8/6/02	DI blank from Toolik Field Station DI supply						0.710607	0.000071
NS-04.01	2002-0013	6/17/02	E5 inlet S	Sag 2	68.6444	149.4306			0.716413	0.000191
NS-04.02	2002-0012	6/17/02	E5 inlet W	Sag 2	68.6450	149.4600			0.718806	0.000026
NS-04.03	2002-0011	6/17/02	E5 outlet	Sag 2	68.6461	149.4556			0.715150	0.000029
NS-04.05	2002-0547	7/29/02	E5 inlet S	Sag 2	68.6444	149.4306			0.716328	0.000021
NS-07.01	2002-0017	6/19/02	Imnaviat weir	Sag 1	68.6170	149.3179	10.4	5.8	0.717192	0.000143

sample number	LTER ID	Date	location name	surface	latitude (dec. deg. N)	longitude (dec. deg. W.)	temp. (deg. C)	pH	$^{87}Sr/^{86}Sr$	2 sigma
NS-07.02	2002-0018	6/19/02	Imnaviat site 2	Sag 1						
NS-07.03	2002-0019	6/19/02	Imnaviat site 3	Sag 1						
NS-07.04	2002-0020	6/19/02	Imnaviat site 4	Sag 1					0.716532	0.000057
NS-07.05	2002-0551	7/31/02	Imnaviat Weir	Sag 1	68.6170	149.3179			0.716905	0.000021
NS-07.21		8/15/03	Imnaviat Weir	Sag 1	68.6170	149.3179			0.716954	0.000015
NS-08.20	2002-1162	7/14/02	It 1 pit	It 1	68.6255	149.5774			0.719586	0.000037
NS-101.15		8/7/03	It 1 Pit 2 lysimeter	It 1	68.6251	149.5718			0.717537	0.000016
NS-101.16		8/7/03	It 1 Pit 2 lysimeter	It 1	68.6251	149.5718			0.716692	0.000016
NS-103.13		8/7/03	Sag 2 Pit 2	Sag 2	68.6451	149.4352			0.715384	0.000020
NS-103.14		8/7/03	Sag 2 Pit 2	Sag 2	68.6451	149.4352			0.713668	0.000013
NS-105.11		8/8/03	Sag 1 Pit 2	Sag 1	68.6178	149.3231			0.716127	0.000014
NS-105.12		8/8/03	Sag 1 Pit 2	Sag 1	68.6178	149.3231			0.715558	0.000026
NS-110.16		8/17/03	It 2 Pit 3	It 2	68.6414	149.5995			0.709537	0.000018
NS-110.17		8/17/03	It 2 Pit 3	It 2	68.6414	149.5995			0.709513	0.000014
NS-112.05		8/13/03	upper glacier stream near neo 1 pit 1	neo 1			1.1	7.7	0.717296	0.000016
NS-115.01		8/13/03	middle glacier stream	neo 2			10.8	7.5	0.718228	0.000015
NS-116.01		8/13/03	lower glacier stream	neo 3	68.3776	149.5216	3.1	8.6	0.713828	0.000019
NS-120.01		8/14/03	Anak Stream	Anak	68.9050	149.3842			0.712417	0.000014
NS-125.01	2003-1016	8/15/03	Gunsight Stream	Gunsight	69.2764	148.9274			0.711356	0.000016
NS-126.01	2003-1015	8/15/03	Toolik River Ice Lens Melt-Out Upstream	Sag 1	68.6924	149.2033			0.717341	0.000016
NS-127.01	2003-1014	8/15/03	Toolik River Ice Lens Melt-Out Downstream	Sag 1	68.6924	149.2033			0.713121	0.000019
NS-129.01		8/17/03	Underwillow Stream	Silicate bedrock	68.3342	149.3200	2.3	7.5	0.719893	0.000020
NS-13.25	2002-1141	8/8/02	It 2 pit/lysimeter	It 2	68.6412	149.6030			0.711459	0.000023
NS-16.01	2002-1142	7/9/02	field station gravel pad	gravel pad	68.6269	149.5978			0.709740	0.000013
NS-16.05	2002-1143	8/5/02	precipitation/field station gravel pad	precip	68.6269	149.5978			0.709485	0.000165
NS-16.06	2002-1144	8/6/02	precipitation/field station gravel pad	precip	68.6269	149.5978			0.708781	0.000042
NS-17.01	2002-1145	7/10/02	N1 feeder stream	It 2	68.6412	149.6107	15		0.710600	0.000050

sample number	LTER ID	Date	location name	surface	latitude (dec. deg. N)	longitude (dec. deg. W.)	temp. (deg. C)	pH	$^{87}Sr/^{86}Sr$	2 sigma
NS-20.01	2002-1146	7/13/02	Roche Moutonee Creek	mixed bedrock	68.3739	149.3101			0.713375	0.000021
NS-20.21		8/17/03	Roche Moutonee Creek	Mixed bedrock	68.3739	149.3101	4.8	9.6	0.713843	0.000016
NS-21.01	2002-1147	7/14/02	It 1 stream	It 1	68.6255	149.5774			0.710995	0.000024
NS-25.01	2002-1148	7/20/02	TW Lower stream	It 2 outwash	68.6198	149.6095			0.713314	0.000016
NS-30.01	2002-1149	7/28/02	PMI Atigun feeder stream	carbonate bedrock	68.4503	149.3464	8.3		0.710550	0.000033
NS-31.01	2002-1150	7/28/02	Atigun River	mixed bedrock	68.4614	149.3279	12.2		0.714458	0.000021
NS-33.01	2002-1151	7/28/02	It 3 stream	It 3	68.4818	149.4757	11		0.710391	0.000039
NS-35.01	2002-1152	7/30/02	Sagavanirktok River	mixed bedrock	68.9585	148.8591	7		0.710453	0.000017
NS-36.04	2002-1153	7/30/02	Aufeis near Galbraith	carbonate bedrock	68.4639	149.5402	7.7		0.708802	0.000020
NS-39.01	2002-1154	8/1/02	Island Lake	It 3	68.5200	149.4917	9.1		0.710234	0.000020
NS-40.01	2002-1155	8/3/02	Kuparuk	Sag 1	68.6471	149.4086	15.4		0.707870	0.000018
NS-41.01	2002-1156	8/3/02	Holden Creek	mixed bedrock	68.4074	149.3194	10.9		0.709819	0.000013
NS-41.21		8/17/03	Holden Creek	Mixed bedrock	68.4074	149.3194	4.3	7	0.709772	0.000016
NS-42.01	2002-1157	8/3/02	Bad idea stream-drains MDk only	mixed bedrock	68.3905	149.3122	5.2		0.711232	0.000048
NS-42.21		8/17/03	Bad Idea Stream	Mixed bedrock	68.3905	149.3122	4.3	9.2	0.711382	0.000013
NS-43.01	2002-1158	8/6/02	Kuparuk upstream from dripper	Sag 1	68.6363	149.4050	4.8		0.707878	0.000086
NS-44.01	2002-1159	8/6/02	Atigun upstream	silicate bedrock	68.2144	149.4070	5		0.719655	0.000035
NS-45.01	2002-1160	8/6/02	Trevor Creek	mixed bedrock	68.2839	149.3688	3.3		0.714855	0.000031
NS-45.21		8/17/03	Trevor Creek	Mixed bedrock	68.2839	149.3688	4.6	8.9	0.715054	0.000016
NS-46.01	2002-1161	8/6/02	Kayak Creek	carbonate bedrock	68.4116	149.3282	3.9		0.708469	0.000018
NS-46.21		8/17/03	Kayak Stream	Carbonate bedrock	68.4116	149.3282	5.1	8.1	0.708488	0.000015
NS-I1OUT.01	2002-0071	6/25/02	I1 outlet	It 2	68.5724	149.5812			0.714930	0.000019
NS-I1OUT.03	2002-0638	8/6/02	I1 outlet	It 2	68.5724	149.5812			0.715188	0.000078
NS-I1out.08		8/6/03	I1 outlet	It 2	68.5724	149.5812			0.715016	0.000024
NS-I2OUT.01	2002-0070	6/25/02	I2 outlet	It 2	68.5727	149.5705			0.716396	0.000019

sample number	LTER ID	Date	location name	surface	latitude (dec. deg. N)	longitude (dec. deg. W.)	temp. (deg. C)	pH	$^{87}Sr/^{86}Sr$	2 sigma
NS-I2OUT.03	2002-0640	8/6/02	I2 outlet	lt 2	68.5727	149.5705			0.716473	0.000037
NS-I2OUT.08		8/6/03	I2 outlet	lt 2	68.5727	149.5705			0.716675	0.000033
NS-I3INEAST	2002-0073	6/25/02	I3 inlet east	lt 2						
NS-I3INWEST	2002-0072	6/25/02	I3 inlet west	lt 2						
NS-I3OUT	2002-0074	6/25/02	I3 outlet	lt 2						
NS-I4OUT.01	2002-0075	6/25/02	I4 outlet	lt 2	68.5815	149.5864			0.715633	0.000019
NS-I4OUT.04	2002-0642	8/6/02	I4 outlet	lt 2	68.5815	149.5864			0.715593	0.000024
NS-I5IN	2002-0076	6/25/02	I4 into I5	lt 2						
NS-I5OUT	2002-0077	6/25/02	I5 outlet	lt 2						
NS-I6HWIN.01	2002-0081	6/25/02	I6 headwater inlet	lt 1	68.5790	149.6225			0.711416	0.000019
NS-I6HWIN.04	2002-0648	8/7/02	I6 headwater inlet	lt 1	68.5790	149.6225			0.711281	0.000011
NS-I6HWIN.08		8/6/03	I6 headwater inlet		68.5790	149.6225			0.710947	0.000014
NS-I6INE.08		8/6/03	I6 inlet east						0.715408	0.000011
NS-I6INEAST.01	2002-0078	6/25/02	I5 into I6	lt 2 outwash	68.5949	149.5863			0.715357	0.000034
NS-I6INEAST.04	2002-0645	8/7/02	I5 into I6	lt 2 outwash	68.5949	149.5863			0.715257	0.000018
NS-I6INWEST.01	2002-0079	6/25/02	I6HW into I6	lt 2 outwash	68.5969	149.6013			0.711315	0.000018
NS-I6INWEST.03	2002-0646	8/7/02	I6HW into I6	lt 2 outwash	68.5969	149.6013			0.710864	0.000014
NS-I6INWEST.08		8/6/03	I6HW into I6	lt 2 outwash	68.5969	149.6013			0.711263	0.000021
NS-I6OUT	2002-0080	6/25/02	I6 outlet	lt 2 outwash						
NS-I7OUT.01	2002-0085	6/26/02	I7 outlet	lt 2 outwash	68.6020	149.5969			0.712616	0.000024
NS-I7OUT.03	2002-0650	8/7/02	I7 outlet	lt 2 outwash	68.6020	149.5969			0.712520	0.000013
NS-I8HW.01	2002-0069	6/25/02	I8 Headwater	lt 1	68.5723	149.5409			0.713464	0.000051
NS-I8HW.04	2002-0636	8/6/02	I8 Headwater	lt 1	68.5723	149.5409				
NS-I8HW.08		8/6/03	I8 Headwater		68.5723	149.5409			0.712549	0.000014
NS-I8IN.01	2002-0086	6/26/02	I8 inlet	lt 2 outwash	68.6085	149.5876			0.712523	0.000023
NS-I8IN.03	2002-0651	8/7/02	I8 inlet	lt 2 outwash	68.6085	149.5876			0.712210	0.000017
NS-I8OUT	2002-0087	6/26/02	I8 outlet	lt 2 outwash						
NS-I9INEAST.01	2002-0091	6/26/02	I8 into I9	lt 2 outwash	68.6184	149.5965			0.712172	0.000017
NS-I9INEAST.03	2002-0656	8/7/02	I8 into I9	lt 2 outwash	68.6184	149.5965			0.712015	0.000017

sample number	LTER ID	Date	location name	surface	latitude (dec. deg. N)	longitude (dec. deg. W.)	temp. (deg. C)	pH	$^{87}Sr/^{86}Sr$	2 sigma
NS-I9INW.08		8/6/03	I9 inlet west		68.6182	149.5968			0.712542	0.000015
NS-I9INWEST.01	2002-0090	6/26/02	I7 into I9	lt 2 outwash	68.6182	149.5968			0.712503	0.000020
NS-I9INWEST.03	2002-0655	8/7/02	I7 into I9	lt 2 outwash	68.6182	149.5968			0.712142	0.000011
NS-I9OUT.01	2002-1163	6/26/02	I9 outlet	lt 2 outwash	68.6194	149.5953			0.712250	0.000014
NS-I9OUT.05	2002-1164	8/7/02	I9 outlet	lt 2 outwash	68.6194	149.5953			0.712026	0.000019
NS-IMINUSIN.01	2002-0083	6/26/02	I minus inlet	lt 2 outwash	68.5568	149.5551			0.712971	0.000014
NS-IMINUSOUT.01	2002-0084	6/26/02	I minus outlet	lt 2 outwash	68.5567	149.5747			0.713132	0.000016
NS-ISWAMPIN	2002-0088	6/26/02	I Swamp inlet	lt 2 outwash						
NS-ISWAMPOUT	2002-0089	6/26/02	I Swamp outlet	lt 2 outwash						
NS-MWL.01	2002-0092	6/26/02	Milky Way lower	lt 2 outwash	68.6197	149.5961			0.710943	0.000107
NS-MWL.03	2002-0657	8/7/02	Milky Way lower	lt 2 outwash	68.6197	149.5961			0.710598	0.000041
NS-MWL.08		8/6/03	Milky Way lower		68.6197	149.5961			0.710948	0.000014
NS-MWL.09		8/15/03	Milky Way lower		68.6197	149.5961			0.711577	0.000014
NS-MWU.01	2002-0093	6/26/02	Milky Way upper	lt 2 outwash	68.6191	149.5806				
NS-MWU.03	2002-0702	8/9/02	Milky Way upper	lt 2 outwash	68.6191	149.5806			0.712085	0.000031
NS-MWU.08		8/6/03	Milky Way upper		68.6191	149.5806			0.712546	0.000016
NS-MWU.09		8/15/03	Milky Way upper		68.6191	149.5806			0.712632	0.000016
NS-TOOLIKIN.01	2002-0094	6/26/02	Toolik Inlet	lt 2 outwash	68.6256	149.5961			0.712323	0.000080
NS-TOOLIKIN.03	2002-0659	8/7/02	Toolik Inlet	lt 2 outwash	68.6256	149.5961			0.711850	0.000140
NS-TOOLIKIN.08		8/6/03	Toolik Inlet		68.6256	149.5961			0.712110	0.000014
NS-TOOLIKIN.09		8/15/03	Toolik Inlet		68.6256	149.5961			0.712248	0.000014
NS-TOOLIKIN.10		8/10/03	Toolik Inlet		68.6256	149.5961			0.712072	0.000014
NS-TOOLIKIN.11		8/10/03	Toolik Inlet		68.6256	149.5961			0.712074	0.000008

Stream water chemistry data, mg/L.

sample number	Ba	Ca	Fe	K	Mg	Mn	Na	Ni	P	Rb	S	Si	Sr	V	Zn	Alk (uEQ/L)
2005-tk1	0.01	0.66	3.44	0.02	0.30	0.08	0.05	0.06	0.00	0.00	0.10	1.26	0.00	0.00	0.02	126.6
2005-tk2	0.02	1.40	3.04	0.12	0.40	0.11	0.20	0.10	0.00	0.00	0.35	1.98	0.00	0.01	0.03	98.0
2005-tk3	0.03	2.54	3.88	0.31	0.60	0.17	0.29	0.14	0.00	0.00	0.53	2.86	0.01	0.02	0.01	158.3
2005-tk4	0.03	3.26	4.90	0.39	0.70	0.24	0.44	0.12	0.00	0.00	0.53	2.37	0.01	0.01	0.02	185.0
DH-01.01	0.01	1.91	0.89	0.23	0.42	0.05	1.44	1.08	0.02	0.00	0.67	1.27	0.07	0.00	0.00	114.0
DH-02.01	0.00	1.03	1.29	0.26	0.43	0.02	1.47	1.50	0.02	0.45	0.67	0.77	0.07	0.00	0.00	
DH-03.01	0.00	4.09	0.02	0.22	0.64	0.00	1.04	1.19	0.02	0.52	0.67	1.11	0.07	0.00	0.00	90.5
DH-04.01	0.00	3.05	0.00	0.26	0.49	0.00	1.27	1.58	0.02	0.27	0.67	0.68	0.06	0.00	0.00	136.7
DH-05.01	0.00	1.57	0.74	0.17	0.31	0.02	0.74	0.77	0.02	0.22	0.67	1.64	0.07	0.00	0.00	37.3
DH-06.01	0.01	6.03	0.00	0.52	0.93	0.00	1.46	1.05	0.02	0.20	0.67	1.31	0.06	0.00	0.00	349.9
DH-101.01	0.01	2.30	0.25	0.35	0.61	0.01	0.90	0.04	0.00	0.00	0.87	2.90	0.02	0.04	0.00	
DH-130.01	0.04	30.5	0.06	1.43	7.45	0.00	2.83	0.03	0.00	0.00	12.3	2.30	0.12	0.08	0.00	
KP-02.01	0.01	3.47	0.33	0.11	0.37	0.02	1.89	0.05	0.00	0.00	0.13	4.17	0.03	0.05	0.00	
NS-00.00	0.00	0.00	0.00	0.02	0.00	0.00	0.00	0.01	0.02	0.00	0.67	2.59	0.07	0.00	0.00	
NS-04.01	0.01	1.50	0.21	0.02	0.40	0.01	0.38	0.24	0.02	0.17	0.67	2.31	0.07	0.00	0.00	
NS-04.02	0.01	0.79	0.11	0.03	0.30	0.01	0.35	0.35	0.02	0.38	0.67	2.16	0.07	0.00	0.00	
NS-04.03	0.01	1.92	0.10	0.28	0.44	0.06	0.27	0.20	0.02	0.42	0.67	2.35	0.07	0.00	0.00	
NS-04.05	0.01	1.77	0.36	0.03	0.49	0.02	0.25	0.04	0.08	0.00	0.10	1.05	0.00	0.01	0.02	
NS-07.01	0.01	1.13	0.32	0.02	0.34	0.01	0.32	0.16	0.02	0.66	0.67	2.41	0.07	0.00	0.00	
NS-07.02	0.01	1.13	0.28	0.02	0.33	0.01	0.28	0.15	0.02	0.33	0.67	2.42	0.07	0.00	0.00	
NS-07.03	0.01	1.09	0.26	0.02	0.31	0.01	0.25	0.16	0.02	0.13	0.67	2.41	0.07	0.00	0.00	
NS-07.04	0.01	1.15	0.26	0.02	0.30	0.01	0.22	0.13	0.02	0.46	0.67	2.45	0.07	0.00	0.00	
NS-07.05	0.01	1.13	0.76	0.02	0.35	0.03	0.09	0.03	0.08	0.00	0.04	0.57	0.00	0.01	0.01	
NS-07.21	0.01	1.14	0.24	0.01	0.31	0.02	0.13	0.01	0.00	0.00	0.05	0.87	0.00	0.04	0.00	
NS-08.20	0.12	2.81	4.60	1.81	0.87	0.29	0.44	4.47	0.02	1.99	0.67		0.07	0.06	0.00	
NS-101.15	0.07	2.62	0.08	0.09	0.52	0.07	0.37	0.02	0.00	0.00	0.19	1.55	0.01	0.04	0.15	
NS-101.16	0.04	2.41	0.08	0.13	0.54	0.05	0.53	0.02	0.00	0.00	0.11	1.60	0.01	0.04	0.02	
NS-103.13	0.10	2.19	0.15	0.30	0.62	0.20	0.52	0.03	0.00	0.00	0.21	1.80	0.01	0.05	0.03	
NS-103.14	0.47	1.36	0.58	0.18	0.44	0.31	0.54	0.03	0.00	0.00	0.35	2.03	0.01	0.04	0.19	
NS-105.11	0.06	1.06	0.14	0.07	0.44	0.02	0.36	0.02	0.00	0.00	0.25	1.68	0.00	0.04	0.13	
NS-105.12	0.06	1.02	0.14	0.07	0.42	0.04	0.34	0.02	0.00	0.00	0.23	1.75	0.00	0.04	0.05	
NS-110.16	0.20	70.9	0.02	0.18	7.28	0.01	0.78	0.02	0.00	0.00	2.07	1.68	0.09	0.07	0.89	
NS-110.17	0.14	109	0.05	2.19	12.1	0.03	1.55	0.02	0.00	0.00	15.7	1.39	0.13	0.10	0.36	
NS-112.05	0.00	0.72	0.00	0.12	1.07	0.00	0.07	0.00	0.00	0.00	0.26	0.09	0.00	0.04	0.00	101.6
NS-115.01	0.02	3.17	0.01	0.58	3.42	0.00	0.26	0.00	0.00	0.00	0.92	0.34	0.02	0.05	0.00	414.9
NS-116.01	0.03	10.8	0.00	0.46	3.95	0.00	0.22	0.00	0.00	0.00	0.77	0.29	0.03	0.06	0.00	
NS-120.01	0.01	3.13	0.25	0.02	0.44	0.00	0.27	0.02	0.00	0.00	0.07	1.32	0.01	0.04	0.00	
NS-125.01	0.01	6.64	0.31	0.00	1.08	0.00	0.21	0.02	0.00	0.00	0.11	1.65	0.01	0.05	0.00	204.3
NS-126.01	0.01	0.47	0.47	0.02	0.26	0.04	0.09	0.01	0.00	0.00	0.08	0.81	0.00	0.04	0.00	184.0
NS-127.01	0.06	4.96	1.40	0.57	0.72	0.12	0.28	0.05	0.09	0.00	0.16	3.90	0.02	0.12	0.01	331.4
NS-129.01	0.04	10.2	0.02	0.89	4.74	0.00	6.79	0.01	0.00	0.00	10.2	0.89	0.04	0.06	0.00	648.6
NS-13.25	0.03	15.3	0.14	0.20	1.36	0.00	1.45	0.37	0.02	0.00	0.67	2.17	0.07	0.00	0.00	
NS-16.01	0.15	54.2	2.02	0.80	5.23	0.18	1.47	0.64	0.02	0.00	0.66	1.86	0.06	0.02	0.00	6532.9
NS-16.05	0.00	4.10	0.00	3.27	0.11	0.02	5.01	0.03	0.02	0.29	0.67	2.59	0.07	0.00	0.00	
NS-16.06	0.00	3.40	0.00	0.74	0.05	0.01	1.30	0.02	0.02	0.25	0.67	2.59	0.07	0.00	0.00	
NS-17.01	0.01	21.8	0.04	0.05	2.86	0.00	0.30	0.29	0.02	0.00	0.67	2.26	0.07	0.01	0.00	1195.8
NS-20.01	0.02	18.4	0.01	0.36	3.01	0.00	1.39	0.21	0.02	0.08	0.67	2.35	0.06	0.01	0.00	5005.9
NS-20.21	0.02	14.9	0.01	0.39	2.68	0.00	1.28	0.01	0.00	0.00	2.66	0.67	0.04	0.05	0.00	867.9

sample number	Ba	Ca	Fe	K	Mg	Mn	Na	Ni	P	Rb	S	Si	Sr	V	Zn	Alk (uEQ/L)
NS-21.01	0.03	17.7	0.04	0.10	1.78	0.00	0.44	0.38	0.02	0.00	0.67	2.14	0.07	0.01	0.00	1019.0
NS-25.01	0.01	10.8	0.05	0.04	1.40	0.02	0.17	0.34	0.02	0.00	0.67	2.19	0.07	0.00	0.00	585.9
NS-30.01	0.04	62.5	0.00	0.52	6.98	0.00	2.23	0.32	0.02	0.00	0.66	2.25	0.06	0.02	0.00	12119
NS-31.01	0.02	27.7	0.00	0.48	7.89	0.00	2.80	0.29	0.02	0.00	0.66	2.27	0.06	0.02	0.00	8090.3
NS-33.01	0.01	22.1	0.22	0.09	2.55	0.02	0.82	0.58	0.02	0.00	0.67	1.90	0.06	0.01	0.00	1117.4
NS-35.01	0.03	37.0	0.00	0.35	6.87	0.00	1.84	0.39	0.02	0.00	0.66	2.16	0.06	0.02	0.00	1709.5
NS-36.04	0.05	49.2	0.00	0.21	6.61	0.00	0.49	0.51	0.02	0.00	0.67	1.99	0.06	0.01	0.00	2391.8
NS-39.01	0.02	20.9	0.00	0.40	4.46	0.00	1.78	0.17	0.02	0.07	0.67	2.41	0.06	0.01	0.00	949.6
NS-40.01	0.04	7.78	0.00	0.30	1.65	0.00	1.78	0.60	0.02	0.00	0.67	1.86	0.07	0.00	0.00	358.6
NS-41.01	0.02	36.8	0.00	0.49	3.99	0.00	4.92	0.27	0.02	0.00	0.66	2.30	0.06	0.01	0.00	1538.6
NS-41.21	0.01	22.8	0.01	0.34	2.49	0.00	2.03	0.01	0.00	0.00	3.93	0.60	0.11	0.04	0.00	1251.2
NS-42.01	0.04	60.2	0.00	0.63	7.07	0.00	5.15	0.41	0.02	0.00	0.66	2.14	0.05	0.02	0.00	1980.4
NS-42.21	0.02	34.7	0.00	0.58	4.07	0.00	3.88	0.01	0.00	0.00	12.7	0.97	0.13	0.05	0.00	1642.7
NS-43.01	0.04	7.98	0.02	0.26	1.73	0.00	1.78	0.62	0.02	0.04	0.67	1.83	0.07	0.01	0.00	357.4
NS-44.01	0.01	22.9	0.00	0.48	9.62	0.00	6.22	0.36	0.02	0.00	0.66	2.18	0.06	0.02	0.00	1327.6
NS-45.01	0.04	28.3	0.00	0.41	6.42	0.00	2.16	0.23	0.02	0.00	0.66	2.35	0.06	0.01	0.00	1282.7
NS-45.21	0.03	18.3	0.00	0.38	4.62	0.00	1.36	0.01	0.00	0.00	4.81	0.61	0.06	0.05	0.00	1082.8
NS-46.01	0.02	64.4	0.00	0.29	4.04	0.00	0.47	0.31	0.02	0.00	0.67	2.27	0.05	0.01	0.00	2857.4
NS-46.21	0.01	47.6	0.00	0.29	2.96	0.00	0.34	0.01	0.00	0.00	2.09	0.76	0.19	0.05	0.00	2618.0
NS-I1OUT.01	0.00	5.22	0.02	0.29	0.91	0.03	0.20	0.12	0.02	0.42	0.67	2.46	0.07	0.00	0.00	
NS-I1OUT.03	0.00	4.93	0.08	0.25	0.89	0.01	0.32	0.00	0.33	0.12	0.26	0.02	0.01	0.09	0.03	
NS-I1out.08	0.00	4.13	0.03	0.24	0.71	0.01	0.15	0.00	0.00	0.00	0.07	0.26	0.01	0.04	0.00	
NS-I2OUT.01	0.01	4.88	0.06	0.33	1.11	0.02	0.21	0.15	0.02	0.83	0.67	2.43	0.07	0.00	0.00	
NS-I2OUT.03	0.01	5.20	0.26	0.26	1.23	0.00	0.32	0.01	0.34	0.12	0.22	0.29	0.01	0.10	0.03	
NS-I2OUT.08	0.01	3.46	0.06	0.26	0.79	0.01	0.15	0.01	0.00	0.00	0.10	0.44	0.01	0.03	0.00	
NS-I3INEAST	0.00	4.36	0.07	0.25	1.01	0.00	0.20	0.15	0.02	0.36	0.67	2.43	0.07	0.00	0.00	
NS-I3INWEST	0.00	4.61	0.03	0.24	0.80	0.00	0.18	0.12	0.02	0.51	0.67	2.46	0.07	0.00	0.00	
NS-I3OUT	0.00	4.53	0.07	0.24	0.88	0.00	0.20	0.10	0.02	0.57	0.67	2.49	0.07	0.00	0.00	
NS-I4OUT.01	0.00	4.42	0.17	0.27	0.85	0.01	0.19	0.10	0.02	0.75	0.67	2.49	0.07	0.00	0.00	
NS-I4OUT.04	0.01	4.21	0.15	0.20	0.84	0.02	0.31	0.00	0.34	0.12	0.27		0.01	0.09	0.03	
NS-I5IN	0.00	4.37	0.18	0.25	0.84	0.00	0.18	0.10	0.02	0.42	0.67	2.49	0.07	0.00	0.00	
NS-I5OUT	0.00	4.23	0.05	0.25	0.79	0.03	0.18	0.13	0.02	0.80	0.67	2.44	0.07	0.00	0.00	
NS-I6HWIN.01	0.00	16.7	0.08	0.04	1.58	0.00	0.28	0.34	0.02	0.48	0.67	2.20	0.07	0.01	0.00	
NS-I6HWIN.04	0.01	23.8	0.51	0.04	2.38	0.04	0.46	0.04	0.33	0.11	0.21	0.97	0.04	0.10	0.03	
NS-I6HWIN.08	0.00	18.5	0.05	0.04	1.64	0.00	0.28	0.01	0.00	0.00	0.42	1.07	0.03	0.04	0.00	
NS-I6INE.08	0.00	3.45	0.10	0.20	0.64	0.01	0.14	0.01	0.00	0.00	0.07	0.37	0.01	0.03	0.00	
NS-I6INEAST.01	0.00	4.35	0.10	0.24	0.80	0.00	0.18	0.13	0.02	0.90	0.67	2.45	0.07	0.00	0.00	
NS-I6INEAST.04	0.01	4.92	0.33	0.18	0.90	0.03	0.32	0.00	0.33	0.11	0.28	0.07	0.01	0.09	0.03	
NS-I6INWEST.01	0.01	11.1	0.02	0.11	1.05	0.00	0.20	0.27	0.02	0.35	0.67	2.29	0.07	0.00	0.00	
NS-I6INWEST.03	0.02	27.2	0.02	0.10	2.56	0.00	0.45	0.04	0.33	0.11	0.58	0.94	0.04	0.10	0.03	
NS-I6INWEST.08	0.01	11.3	0.02	0.11	1.07	0.00	0.19	0.01	0.00	0.00	0.17	0.92	0.02	0.04	0.00	
NS-I6OUT	0.01	7.96	0.03	0.28	1.03	0.02	0.20	0.16	0.02	0.17	0.67	2.41	0.07	0.00	0.00	
NS-I7OUT.01	0.01	8.46	0.03	0.28	1.05	0.03	0.21	0.16	0.02	0.13	0.67	2.41	0.07	0.00	0.00	
NS-I7OUT.03	0.01	7.85	0.04	0.21	1.00	0.00	0.33	0.01	0.34	0.12	0.31	0.17	0.01	0.09	0.03	
NS-I8HW.01	0.01	6.74	0.13	0.11	1.28	0.01	0.31	0.32	0.02	0.25	0.67	2.21	0.07	0.00	0.00	
NS-I8HW.04	0.01	13.2	0.71	0.13	2.93	0.11	0.44	0.05	0.03	0.00	0.40	1.08	0.03	0.02	0.01	
NS-I8HW.08	0.01	8.56	0.08	0.08	1.23	0.02	0.27	0.01	0.00	0.00	0.26	1.04	0.02	0.04	0.00	
NS-I8IN.01	0.01	9.30	0.05	0.13	1.37	0.00	0.32	0.27	0.02	0.45	0.67	2.28	0.07	0.01	0.00	

sample number	Ba	Ca	Fe	K	Mg	Mn	Na	Ni	P	Rb	S	Si	Sr	V	Zn	Alk (uEQ/L)
NS-I8IN.03	0.02	21.2	0.11	0.12	3.62	0.00	0.55	0.03	0.34	0.11	0.69	0.78	0.04	0.11	0.03	
NS-I8OUT	0.01	9.41	0.04	0.26	1.33	0.00	0.30	0.26	0.02	0.61	0.67	2.29	0.07	0.01	0.00	
NS-I9INEAST.01	0.01	9.61	0.03	0.26	1.33	0.00	0.30	0.23	0.02	0.47	0.67	2.33	0.07	0.00	0.00	
NS-I9INEAST.03	0.01	12.5	0.02	0.12	1.78	0.00	0.47	0.01	0.34	0.11	0.50	0.38	0.02	0.10	0.03	
NS-I9INW.08	0.01	6.72	0.07	0.16	0.82	0.00	0.15	0.01	0.00	0.00	0.09	0.57	0.01	0.03	0.00	
NS-I9INWEST.01	0.01	8.21	0.06	0.23	1.01	0.00	0.21	0.17	0.02	0.40	0.67	2.40	0.07	0.00	0.00	
NS-I9INWEST.03	0.00	0.00	0.00	0.00	-0.03	0.00	0.22	-0.01	0.48	0.14	0.18		0.00	0.07	0.04	
NS-I9OUT.01	0.01	8.91	0.04	0.23	1.20	0.00	0.26	0.20	0.02	0.00	0.67	2.36	0.07	0.00	0.00	440.3
NS-I9OUT.05	0.01	14.2	0.10	0.18	1.88	0.01	0.34	0.23	0.02	0.00	0.67	2.33	0.07	0.01	0.00	695.2
NS-IMINUSIN.01	0.01	5.46	0.13	0.19	0.92	0.01	0.29	0.32	0.02	0.72	0.67	2.21	0.07	0.00	0.00	
NS-IMINUSOUT.01	0.01	8.80	0.06	0.33	1.50	0.02	0.36	0.34	0.02	0.51	0.67	2.20	0.07	0.00	0.00	
NS-ISWAMPIN	0.01	8.94	0.06	0.28	1.06	0.00	0.22	0.17	0.02	0.04	0.67	2.40	0.07	0.00	0.00	
NS-ISWAMPOUT	0.01	8.23	0.05	0.23	1.00	0.00	0.20	0.17	0.02	0.44	0.67	2.40	0.07	0.00	0.00	
NS-MWL.01	0.02	16.6	0.01	0.13	1.74	0.00	0.54	0.36	0.02	0.00	0.67	2.17	0.07	0.01	0.00	
NS-MWL.03	0.03	31.1	0.00	0.14	2.82	0.00	0.72	0.04	0.33	0.11	0.80	1.14	0.05	0.10	0.03	
NS-MWL.08	0.02	15.0	0.03	0.11	1.49	0.00	0.43	0.01	0.00	0.00	0.45	1.07	0.03	0.04	0.00	
NS-MWL.09	0.01	11.6	0.02	0.12	1.37	0.00	0.41	0.01	0.00	0.00	0.46	1.11	0.02	0.04	0.00	
NS-MWU.01	0.01	6.91	0.04	0.08	1.04	0.00	0.49	0.33	0.02	0.17	0.67	2.20	0.07	0.00	0.00	
NS-MWU.03	0.02	10.2	0.09	0.09	1.52	0.01	0.63	0.04	0.34	0.11	0.59	1.13	0.02	0.10	0.03	
NS-MWU.08	0.01	5.94	0.03	0.05	0.90	0.00	0.37	0.01	0.00	0.00	0.37	1.10	0.01	0.04	0.00	
NS-MWU.09	0.01	5.84	0.03	0.09	0.89	0.00	0.37	0.01	0.00	0.00	0.37	1.10	0.01	0.03	0.00	
NS-TOOLIKIN.01	0.01	10.2	0.03	0.25	1.32	0.00	0.30	0.22	0.02	0.28	0.67	2.35	0.07	0.00	0.00	
NS-TOOLIKIN.03	0.01	14.8	0.02	0.16	1.91	0.00	0.48	0.02	0.34	0.11	0.50	0.57	0.03	0.10	0.03	
NS-TOOLIKIN.08	0.01	9.38	0.05	0.11	1.24	0.00	0.26	0.01	0.00	0.00	0.26	0.88	0.02	0.03	0.00	
NS-TOOLIKIN.09	0.01	8.12	0.07	0.14	1.08	0.00	0.24	0.01	0.00	0.00	0.22	0.89	0.01	0.04	0.00	
NS-TOOLIKIN.10	0.01	9.98	0.05	0.12	1.30	0.00	0.27	0.01	0.00	0.00	0.27	0.86	0.02	0.04	0.00	
NS-TOOLIKIN.11	0.02	10.0	0.07	0.12	1.30	0.00	0.28	0.01	0.00	0.00	0.29	0.87	0.02	0.04	0.00	

Appendix D: Toolik Inlet stream and Milky Way Upper stream $^{87}Sr/^{86}Sr$.

Toolik inlet Stream

Date and Time	LTER ID	$^{87}Sr/^{86}Sr$	2 sigma
6/23/93 0:00	1993-0338	0.712135	0.000019
9/12/93 0:00	1993-1386	0.712227	0.000018
7/8/94 12:00	1994-0371	0.712260	0.000020
7/13/94 12:00	1994-0434	0.712247	0.000019
7/15/94 12:00	1994-0489	0.712270	0.000013
7/19/94 12:00	1994-0603	0.712203	0.000019
7/22/94 12:00	1994-0655	0.712354	0.000016
7/27/94 12:00	1994-0718	0.712177	0.000020
7/29/94 12:00	1994-0776	0.712054	0.000021
8/3/94 12:00	1994-0882	0.712212	0.000015
8/5/94 12:00	1994-0927	0.712122	0.000014
8/9/94 12:00	1994-1040	0.712231	0.000030
8/12/94 12:00	1994-1059	0.712205	0.000019
8/19/94 12:00	1994-1152	0.712125	0.000016
8/24/94 12:00	1994-1214	0.712274	0.000016
5/15/96 15:00	1996-0002	0.712146	0.000016
5/23/96 23:00	1996-0019	0.712258	0.000021
5/24/96 15:00	1996-0023	0.712209	0.000023
5/24/96 21:00	1996-0024	0.712387	0.000021
5/26/96 18:00	1996-0033	0.712481	0.000012
5/29/96 18:00	1996-0071	0.712505	0.000027
5/30/96 16:00	1996-0074	0.712504	0.000016
5/31/96 15:00	1996-0077	0.712452	0.000015
6/3/96 12:00	1996-0081	0.712451	0.000029
6/4/96 12:00	1996-0824	0.712559	0.000011
6/5/96 11:00	1996-0088	0.712514	0.000014
6/6/96 12:00	1996-0095	0.712436	0.000019
6/21/96 11:00	1996-0192	0.712157	0.000011
6/28/96 10:00	1996-0231	0.712136	0.000012
6/29/96 14:00	1996-0234	0.712087	0.000021
7/5/96 11:00	1996-0312	0.712060	0.000014
7/12/96 10:00	1996-0332	0.711944	0.000019
7/19/96 12:00	1996-0389	0.712175	0.000017
7/19/96 12:00	1996-0389.1	0.712247	0.000028
7/23/96 12:00	1996-0832	0.712235	0.000014
7/26/96 14:00	1996-0469	0.712102	0.000013
7/30/96 15:00	1996-0502	0.712063	0.000011
7/31/96 14:00	1996-0524	0.712183	0.000033
8/12/96 15:00	1996-0638	0.711985	0.000023
8/20/96 13:00	1996-0724	0.711968	0.000013
8/22/96 12:00	1996-0737	0.711948	0.000016

Date and Time	LTER ID	$^{87}Sr/^{86}Sr$	2 sigma
9/2/96 16:00	1996-0798	0.711923	0.000014
6/6/97 13:00	1997-0001	0.712366	0.000013
6/9/97 15:00	1997-0012	0.712368	0.000018
6/18/97 14:00	1997-0065	0.712392	0.000027
6/20/97 11:00	1997-0094	0.712288	0.000012
7/1/97 11:00	1997-0163	0.712007	0.000023
7/9/97 13:00	1997-0265	0.712101	0.000008
7/19/97 14:00	1997-0455	0.712072	0.000016
7/26/97 11:00	1997-0547	0.712152	0.000034
8/2/97 12:00	1997-0641	0.712000	0.000009
8/15/97 16:00	1997-0807	0.712319	0.000018
8/16/97 17:00	1997-0810	0.712218	0.000010
8/18/97 17:00	1997-0831	0.712163	0.000012
6/11/98 15:00	1998-0001	0.712107	0.000017
6/16/98 12:00	1998-0025	0.712235	0.000025
6/24/98 10:00	1998-0123	0.712021	0.000021
7/3/98 15:00	1998-0222	0.712021	0.000014
7/10/98 11:00	1998-0335	0.711897	0.000011
7/15/98 10:00	1998-0400	0.711870	0.000014
7/20/98 9:00	1998-0464	0.711836	0.000020
8/3/98 10:00	1998-0608	0.712045	0.000020
8/7/98 13:00	1998-0639	0.712104	0.000021
8/14/98 15:00	1998-0686	0.712009	0.000016
6/23/99 16:00	1999-0075	0.712121	0.000022
6/25/99 17:00	1999-0080	0.712059	0.000016
6/28/99 15:00	1999-0125	0.711987	0.000012
7/6/99 21:00	1999-0251	0.711928	0.000020
7/8/99 19:00	1999-0282	0.712020	0.000011
7/13/99 13:00	1999-0385	0.711996	0.000017
7/28/99 12:00	1999-0613	0.712001	0.000009
8/2/99 12:00	1999-0682	0.711930	0.000014
8/6/99 14:00	1999-0734	0.711874	0.000018
8/11/99 9:00	1999-0806	0.712019	0.000017
8/16/99 14:00	1999-0827	0.712052	0.000019
6/21/00 11:00	2000-0017	0.712180	0.000019
6/28/00 16:00	2000-0099	0.712077	0.000026
7/4/00 12:00	2000-0181	0.712084	0.000014
7/6/00 17:00	2000-0227	0.712192	0.000019
7/12/00 11:00	2000-0308	0.712023	0.000021
7/24/00 11:00	2000-0434	0.712007	0.000014
7/28/00 12:00	2000-0501	0.711675	0.000016
8/1/00 11:00	2000-0539	0.711918	0.000016
8/7/00 11:00	2000-0580	0.711853	0.000020
8/14/00 11:00	2000-0655	0.712013	0.000012

Date and Time	LTER ID	$^{87}Sr/^{86}Sr$	2 sigma
6/30/01 17:00	2001-0136	0.712009	0.000018
7/4/01 15:00	2001-0220	0.712104	0.000013
7/6/01 11:00	2001-0232	0.712057	0.000021
7/7/01 20:00	2001-0249	0.712136	0.000013
7/18/01 13:00	2001-0377	0.711984	0.000019
7/20/01 12:00	2001-0444	0.711986	0.000028
7/27/01 12:00	2001-0529	0.712088	0.000019
8/1/01 11:00	2001-0554	0.712154	0.000023
8/8/01 12:00	2001-0630	0.712107	0.000031
8/13/01 12:00	2001-0696	0.712071	0.000014
6/21/02 15:00	2002-0040	0.712085	0.000026
6/26/02 12:00	2002-0094	0.712119	0.000053
6/28/02 17:00	2002-0150	0.712155	0.000021
7/5/02 16:00	2002-0218	0.712166	0.000030
7/12/02 3:00	2002-0301	0.712114	0.000022
7/17/02 16:00	2002-0377	0.712086	0.000028
7/19/02 12:00	2002-0421	0.712062	0.000022
7/26/02 12:00	2002-0521	0.711968	0.000021
8/2/02 11:00	2002-0576	0.711872	0.000009
8/7/02 14:00	2002-0659	0.711939	0.000025
8/9/02 11:00	2002-0703	0.711887	0.000014
5/21/03 14:00	2003-0047	0.711921	0.000031
5/28/03 13:00	2003-0473	0.711946	0.000021
5/29/03 10:00	2003-0474	0.711917	0.000023
5/29/03 16:00	2003-0475	0.711842	0.000036
5/30/03 10:00	2003-0477	0.711846	0.000019
5/30/03 16:00	2003-0478	0.711975	0.000018
5/31/03 11:00	2003-0480	0.712162	0.000021
5/31/03 16:00	2003-0481	0.712189	0.000027
6/1/03 16:00	2003-0482	0.712246	0.000035
6/3/03 9:00	2003-0488	0.712245	0.000013
6/4/03 11:00	2003-0492	0.712434	0.000018
6/5/03 20:00	2003-0499	0.712418	0.000014
6/7/03 10:00	2003-0500	0.712469	0.000016
6/9/03 10:00	2003-0507	0.712453	0.000028
6/14/03 14:00	2003-0529	0.712279	0.000027
6/17/03 9:00	2003-0539	0.712198	0.000016
6/20/03 17:00	2003-0239	0.712114	0.000016
6/25/03 16:00	2003-0310	0.712049	0.000026
6/27/03 12:00	2003-0245	0.712052	0.000028
7/4/03 12:00	2003-0251	0.712125	0.000018
7/11/03 11:00	2003-0257	0.712166	0.000026
7/14/03 18:00	2003-0760	0.712276	0.000021
7/16/03 15:00	2003-0334	0.712208	0.000026

Date and Time	LTER ID	$^{87}Sr/^{86}Sr$	2 sigma
7/28/03 11:00	2003-0841	0.712278	0.000022
8/1/03 12:00	2003-0275	0.712199	0.000024
8/6/03 15:00	2003-0358	0.712102	0.000023
8/15/03 13:00	2003-0281	0.712239	0.000017
6/18/04 16:00	2004-0130	0.711827	0.000022
6/23/04 14:00	2004-0178	0.711812	0.000015
6/25/04 14:00	2004-0179	0.711811	0.000016
7/2/04 11:00	2004-0238	0.711797	0.000016
7/9/04 13:00	2004-0296	0.711871	0.000019
7/14/04 11:00	2004-0344	0.712001	0.000014
7/16/04 11:00	2004-0345	0.712020	0.000015
7/23/04 12:00	2004-0404	0.712109	0.000013
7/30/04 11:00	2004-0462	0.712000	0.000017
8/4/04 13:00	2004-0510	0.712218	0.000009
8/6/04 11:00	2004-0511	0.712048	0.000011
8/13/04 12:00	2004-0570	0.711932	0.000014
8/19/04 16:00	2004-0628	0.711955	0.000014

Toolik Inlet

Rain Event Date	LTER ID	$^{87}Sr/^{86}Sr$	2 sigma
26-Jul-03	2003-0837	0.712365	0.000026
27-Jul-03	2003-0838	0.712381	0.000028
27-Jul-03	2003-0839	0.712346	0.000063
28-Jul-03	2003-0840	0.712300	0.000018

Milky Way

Upper Stream Date	LTER ID	$^{87}Sr/^{86}Sr$	2 sigma
12-Jun-96	1996-0112	0.712555	0.000016
21-Jun-96	1996-0194	0.712324	0.000013
28-Jun-96	1996-0233	0.712461	0.000016
20-Aug-96	1996-0726	0.712337	0.000014
27-Aug-96	1996-0784	0.712256	0.000033
26-Jun-02	2002-0093	0.712538	0.000043
28-Jun-02	2002-0152	0.712625	0.000022
05-Jul-02	2002-0213	0.712581	0.000017
12-Jul-02	2002-0297	0.712554	0.000013
17-Jul-02	2002-0376	0.712406	0.000015
19-Jul-02	2002-0417	0.712359	0.000014
26-Jul-02	2002-0517	0.712237	0.000039
02-Aug-02	2002-0572	0.712000	0.000019
07-Aug-02	2002-0658	0.711981	0.000032

Date	LTER ID	$^{87}Sr/^{86}Sr$	2 sigma
09-Aug-02	2002-0702	0.712085	0.000031
09-Aug-02	2002-0702.0-gff	0.712028	0.000014
20-Jun-03	2003-0241	0.712408	0.000031
27-Jun-03	2003-0247	0.712183	0.000027
4-Jul-03	2003-0253	0.712523	0.000024
11-Jul-03	2003-0259	0.712552	0.000019
25-Jul-03	2003-0271	0.712566	0.000019
1-Aug-03	2003-0277	0.712558	0.000016
25-Jun-03	2003-0307	0.712304	0.000019
16-Jul-03	2003-0331	0.712570	0.000020
6-Aug-03	2003-0355	0.712594	0.000032
15-Aug-03	2003-0283	0.712600	0.000016

Appendix E: Vegetation and soil road-influence transect chemistry data and graph. Soil and vegetation was sampled at progressive distances away from the Dalton Highway on the Sag 2 glacial surface in order to detect the influence of road dust on soil chemistry and nutrient supply to vegetation.

sample	distance from road (m)	horizon or veg type	Ba	Ca	Fe	K	Mg	P	Sr	Ca/Sr	87Sr/86Sr	2 sigma
NS-22.07	200	turf	0.21	7.78	6.80	2.32	1.95	0.62	0.02	797	0.715349	0.000026
NS-22.07b	200	moss	0.26	7.29	8.83	3.29	2.30	0.90	0.02	713	0.716601	0.000021
NS-22.08 ex	200	O	0.03	1.16	0.06	0.17	0.25	0.03	0.00	590	0.713771	0.000013
NS-22.08 HNO3 leach	200	O	0.13	1.51	2.88	0.00	0.04	0.30	0.00	721	0.713702	0.000027
NS-22.09 ex	200	A	0.06	0.34	0.01	0.05	0.06	0.00	0.00	564	0.713989	0.000031
NS-22.09 HNO3 leach	200	A	0.05	0.31	5.86	0.04	0.24	0.00	0.00	782	0.712777	0.000031
NS-22.10 ex	200	B	0.24	1.45	0.04	0.12	0.21	0.00	0.00	646	0.713286	0.000024
NS-22.10 HNO3 leach	200	B	0.15	0.52	14.4	0.10	0.36	0.00	0.00	721	0.713302	0.000023
NS-22.11 ex	200	perm	0.25	2.23	0.04	0.20	0.27	0.00	0.01	764	0.711905	0.000011
NS-22.11 HNO3 leach	200	perm	0.17	0.97	8.87	0.11	0.24	0.00	0.00	894	0.711978	0.000028
NS-22.22	200	willow	0.05	11.2	0.93	6.33	3.62	2.80	0.02	1074	0.713657	0.000018
NS-22.23	200	birch	0.19	10.1	0.74	9.70	4.13	4.31	0.01	1478	0.713429	0.000024
NS-22.24	200	ledum	0.16	6.45	0.75	6.82	1.34	1.65	0.00	3315	0.713418	0.000017
NS-22.25	200	turf	0.21	6.45	7.89	3.17	2.41	0.72	0.02	858	0.715783	0.000019
NS-22.26 ex	50	O	0.03	4.85	0.04	0.02	0.22	0.01	0.01	945	0.709979	0.000023
NS-22.26 HNO3 leach	50	O	0.13	9.56	3.74	0.00	0.08	0.18	0.02	1142	0.709937	0.000027
NS-22.27 ex	50	A	0.03	0.25	0.00	0.03	0.04	0.00	0.00	593	0.713414	0.000017
NS-22.27 HNO3 leach	50	A	0.03	0.16	2.66	0.04	0.15	0.01	0.00	819	0.712500	0.000054
NS-22.30	50	willow	0.12	26.1	2.15	15.3	5.29	3.78	0.04	1331	0.711309	0.000015
NS-22.31	50	birch	0.11	8.87	0.90	11.8	4.07	1.79	0.01	2103	0.711791	0.000022
NS-22.32	50	ledum	0.15	8.17	0.82	6.51	1.89	1.57	0.01	3477	0.711569	0.000017
NS-22.33	50	turf	0.24	13.7	6.88	3.95	2.84	0.52	0.03	1101	0.711571	0.000019
NS-22.33b	50	moss	0.19	10.7	7.70	4.27	2.10	0.54	0.02	1042	0.712764	0.000016
NS-22.34	250	willow	0.02	11.9	0.31	10.8	4.10	2.14	0.02	1392	0.713384	0.000022
NS-22.35	250	moss	0.10	4.38	1.88	3.82	1.30	0.83	0.01	1438	0.714143	0.000024
NS-22.36	250	sedge	0.06	3.86	0.35	11.0	1.47	1.55	0.01	1137	0.713378	0.000026
NS-22.37	250	evergrn	0.10	6.96	1.58	2.43	1.22	0.87	0.01	1724	0.714000	0.000015
NS-22.38	250	birch	0.06	7.68	0.27	11.6	3.35	2.40	0.01	1878	0.713085	0.000019
NS-22.38 dup	200	birch	0.06	7.59	0.28	11.2	3.24	2.30	0.01	1815	0.713107	0.000038
NS-22.39	250	ledum	0.21	8.39	0.27	5.91	1.70	1.48	0.00	5237	0.714125	0.000016

NS-47.03 ex	10O	0.03	3.63	0.21	0.0	0.25	0.00	0.01	759	0.712250	0.000026
NS-47.03 HNO3 leach	10O	0.13	7.24	18.6	0.0	0.13	0.03	0.02	875	0.712191	0.000017
NS-47.04 ex	10A	0.08	1.84	0.06	0.04	0.15	0.00	0.01	743	0.712336	0.000019
NS-47.04 HNO3 leach	10A	0.16	1.39	8.47	0.05	0.26	0.00	0.00	968	0.712197	0.000024
NS-47.05	10turf	0.90	16.4	32.2	6.26	10.4	0.81	0.04	904	0.714152	0.000018
NS-47.06	10willow	0.09	9.83	2.48	8.08	2.39	1.80	0.02	1018	0.712611	0.000017
NS-47.07	10ledum	0.22	13.0	3.89	5.15	2.64	1.40	0.02	1323	0.711284	0.000024
NS-47.08	10reticulata	0.33	31.2	7.79	16.7	6.55	2.48	0.07	1011	0.710968	0.000015
NS-48.01 ex	0road	0.07	1.62	0.03	0.03	0.07	0.00	0.00	718	0.708697	0.000012
NS-48.01 HNO3 leach	0road	0.13	12.2	3.29	0.05	1.13	0.44	0.02	1166	0.708407	0.000026

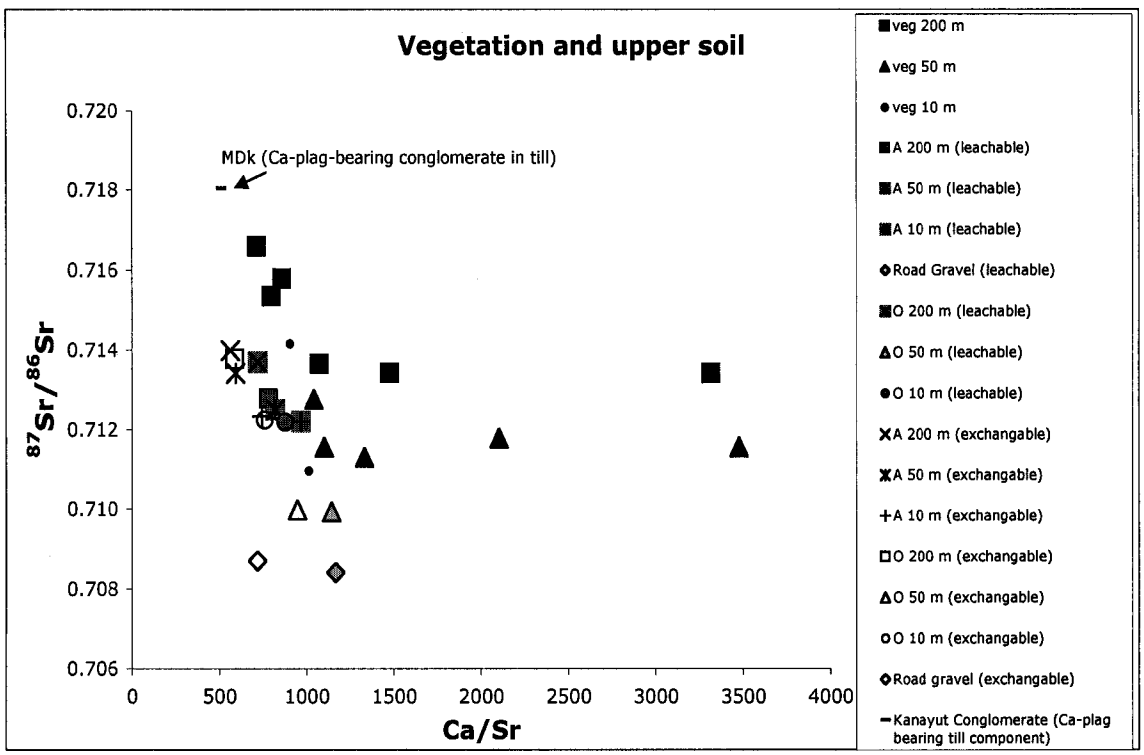

Appendix F: Permafrost sequential water leach chemistry. Permafrost samples from several surfaces were leached in a batch-reaction method on a shaker table with 2x DI water (pH=5.5) for durations ranging from 3 days to 3 weeks in an effort to simulate the effects of permafrost thaw and progressive exposure to natural water. The entire water leach lasted 72 days to approximate the duration of an arctic summer; upon completion of the leach the permafrost samples were digested with 1M HNO_3 at room temperature to estimate the remaining carbonate content.

Experimental design:

stage	leach type	leach duration (days)	total days of experiment
1	water	3	3
2	water	3	6
3	water	3	9
4	water	7	16
5	water	7	23
6	water	7	30
7	water	21	51
8	water	21	72
9	1M HNO_3	3	75

Sequential leach fraction chemistry, in mg/g sample.

	mg/g									
sample	**Ba**	**Ca**	**Fe**	**K**	**Mg**	**Na**	**P**	**S**	**Si**	**Sr**
NS-13.23 - 1	0.00	0.59	0.00	0.03	0.08	0.03	0.00	0.50	0.01	0.001
NS-13.23 - 2	0.00	0.29	0.01	0.03	0.04	0.01	0.00	0.11	0.04	0.001
NS-13.23 - 3	0.00	0.26	0.00	0.01	0.03	0.00	0.00	0.05	0.01	0.001
NS-13.23 - 4	0.00	0.25	0.01	0.02	0.03	0.00	0.00	0.03	0.04	0.001
NS-13.23 - 5	0.00	0.23	0.00	0.01	0.02	0.00	0.00	0.02	0.03	0.001
NS-13.23 - 6	0.00	0.21	0.01	0.01	0.02	0.00	0.00	0.01	0.03	0.000
NS-13.23 - 7	0.00	0.27	0.00	0.01	0.02	0.00	0.00	0.02	0.02	0.001
NS-13.23 - 8	0.27	0.04	0.02	0.00	0.00	0.00	0.00	0.08	0.00	0.000
NS-13.23 - cold HNO3	0.33	13.9	14.9	0.19	3.74	0.01	0.75	0.04	2.74	0.022
NS-101.05 - 1	0.00	0.02	0.23	0.11	0.03	0.01	0.00	0.00	0.64	0.000
NS-101.05 - 2	0.01	0.01	0.30	0.15	0.03	0.01	0.01	0.00	0.80	0.000
NS-101.05 - 3	0.00	0.01	0.16	0.07	0.02	0.01	0.00	0.00	0.38	0.000
NS-101.05 - 4	0.00	0.01	0.14	0.05	0.01	0.00	0.00	0.00	0.29	0.000
NS-101.05 - 5	0.00	0.00	0.07	0.02	0.01	0.00	0.00	0.00	0.12	0.000
NS-101.05 - 6	0.00	0.00	0.06	0.02	0.00	0.00	0.00	0.00	0.10	0.000
NS-101.05 - 7	0.00	0.01	0.13	0.04	0.01	0.00	0.00	0.00	0.22	0.000
NS-101.05 - 8	0.00	0.01	0.23	0.07	0.02	0.01	0.01	0.00	0.41	0.000
NS-101.05 - cold HNO3	0.11	0.88	10.8	0.11	0.65	0.00	0.42	0.02	1.63	0.004
NS-102.06 - 1	0.00	0.01	0.26	0.13	0.03	0.01	0.01	0.01	0.61	0.000
NS-102.06 - 2	0.00	0.00	0.12	0.05	0.01	0.00	0.00	0.00	0.25	0.000
NS-102.06 - 3	0.00	0.00	0.07	0.03	0.01	0.00	0.00	0.00	0.14	0.000
NS-102.06 - 4	0.00	0.00	0.05	0.01	0.00	0.00	0.00	0.00	0.08	0.000
NS-102.06 - 5	0.00	0.00	0.07	0.02	0.01	0.00	0.00	0.00	0.13	0.000
NS-102.06 - 6	0.00	0.00	0.03	0.01	0.00	0.00	0.00	0.00	0.06	0.000
NS-102.06 - 7	0.00	0.00	0.08	0.02	0.01	0.00	0.00	0.00	0.14	0.000
NS-102.06 - 8	0.00	0.00	0.07	0.02	0.00	0.00	0.00	0.00	0.11	0.000
NS-102.06 - cold HNO3	0.03	0.32	5	0.07	0.46	0.00	0.25	0.01	1.26	0.001
NS-102.05 - 1	0.00	0.01	0.28	0.10	0.02	0.01	0.00	0.00	0.50	0.000
NS-102.05 - 2	0.00	0.00	0.17	0.05	0.01	0.00	0.00	0.00	0.28	0.000
NS-102.05 - 3	0.00	0.00	0.11	0.03	0.01	0.00	0.00	0.00	0.16	0.000
NS-102.05 - 4	0.00	0.00	0.08	0.02	0.00	0.00	0.00	0.00	0.10	0.000
NS-102.05 - 5	0.00	0.00	0.07	0.01	0.00	0.00	0.00	0.00	0.08	0.000
NS-102.05 - 6	0.00	0.00	0.07	0.01	0.00	0.00	0.00	0.00	0.08	0.000
NS-102.05 - 7	0.00	0.00	0.14	0.03	0.01	0.00	0.00	0.00	0.17	0.000
NS-102.05 - 8	0.00	0.00	0.12	0.02	0.01	0.00	0.00	0.00	0.14	0.000
NS-102.05 - cold HNO3	0.05	0.38	9.84	0.08	0.57	0.00	0.23	0.01	1.49	0.002
NS-101.06 - 1	0.00	0.41	0.01	0.02	0.02	0.00	0.00	0.01	0.05	0.000
NS-101.06 - 2	0.00	0.29	0.01	0.01	0.01	0.00	0.00	0.00	0.04	0.000
NS-101.06 - 3	0.00	0.21	0.01	0.01	0.01	0.00	0.00	0.00	0.03	0.000
NS-101.06 - 4	0.00	0.23	0.01	0.01	0.01	0.00	0.00	0.00	0.04	0.000
NS-101.06 - 5	0.00	0.19	0.01	0.01	0.00	0.00	0.00	0.00	0.04	0.000
NS-101.06 - 6	0.00	0.20	0.01	0.01	0.00	0.00	0.00	0.00	0.05	0.000
NS-101.06 - 7	0.00	0.22	0.01	0.01	0.00	0.00	0.00	0.00	0.05	0.000

NS-101.06 - 8	0.00	0.24	0.03	0.01	0.01	0.00	0.00	0.00	0.07	0.000
NS-101.06 - cold HNO3	0.15	8.4	13.3	0.15	0.82	0.00	0.29	0	1.66	0.009
NS-110.05 - 1	0.00	0.41	0.08	0.04	0.03	0.01	0.01	0.10	0.10	0.001
NS-110.05 - 2	0.00	0.22	0.16	0.05	0.03	0.00	0.00	0.05	0.21	0.000
NS-110.05 - 3	0.00	0.13	0.10	0.03	0.02	0.00	0.00	0.02	0.13	0.000
NS-110.05 - 4	0.00	0.15	0.15	0.04	0.02	0.00	0.00	0.01	0.18	0.000
NS-110.05 - 5	0.00	0.12	0.10	0.02	0.01	0.00	0.00	0.01	0.11	0.000
NS-110.05 - 6	0.00	0.11	0.09	0.02	0.01	0.00	0.00	0.01	0.10	0.000
NS-110.05 - 7	0.00	0.17	0.20	0.03	0.02	0.00	0.00	0.01	0.18	0.000
NS-110.05 - 8	0.00	0.16	0.25	0.03	0.02	0.00	0.01	0.01	0.20	0.000
NS-110.05 - cold HNO3	0.38	9.27	7.04	0.08	1.05	0.00	0.4	0.21	1.74	0.019
NS-121.02 - 1	0.00	0.07	0.12	0.04	0.02	0.01	0.00	0.02	0.22	0.000
NS-121.02 - 2	0.00	0.04	0.12	0.04	0.01	0.00	0.00	0.00	0.22	0.000
NS-121.02 - 3	0.00	0.03	0.14	0.06	0.02	0.00	0.00	0.00	0.30	0.000
NS-121.02 - 4	0.00	0.03	0.09	0.02	0.01	0.00	0.00	0.00	0.14	0.000
NS-121.02 - 5	0.00	0.02	0.08	0.02	0.01	0.00	0.00	0.00	0.13	0.000
NS-121.02 - 6	0.00	0.02	0.06	0.02	0.01	0.00	0.00	0.00	0.11	0.000
NS-121.02 - 7	0.00	0.03	0.15	0.04	0.01	0.00	0.00	0.00	0.23	0.000
NS-121.02 - 8	0.00	0.03	0.16	0.03	0.01	0.00	0.00	0.00	0.24	0.000
NS-121.02 - cold HNO3	0.06	1.22	6.27	0.05	0.57	0.00	0.52	0.03	1.36	0.004
NS-121.01 - 1	0.00	0.28	0.01	0.03	0.02	0.03	0.00	0.20	0.04	0.001
NS-121.01 - 2	0.01	0.16	0.16	0.16	0.04	0.02	0.00	0.04	0.68	0.001
NS-121.01 - 3	0.00	0.14	0.12	0.12	0.03	0.01	0.00	0.01	0.51	0.001
NS-121.01 - 4	0.00	0.13	0.03	0.04	0.01	0.00	0.00	0.01	0.16	0.001
NS-121.01 - 5	0.00	0.13	0.02	0.03	0.01	0.00	0.00	0.01	0.12	0.000
NS-121.01 - 6	0.00	0.12	0.03	0.04	0.01	0.00	0.00	0.01	0.15	0.001
NS-121.01 - 7	0.00	0.15	0.02	0.03	0.01	0.00	0.00	0.01	0.11	0.001
NS-121.01 - 8	0.00	0.15	0.02	0.02	0.01	0.00	0.00	0.02	0.09	0.001
NS-121.01 - cold HNO3	0.15	6.89	13.4	0.19	2.03	0.00	0.6	0.19	3.07	0.017

Ca (mg/g) released into water by permafrost samples over time.

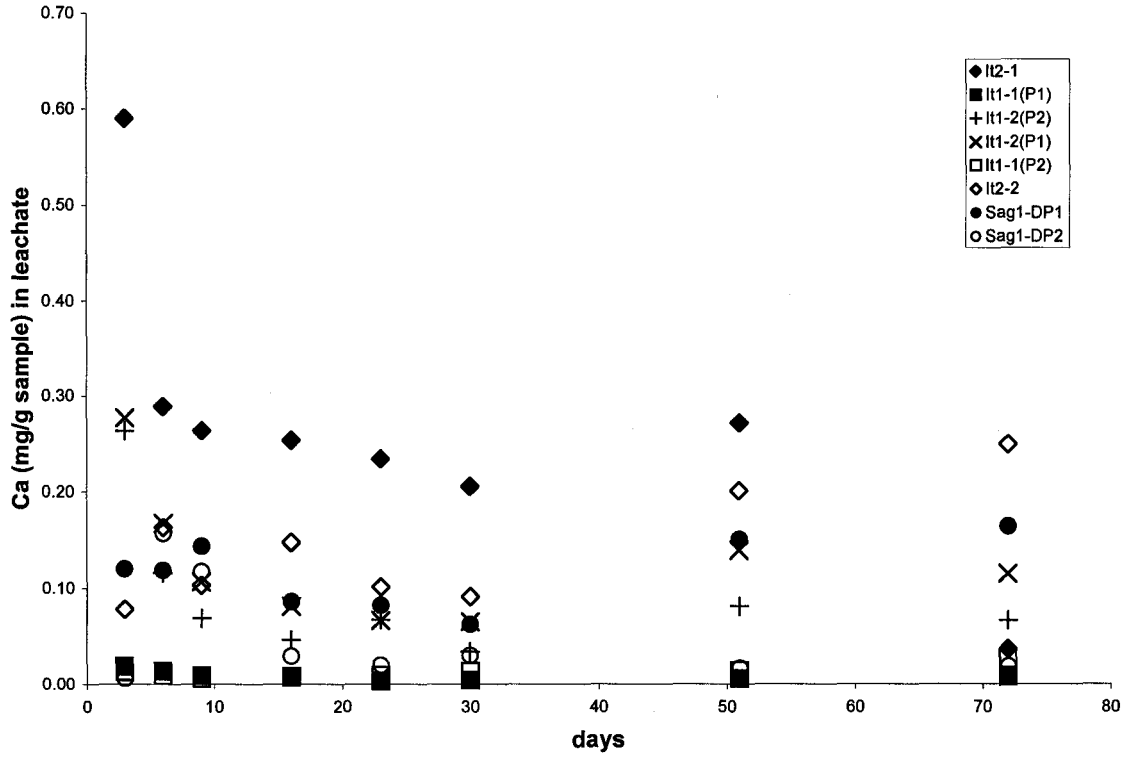

Appendix G: Statistics and graph for seasonal trends in stream geochemistry. Some years during the 1994-2004 analysis period showed significant ($p<0.05$) seasonal increases in Toolik Inlet stream Ca/Na and Ca/Ba and decreases in $^{87}Sr/^{86}Sr$ (Figure G), as seasonal thaw depth increased. These trends were not significant during every summer season for each geochemical indicator due to small sample size and variability caused by environmental factors. However, there were non-significant trends in most years for Ca/Na (which increased overall in seven out of the nine seasons for which there is useable data) and $^{87}Sr/^{86}Sr$ (which decreased overall in eight out of nine seasons). These significant and non-significant trends, detectable during times when seasonal thaw depth is known to be increasing, suggest that stream geochemistry is in fact an indicator of changing thaw depth and can be used to indicate longer-term trends.

Figure G: Late-summer low-discharge (Q<1.1) significant seasonal trends in Toolik Inlet stream geochemistry. A) Ca/Na (molar ratio) increases significantly with summer date. For 2004 (filled diamonds), R^2= ,p= ; for 1998 (open triangles), R^2= ,p= ; for 1996 (filled squares), R^2= ,p= ; for 1994 (open circles), R^2=0.79,p<0.001. B) Ca/Ba (molar ratio) increases significantly with summer date in 1996; R^2=0.59, p=0.02. C) 87Sr/86Sr decreases significantly with summer date in 2002; R^2=0.90,p=0.001.